

Role of Neutrophils and NETs in Coagulation

Yu Shi

Submitted in accordance with the requirements for the degree of Doctor of
Philosophy

The University of Leeds

School of Medicine

Faculty of Medicine & Health

January, 2022

Intellectual Property and Publication Statements

The candidate confirms that the work submitted is her own, except where work which has formed part of jointly authored publications has been included. The contribution of the candidate and the other authors to this work has been explicitly indicated below. The candidate confirms that appropriate credit has been given within the thesis where reference has been made to the work of others.

Publication which has arisen from the work presented in this thesis is:

Neutrophils can promote clotting via FXI and impact clot structure via neutrophil extracellular traps in a distinctive manner *in vitro*. Shi Y, Baker SR, Gauer JS, Philippou H, Connell SD, Ariens RAS. *Sci Rep* 11, 1718 (2021).

<https://doi.org/10.1038/s41598-021-81268-7>. Methods from this paper appear in Chapter 2 of this thesis. Results, adapted figures and discussion from this paper appear partially in Chapters 3-6.

This copy has been supplied on the understanding that it is copyright material, and no quotation from this thesis may be published without proper acknowledgement.

Acknowledgements

First, I would like to say a massive thank you to all those who played a role in the formation of this PhD thesis. I would like to say a huge thank you to my supervisors Prof Robert A. S. Ariëns, Prof Helen Philippou, Dr Simon D. Connell, Dr Julia Sandrin Gauer and my former co-supervisor Dr Stephen R. Baker who offered me patience, encouragement, constructive comments, and helpful advice throughout my PhD. I most sincerely thank my previous supervisors Prof Chris Peers, Dr Heiko Wurdak and Professor Susan Short, for taking care of me for 4 months at the beginning of my PhD, it is regrettable that my previous project has been cancelled. I would also thank my research tutors Dr Neil A. Turner and Prof David Buckley for their guidance, advice and supporting me during my PhD. A big thank you goes to the Ariëns group and Philippou group for your laboratory guidance, friendship, and for offering many helps whenever I need over the last three years.

I would like to thank Ms Helen McPherson for teaching me cell culture and fibrinogen purification. She also contributed to Scanning Electron Microscopy (SEM) by coating and imaging of all the samples. I would also like to thank Mr Martin Fuller for carrying out critical point drying of all SEM samples.

I would like to thank Dr Julia Sandrin Gauer for teaching me in permeation, sample preparation for SEM and helping me with the analysis of turbidity and SEM data.

I would like to thank Dr Simon D. Connell and Dr Lekshmi Kailas for training me in Atomic Force Microscopy (AFM) and giving me great suggestions. Many thanks to Simon for generously providing many cantilever tips for my experiments!

I would like to thank Dr Timea Feller for supporting and helping me with AFM scanning and providing a lot of helpful advice. I could not get those lovely AFM images without her help.

I would like to thank Dr Stephen R. Baker and Dr Fraser Macrae for helping me check the self-coagulation of normal pooled plasma, and giving me suggestions on how to avoid it.

I would like to thank Dr Fraser Macrae and Dr Cedric Duval for designing the Fiji-Image J macros that were used in counting fibrin fibres in confocal images.

I would also like to thank Ms Rachel George for carrying out mass spectrometry of neutrophil supernatant.

My gratitude also goes to Dr Samantha Heal and Dr Lewis Hardy for helping me with turbidity experiments, and providing useful suggestions on my research.

Samantha trained me in turbidity and chromogenic activity assay. Lewis suggested using deficient plasmas when the inhibitors did not work.

I would like to acknowledge Dr Matthew Hindle, Dr Clare Wilson who have helped me with flow cytometry experiments. They also taught me how to analyse flow data.

I would like to express special gratitude to Dr Ruigang Xu, Dr Ya Xu and Dr Lih Cheah who took care of me like a big brother and sister during my PhD time. I really appreciate their help, advice and support in both research and my daily life.

I would like to thank Miss Helen McPherson and Dr Cedric Duval for helping me with ordering all lab materials and reagents during my PhD. I would like to thank all the members in the LIGHT Laboratories, especially, Dr Emma Hethershaw, Dr Jian Shi, Prof Khalid Naseem, Ms Ping Jin, Ms Kay White, Mr Alan Burnett, Ms Julie Mawson, Dr Jianping Lu, Ms Yilizila Abudushalamu, Miss Hang Wu, Dr Xiaoxi Pan, Miss Yu Sun, Miss Cheuk Yau Luk and Ms Ghadir Alkarithi, for their support and friendship. I apologise if you haven't made the list above, but you have all contributed to making the last three years a success.

I would like to offer my heartfelt thanks to all the phlebotomists and donors. I also thank British Heart Foundation and Wellcome Investigator Award for

funding the lab. Finally, I deeply extend my loads of thanks and my heartiest gratitude to my parents for their love, support and encouragement.

Abstract

Neutrophils and NETs have recently been associated with crosstalk between inflammation and thrombosis. Besides playing a role in innate immunity, neutrophils are involved in thrombosis by releasing procoagulant and anticoagulant mediators. Neutrophil Extracellular Traps (NETs), which are extruded from neutrophils on activation by inflammatory stimuli, have been shown to provide a “scaffold” for thrombosis and to increase the resistance of clots to fibrinolysis. However, the exact cellular and biochemical mechanisms behind some of these reactions are not yet fully understood.

This thesis describes the use of human neutrophils and a neutrophil-like cell model (PLB-985 cell line) to investigate the role of neutrophils/NETs in blood coagulation, fibrin formation, clot stability and clot porosity. Specifically, the experiments were aimed at investigating the effects of neutrophils on fibrinopeptide A and B release and comparing the effects of neutrophil-like cells, human neutrophils and their NETs on the structure of fibrin fibres amongst other investigations, in order to decipher how neutrophils/NETs interact with the fibrin network.

Results using coagulation factor-specific deficient plasmas showed that NETs promoted clotting independently of FXII, FXI and FVII, and contributed to the formation of a denser clot architecture that is more resistant to lysis. Neutrophils induced blood clotting in a different manner than NETs, more

specifically mediated by FXI. Both neutrophils and NETs also delayed clot lysis in plasma. Neutrophil-like cells, PLB-985 NETs and human NETs induced the formation of a fibrin fibre network structure, and significantly increased the diameter of fibrin fibres. Human neutrophils increased the release of fibrinopeptide B in plasma, but human neutrophil-induced clots lack a substantial fibrin scaffold and form only short and thin fibrin fibres. This study shows a distinctive role for neutrophils and NETs in coagulation and contributes to a better understanding of their mechanisms.

Contents

List of Figures	xiii
List of Tables	xvi
Chapter 1 Introduction	1
1.1 Coagulation	2
1.1.1 Triggers of Coagulation	3
1.1.2 Consolidation Phase	6
1.1.3 Formation of The Clot.....	7
1.1.4 Prevention Mechanisms.....	7
1.2 Fibrin(ogen)	8
1.2.1 Fibrinogen Structure	8
1.2.2 Fibrin Formation.....	9
1.2.3 Cross-Linking by FXIII	10
1.3 Fibrinolysis	11
1.4 Thrombosis.....	13
1.5 Clot Structure	14
1.6 Neutrophils	16
1.7 NETs Formation	18
1.8 Role of NETs in Coagulation	20
1.9 Platelets.....	21
1.9.1 Role of Platelets in Haemostasis	21
1.9.2 Interactions between Platelets and Neutrophils (or NETs).....	23
1.10 Thromboinflammation.....	24
1.11 Hypothesis.....	26
1.12 Aims.....	27
Chapter 2 Methods and Materials.....	29
2.1 Human Blood Samples Preparation	30
2.1.1 Neutrophils Isolation	30
2.1.2 Neutrophil Supernatant Collection	32
2.1.3 Platelet-rich Samples Collection	32
2.1.4 Normal Pooled Plasma	33
2.2 PLB-985 Cell Culture and Differentiation	33
2.3 Coverslips and Slides Surface Coating	34
2.4 NETs Generation.....	34
2.4.1 For Microscopy Experiments.....	34

2.4.2 For Turbidity Measurements	35
2.5 Flow Cytometry	35
2.5.1 Antibodies	37
2.5.2 Human Neutrophil or PLB-985 Cell Sample Preparation	37
2.5.3 Platelet-rich Sample Preparation	37
2.5.4 Gating and Compensation	38
2.6 Morphological Staining	39
2.7 Immunofluorescence	40
2.8 Fluorescent Labeling	41
2.9 Turbidity Measurements	42
2.9.1 In a Fibrinogen System	42
2.9.2 In a Plasma System	43
2.10 Chromogenic Activity Assay	43
2.11 Mass Spectrometry	44
2.12 Atomic Force Microscopy (AFM)	45
2.13 Scanning Electron Microscope (SEM)	46
2.14 Clot Supernatant Collection	48
2.15 Clot Permeation	48
2.16 Enzyme-Linked Immunosorbent Assay (ELISA)	50
2.17 Data Analysis	52
Chapter 3 Establishing a Neutrophil-Like Model Using PLB-985 Cells and NETs Generation	54
3.1 Introduction	55
3.2 Objectives	57
3.3 Methods	58
3.3.1 Human Neutrophil Isolation and PLB-985 Cell Model Establishment	58
3.3.2 Purity of Isolated Neutrophils and the Availability of Neutrophil-like Cell Model	58
3.3.3 NETs Generation and Visualization	58
3.3.4 Data Analysis	59
3.4 Results	59
3.4.1 Morphology of Human Neutrophils and Differentiated PLB-985 Cells	59
3.4.2 Qualitative Identification of Isolated Cells	65
3.4.3 Quantification of platelets in isolated Human Neutrophils	66
3.4.4 Expression of Neutrophil Surface Antigens on Differentiated PLB-985 Cells	69
3.4.5 Generation and Visualization of NETs	72
3.5 Discussion	75
Chapter 4 Effects of Neutrophils and NETs on Coagulation	78

4.1 Introduction	79
4.2 Objectives	80
4.3 Methods	80
4.3.1 Role of Neutrophils and NETs in Clot Formation and Dissolution	80
4.3.2 Data Analysis	80
4.4 Results	81
4.4.1 Effects of Neutrophils and NETs on Clot Formation with Purified Fibrinogen	81
4.4.2 Effects of Neutrophils and NETs on Clot Formation in Plasma	84
4.4.3 Effects of Neutrophils and NETs on Clot Dissolution in Plasma	92
4.5 Discussion	94
Chapter 5 Role of Neutrophils and NETs in Overall Structure of Clots ..	97
5.1 Introduction	98
5.2 Objectives	99
5.3 Methods	99
5.3.1 Visualization of inner Structure of Clots	99
5.3.2 Permeability of Clots	100
5.3.3 Data Analysis	100
5.4 Results	101
5.4.1 Effects of Neutrophil-like Cells and Human Neutrophils on Clot Structure ..	101
5.4.2 Effects of PLB-985 NETs and Human NETs on Clot Structure	106
5.4.3 AFM Scanning of Neutrophil-like Cell Model	113
5.4.4 Effects of Human Neutrophils and NETs on Clot Permeability	119
5.5 Discussion	120
Chapter 6 Potential Mechanisms of Neutrophil- and NET-Induced Clotting	125
6.1 Introduction	126
6.2 Objectives	127
6.3 Methods	127
6.3.1 Inhibition of FXII and TF in Plasma	127
6.3.2 Detection of Procoagulant Mediators Released from Neutrophils	128
6.3.4 Quantitative Detection of FpA and FpB Release in Neutrophil-induced Clots by ELISA	128
6.3.5 Data Analysis	129
6.4 Results	129
6.4.1 Coagulation Pathway Mechanisms Involved in Neutrophil- and NETs-induced Clotting	129
6.4.2 Release of FpA and FpB during Neutrophil-induced Clotting	134
6.4.3 Mediators that may Contribute to Neutrophil-induced Clotting	135
6.5 Discussion	138
Chapter 7 General Discussion	142

7.1 General discussion	143
7.1.1 NETs and Mediators Released by Neutrophils Induced Coagulation in Plasma	143
7.1.2 Neutrophil and NETs Altered Clot Structure in a Different Manner	145
7.1.3 Neutrophil and NETs Initiated Different Coagulation Pathways	147
7.1.4 Comparison of Neutrophil and Neutrophil-like Cells	149
7.2 Conclusion	151
7.3 Future Studies	152
References	154
Appendices	172

List of Figures

Figure 1-1 Coagulation pathways.	5
Figure 1-2 Fibrinogen and the formation of fibrin.	9
Figure 1-3 Fibrinolysis pathway.....	13
Figure 1-4 Role of neutrophil released mediators in the coagulation pathways.	17
Figure 1-5 NETosis process.....	20
Figure 1-6 Interactions between platelets and neutrophils.....	24
Figure 2-1 Neutrophil isolation from human blood.....	32
Figure 2-2 Basic principles of flow cytometry	36
Figure 2-3 An example of gating	39
Figure 2-4 An example of parameters measured on turbidity and lysis curve.	43
Figure 2-5 Schematic of atomic force microscopy (AFM)	45
Figure 2-6 Graphical representation of SEM sample preparation.....	47
Figure 2-7 Schematic of permeation measurements.	50
Figure 2-8 Schematic of the sandwich ELISA method.....	51
Figure 3-1 Morphological photographs of 5 WBC subtypes.....	57
Figure 3-2 Wright's stain images of isolated human neutrophils.	61
Figure 3-3 Wright's stain images of DMSO-differentiated PLB-985 cells.	63
Figure 3-4 Physical characteristics of isolated human neutrophils, platelets and differentiated PLB-985 cells were reflected by FSC and SSC properties.....	65
Figure 3-5 Identification and quantification of neutrophils isolated from human blood by CD16 and CD66b.	66
Figure 3-6 Effectiveness of CD41 in detecting platelets.	67

Figure 3-7 Effectiveness of CD42b in detecting platelets.	67
Figure 3-8 Quantification of platelets in isolated neutrophils by CD41.	68
Figure 3-9 Quantification of platelets in isolated neutrophils by CD42b.	69
Figure 3-10 Expression level of human neutrophil-surface antigens (CD66b and CD16) on differentiated PLB-985 cells.....	70
Figure 3-11 Expression level of human neutrophil-surface antigen CD11b on differentiated PLB-985 cells.	71
Figure 3-12 Expression level of human neutrophil-surface antigen CD11b on differentiated PLB-985 cells.	72
Figure 3-13 Immunofluorescence images of NETs.	73
Figure 3-14 Immunofluorescence staining controls.....	74
Figure 4-1 Comparison of clot formation in a purified fibrinogen system in the presence of PLB NETs and cells versus human NETs and neutrophils.....	83
Figure 4-2 Comparison of clot formation in plasma in the presence of PLB NETs and cells versus human NETs and neutrophils..	86
Figure 4-3 Effects of PMA on clot formation in purified fibrinogen and plasma.	88
Figure 4-4 Effects of human serum albumin (HSA) on clot formation in purified fibrinogen.	89
Figure 4-5 Effects of human neutrophil supernatant on clot formation in plasma.	90
Figure 4-6 Effects of RBC lysis buffer on the procoagulant effects of human neutrophils in plasma.....	91
Figure 4-7 Effect of human neutrophils or human NETs on clot dissolution in plasma.....	93
Figure 5-1 Confocal Z-stacks images of differentiated PLB-985 cell-induced and human neutrophil-induced plasma clots.	102
Figure 5-2 SEM images of normal PLB-985 cells, differentiated PLB-985 cell and human neutrophil.....	104

Figure 5-3 SEM images of differentiated PLB-985 cell-induced and human neutrophil-induced plasma clots.....	105
Figure 5-4 Confocal Z-stacks images of PLB-985 NET-induced and human NET-induced plasma clots.	107
Figure 5-5 SEM images of PLB-985 NETs and human NETs.	109
Figure 5-6 SEM images of PLB-985 NET-induced plasma clots.	110
Figure 5-7 SEM images of human NET-induced plasma clots.	111
Figure 5-8 Effects of human neutrophils, human NETs, differentiated PLB-985 cells and PLB-985 NETs on the fibrin fibre thickness in plasma.....	112
Figure 5-9 Effects of human neutrophils, human NETs, differentiated PLB-985 cells and PLB-985 NETs on the density (fibrin fibre counts) of plasma clots.	113
Figure 5-10 AFM analyses of air-dried differentiated PLB-985 cells.	115
Figure 5-11 AFM analyses of air-dried PLB-985 NETs.....	116
Figure 5-12 AFM analyses of the single fibres of air-dried PLB-985 NETs..	117
Figure 5-13 AFM analyses of differentiated PLB-985 cells in PBS buffer. ...	118
Figure 5-14 Effects of human neutrophils and human NETs on the permeability of plasma clots.....	119
Figure 6-1 Role of TF inhibitor (TF antibody) and FXII Inhibitor (CTI) in the procoagulant effects of human neutrophils and NETs in plasma.....	130
Figure 6-2 Effects of FXII-, FXI- and FVII-deficient plasmas on the procoagulant effects of human neutrophils, NETs and neutrophil supernatant.	132
Figure 6-3 Self-coagulation of plasmas before and after centrifugation and filtration.....	134
Figure 6-4 Release of FPA and FPB in neutrophil-induced clots.....	135

List of Tables

Table 6-1 Mass spectrometry data showing the composition of human neutrophil supernatant.....	137
Table 7-1 A summary of effects of human neutrophils, human NETs, differentiated PLB-985 cells and PLB-985 NETs on coagulation.....	145

Abbreviations

AFM - Atomic force microscopy

APC – Activated protein C

BSA - Bovine serum albumin

Ca²⁺ - Calcium ions

CaCl₂ - Calcium chloride

cDNA - Complementary DNA

CF-DNA - Cell-free DNA

citH3 – Citrullinated histone H3

CTI – Corn trypsin inhibitor

CO₂ - Carbon dioxide

DAPI – 4',6-Diamidino-2-Phenylindole, Dihydrochloride

ddH₂O – Double-distilled water

DIC – Disseminated intravascular coagulation

DNA - Deoxyribose nucleic acid

dsDNA – Double-stranded DNA

DMSO - Dimethyl Sulfoxide

DVT - Deep vein thrombosis

EDTA - Ethylenediaminetetraacetic acid

ELISA - Enzyme linked immunosorbent assay

FBS – Fetal bovine serum

FDPs - Fibrin degradation products

FIX - Factor IX

FIXa - Activated factor IX

Fluor - Fluorescence

FpA - Fibrinopeptide A

FpB - Fibrinopeptide B

FSC – Forward scatter channel

FV - Factor V

FVa - Activated factor V

FVII - Factor VII

FVIIa - Activated factor VII

FVIII - Factor VIII

FVIIIa - Activated factor VIII

FX - Factor X

FXa - Activated factor X

FXI - Factor XI

FXIa - Activated factor XI

FXII - Factor XII

FXIIa – Activated factor XII

FXIII - Factor XIII

FXIIIa - Activated factor XIII

g - Gram

Gla - Gamma-carboxyglutamic acid

GP – Glycoprotein

h - Hour

HBSS - Hanks' Balanced Salt solution

HBS - HEPES-buffered saline

HRP - Horseradish peroxidase

HSA - Human serum albumin

H₂O₂ – Hydrogen peroxide

Ks - Permeability coefficient (Darcy constant)

Kg - Kilogram

M – Molar

MaxOD - Maximum optical density

mg - Milligram

Mg²⁺ - Magnesium ions

min - Minute

ml - Millilitre

mm - Millimetre

mM - Millimolar

MMP - Matrix metalloproteinases

MPO - Myeloperoxidase

NADPH - Nicotinamide adenine dinucleotide phosphate

N/A - Not analyzable

N/D - Not detectable

NaCl - Sodium chloride

NETs - Neutrophil extracellular traps

ng - Nanogram

NPP - Normal pooled plasma

OD - Optical density

PAI-1 - Plasminogen activator inhibitor 1

PAR – Protease activated receptor

PBS - Phosphate buffered saline

PBST – PBS with 0.1% v/v Tween 20

PEG – Polyethylene glycol

PFA – Paraformaldehyde

PK - Prekallikrein

PMA - Phorbol 12-myristate 13-acetate

PS - Phosphatidylserine

PSGL-1 – P-selectin glycoprotein ligand 1

RBC - Red blood cell

ROS - Reactive oxygen species

SABC - HRP-streptavidin conjugate

SD - Standard deviation

SEM - Scanning electron microscopy

SSC – Side scatter channel

TAFI – Thrombin activated fibrinolysis inhibitor

TEM – Transmission electron microscopy

TF - Tissue factor

TFPI - Tissue factor pathway inhibitor

TMB - 3,3',5,5'-tetramethylbenzidine

tPA - Tissue plasminogen activator

uPA - Urokinase plasminogen activator

V_{max} - Maximum rate

vWF - Von Willebrand factor

WBCs – White blood cells

μg - Microgram

μl - Microliter

μM - Micrometre

μN - Micronewton

°C - Degrees centigrade

Chapter 1 Introduction

1.1 Coagulation

Coagulation (clotting) is the process by which blood forms a clot from fluid. This physiologically occurs after an injury to the blood vessel, resulting in haemostasis, a multistep process that helps to stop bleeding (Palta et al., 2014). Four main steps of haemostasis are: vasoconstriction, formation of platelet plugs, activation of the coagulation pathways and formation of fibrin plugs (LaPelusa and Dave, 2021). Immediately after an injury, the walls of the vessel vasoconstrict to slow blood flow to the site of damage and minimize blood loss (Furie and Furie, 2008). Circulating platelets are activated and aggregate to form a platelet plug at the injured site. This process is induced by collagen exposed from the injured vessel's endothelium (Periyah et al., 2017). In the meantime, the coagulation cascade is activated, leading to the formation of an insoluble fibrin clot that interacts with the initial platelet plug (Mussbacher et al., 2019). Then, normal tissue at the site of the injury recovers, the blood clot slowly dissolves, and eventually the damage heals (LaPelusa and Dave, 2021). The coagulation process is regulated by a dynamic balance between pro-coagulant and anti-coagulant mechanisms, involving both cellular and plasmatic protein components (e.g., platelets, coagulation factors, antithrombin, etc.) (Palta et al., 2014). Thrombosis or bleeding may occur if this balance is disturbed (Colman, 2006).

1.1.1 Triggers of Coagulation

The coagulation cascade is traditionally separated into extrinsic and intrinsic pathways, which converge at the level of a common pathway when activating factor X (FX). Current understanding of the coagulation pathways is that there is only one pathway but initiated by different triggers, tissue factor (TF) or contact activation (Figure 1-1) (Palta et al., 2014). TF, a 263/261 amino acid transmembrane glycoprotein (~33 kDa), is expressed by sub-endothelial cells (e.g. smooth muscle cells, fibroblasts), and thus exposed to the circulating blood when the vessel wall is damaged (Butenas, 2012). TF binds the serine protease precursor factor VII (FVII) which is activated into FVIIa (Owens and Mackman, 2010). The TF-FVIIa complex provides a link between classical extrinsic and intrinsic pathways by activating both factor IX (FIX, a highly post-translationally modified glycoprotein) and factor X (FX, a liver-synthesized vitamin K-dependent glycoprotein, ~59 kDa) (Venkateswarlu et al., 2002; Palta et al., 2014; Zacchi et al., 2021). Activated FX (FXa) binds to its cofactor FVa (activated factor V) to form FXa-FVa complex (the prothrombinase complex) on cell surfaces (e.g., platelets, monocytes) (Tracy et al., 1983; Monroe et al., 1996; Lam and Moosavi, 2019). The coagulation reaction needs to be kept in careful balance and thus FXa is kept in check and is inhibited by the TF pathway inhibitor (TFPI) or antithrombin when it spreads from the surfaces on which it was activated (Monroe et al., 2002). The prothrombinase complex subsequently cleaves prothrombin (factor II, a glycoprotein, ~72 kDa) into small amounts of thrombin (factor IIa, an allosteric serine protease, ~36 kDa) (Licari

and Kovacic, 2009; Whelihan et al., 2012). This small amount of thrombin plays an important role in initiating the consolidation phase of coagulation (section 1.1.2).

In a slower reaction (Figure 1-1), the contact activation pathway is initiated by the autoactivation of factor XII (FXII, a glycoprotein, ~80 kDa), when blood contacts negatively charged surfaces (e.g., platelet polyphosphates and extracellular DNA) (G and S, 2017). Activated FXII (FXIIa) goes on to activate factor XI (FXI, a homolog of prekallikrein (PK), ~80 kDa) into FXIa. FXIa subsequently activates FIX into FIXa (Mohammed et al., 2018). Factor VIII (FVIII, ~ 300 kDa), also known as antihemophilic factor, is proteolytically activated (to form FVIIIa) by thrombin or FXa (Fay, 2004). FIXa and FVIIIa generate the FIXa-FVIIIa or tenase complex which activates FX (Mazurkiewicz-Pisarek et al., 2016).

Tissue Factor (Extrinsic) Pathway

Contact Activation (Intrinsic) Pathway

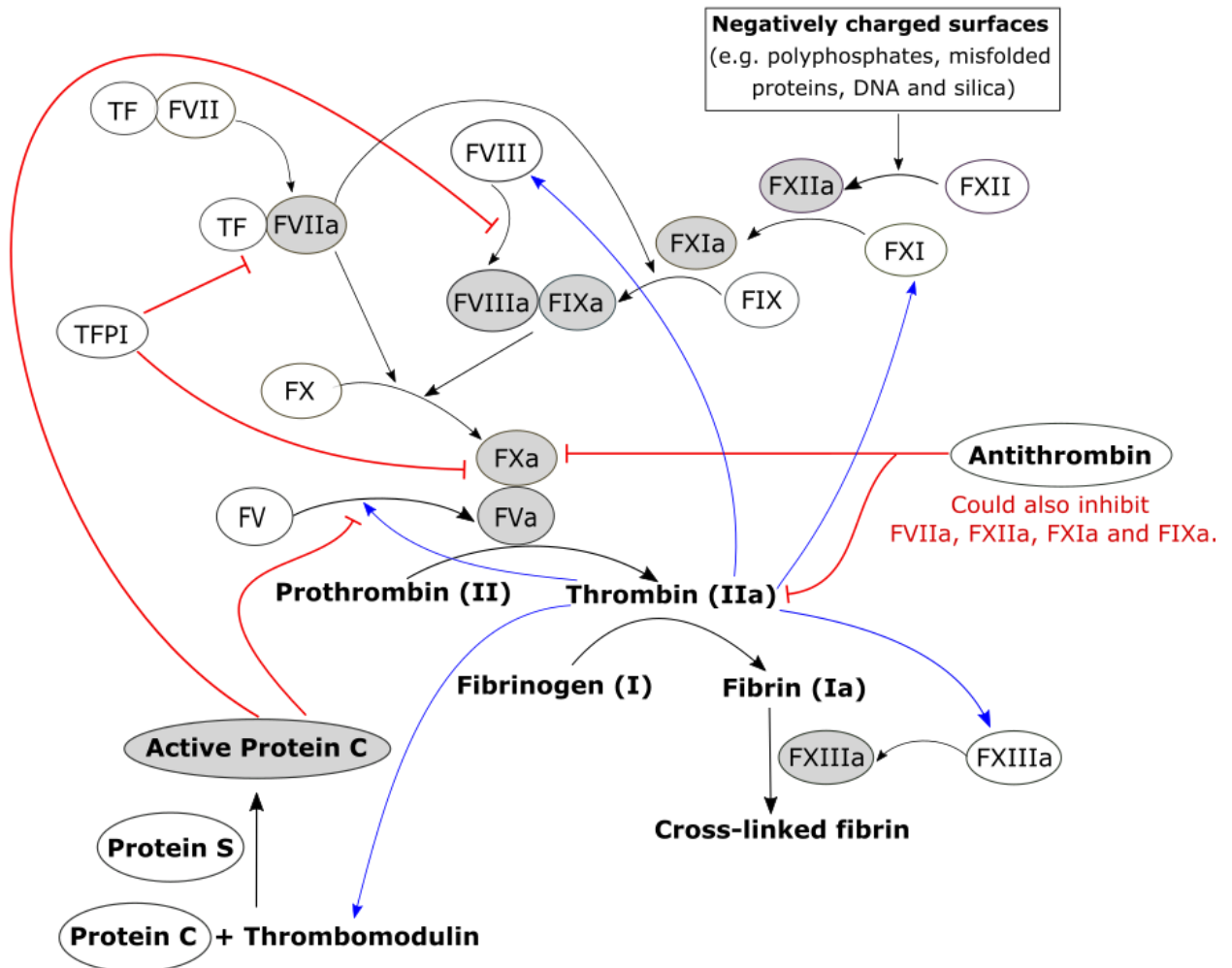


Figure 1-1. Coagulation pathways. Black and blue arrows denote stimulation and activation, red blunt arrows denote inhibition. The coagulation cascade involves the tissue factor (extrinsic) and contact activation (intrinsic) pathways, both of which converge on a common pathway. The contact activation pathway is initiated when FXII is activated by negatively charged surfaces. The tissue factor (TF) pathway is initiated when TF binds to FVII, resulting in thrombin formation. Thrombin can positively feedback (blue arrows) to activate FV, FVIII, FXI and FXIII, and negatively feedback to protein C which inactivate FV and FVIII. Tissue factor pathway inhibitor (TFPI) inhibits TF–FVIIa complexes and early forms of prothrombinase (FXa-FVa complex) (Kato, 2002; Mast, 2016). Antithrombin mainly inhibits FXa and thrombin, but also inhibits FVIIa, FXIIa, FXIa and FIXa (Rezaie and Giri, 2020).

1.1.2 Consolidation Phase

There are several positive feedback mechanisms that are triggered by the initially small amount of thrombin generated, which allow for the generation of a more substantial thrombin burst that is required for the conversion of fibrinogen into fibrin (Figure 1-1). The small amount of initial thrombin (described above) binds to platelets which have aggregated at the site of injury. Thrombin cooperates with collagen to activate platelets, resulting in the release of partially activated factor V (FV, 330 kDa glycoprotein) from platelet granules (Viskup et al., 1987; Monroe et al., 2002). Partially activated FV and FXI are fully activated into FVa and FXIa by thrombin on the platelet surface (Monroe et al., 2002). FVIII is also activated and released from von Willebrand factor (vWF) by thrombin (Pieters et al., 1989). The above reactions are enhanced by gamma-carboxyglutamic acid (Gla) domains in thrombin, FIXa and FXa, which bind the exposed phosphatidylserine on the activated platelet membrane via positively charged calcium ions that bridge these two negatively charged structures (Monroe et al., 1994). The FIXa-FVIIIa complex accumulated on the platelet surface activates FX, leading to the formation of many more FXa-FVa complexes (Scandura and Walsh, 1996). A large amount of thrombin is generated by the exponentially increasing FXa-FVa complexes on the platelet surface (Walsh, 2004).

1.1.3 Formation of The Clot

The large amounts of thrombin generated through the consolidation phase of coagulation convert fibrinogen to fibrin and also activate factor XIII (FXIII, a transglutaminase, ~320 kDa) into FXIIIa (Malkhassian and Sharma, 2019; LaPelusa and Dave, 2021). Upon the consolidation of the platelet plug, fibrin monomers are cross-linked to a stable fibrin meshwork by FXIIIa (discussed in section 1.2.3) (Bombeli and Spahn, 2004).

1.1.4 Prevention Mechanisms

Thrombin also generates negative feedback to prevent excessive coagulation (Figure 1-1). Thrombomodulin is a transmembrane glycoprotein expressed by endothelial cells (Watanabe-Kusunoki et al., 2020). Thrombomodulin reversibly binds to thrombin and modulates its procoagulant effects (Ito et al., 2019).

Once thrombin complexes with thrombomodulin, it cleaves and activates protein C (Nesheim, 2003). Activated protein C (APC) goes on to proteolytically degrade FVa and FVIIIa on negatively charged phospholipid membranes, resulting in an inhibition of thrombin generation (Dahlbäck and Villoutreix, 2005). Protein S acts as a cofactor to APC in this reaction, and it also directly inhibits the activity of prothrombinase complex (FVa + FXa) (Koshiar et al., 2014).

Tissue factor pathway inhibitor (TFPI) and antithrombin also play an important role in regulating coagulation. TFPI is a protease inhibitor that contains three Kunitz domains (Kato, 1996). It binds FVIIa via the first Kunitz domain and binds

FXa via the second Kunitz domain, leading to an inhibition of the FXa-FVIIa complex (Kato, 2002). In the early stages of blood coagulation, TFPI also inhibits early forms of prothrombinase (FXa-FVa complex), which retain the acidic region of the FV B-domain. The basic region of TFPI binds to the acidic region of the FV B-domain, resulting in an inhibition of prothrombinase (Mast, 2016). Antithrombin, a serpin synthesized in the liver, has a potent anticoagulant activity (Rodgers, 2009). Antithrombin interacts with heparin via a basic D-helix, to inhibit FXa and thrombin and other procoagulant factors (e.g., FVIIa, FXIIa, FXIa and FIXa) (Rezaie and Giri, 2020).

1.2 Fibrin(ogen)

1.2.1 Fibrinogen Structure

Fibrinogen is a 340 kDa glycoprotein that is generated by the liver (Kattula et al., 2017). It circulates in healthy human blood at a relatively high concentration (2-4 mg/ml) (Wolberg, 2007). As shown in Figure 1-2, the fibrinogen molecule consists of two sets of A α -, B β -, and γ -polypeptide chains, which are held together in a large hexamer by 29 disulfide bridges (Undas and Ariëns, 2011). The structure of fibrinogen, which is 45 nm in length and about 2-5 nm in diameter, contains two outer regions (D-region) converged by coiled-coil segments in a central globular region (E-region) (Weisel and Litvinov, 2017). The E-region contains fibrinopeptide (Fp) A, FpB and the N-termini of all six chains. The D-region consists of the globular regions (C-termini) of the B β - and γ -chains. The C-termini of A α -chains are flexible and situated close to the

central E-region of fibrinogen (Mosesson, 2005; Wolberg, 2007). Cleavage of both FpA and FpB from E-region allows the C-termini of α -chains dissociate, leading to a lateral aggregation of protofibrils (Mosesson, 2005).

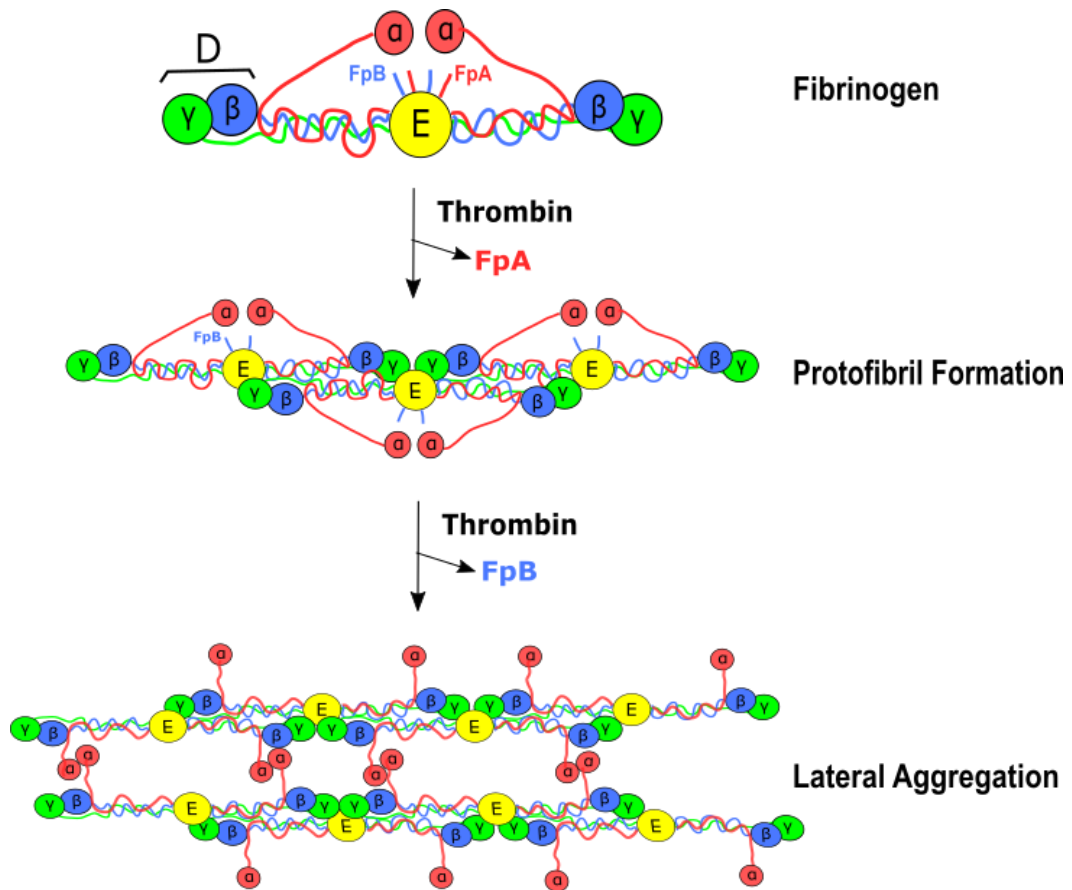


Figure 1-2. Fibrinogen and the formation of fibrin. Fibrinogen is comprised of two sets of α (red), β (blue), and γ (green) polypeptide chains. Fibrinopeptide (Fp) A and B are located in the E-region. The D-region is composed of the globular C-terminal domains of the β and γ chains. Fibrinogen is converted into protofibrils when the FpA is cleaved by thrombin. Protofibrils laterally aggregate into fibres when FpB is cleaved by thrombin (Undas and Ariëns, 2011).

1.2.2 Fibrin Formation

Conversion of soluble fibrinogen into insoluble fibrin is one of the major steps of the coagulation cascade (Kattula et al., 2017). As Figure 1-2 shows, FpA is first released from the N-termini of α -chains by thrombin, allowing exposure of two

binding sites in the E-region, which can then bind to constitutively exposed binding pockets in the γ -chain C-terminal of two other fibrin monomers. Thus, one fibrin monomer binds two other fibrin monomers which are converted into half-staggered protofibrils (Wolberg, 2007). FpB is released subsequently from the N-termini of B β -chains by thrombin, as it is cleaved at a slower rate than FpA. The cleavage of FpB allows two more binding sites to be exposed and releases the α -chain C-termini from protofibrils. Thus, the E-region can bind to the β -chain C-terminal of other fibrin monomers, and the α -chain C-termini of protofibrils can interact with each other, acting as Velcro between two protofibril strands (Figure 1-2). These reactions permit the laterally aggregation of protofibrils into fibres (Weisel and Litvinov, 2017).

1.2.3 Cross-Linking by FXIII

FXIII, which was previously also called fibrin stabilizing factor, plays an important role in the cross-linking of fibrin, which stabilizes the initial platelet plug at the injure site (Schwartz et al., 1973). FXIII is composed of two ~83 kD catalytic A subunits and two ~80 kD inhibitory B subunits (Muszbek et al., 2011). The B subunit binds and carries the A subunit to form an A₂B₂ tetramer in the circulating plasma. About half of the B subunits are engaged in generating the tetrameric complex with the A subunit, while the other half circulates free (Ariëns et al., 2002; Muszbek et al., 2011). In addition to the blood plasma, the FXIII A subunit (a pro-transglutaminase) is also present in platelets, and in the cytoplasm of monocytes and macrophages (Schwartz et al.,

1973; Muszbek et al., 2011). As mentioned in section 1.1.3, when thrombin generation reaches its maximum capacity, thrombin rapidly activates Factor XIII in the presence of Ca^{2+} and fibrin (Bombeli and Spahn, 2004). Val34Leu, a FXIII A-subunit genetic polymorphism, leads to faster activation of FXIII by thrombin, and eventually alters the clot structure to a denser architecture with thinner fibrin fibres (Ariens et al., 2000). Activated FXIII binds to the fibrin substrate unmasking its active site cysteine residues on each A subunit, which are exposed by the dissociation of B subunits from FXIII (Ariens et al., 2002). Cross-linking by FXIII occurs fastest (within 5-10 minutes) within the fibrin γ -chains while that of the fibrin α -chains occurs much slower, and is not complete until approximately 2 hours after clot formation. Cross-linking of the fibrin γ -chains by FXIIIa increases clot density while that of the α -chains enhances clot stiffness (Duval et al., 2014)

1.3 Fibrinolysis

Fibrinolysis is an important protective process that aims to limit the size of clot and prevent clogging of blood vessels, to remove thrombi after the wound heals (Chandler, 2013; Chapin and Hajjar, 2015). As shown in Figure 1-3, the fibrinolysis process is initiated by tissue plasminogen activator (tPA) or urokinase plasminogen activator (uPA). TPA is a ~70 kDa serine protease and released from endothelial cells and could be stimulated by thrombin, tissue occlusion, adrenaline, etc. (Flemmig and Melzig, 2012; Palta et al., 2014; Chapin and Hajjar, 2015). UPA is a ~54 kD serine protease and released from

urothelial cells, monocytes and macrophages (Flemmig and Melzig, 2012; Chapin and Hajjar, 2015). Both tPA and uPA can convert plasminogen into plasmin, the proteolytic enzyme that degrades the fibrin clot into fibrin degradation products (FDPs) (Palta et al., 2014). A difference between tPA and uPA is that tPA activates plasminogen by bind to fibrin, while uPA could not directly bind to fibrin and can activate plasminogen in solution (Longstaff and Kolev, 2015; Whyte and Mutch, 2021). To avoid excessive fibrinolysis, plasmin activity is limited by plasminogen activator inhibitor 1 (PAI-1), alpha-2 plasmin inhibitor (α -2 antiplasmin) and thrombin activated fibrinolysis inhibitor (TAFI) (Palta et al., 2014). PAI-1 can irreversibly inhibit tPA and uPA. Alpha-2 plasmin inhibitor, a serpin synthesized from liver, directly inhibits the active site of plasmin (Eddy et al., 2015). TAFI (60 kDa carboxypeptidase) is activated by thrombin, when thrombin is converted to an antifibrinolytic form by the complex with thrombomodulin (Nesheim, 2003; Sillen and Declerck, 2021). Activated TAFI reduces the binding of plasminogen to fibrin by removing the lysine and arginine residues from partially degraded fibrin, resulting in the reduction of plasminogen binding sites which are required for efficient plasmin generation by tPA (Chapin and Hajjar, 2015).

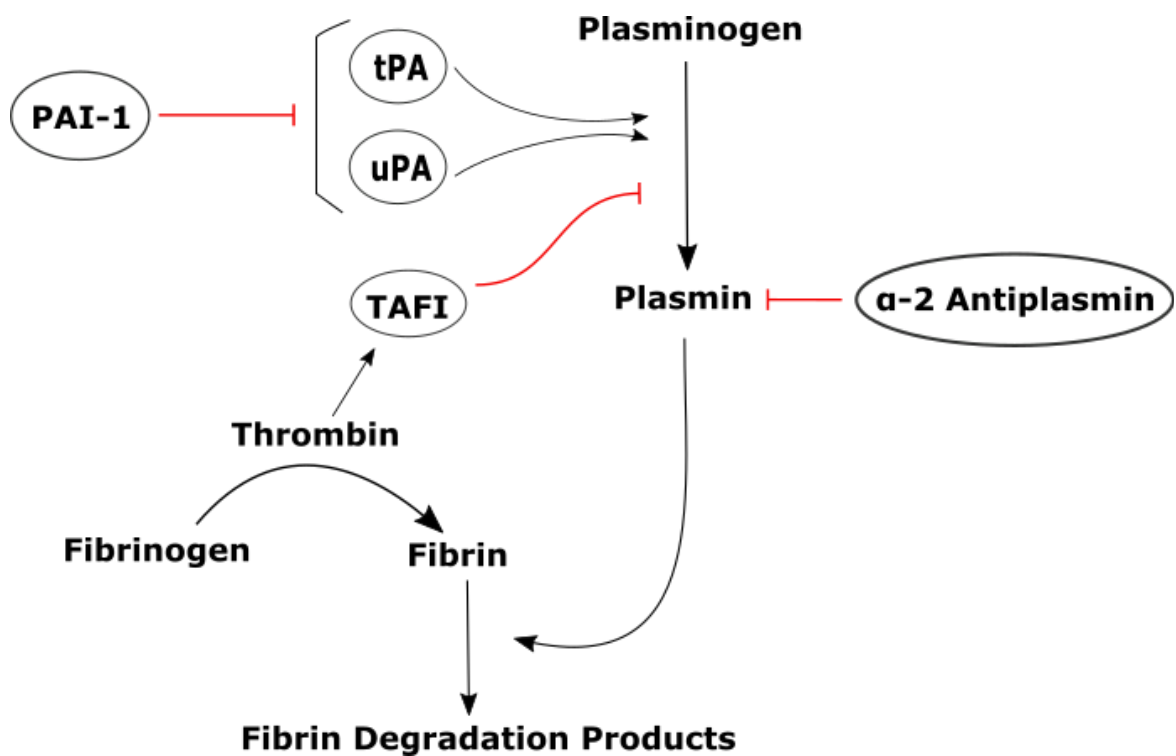


Figure 1-3. Fibrinolysis pathway. Black arrows denote stimulation and activation, red blunt arrows denote inhibition. Fibrinolysis is initiated by tissue plasminogen activator (tPA) or urokinase plasminogen activator (uPA). Plasminogen is activated by tPA or uPA into plasmin. Plasmin degrades the fibrin clot into fibrin degradation products. Plasmin activity and generation is limited by plasminogen activator inhibitor 1 (PAI-1), alpha-2 plasmin inhibitor (α -2 antiplasmin) and thrombin activated fibrinolysis inhibitor (TAFI). (Meltzer et al., 2009)

1.4 Thrombosis

Thrombosis is one of the leading causes of death globally (Raskob et al., 2014).

Moreover, in the recent SARS-CoV-2 pandemic, thrombosis has been shown to contribute to mortality of patients with coronavirus disease 2019 (Covid-19).

(Kashi et al., 2020; Kerbikov et al., 2021). The pathways that regulate normal coagulation and thrombosis do not appear to be exactly the same, as previous studies have shown that FXII is critical for thrombosis, but inhibition of FXII does not increase bleeding (Renné et al., 2005; Kleinschnitz et al., 2006).

Thrombosis is classified into two main types: venous thrombosis and arterial thrombosis. Venous thrombosis is commonly found as pulmonary embolism and deep vein thrombosis (DVT) (Næss et al., 2007). Genetic risk factors of venous thrombosis include deficiencies of the anticoagulants (e.g., antithrombin, protein C, protein S), and the factor V Leiden and prothrombin 20210A mutations (Zöller et al., 2020). Most commonly acquired risk factors of venous thrombosis include advanced age, obesity, history of venous thromboembolism, cancer, immobility, pregnancy and major surgery (Goldhaber, 2010; Previtali et al., 2011). Arterial thrombosis usually occurs as ischaemic stroke, acute myocardial infarction and peripheral artery disease (Lippi and Favalaro, 2018). The risk factors for arterial thrombosis include advanced age, smoking, diabetes, poor diet, high blood pressure, lack of activity and obesity (Previtali et al., 2011). Unlike venous thrombosis, the genetic risk factors associated with coagulation factors have limited effects on arterial thrombosis (Voetsch and Loscalzo, 2004). The risk factors for arterial thrombosis are usually acquired risk factors, which are largely different from the risk factors for venous thrombosis, and which involve risk factors that drive atherosclerosis, the main triggering mechanism for an arterial thrombus.

1.5 Clot Structure

Previous studies have shown that clot structure plays a possible role in assessing the risk of cardiovascular disease (Wolberg, 2007; Undas and Ariëns, 2011; Kattula et al., 2017). Clots that are denser, have smaller pores and are

more resistant to fibrinolysis are associated with an increased risk of cardiovascular disease (Ariëns, 2013; Bridge et al., 2014). For example, a recent study has shown that resistance to fibrinolysis predicts an increased risk of cardiovascular death and spontaneous myocardial infarction in acute coronary syndrome patients with diabetes (Sumaya et al., 2020). Various factors can influence the structure of clot, such as thrombin generation, FXIIIa concentration, inflammatory status, hyperglycemia, smoking and genetic variation (Undas and Ariëns, 2011; Ariëns, 2013). A recent study showed that clots in arterial, venous and pulmonary vessels all have different clot structures and components, suggesting the origin and destination of clots can alter their structure. For example, there are more fibrin bundles in arterial clots than in venous thrombi and pulmonary emboli, while there are more single fibrin fibers in pulmonary emboli (Chernysh et al., 2020). Additionally, the role of FXIIIa in fibrin cross-linking has been widely studied (Lorand, 2001; Duval et al., 2014; Duval et al., 2016). FXIIIa reduces the thickness of individual fibrin fibres and increases the density of clots, contributing to the increased resistance of clots to fibrinolysis (Hethershaw et al., 2014). However, other factors that influence clot structure still need to be further understood, which may bring new strategies for the treatment of cardiovascular disease.

1.6 Neutrophils

Neutrophils, which are generated from the myeloid cell lineage in the bone marrow, are the most abundant leukocyte in the blood. They act as the first line of defense in innate inflammatory responses, effectively catching and killing bacteria and pathogens (Rosales, 2018). The main antimicrobial function of neutrophils are phagocytosis, degranulation, generation of reactive oxygen species (ROS) and the formation of neutrophil extracellular traps (NETs) (Mayadas et al., 2014). Recently, neutrophils have been involved in the crosstalk between innate immunity and haemostasis. As shown in Figure 1-4, mediators released by neutrophils, such as matrix metalloproteinases (MMP), cell-free DNA (CF-DNA), histones, cathepsin G and elastase, can activate coagulation factors (e.g., FXII, FXI, FVIII, FX, FV, thrombin), inhibit anticoagulant factors (e.g., TFPI, antithrombin), and influence the fibrinolysis pathway (Swystun and Liaw, 2016; Alkarithi et al., 2021). But the role of neutrophils in coagulation is likely to be complex. For example, neutrophil elastase has been shown to inactivate TFPI and antithrombin (procoagulant effects), but it can also cleave fibrinogen (anticoagulant effects) (Jochum et al., 1981; Petersen et al., 1992; De Lau et al., 2008). Additionally, the expression of TF in neutrophils is still a matter of debate in the literature. Some studies indicate that neutrophils are able to express TF in human blood and in different types of animal models (Higure et al., 1996; Todoroki et al., 2000; Nakamura et al., 2004; Ritis et al., 2007; Maugeri and Manfredi, 2015). But other studies find that neutrophils may not express TF themselves, but instead may obtain TF

expressed by monocytes through cell-cell interactions (Østerud et al., 2000; Østerud, 2004; Sovershaev et al., 2008). Therefore, many questions remain about how neutrophils influence coagulation that need to be further investigated.

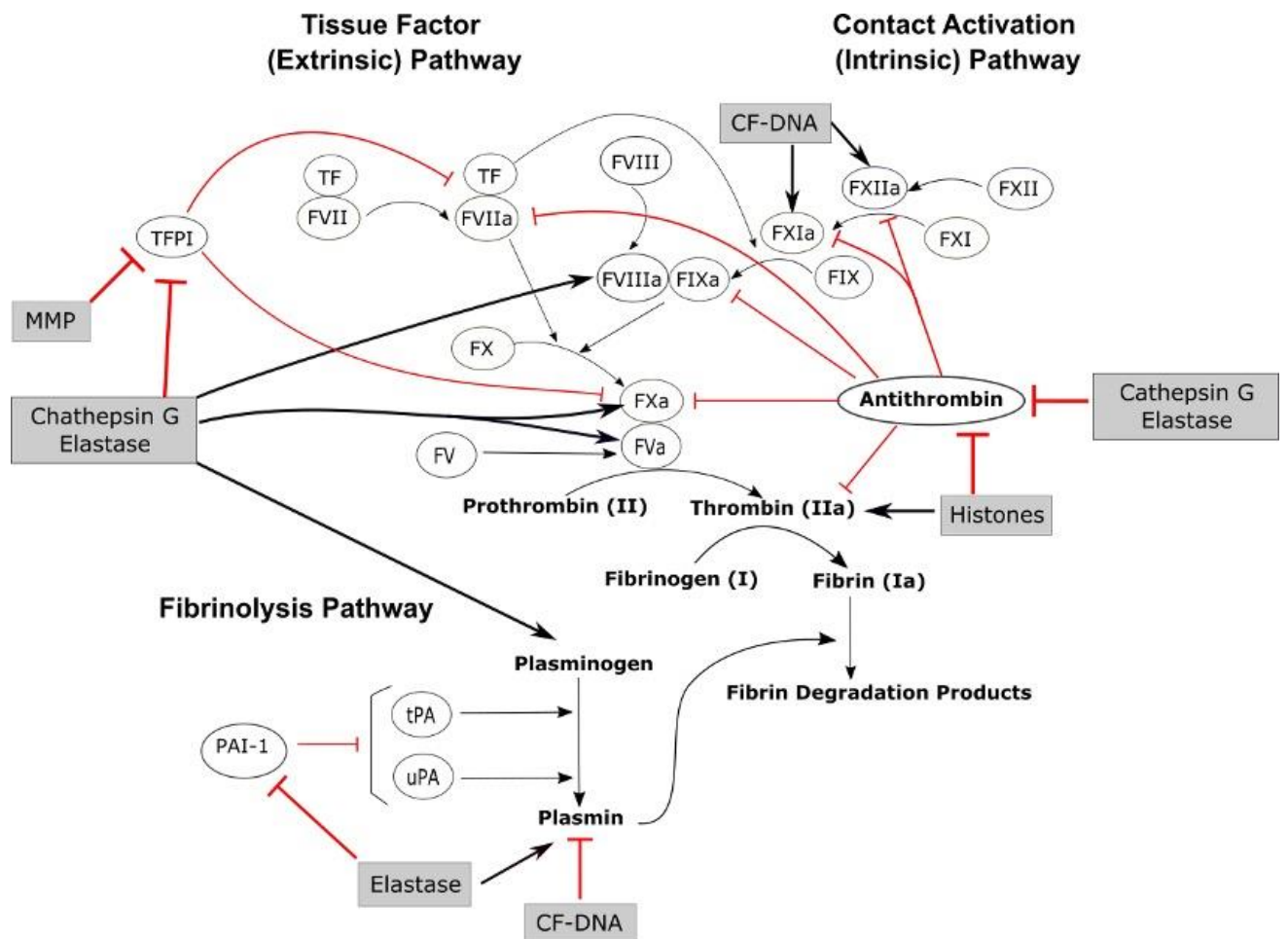


Figure 1-4. Role of neutrophil released mediators in the coagulation pathways. Black arrows denote stimulation and activation, red blunt arrows denote inhibition. Matrix metalloproteinases (MMP), cell-free DNA (CF-DNA), histones, cathepsin G, and elastase influence the coagulation pathways by directly activate procoagulant and fibrinolytic factors, and inhibit the activity of anticoagulants. TFPI: tissue factor pathway inhibitor, tPA: tissue plasminogen activator, uPA: urokinase plasminogen activator, PAI: plasminogen activator inhibitor. (Swystun and Liaw, 2016)

1.7 NETs Formation

As mentioned above, one of the functions of neutrophils is to form NETs. The process of NET formation, also called NETosis, occurs when neutrophils are activated and extrude a modified form of chromatin which is decorated with cytoplasmic, histones and granular proteins (Sollberger et al., 2018). During NETosis, histones are citrullinated to induce decondensation of chromatin, then chromatin is decorated with other components inside the neutrophil when the nuclear membrane disintegrates, followed by the rupture of cytoplasmic membrane, resulting in the release of NETs which normally appear in a fibrous network structure (Figure 1-5) (Von Köckritz-Blickwede and Nizet, 2009; Sollberger et al., 2018). NETosis occurs when neutrophils are exposed to microbial and inflammatory stimuli, such as bacteria, fungi and Phorbol 12-myristate 13-acetate (PMA) (Zawrotniak and Rapala-Kozik, 2013). Fuchs et al. demonstrated that NETosis is a type of active neutrophil death process, which easily occurs at $\leq 2\%$ fetal calf serum concentrations. NETosis includes unique morphological changes of the nucleus, such as disintegration of nuclear membrane. This is different from apoptosis and necrosis, where the nuclear membrane remains intact. They also found that the production of hydrogen peroxide (H_2O_2), a reactive oxygen species (ROS) generated by the nicotinamide adenine dinucleotide phosphate (NADPH) oxidase, is essential for NETosis. But caspase, which plays an important role in apoptosis, is not required in NETosis (Fuchs et al., 2007). NETosis has been classified into two types: suicidal NETosis and vital NETosis. Suicidal NETosis is normally slow

and mostly stimulated by chemical stimuli (e.g., PMA), while vital NETosis is rapid and stimulated by microbial-specific stimuli (e.g., lipopolysaccharides of gram-negative bacteria) (Yipp and Kubes, 2013). A big difference between these two types of NETosis is that during vital NETosis neutrophil functions remain alive as it occurs independent of cellular suicide (Pilszczek et al., 2010; Yipp and Kubes, 2013).

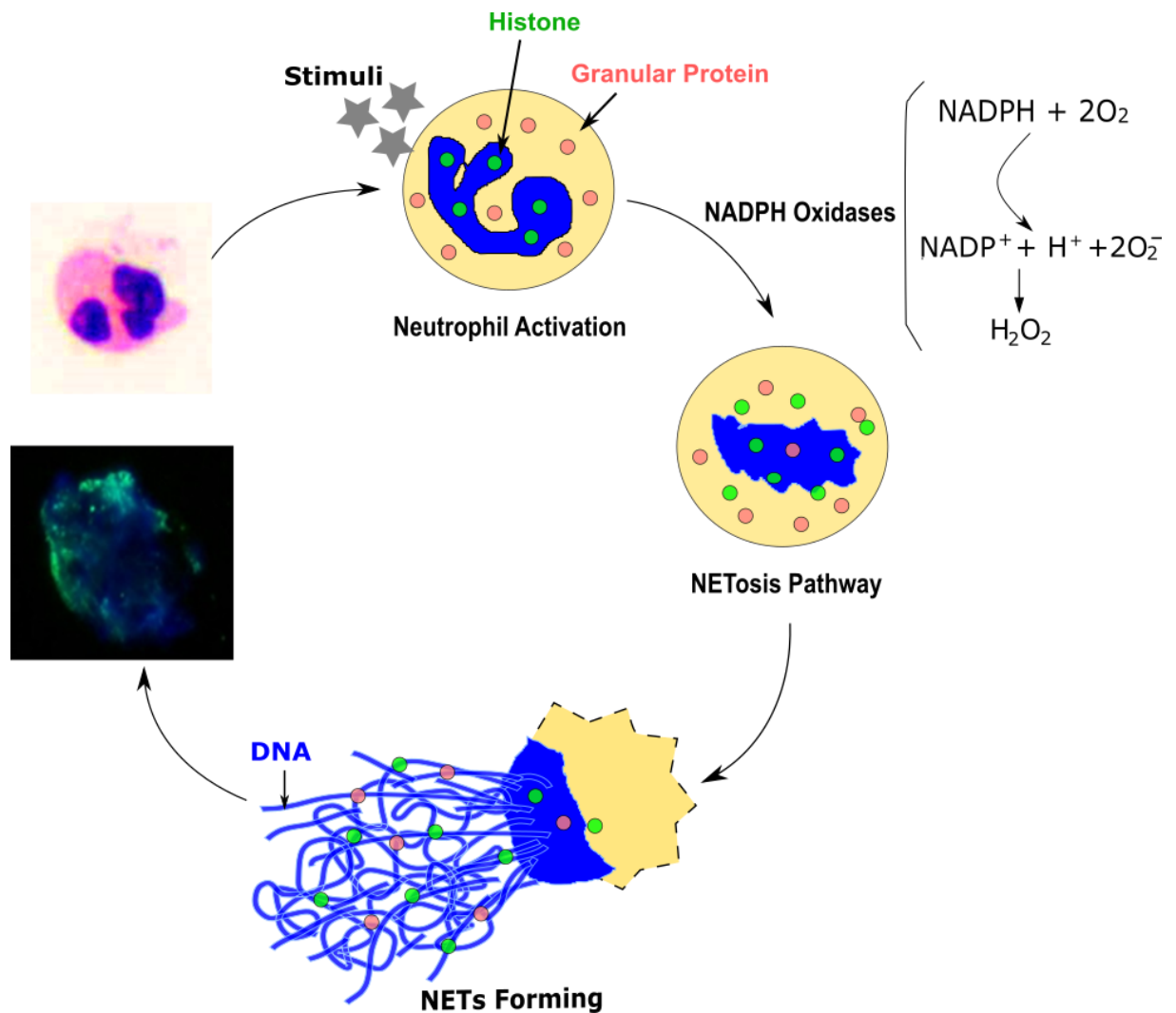


Figure 1-5. NETosis process. Neutrophils are activated by stimuli. The nicotinamide adenine dinucleotide phosphate (NADPH) oxidases are activated, resulting in the formation of reactive oxygen species (e.g., H_2O_2), which plays an important role in the NETosis pathway. Next, neutrophils extrude their DNA and granular proteins to form NETs (Von Köckritz-Blickwede and Nizet, 2009). In Wright's stain image of isolated human neutrophil, eosin ions stain the basic cell components orange to pink, methylene blue ions stain the acidic cell components in different shades of blue. In the immunofluorescence images of NETs, blue showing DAPI-stained DNA, green (cyan in overlay with blue) showing Alexa Fluor 488 labelled Histone H3 (citrulline R2 + R8 + R17).

1.8 Role of NETs in Coagulation

Besides their well-known antibacterial function, the contribution of NETs to haemostasis has also been appreciated with accumulating data emerging during recent years (Kapoor et al., 2018). NETs are considered to promote

blood clotting via various mechanisms. NETs contain DNA that is negatively charged, so they are hypothesized to initiate the intrinsic pathway (von Brühl et al., 2012). Von Bruhl et al. found that NETs contributed to DVT via FXII but independent of FXI in mice models. They also indicated that NETs were decorated with TF, suggesting that they may also initiate the extrinsic pathway (von Brühl et al., 2012; Martinod and Wagner, 2014). An *in-vitro* study showed that NETs promoted clotting by providing a “scaffold” for platelet aggregation, and that NETs can activate platelets. It has also been reported that the “scaffold” of NETs could act as a basis for clot formation independent of fibrin (Fuchs et al., 2010). In addition, citrullinated histone H3 (citH3), a biomarker of NETs, has been shown to bind to vWF, and to contribute to the formation of red blood cell (RBC) and platelet rich DVT in mice (Brill et al., 2012). However, a recent *in-vitro* study questioned the role of intact NETs in coagulation. In this report, purified NET components was able to promote clotting by themselves, but any procoagulant effect was lost in intact NETs due to the interactions between histones and DNA (Denis F Noubouossie et al., 2019). Since conflicting data have been obtained in previous studies, the role of NETs in coagulation deserves further investigation.

1.9 Platelets

1.9.1 Role of Platelets in Haemostasis

As mentioned above, platelets play a crucial role in haemostasis. The platelet receptor glycoprotein (GP) Iba binds to the A1 domain of vWF, while vWF binds

to collagen via its A3 domain. These interactions allow the aggregation and adhesion of platelets to the injury site, resulting in the formation of a platelet plug (Ruggeri, 2007; Ruggeri and Mendolicchio, 2007). Besides forming platelet plugs at the sites of injury of a blood vessel, platelets directly or indirectly interact with many coagulation factors, including FXIIa, FXI, FXIII, FXa, fibrin(ogen), thrombin, etc. (Sang et al., 2021). There are multiple pathways, which can activate platelets. For instance, platelets are activated by thrombin via proteolytic cleavage of G-protein coupled protease activated receptors (PAR-1 and PAR-4), or binding to GPIIb α (Heemskerk et al., 2013; Sang et al., 2021). Collagen activates platelets via interaction with the 62 kDa membrane receptor GPVI (Moroi and Jung, 2004). This GPVI-mediated activation can be enhanced by adenosine diphosphate, thromboxane A₂ and thrombin generation (Nieswandt and Watson, 2003). Additionally, GPVI has recently been shown to interact with fibrinogen via its α C-region (Xu et al., 2021). Platelets are able to increase the density of clots through clot contraction because of the strong adhesion between platelets and fibrin (Longstaff and Kolev, 2015). Activated platelets expose phosphatidylserine (PS), which contributes to platelet-dependent thrombin generation (Heemskerk et al., 2013). Plasma P2Y₁₂ receptor and integrin α _{IIb} β ₃ are crucially involved in PS exposure (Sang et al., 2021). A previous study indicated that a full exposure of PS from platelets requires both Cl⁻ and Ca²⁺ channels (Harper and Poole, 2013).

1.9.2 Interactions between Platelets and Neutrophils (or NETs)

Interestingly, there likely is a positive feedback loop between platelets and NETs. Previous studies found that platelets can be activated by NETs, and vice versa that activated platelets can promote NETs formation (Clark et al., 2007; Zucoloto and Jenne, 2019; Zhou et al., 2020). These findings are consistent with another study that showed an interaction between NETs and platelets during NET-induced clotting (McDonald et al., 2017). As mentioned in above, VWF, which binds to NETs, also binds to GPIIb α in the GPIIb-IX-V complex and integrin α IIb β 3 on the platelet, and thus may act as a bridge in the interactions between NETs and platelet (Peyvandi et al., 2011; Brill et al., 2012). Platelets also contribute to the recruitment of neutrophils. The interaction between platelets and neutrophils mainly occurs via P-selectin on the platelet interacting with P-selectin glycoprotein ligand 1 (PSGL-1) on the neutrophil (Duerschmied et al., 2013; Pitchford et al., 2017), but also through other mechanisms, such as platelet GPIIb α binding to neutrophil MAC-1, platelet ICAM-2 binding to neutrophil LFA-1, and platelet α IIb β 3 indirectly binding to neutrophil MAC-1 via fibrinogen (Figure 1-6) (Simon et al., 2000; Rossaint et al., 2018).

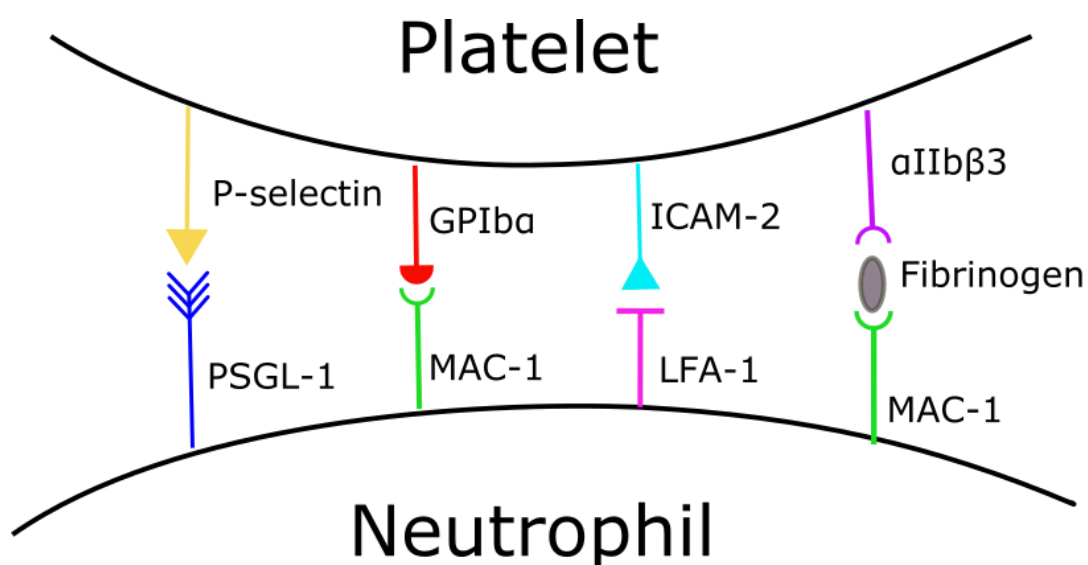


Figure 1-6. Interactions between platelets and neutrophils. Interactions between platelets and neutrophils are mainly mediated through P-selectin interacting with P-selectin glycoprotein ligand 1 (PSGL-1), but also through GPIIb α interacting with MAC-1, ICAM-2 interacting with LFA-1, and α IIb β 3 interacting with MAC-1 via fibrinogen (Rossaint et al., 2018).

1.10 Thromboinflammation

The term ‘thromboinflammation’ was first created to describe the interactions between platelets and neutrophils (Tanguay et al., 2004). Nowadays, it is commonly used to describe the crosstalk between inflammation and thrombosis, in which neutrophils and NETs are widely involved (Martinod and Deppermann, 2021; McAdoo and Dhaun, 2021). Thromboinflammation is associated with a wide range of human diseases, including stroke, sepsis, myocardial infarction, COVID-19, etc. (Martinod and Deppermann, 2021). The close interdependence of inflammation and thrombosis has become increasingly appreciated with the recognition that they could stimulate each other (Jackson et al., 2019). Interleukin 1, interleukin 6, and proinflammatory

cytokines tumor necrosis factor-alpha are the main mediators involved in the reactions of thromboinflammation (Margetic, 2012). Thromboinflammation normally occurs when all the coagulation components are present. Among them, thrombin, TF, the fibrinolytic system, and the protein C pathway play a key role. (Levi and Van Der Poll, 2005; Margetic, 2012). For example, inflammatory cells (e.g., mononuclear cells) and endothelial cells can be activated by thrombin, FXa and fibrin to produce interleukin 6, which is normally rapidly produced in response to infections (Van der Poll et al., 2001; Levi and Van Der Poll, 2005; Tanaka et al., 2014). TF can be expressed and exposed to the blood by inflammatory cells in ruptured atherosclerotic plaques, e.g. in the coronary or carotid artery, thereby initiating thrombosis (Libby and Aikawa, 2002).

1.11 Hypothesis

Previous studies have shown conflicting data on the effects of neutrophils and NETs on coagulation. Most studies indicate that neutrophils could promote coagulation via the generation of NETs. NETs have been shown to provide a “scaffold” for platelet aggregation and fibrin formation, which could enhance the stability of clots. However, a recent study showed that whole NETs could not induce clotting, while NETs components could. Some previous studies suggested that neutrophils could release TF. But there are also other studies that indicated that neutrophils cannot release TF themselves. Based on the existing literature, the overarching hypothesis of this PhD study is to investigate whether neutrophils can promote clotting directly themselves and/or via the formation of NETs. Neutrophils and/or NETs may contribute to the formation of a denser clot architecture, impact clot stability, and through these procoagulant effects lead to an increased risk of thrombosis.

Specific sub-hypotheses to be tested are:

1. NETs can promote clotting via FXII, as they contain DNA.
2. Neutrophils can release TF and other procoagulant enzymes, in which case, neutrophils promote clotting directly themselves or via the formation of NETs.
3. NETs contribute to the formation of a denser clot architecture, thicker fibrin fibres, eventually resulting in an increased fibrinolysis resistance of clots.
4. Neutrophils and NETs have similar effects on coagulation, since NETs are

generated from neutrophils, and both can contribute to an increased risk of thrombosis.

1.12 Aims

Although many previous studies have shown that neutrophils and NETs participate in coagulation, thereby providing a link between thrombosis and inflammation, the exact mechanisms behind this are not yet fully understood. This study aims to investigate the role of neutrophils and/or NETs in blood coagulation, fibrin formation, clot stability and clot structure, and explore the interaction between neutrophil (NETs) and fibrin(ogen) in order to decipher novel mechanisms that contribute to thrombosis.

My specific aims were:

1. To isolate human neutrophils from whole blood and generate NETs.
2. To establish a functional neutrophil-like cell model which is suitable for studying neutrophils and NETs in coagulation aspects.
3. To investigate the role of neutrophils and/or NETs in coagulation.
4. To investigate which factors or mediators may be involved in the procoagulant effects of neutrophils and/or NETs.
5. To determine the effects of neutrophils and/or NETs on the thrombolysis resistance of clots.
6. To detect the permeability of neutrophil- and/or NET-induced clots.
7. To explore the role of neutrophils and/or NETs in the clot structure. .

8. To optimise AFM in order to investigate the interactions between NET fibres and fibrin fibres.

Chapter 2 Methods and Materials

All reagents that could be filtered were filtered through a 0.2 µm filter prior to use.

2.1 Human Blood Samples Preparation

All blood donors provided informed written consent according to the declaration of Helsinki, and this study was approved by the University of Leeds Medicine and Health Faculty Research Ethics Committee, reference number HSLTLM12045.

2.1.1 Neutrophils Isolation

Whole blood samples were obtained from the antecubital vein of healthy volunteers with minimal stasis, discarding the first 2.5 ml, and collected on 0.5 M Ethylenediaminetetraacetic acid (EDTA) or using EDTA Vacutainers (Greiner Bio-One). Human neutrophils were isolated as previously described (Oh et al., 2008). All reagents were brought to room temperature for 30 minutes prior to use. First, 5 ml Lympholyte-poly (Cedarlane) was added to a 15 ml Falcon tube, then 5 ml whole blood was carefully layered on top. Tubes were centrifuged at 500 RCF for 35 minutes at 23°C without brakes. As shown in Figure 2-1, the blood was separated into six clear layers after centrifugation, from top to bottom: plasma, mononuclear cells, isolation media, polymorphonuclear cells (neutrophils), isolation media and red blood cells, respectively. If these layers were not clear, samples were centrifuged again for 15-20 minutes. The top three layers were carefully aspirated and discarded, after which the layer of

neutrophils and all of the isolation media below this layer were carefully transferred into a new Falcon tube. Cells were then washed with 10 ml Hanks' Balanced Salt solution (HBSS) (without $\text{Ca}^{2+}/\text{Mg}^{2+}$) and centrifuged at 350 RCF for 10 minutes. After centrifugation, the supernatant was removed, then 2 ml Red Blood Cell (RBC) Lysis Buffer (Roche) was added to the tube to lyse the residual RBC, and the cell pellet was gently resuspended. Cells were washed once with 10 ml HBSS (without $\text{Ca}^{2+}/\text{Mg}^{2+}$) and centrifuged at 250 RCF for 5 mins, after which the supernatant was discarded. The lysis process was repeated if required. Finally, the cell pellet was resuspended in HBSS (with $\text{Ca}^{2+}/\text{Mg}^{2+}$) or HEPES-buffered saline (HBS) ((If required for subsequent experiments, these buffers were supplemented with 2% w/v human serum albumin (HSA) or 2% v/v fetal bovine serum (FBS)). Following neutrophil isolation, the number of live neutrophils was determined by mixing 10 μl cell suspension and 90 μl Trypan Blue then transferring 10 μl of mixture onto a haemocytometer. The number of live neutrophils was counted under an Olympus CKX41 inverted microscope.

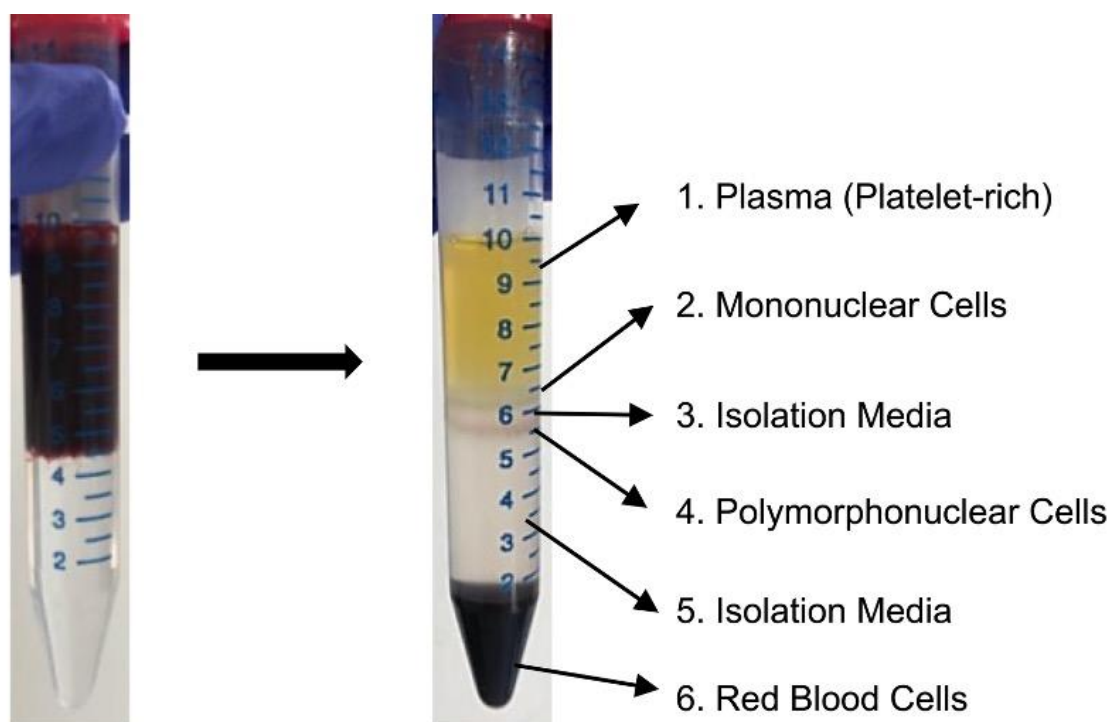


Figure 2-1. Neutrophil isolation from human blood. 5 ml whole blood was layered carefully on top of 5 ml Lympholyte-poly (cell isolation media). After centrifugation, the blood was separated into six clear bands, from top to bottom: plasma, mononuclear cells, isolation media, polymorphonuclear cells (neutrophils), isolation media and the RBCs, respectively.

2.1.2 Neutrophil Supernatant Collection

The neutrophil sample was centrifuged at 500 RCF for 5 minutes to pellet the cells and obtain the supernatant. These neutrophil supernatant samples were either used directly in turbidity measurements or frozen at -20°C for subsequent protein identification via mass spectrometry.

2.1.3 Platelet-rich Samples Collection

Along with neutrophil isolation, after the blood was separated into six clear layers (Figure 2-1), the first layer which contained platelets was carefully

transferred into a new Falcon tube. These platelet-rich samples were labeled with platelet markers and then directly analysed by flow cytometry.

2.1.4 Normal Pooled Plasma

Normal pooled plasma (NPP) was produced as previously described (Macrae et al., 2018). Free-flowing blood samples were collected from the antecubital vein of at least 25 healthy donors using 19 gauge butterfly needles. Blood samples were taken into 0.109 M trisodium citrate and were used within 1 hour. Samples were centrifuged at 3,000 RCF for 20-30 minutes to obtain platelet poor plasma, and then pooled. Normal pooled plasma (NPP) was divided into 0.8-1 ml aliquots, snap-frozen in liquid nitrogen, and then stored at -80°C . Before the experiments, plasmas were defrosted in $\sim 37^{\circ}\text{C}$ water bath for 5 minutes, followed by spinning at 10,000 RCF for 10 min at room temperature, and then filtered through a 0.2 μm filter.

2.2 PLB-985 Cell Culture and Differentiation

A PLB-985 cell line (ACC-139), established from human acute myeloid leukemia, was purchased from DSMZ. PLB-985 cells (1×10^6 cells/ml) were aliquoted into vials and frozen with 70% RPMI 1640 medium, 20% FBS, 10% Dimethyl Sulfoxide (DMSO, Sigma-Aldrich) in liquid nitrogen for long-time storage. Before cell culture, a vial of cells was defrosted in a 37°C water bath for 5 minutes, then transferred into T225 with 10 ml pre-warmed cell culture media. Media was changed the next day to reduce the concentration of DMSO.

PLB-985 cells were cultured in RPMI 1640 medium (R8758, Sigma-Aldrich) supplemented with 10% heat-inactivated FBS at 37°C in a 5% CO₂ with air humidified incubator. Medium was renewed every 2 days. For differentiation, cells were treated in RPMI 1640 medium supplemented with 1.25% DMSO and 5% heat-inactivated FBS at 37°C in 5% CO₂ for 5 days. This differentiation medium was renewed on day 3. The differentiated cells were used in experiments on day 6.

2.3 Coverslips and Slides Surface Coating

Coverslips and slides used in this study were washed once with 70% Ethanol and then washed twice with 1x Phosphate Buffered Saline (PBS, filtered). Then they were coated by being soaked in an excess of 0.01% poly-L-lysine (Sigma-Aldrich) for 15 to 30 minutes at room temperature. The coverslips and slides were subsequently taken out of the poly-L-lysine, allowed to air dry completely, and stored in a clean container for future experiments.

2.4 NETs Generation

2.4.1 For Microscopy Experiments

Round coverslips that were pre-coated with poly-L-lysine were placed in wells of a 24-well cell culture plate. Isolated neutrophils were seeded (~200,000 cells) in 500 µl HBSS (with Ca²⁺/Mg²⁺, 2% w/v HSA) per well. PLB-985 cells were seeded (~200,000 cells) in 500 µl RPMI 1640 medium (2% v/v FBS) per well.

Samples were incubated at 37°C in an incubator for 1 hour to allow the cells to settle down. Then the supernatant was gently removed, after which 20 or 100 nM phorbol 12-myristate 13-acetate (PMA) (Sigma-Aldrich), diluted in either HBSS or RPMI 1640, was added in each well. Cells were incubated at 37°C in an incubator for 2 hours or overnight.

2.4.2 For Turbidity Measurements

Cells were treated with 20 or 100 nM PMA in a T25 flask, incubated at 37°C in an incubator for 4 hours or overnight prior to experiments. After treatment, samples were centrifuged at 500 RCF for 5 mins to pellet residual cells or debris, and then the supernatant was centrifuged at 17,000 RCF for 15 mins at 4°C to harvest NETs. NETs were washed once with HBS by centrifugation at 17,000 RCF for 15 mins at 4°C, the supernatant was discarded, and NETs were resuspended in HBS. Before the resuspended NETs were used in experiments, double-stranded DNA (dsDNA) was quantified using LabTech-Nanodrop ND100 spectrophotometer at a wavelength of 260 nm to confirm that the NETs concentrations were consistent across all experiments.

2.5 Flow Cytometry

Flow cytometry has been used to identify, characterize and count particles in a liquid media for many years. According to a review by Adan et al. (2017), the fluidics system, where hydrodynamic focusing takes place, allows particles to pass the laser beams in a single row (Figure 2-2). The forward scatter channel

(FSC) collects light that is scattered in the forward direction. FSC reflects the size of particles. The side scatter channel (SSC) collects light that is scattered at a 90° angle to the laser beam. It reflects the granularity of particles. Light scattering and fluorescence emission are collected by appropriate detectors. Finally, the light signal is converted into digital data by detectors and a computer (Adan et al., 2017).

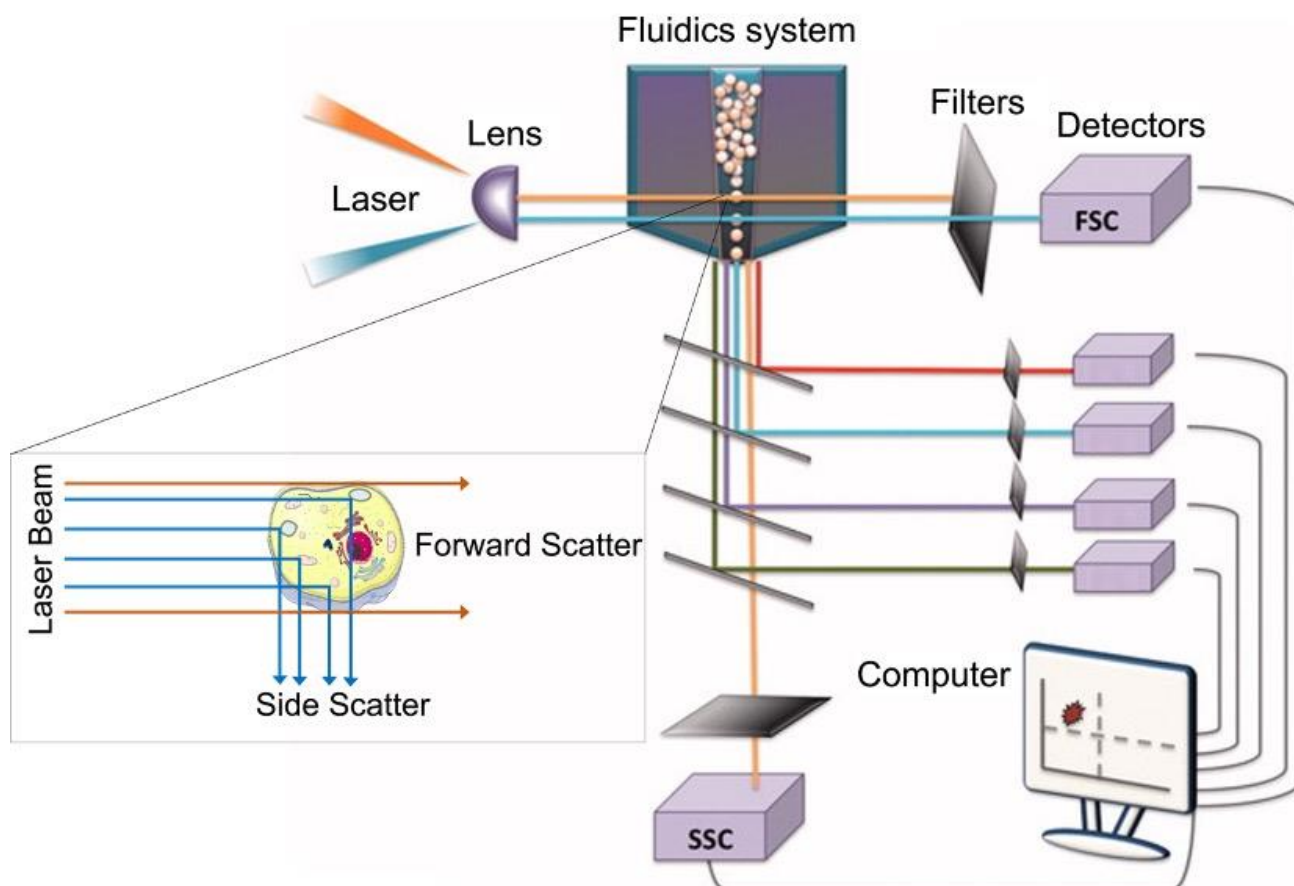


Figure 2-2. Basic principles of flow cytometry. In a fluidics system, particles pass through the laser beams in a single row. The forward-scattered light, side-scattered light or fluorescence emission are collected, and converted into digital data by detectors and computer (Adan et al., 2017). Original images were adapted from Adan et al., 2017 and <https://smart.servier.com>.

2.5.1 Antibodies

PE anti-human CD11b Antibody (clone: RUO), APC/Fire 750 anti-human CD16 Antibody (clone: B73.1), FITC anti-human CD66b Antibody (clone: G10F5), PE anti-human CD41 Antibody (clone: HIP8) and PE Mouse IgG1 κ Isotype Ctrl Antibody (Clone: MOPC-21) were purchased from BioLegend. APC Mouse Anti-Human CD42b (Clone: HIP1) and APC Mouse IgG1 κ Isotype Control (Clone: MOPC-21) were purchased from BD Biosciences.

2.5.2 Human Neutrophil or PLB-985 Cell Sample Preparation

Cells were counted and adjusted to a concentration of 1,000,000 cells/ml in 15 ml Falcon tubes, and then washed once with PBS (with 10% v/v FBS) by centrifugation at 250 RCF for 5 minutes. Cells were incubated in Human BD Fc Block (BD Biosciences) (5 μ l per 100 μ l ice cold PBS) for at least 10 mins. Then 5 μ l conjugated antibodies were added directly in each tube without washing. After 30 mins incubation at 4°C in the dark, cells were washed 3 times with PBS (10% v/v FBS) by centrifugation at 250 RCF for 5 minutes, after which each pellet was resuspended in 500 μ l to 1 ml PBS (10% v/v FBS). Samples were analysed using a CytoFLEX S - 4 laser flow cytometer. Experiments were performed at least in triplicate.

2.5.3 Platelet-rich Sample Preparation

Samples were incubated in Human BD Fc Block (5 μ l per 100 μ l ice cold PBS) for at least 10 mins. Then 5 μ l conjugated antibodies were added directly in

each tube without washing. After 30 mins incubation at 4°C in the dark, samples were directly fixed in 0.9% v/v paraformaldehyde (90 µl of 1% solution were added in the tube). Samples were analysed using a CytoFLEX S - 4 laser flow cytometer.

2.5.4 Gating and Compensation

In order to make the flow data more accurate, gating and compensation are normally used in flow cytometry analysis. *Gating*: a simple gating process is to use FSC and SSC together to gate out debris and dead cells, because they may cause more non-specific interactions and a high background. An example of gating by CytExpert (v.2.1) is shown in Figure 2-3. *Compensation*: The spectral overlap between fluorophores in adjacent channels was calculated by compensation. Compensation was calculated automatically by CytExpert (v.2.1) by comparing each single fluorophore labeled sample to an unstained control.

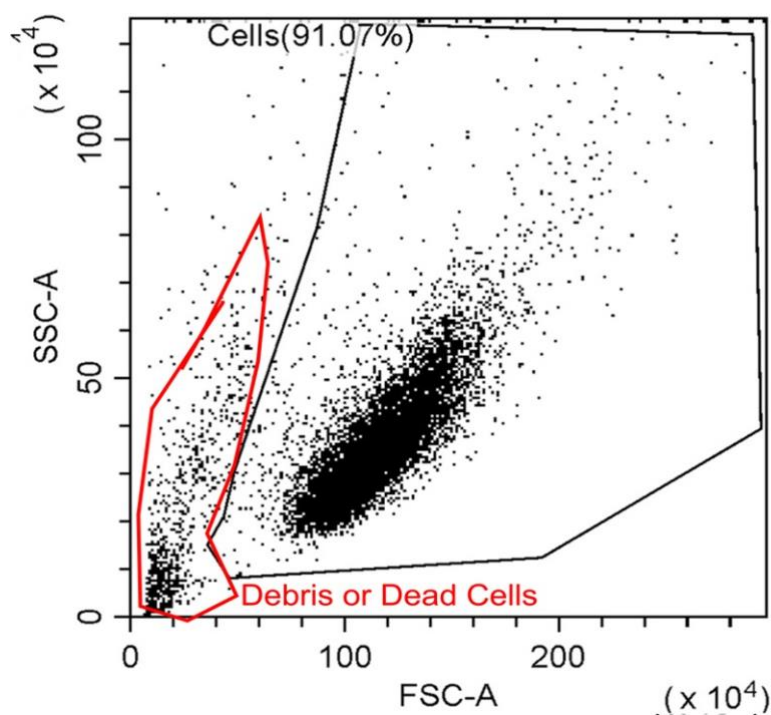


Figure 2-3. An example of gating. Cells (black) and a small amount of debris (red) can be identified and gated using physical characteristics on forward scatter channel (FSC) and side scatter channel (SSC).

2.6 Morphological Staining

Wright's stain was used to identify the morphological features of isolated cells and differentiated PLB-985 cells. A drop of medium (10-20 μ l) containing cells was placed on a glass-slide, a square coverslip was used to touch the drop of medium at an angle of about 45 degrees, and was pushed along the length of the glass-slide to make a smear. Then inside the fume hood, 1 ml Wright's stain buffer was added to the smear when it was almost dry. After 30 seconds, 1 ml deionized water was added and mixed thoroughly with Wright's stain buffer by gently blowing. After 1 minute, slides were rinsed with deionized water and

allowed to air dry. Slides were mounted with DPX Mounting. Finally, slides were visualized under 20x and 40x lenses using an Olympus Microscope.

2.7 Immunofluorescence

Immunofluorescence was carried out to visualize NETs as previously described (Shi et al., 2021). Anti-Histone H3 (citrulline R2 + R8 + R17) antibody (ab5103) and Goat anti-Rabbit IgG H&L (Alexa Fluor 488) (ab150077) were obtained from Abcam. NETs samples were prepared as described in section 2.4.1.

Human neutrophil and PLB-985 cell samples were prepared in the same way as NETs (section 2.4.1), except stimulation with PMA. Samples on 24-well plates were fixed with paraformaldehyde (PFA, 4% in PBS, Sigma-Aldrich) for 30 mins inside a fume hood at room temperature, followed by washing 3x with 1 ml PBS per well. Then samples were incubated in 0.5% Triton X-100 (diluted in PBS) for 1 min at room temperature. After washing 3x with PBS, samples were incubated in blocking buffer (1% w/v bovine serum albumin (BSA), 22.52 mg/ml glycine in PBST (PBS with 0.1% v/v Tween 20)) for 30 mins at room temperature to block non-specific binding of the antibodies. Following one washing step with 1% BSA in PBST, samples were incubated in 500 μ l primary antibody (anti-Histone H3, 1:250 diluted in 1% BSA) per well overnight at 4°C.

The following day, coverslips were washed 3x with PBS, and then incubated with secondary antibody (Goat Anti-Rabbit IgG H&L (Alexa Fluor 488), 1:500 diluted in 1% BSA) for 1 hour at room temperature in the dark. Coverslips were

washed 3x with PBS, followed by incubating with 300 nM 4',6-Diamidino-2-Phenylindole, Dihydrochloride (DAPI, Sigma-Aldrich) for 1-5 min in the dark. After washing twice with distilled water, coverslips were mounted upside down onto glass slides with antifade mounting medium (Vector Laboratories). Slides were allowed to dry for at least 1 hour at room temperature in the dark. Slides were imaged via 20x (0.8 NA) or 40x (1.0 NA) lenses with Diode 405 nm laser and Argon 488nm laser filter by using an Airyscan Upright Confocal Microscope (Zeiss LSM880) or Fluorescence Microscope (Zeiss AX10 - Zen software).

2.8 Fluorescent Labeling

Fluorescent Labeling was carried out to visualize the overall structure of clots. FITC labeled fibrinogen (25µg/ml) was added into plasma. The reaction mixture was prepared by diluting plasma (diluted 1:6 or 1:3), CaCl₂ (3.33 mM) and 2 x 10⁶/ml cells (with 100 nM PMA) or NETs (pre-generated from 2 x 10⁶/ml cells) in HBS. Thrombin (0.1U/ml) was added to initiate clotting. Then 30µl of the mixture was immediately transferred into a well of an uncoated 8-well Ibidi slide (Ibidi GmbH). The slide was placed into a dark humidity chamber for 2 hours at room temperature. Slides were imaged using a 40x oil immersion objective lens (1.4 NA) with Diode 405 nm laser and Argon 488nm laser filter by using an Airyscan Inverted Confocal Microscope (Zeiss LSM880). Optical Z-stacks (9.4-10 µm, 21-23 slices) were combined to form 3D images via Fiji-ImageJ.

2.9 Turbidity Measurements

Turbidity measurements were used to analyse the kinetics of clot formation and fibrinolysis as previously described (Baker et al., 2019). Lag time (the time required for protofibrils formation), maximum optical density (MaxOD), turbidity Vmax (maximum rate of clot formation), time to MaxOD, time from MaxOD to 50% lysis and average rate of lysis were investigated by Microsoft Excel. The preparation time for each well was manually added to its lag time. Figure 2-4 shows a basic example of parameters measured on turbidity and lysis curve. All experiments were performed in triplicate. FXII-, FXI- and FVII-deficient plasmas were purchased from George King Bio-Medical, Inc., USA.

2.9.1 In a Fibrinogen System

2 mg/ml Human Fibrinogen (von Willebrand factor and plasminogen depleted, Enzyme Research Laboratories), 1.5 mM CaCl₂ and 2 x 10⁶/ml cells or NETs (pre-generated from 2 x 10⁶/ml cells) were diluted in HBS and premixed in a 96-well plate. 0.1 U/ml thrombin (Merck) was added to initiate clotting. The absorbency was read at 340 nm, every 12 seconds for 4 hours at 37°C by Multiskan FC Microplate Photometer (Thermo Fisher Scientific) or PowerWave HT Microplate Spectrophotometer (BioTek). In lysis measurements, 0.03 mg/μl tPA was added while other conditions remained unchanged.

2.9.2 In a Plasma System

Plasma (diluted 1:6), 3.33 mM CaCl₂ and 2 x 10⁶/ml cells or NETs (pre-generated from 2 x 10⁶/ml cells) were diluted in HBS and premixed in a 96-well plate. 0.1 U/ml thrombin was added to initiate clotting. The absorbency was read at 340 nm, every 12 seconds for 4 hours at 37°C by PowerWave HT Microplate Spectrophotometer (BioTek). In lysis measurements, 0.03 mg/μl tPA was added and all other conditions remained unchanged.

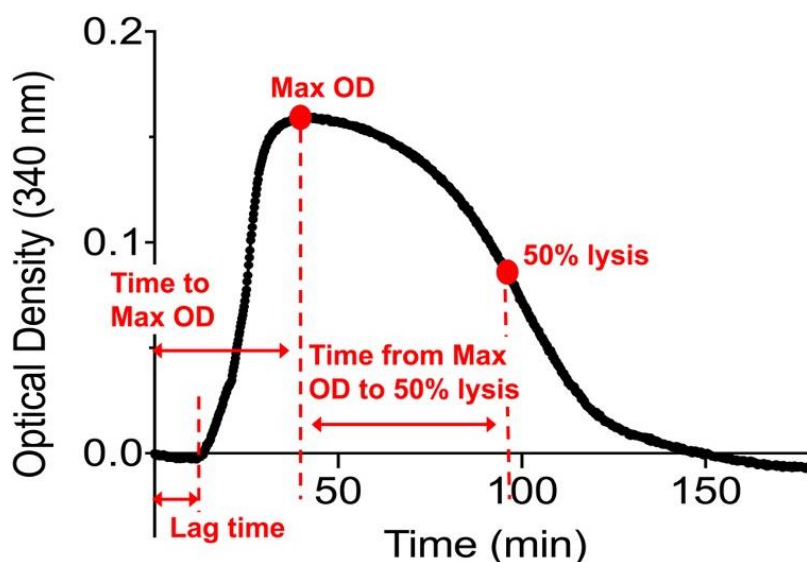


Figure 2-4. An example of parameters measured on turbidity and lysis curve. Lag time reflects the time required for protofibrils formation and shows the time required for the absorbance to begin to increase. MaxOD represents the maximum optical density.

2.10 Chromogenic Activity Assay

Chromogenic activity assay was used to test the efficiency of a FXII inhibitor, corn trypsin inhibitor (CTI) (Enzyme Research Laboratories). FXIIa was purchased from Enzyme Research Laboratories, and the S2302 substrate is

made by Chromogenix and distributed by Quadrantech Diagnostics. This assay was carried out in a purified HBS buffer system, containing 1% polyethylene glycol (PEG) (Sigma-Aldrich). First, gradient concentrations of CTI (0.0125 μ M, 0.05 μ M or 0.2 μ M) were added in each well, followed by adding 30 nM FXIIa. As a control, NPP (diluted 1:5), human neutrophils (200,000 cells/100 μ l) and 5 mM CaCl₂ together were added instead of 30 nM FXIIa, to show an approximate concentration of FXIIa that may be present in the turbidity of plasma system. After 10 mins incubation at 37°C, 200 μ M S2302 substrate was added in each well. The cleavage of S2302 substrate, which reflects any unblocked FXIIa, was monitored at 405 nm by PowerWave HT Microplate Spectrophotometer (BioTek). All experiments were performed in triplicate.

2.11 Mass Spectrometry

Mass spectrometry is used to detect ionized particles qualitatively and quantitatively in a mixture by their mass-to-charge ratio (Murayama et al., 2009). Therefore, this technique has been widely used in protein identification.

Mass spectrometry was carried out by Ms Rachel George, a technician in the Biomolecular Mass Spectrometry Facility, Astbury Centre for Structural Molecular Biology, School of Molecular and Cellular Biology, University of Leeds. A frozen sample of neutrophil supernatant, which prepared as described above, was stored in an ice box and delivered to Ms Rachel George for protein identification.

2.12 Atomic Force Microscopy (AFM)

Atomic force microscopy (AFM) is a high-resolution type of scanning probe microscopy for analyzing a sample surface in liquid, air or ultrahigh vacuum, and has been used as a powerful tool for analyzing biological samples (Carvalho et al., 2010; Kaemmar, 2011; Schillers et al., 2016). A basic operation principle of AFM is shown in Figure 2-5, the tip of the probe contacts with the sample surface. During scanning, the cantilever bends, resulting in changes of deflection of the laser reflected onto the photodiode. A feedback loop is used to hold the cantilever deflection at a constant setpoint thus maintaining a controlled and small interaction force (Kaemmar, 2011).

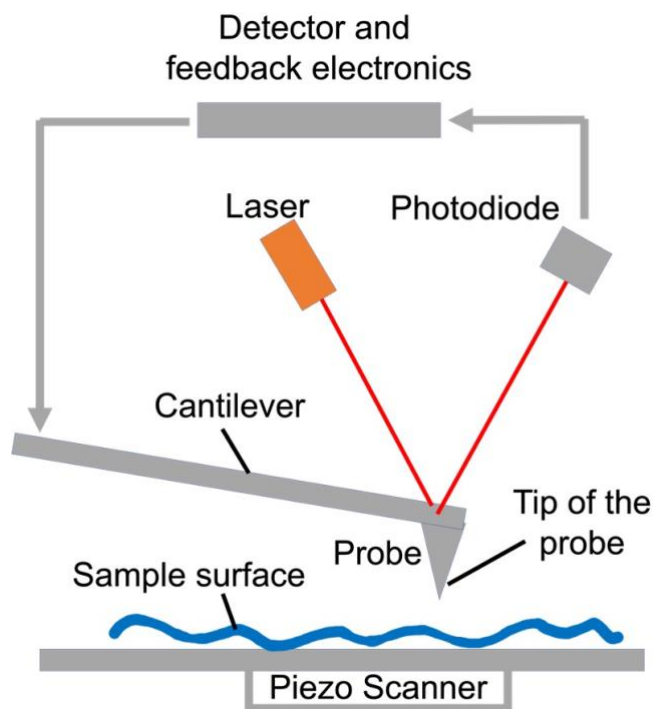


Figure 2-5. Schematic of atomic force microscopy (AFM). An AFM produces images by scanning a cantilever on the surface of a sample. The tip on the probe of cantilever contacts the sample surface, bending the cantilever and changing the amount of laser light reflected onto the photodiode. In tapping mode, the feedback loop is used to keep the amplitude constant (Kaemmar, 2011).

In this study, AFM was used to image and analyse the surface of differentiated PLB-985 cells or their NETs. Samples were prepared in the same way as immunofluorescence (section 2.7). For in-liquid mode, coverslips that have samples on the surface were washed 3 times with PBS after fixation, then coverslips were glued on a metal plate, and finally samples were scanned in PBS. For in-air mode, sample surface of coverslips was washed gently with slow flowing ddH₂O before drying with nitrogen gas, following by the gluing step and AFM scanning. Samples were imaged using the Bruker MultiMode 8 AFM in Tapping mode in air with Bruker TESP-V2 probes or in ScanAsyst PeakForce mode in fluid with Bruker SCANASYST-FLUID probes. Images were analysed using Nanoscope Analysis v1.9 (Bruker).

2.13 Scanning Electron Microscope (SEM)

Scanning Electron Microscopy (SEM) is used to image the detailed structure of clots with high resolution. Cells and NETs samples were prepared in the same way as described in section 2.7. Clot samples were prepared similar to fluorescent labeling samples (section 2.8). Clots for SEM were formed in Eppendorf lids (with 4-6 perforation holes for washing that were sealed during clot formation using parafilm) as shown in Figure 2-6. Final concentrations were: Plasma (diluted 1:3), 10 mM CaCl₂, 1 U/ml thrombin and 2 x 10⁶/ml cells or NETs (pre-generated from 2 x 10⁶/ml cells). This mixture (75 µl) was gently vortexed and immediately transferred into an Eppendorf lid. The Eppendorf lid was kept in a humidity chamber for 1-2 hours to allow for complete clotting to

occur. Following clot formation, the parafilm was removed. The lid with the clot inside was immersed in saline in a 15ml Falcon tube. The Falcon tube was placed on a roller apparatus (set at a medium speed) to wash clots (3 x 40 mins). Then clots were fixed with 2% v/v glutaraldehyde (dilute in Saline) during an overnight step.



Figure 2-6. Graphical representation of SEM sample preparation. Original image of Eppendorf lid was adapted from <https://smart.servier.com>.

On the second day, clots were washed 3 x 40 mins with 50 mM sodium cacodylate buffer (pH 7.4). Then clots were dehydrated using an acetone dehydration series (30%, 50%, 70%, 80%, 90%, 95% and 100% acetone) for 10-15 minutes per concentration. Clots were transferred to fresh 100% acetone. Clots were subjected to critical point drying with carbon dioxide. and mounted onto stubs by Mr Martin Fuller (The Astbury Center, Faculty of Biological Sciences, University of Leeds). Next, samples were sputter coated with 10 nm Iridium using Agar High Resolution Sputter Coater, and the stubs were carbon painted to reduce charging of the samples. Samples were imaged using SU8230 Ultra-High-Resolution Scanning Electron Microscope (Hitachi; Tokyo,

Japan). Coating and imaging were carried out by Ms Helen McPherson, a senior research technician in Leeds Institute of Cardiovascular and Metabolic Medicine, University of Leeds.

2.14 Clot Supernatant Collection

Supernatant of neutrophil-induced clot was collected to detect the release of FpA and FpB by using ELISA. First, clots were produced in 1.5 ml Eppendorf tubes in the same conditions as for SEM samples. After 1-2 hours clotting, clots were manually removed using a pipette tip, and the supernatant was centrifuged at 12,100 RCF for 10 minutes, and transferred to a new tube. These clot supernatant samples were either stored at -20°C or used directly in experiments on the same day.

2.15 Clot Permeation

Permeability of clots was analysed as previously described (Shi et al., 2021). The permeation system was set up as shown in Figure 2-7. Clot samples were prepared using similar methods as described for confocal microscopy above, with the following alterations: plasma was diluted 1:3 and a 6-channel Ibidi slide was used. Clotting slides were placed horizontally in the moist chamber for 2 hours then a syringe was connected to each channel. Syringes were filled with permeation buffer (HBS buffer) to a set height (4 cm) and clots were washed in this manner for 90-120 mins. Flow-through of buffer was subsequently measured by collecting and weighing the buffer flow-through every 5 mins for

20-40 mins. Volume of buffer flow-through, correlated to weight assuming 1 g = 1 ml, over time was plotted and fitted by linear regression ($R^2 \geq 0.99$). The permeability coefficient (K_s , Darcy constant), corresponding to pore size, was calculated as previously described (Pieters et al., 2012).

$$K_s = \frac{Q \times L \times \eta}{T \times A \times \Delta P}$$

K_s = Permeability coefficient (cm^2)

Q = Volume of liquid (1 g = 1 ml = 1 cm^3)

η = Viscosity (10^{-2} poise = 10^{-2} dyne.s/ cm^2 = 10^{-7} N.s/ cm^2), 1 dyne = 10^{-5} N

L = Clot length (1.7 cm)

T = Time (s)

A = Area ($\pi.r^2$) (7.07×10^{-2} cm^2)

ΔP = Pressure drop (density x gravity x height = 1 g/cm^3 x 980 dyne/g x 4cm = 980 dyne/ cm^3 x 4 cm = 0.0098 N/ cm^3 x 4 cm = 0.0392 N/ cm^2)

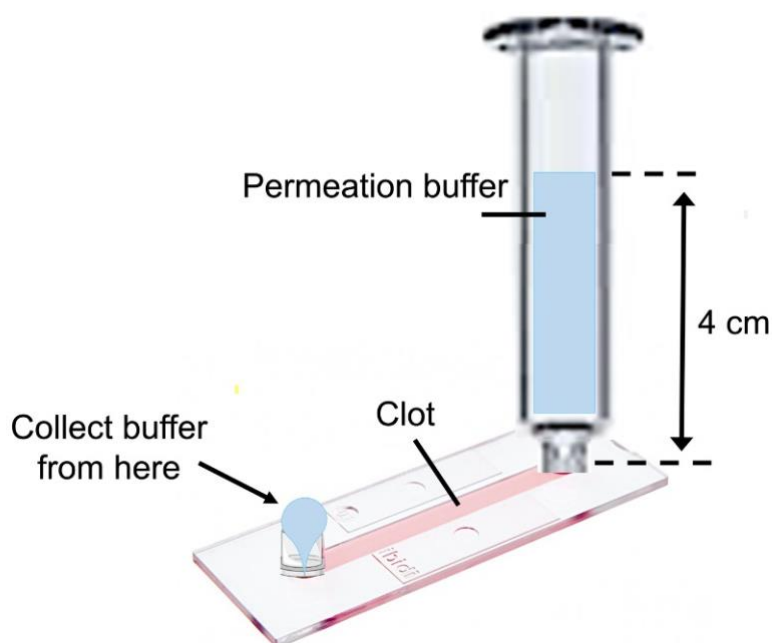


Figure 2-7. Schematic of permeation measurements. Clot was formed in an ibidi slide channel. A syringe was fixed in one of the two end wells of the channel and filled with permeation buffer to a set height (4 cm). Flow-through of buffer was subsequently measured every 5 mins by collecting and weighing the buffer from the other end well of the channel.

2.16 Enzyme-Linked Immunosorbent Assay (ELISA)

Enzyme-linked immunosorbent assays (ELISA) were used to measure the concentration of fibrinopeptide A (FpA) and fibrinopeptide B (FpB) in clot supernatant by following the protocol from the FpA and FpB sandwich ELISA kits (FineTest Inc., US). In a sandwich ELISA, the target antigen is stuck between the capture and detection antibodies (Figure 2-8). Aydin (2015) noted that this type of ELISA has been reported to be more sensitive than all other types (e.g., direct, indirect and competitive).

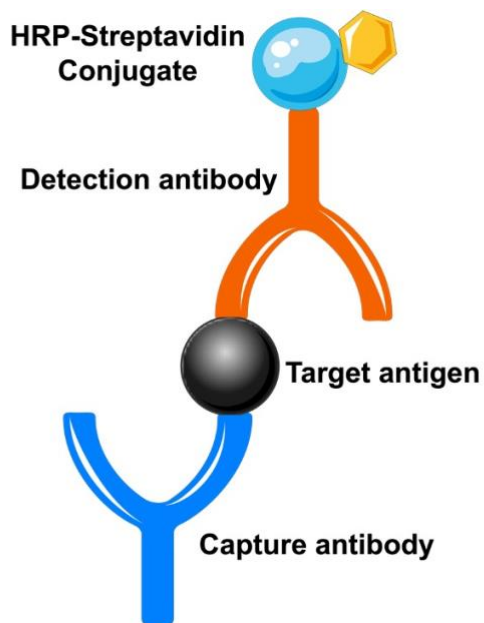


Figure 2-8. Schematic of the sandwich ELISA method. A sandwich ELISA measures target antigen between capture and detection antibodies. Plates are first coated with a capture antibody that is specific to the target antigen. Next, the sample is added, followed by adding a detection antibody that binds to the target antigen. Then a HRP-Streptavidin conjugate is added which binds to the detection antibody. Finally, TMB Substrate is added, which is converted by HRP to a detectable product (Aydin, 2015). Original images were adapted from <https://smart.servier.com>.

All reagents were brought to room temperature for 20 minutes before use.

Clot supernatant samples were diluted 1/2 or 1/4 with Sample Dilution Buffer.

The plate was washed 2 times before adding standards and samples. 100ul of blank control, standards (provided in the kits) or samples were added into wells.

The plate was sealed with a cover and incubate at 37°C for 90 minutes. Wells were washed 2 times with 200 µl Wash Buffer, inverted and tapped 3 times on a paper towel to completely remove any liquid. 100ul Biotin-labeled antibody working solution was added into the wells. The plate was sealed again and incubated at 37°C for 60 minutes. Next, the plate was washed 3 times as

described above. 100ul of HRP-streptavidin conjugate (SABC) Working Solution was added into each well. The plate was sealed once more and incubated at 37°C for 30 minutes. Next, the plate was washed 5 times as described above. Before adding TMB into wells, TMB Substrate were pre-warmed at 37°C for 30 minutes. Then 90ul TMB Substrate was added into each well. The plate was sealed and incubated at 37°C in dark for maximum of 30 minutes. 50ul Stop Solution was added into each well. The adding order of Stop Solution was the same as the TMB Substrate Solution, if the TMB Substrate Solution was added from top left to bottom right, the Stop Solution was added in the same way. The plate was read immediately at a wavelength of 450nm in a PowerWave HT Microplate Spectrophotometer (BioTek). All experiments were performed in duplicate.

2.17 Data Analysis

GraphPad Prism 7 or Microsoft Excel were used to represent data graphically.

All statistical analyses were performed using GraphPad Prism 7. Normal distribution of the data was checked by D'Agostino-Pearson omnibus (K2), Shapiro-Wilk (W) test, Anderson-Darling (A2*) or Kolmogorov-Smirnov (distance) tests. Equality of variance was checked by Brown-Forsythe test or F test. Two-tailed unpaired t-test, two-tailed unpaired t test with Welch's correction, one-way ANOVA followed by Tukey's multiple comparisons test, Brown-Forsythe and Welch ANOVA tests followed by Dunnett's T3 multiple comparisons test were used for parametric data. Mann-Whitney test and

Kruskal-Wallis test followed by Dunn's multiple comparisons test were used for non-parametric data. AFM images were analysed using NanoScope Analysis x86 v190r1. Contrast and brightness of optical, fluorescence and SEM images were adjusted by Fiji-Image J. P-values < 0.05 were considered to indicate statistical significance. Independent repeats are experiments on different days and, where using human neutrophils, used cells from different donors.

Chapter 3 Establishing a Neutrophil-Like Model Using PLB-985 Cells and NETs Generation

3.1 Introduction

PLB-985 cells, a human acute myeloid leukemia cell line, was established by Tucker and colleagues in 1985 from a patient with myeloblastic leukemia (Tucker et al., 1987). The PLB-985 cell line along with other myeloid cell lines, such as HL-60 and NB4, has been suggested to differentiate into mature neutrophils. However, some studies indicate that differentiated PLB-985 cells have a higher capacity to generate reactive oxygen species and to acquire specific granules and secretory vesicles than differentiated HL-60 and NB4 cells (Pedruzzi et al., 2002; Ashkenazi and Marks, 2009). Similar to human neutrophils, differentiated PLB-985 cells can be stimulated by phorbol 12-myristate 13-acetate (PMA) to form neutrophil extracellular traps (NETs) (Marin-Esteban et al., 2012). In addition, a previous study has compared the differentiation of PLB-985 cells using three different inducing agents. Their findings suggest that DMSO-differentiated cells had a higher percentage of morphological changes and higher expression level of neutrophil-surface markers CD63 and CD11b, compared with dbcAMP and DMF (N,N-Dimethyl formamide) (Pivot-Pajot et al., 2010). Therefore, PLB-985 cell line was selected in this study to establish a neutrophil-like cell model by inducing with DMSO.

Human neutrophils were studied to confirm and corroborate the findings and the function of the PLB-985 neutrophil-like cell model. In healthy human blood, neutrophils (50-70%) along with eosinophils (1-5%), basophils (0-1%), lymphocytes (20-45%) and monocytes (2-10%) represent one of five subtypes

of white blood cells (WBCs) (Ramesh et al., 2012; Prinyakupt and Pluempitiwiriyaewej, 2015). According to the morphological features of the cytoplasm and nucleus, the first three subtypes are also classified as granulocytes or polymorphonuclear cells, while the latter two subtypes (lymphocytes and monocytes) are also known as agranulocytes or mononuclear cells. In this chapter, high purity neutrophils were isolated from human blood using existing experimental techniques, where neutrophils were isolated from whole human blood by a standard density gradient centrifugation method (Oh et al., 2008). Samples obtained with this technique are rich in neutrophils, with minimal numbers of eosinophils or basophils.

Wright's stain highlights morphological features of cells using an optical microscope. Wright's stain is a mixture of eosin and methylene blue, negatively charged eosin ions stain the basic cell components orange to pink, while positively charged methylene blue ions stain the acidic cell components in different shades of blue. As previous studies have shown (Figure 3-1) (Chan et al., 2010; Prinyakupt and Pluempitiwiriyaewej, 2015), neutrophils (diameter: 9-15 μm) normally have lower visible granules, which appear pale-purple or pink in blue cytoplasm after staining, as compared with the other two types of granulocytes. The nuclei of neutrophils are multilobed, having between 2 to 5 lobes. On the other hand, eosinophils (diameter: 9-15 μm) have large granules which stained reddish-purple or orange, and nuclei with two lobes only. Basophils (diameter: 10-16 μm) contain bulky granules that are deep blue or

violet when stained, so that their nuclei are often covered. Lymphocytes have a clear blue cytoplasm, which is predominantly filled with a dark purple spherical nucleus. Most of the lymphocytes are smaller than other WBCs (diameter: 7-8 μm), but they could be larger when activated (12-18 μm). Monocytes (diameter: 12-20 μm) have a kidney-bean shaped nucleus in blue abundant cytoplasm. In this chapter, Wright's stain was used to identify neutrophils isolated from blood, and morphological comparisons were made between differentiated PLB-985 cells and primary neutrophils.



Figure 3-1. Morphological photographs of 5 WBC subtypes (Prinyakupt and Pluempitiwiriyawej, 2015).

3.2 Objectives

A primary aim was to establish and optimise a functional neutrophil-like cell model based on previous studies. This model was then compared with human neutrophils isolated from human blood. Another key aim was to establish the purity of the isolated neutrophils. Finally, a key objective was to compare NETs from primary human neutrophils with NETs generated using the PLB-985 neutrophil-like cell model.

3.3 Methods

3.3.1 Human Neutrophil Isolation and PLB-985 Cell Model Establishment

Human neutrophils and platelet-rich samples were harvested from whole blood as described in section 2.1. To establish a neutrophil-like cell model, PLB-985 cells were differentiated as described in chapter 2.2. Wright's stain was used to visualize the morphological features of isolated neutrophils and differentiated PLB-985 cells as described in section 2.6.

3.3.2 Purity of Isolated Neutrophils and the Availability of Neutrophil-like Cell Model

Flow cytometry was carried out to identify isolated neutrophils (CD16, CD66b), to quantify platelets in isolated neutrophils (CD41, CD42b), and to investigate whether PLB-985 cells were differentiated into functional neutrophil-like cells (CD16, CD66b, CD11b) (section 2.5). Mean Fluorescent Intensity (MFI) and percent positive cells were calculated by CytExpert (v.2.1). MFI is often used to describe the mean intensity and level of antibody expression.

3.3.3 NETs Generation and Visualization

NETosis of human neutrophils and differentiated PLB cells was stimulated with 20 or 100 nM PMA (section 2.4). To determine the experimental time for future experiments, the effects of 2-hour and overnight stimulations were investigated in this chapter. Immunofluorescence was used to visualize NETs using DAPI

and a NETosis marker Histone H3 (citrulline R2 + R8 + R17), as described in section 2.7.

3.3.4 Data Analysis

Contrast and brightness of Wright's stain and fluorescence images were adjusted by Fiji-Image J. GraphPad Prism 7 or Microsoft Excel were used to represent the data graphically. All statistical analyses were performed using GraphPad Prism 7. A normal distribution of the data was checked by D'Agostino-Pearson omnibus (K2), Shapiro-Wilk (W) test, Anderson-Darling (A2*) or Kolmogorov-Smirnov (distance) tests. The equality of variances was checked by Brown-Forsythe test or F test. Two-tailed unpaired t-test, two-tailed unpaired t test with Welch's correction, one-way ANOVA followed by Tukey's multiple comparisons test were used for parametric data. Kruskal-Wallis test followed by Dunn's multiple comparisons test was used for non-parametric data. P-values < 0.05 were considered to indicate statistical significance.

3.4 Results

3.4.1 Morphology of Human Neutrophils and Differentiated PLB-985 Cells

The morphological features of isolated human neutrophils are shown in Figure 3-2. Most of the cells isolated from whole blood had 2 to 5 multilobed nuclei surrounded by pale-purple or pink background, containing cytoplasm and granules, and their diameter was roughly 10 to 15 μm , which was consistent with the typical characteristics of neutrophils. Occasionally, other subtypes of

WBCs were observed in isolated neutrophils samples. For example, eosinophils, which had two lobulated nuclei surrounded by reddish-purple or orange background, and basophils that had deep blue granules that covered their nuclei were occasionally observed. Lymphocytes, which were smaller than other cells and containing round dark-purple nuclei, were also occasionally present in the sample. No cells with typical monocyte characteristics could be observed in these samples. In addition, few platelets which appeared as blue-purple spots were also observed.

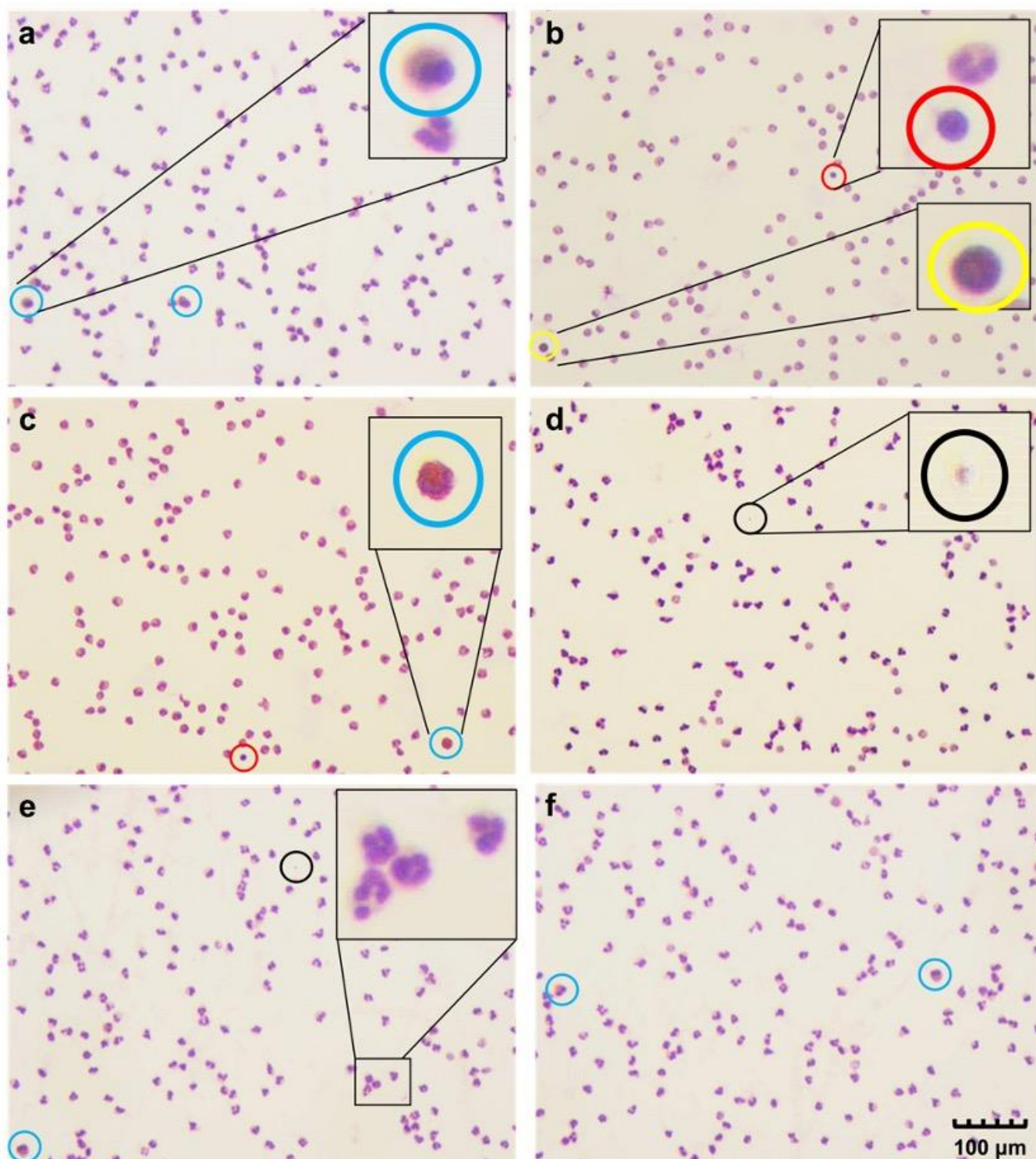


Figure 3-2. Wright's stain images of isolated human neutrophils. A few other blood components were observed and circled here: platelet (black), lymphocyte (red), eosinophils (blue), basophils (yellow). The square black inset box in panel (e) shows a zoom-in on typical neutrophils. Scale bar shows 100 μm. ($n \geq 3$)

The morphological features of differentiated PLB-985 cells are shown in Figure 3-3. The diameter of normal PLB-985 cells was roughly 10 to 20 μm , while the diameter of differentiated cells was smaller (8-12 μm) and closer to primary neutrophils. Both normal PLB-985 cells and differentiated cells had pale-purple or pink cytoplasm. Generally, normal PLB-985 cells were round and had no apparent stained nucleus. Intuitively, they were slightly shrunk into irregular shapes and stained darker after differentiation, with a grainy background that could contain cell debris. However, it was difficult to distinguish whether the darker stain was due to the changes of their nuclei or the increase of granules in the cytoplasm. Moreover, it is also difficult to ascertain whether or not PLB-985 nuclei had changed into multilobed nuclei (typical for neutrophils) after differentiation.

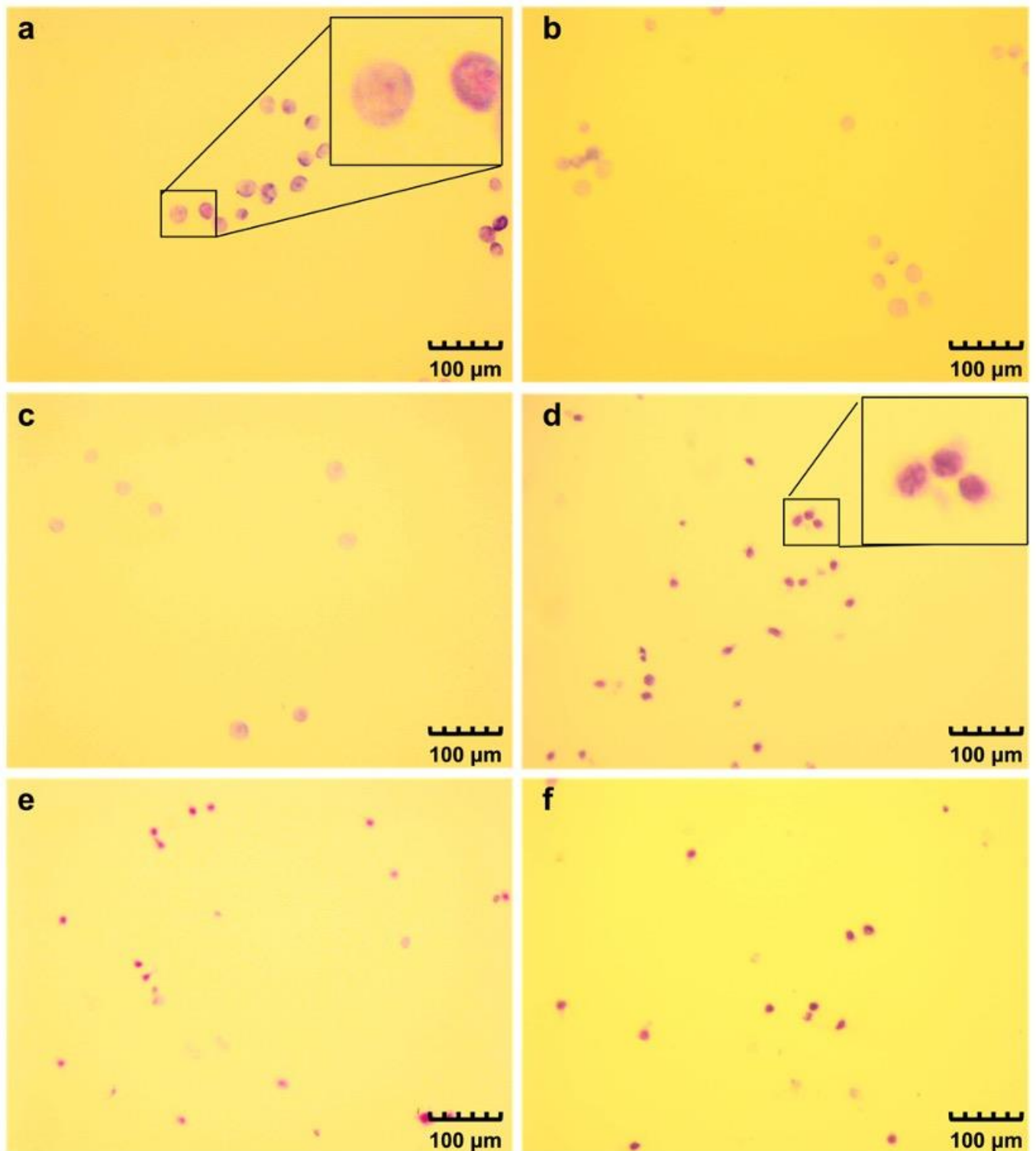


Figure 3-3. Wright's stain images of DMSO-differentiated PLB-985 cells. (a) (b) (c) Normal PLB-985 cells were used as controls. (d) (e) (f) Samples were imaged on day 6 of differentiation. Scale bar showing 100 μm. (n ≥ 3)

The intensity of forward scatter (FSC) in flow cytometry reflects the size and surface area of cells, and the side scatter (SSC) reflects the internal complexity and granularity of cells. Flow data were consistent with Wright's stain images (Figure 3-4) as expected, platelets had the simplest internal structure and were the smallest in size. Overall, normal PLB-985 cells were slightly larger than neutrophils in size. But after differentiation, whether this was following 3-day or 6-day incubation, they became slightly smaller than neutrophils. The internal complexity and granularity PLB-985 cells were relatively simpler than that of primary neutrophils, even after differentiation. There were no significant differences between normal and differentiated PLB-985 cells in the SSC intensity.

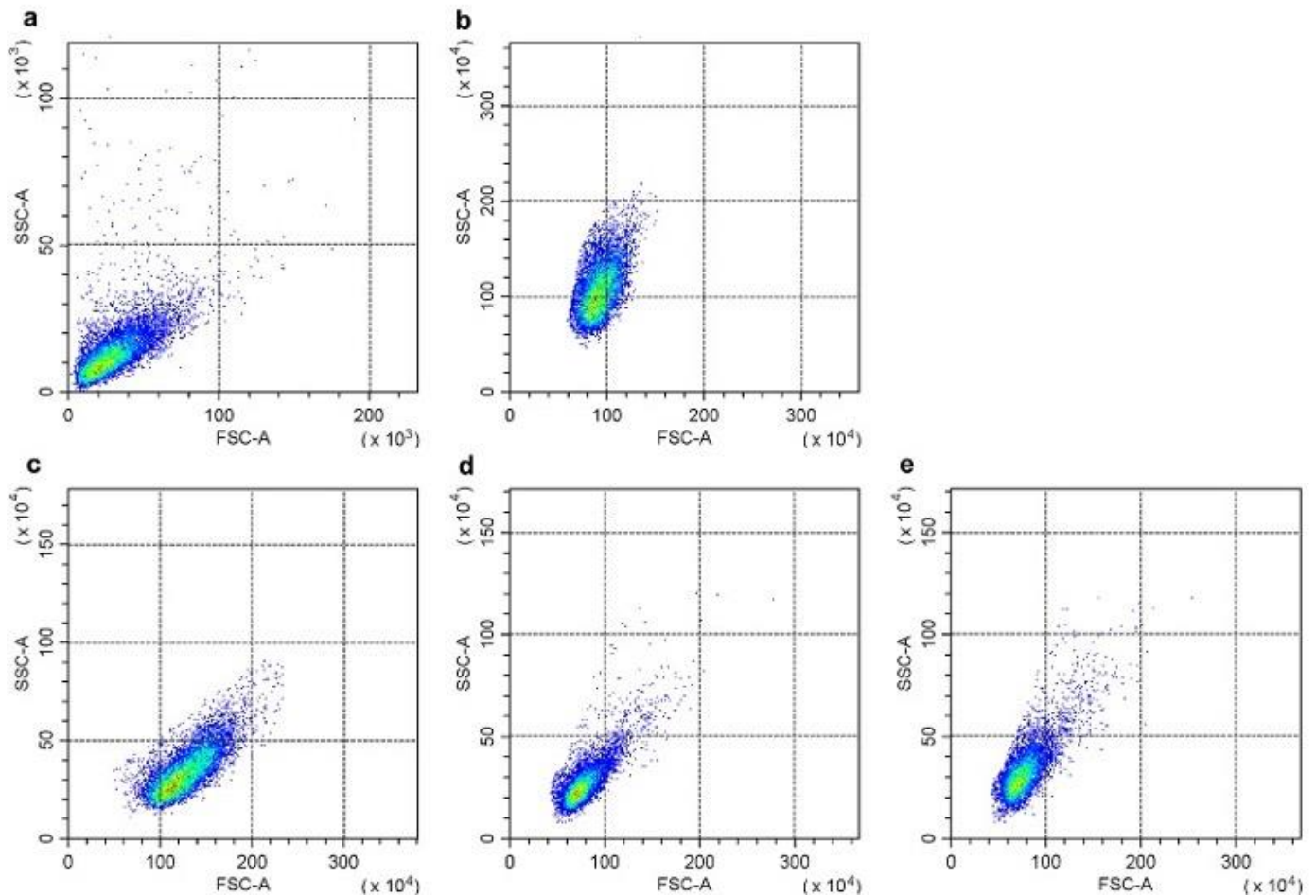


Figure 3-4. Flow cytometric characteristics of isolated human neutrophils, platelets and differentiated PLB-985 cells. Forward scatter characteristics (FSC) and side scatter characteristics (SSC) are plotted on the X- and Y-axes respectively. Dot plots showing: (a) platelets, (b) human neutrophils, (c) normal PLB-985 cells. For differentiated PLB-985 cells, flow cytometry was performed on (d) day 3 and (e) day 6 of DMSO-induced differentiation.

3.4.2 Qualitative Identification of Isolated Cells

Previous studies have shown that CD66b is expressed on neutrophils and eosinophils (Torsteinsdóttir et al., 1999). CD16 is also expressed on neutrophils, but not on eosinophils (Darby et al., 2018). To qualitatively confirm the cells isolated from human blood were neutrophils and not another subtype of WBCs, the expression of both CD66b and CD16 on isolated samples was analysed by flow cytometry. In neutrophil samples prepared from human blood,

99.7% cells expressed CD66b, 94.8% cells expressed CD16, and 94.7% cells simultaneously expressed both markers (Figure 3-5). As these antibodies were used to qualitatively identify whether isolated cells were neutrophils or other cells, no isotype control was used here, and these data may be a bit higher than the actual percentages.

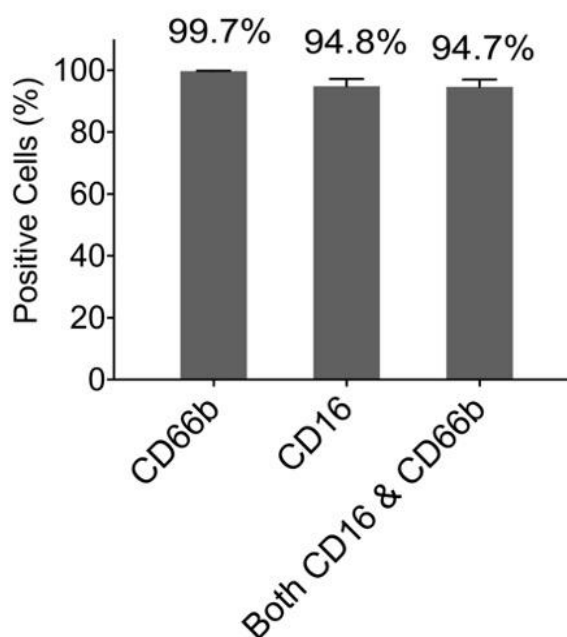


Figure 3-5. Identification and quantification of neutrophils isolated from human blood by CD16 and CD66b. The mean percentage of antibody expression was analyzed. Error bars represent SD of 3 independent repeats ($n = 3$). (Partial data were adapted from Shi et al., 2021)

3.4.3 Quantification of platelets in isolated Human Neutrophils

Flow cytometry was also used to investigate whether CD41 and CD42b can effectively label platelets. Both antibodies were used in platelet-rich (unwashed) samples (section 2.1.3). As compared with unstained and isotype controls, both CD41 (95.89%) and CD42b (96.21%) were highly expressed in platelet-rich

samples, with high MFI values of 334.53×10^3 and 56.07×10^3 , respectively

(Figure 3-6 and Figure 3-7).

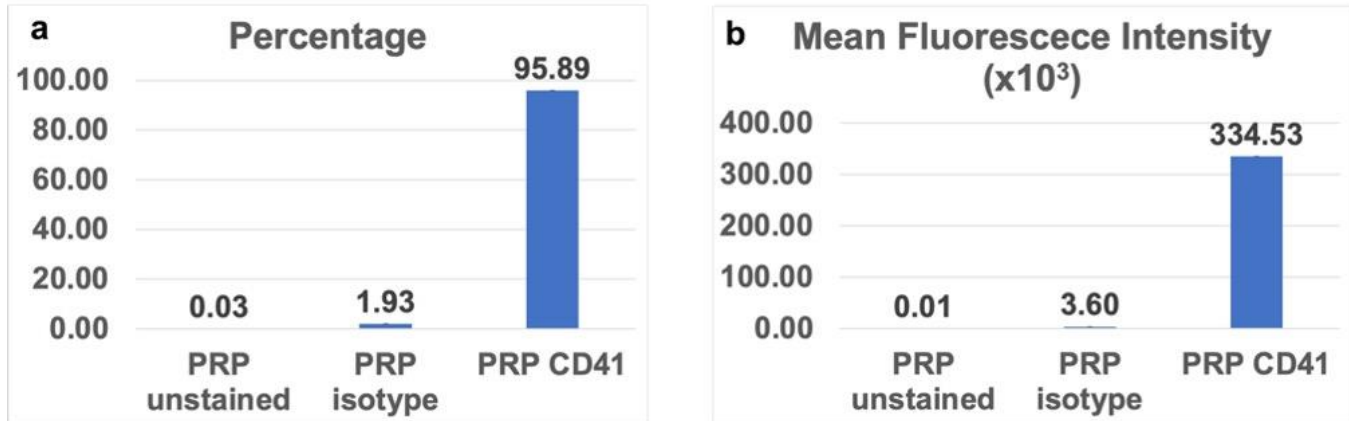


Figure 3-6. Effectiveness of CD41 in detecting platelets. (a) Percentage and (b) mean fluorescence intensity of particles expressed CD41 were quantified by flow cytometry. (n = 1)

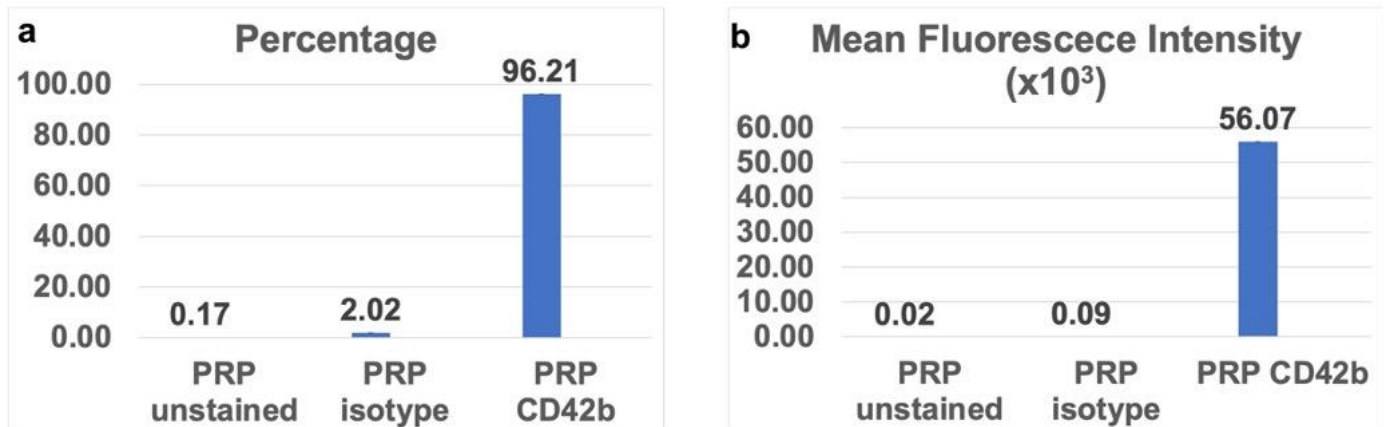


Figure 3-7. Effectiveness of CD42b in detecting platelets. (a) Percentage and (b) mean fluorescence intensity of particles expressed CD42b were quantified by flow cytometry. (n = 1)

As shown in Figure 3-8, 16.14% of particles expressed CD41 in isolated neutrophils samples, but a high expression of IgG-PE isotype (7.7%) was also observed. The MFI value of IgG-PE was 33.99×10^3 , which was significantly higher than that of CD41 antibody (7.52×10^3). Notably, in human neutrophil samples, the IgG-PE isotype had an unusual long tail end to the peak (Figure 3-8 d), which makes the gating difficult and reduced the accuracy of the analysis. The isotype data also indicates that there may be more non-specific binding in neutrophil samples than in platelets-rich control (Figure 3-6 d).

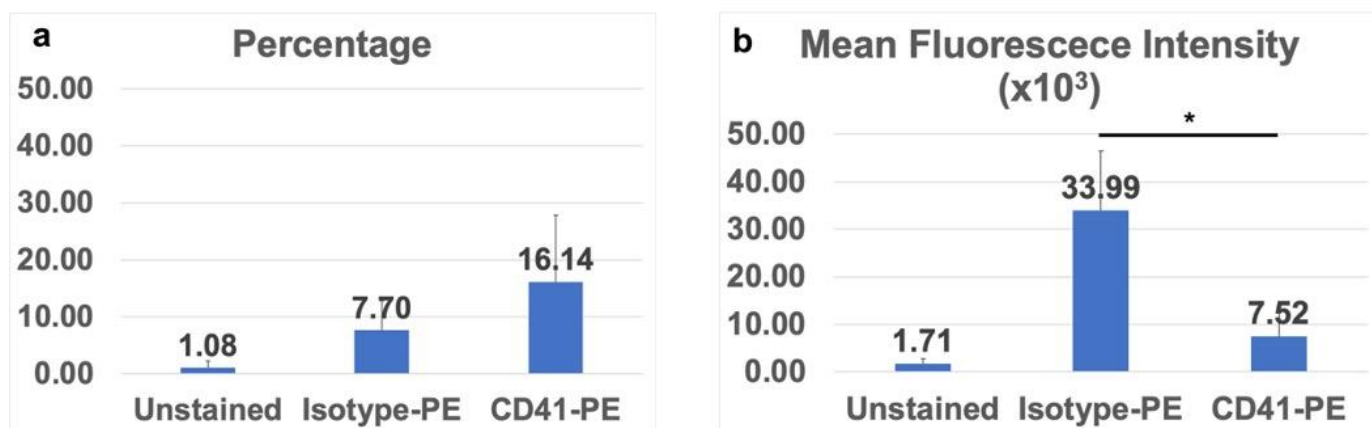


Figure 3-8. Quantification of platelets in isolated neutrophils by CD41. (a) Percentage and (b) mean fluorescence intensity of particles expressed CD41 were quantified by flow cytometry. Error bars represent SD of 3 to 4 independent repeats ($n = 3-4$). * $P < 0.05$.

To confirm the results of CD41, and to find a better antibody for platelet quantification in isolated neutrophils samples, CD42b was used. The expression of Cd42b was quantified by gating a background fluorescence baseline of 1.87% on the IgG-APC isotype control (Figure 3-9 d). The MFI value of IgG-APC was 2.68×10^3 (Figure 3-9 b). Results showed that 2.69% of particles

expressed CD42b in isolated neutrophils, with a MFI value of 4.15×10^3 (Figure 3-9 a & b).

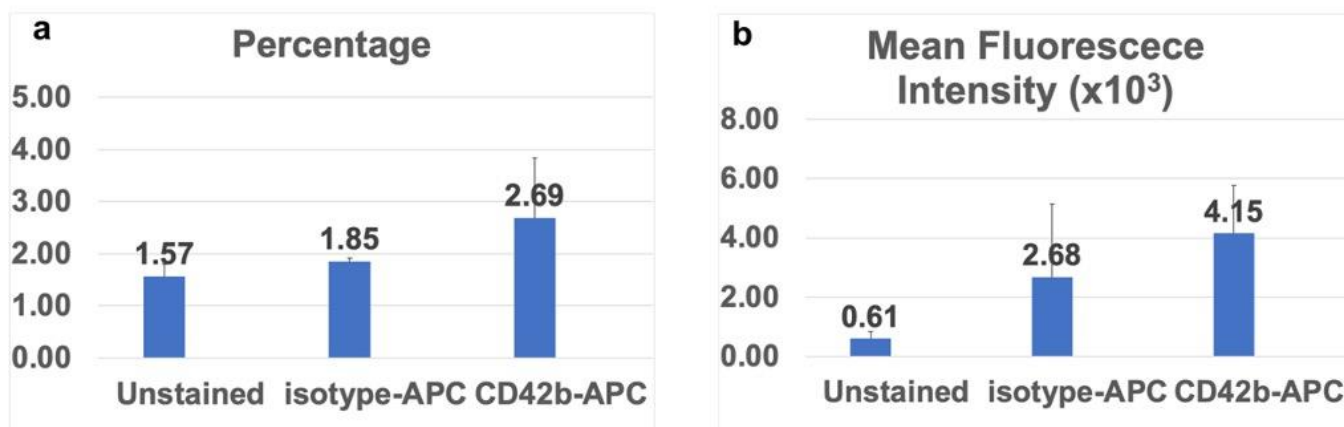


Figure 3-9. Quantification of platelets in isolated neutrophils by CD42b. (a) Percentage and (b) mean fluorescence intensity of particles expressed CD42b were quantified by flow cytometry. Error bars represent SD of 4 independent repeats (n = 4).

3.4.4 Expression of Neutrophil Surface Antigens on Differentiated PLB-985

Cells

The expression of CD16 and CD66b on differentiated PLB-985 cells was detected on day 6 of the differentiation, with normal PLB-985 cells used as controls. Although the expression of CD16 on differentiated cells (1.3%) was significantly higher than that on normal PLB-985 cells (0.2%) (Figure 3-10 f), the expression level was markedly lower in both cell types compared to isolated human neutrophils (94.8%) (Figure 3-5). The expression level of CD66b was also very low, and there were no significant differences in the expression of CD66b in normal PLB-985 cells (3.9%) and differentiated cells (3.3%) (Figure 3-10 c).

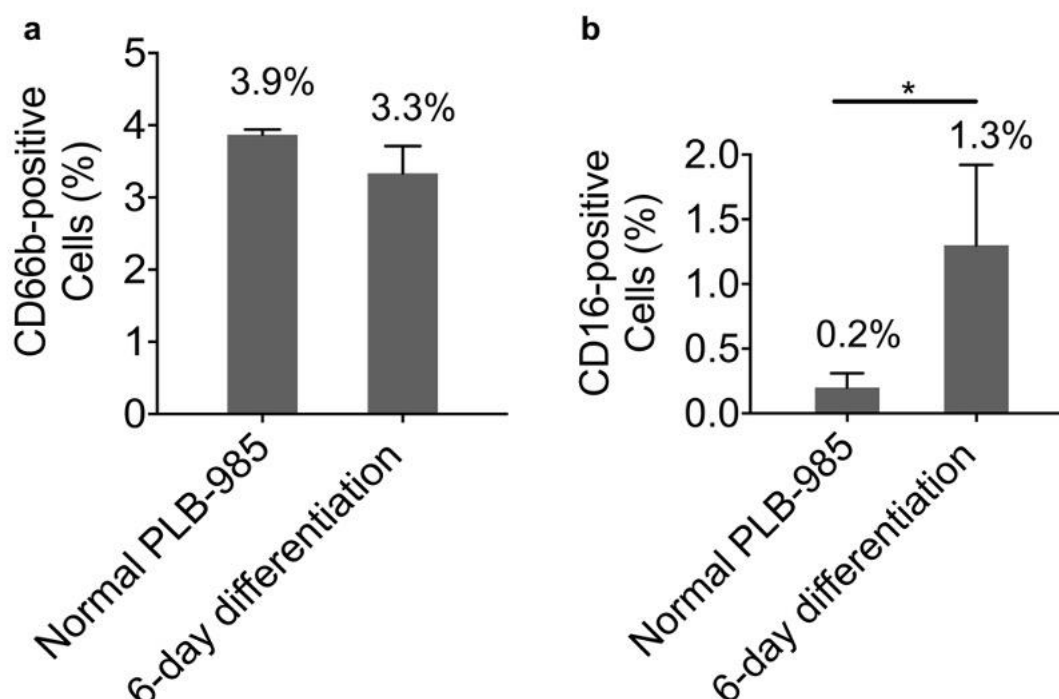


Figure 3-10. Expression level of human neutrophil-surface antigens (CD66b and CD16) on differentiated PLB-985 cells. The mean percentage of (a) CD66b and (b) CD16 expression was analyzed. Normal PLB-985 cells were used as controls. Error bars represent SD of 3 independent repeats (n = 3). * P < 0.05. (Partial data were adapted from Shi et al., 2021)

As a positive marker was required to identify whether PLB-985 cells were differentiated into neutrophil-like cells or not, another human neutrophil surface marker, namely CD11b, was used. Flow cytometry was carried out on day 3 and day 6 of differentiation. Isolated human neutrophils and normal PLB-985 cells were used as positive and negative controls, respectively. As shown in Figure 3-11, the expression level of CD11b significantly increased with time of differentiation, being 14.1% on normal PLB cells, 88.2% on day 3 and 97.0% on day 6 of differentiation. Similarly, the MFI value of CD11b also significantly increased with time of differentiation (Figure 3-12 a). There was no significant difference between 6-day differentiated PLB-985 cells and isolated neutrophils

(98.9 %) in the percentage of expression of CD11b (Figure 3-11 e). However, the CD11b MFI value of 6-day differentiated PLB-985 cells was statistically lower than that of isolated neutrophils (Figure 3-12 b).

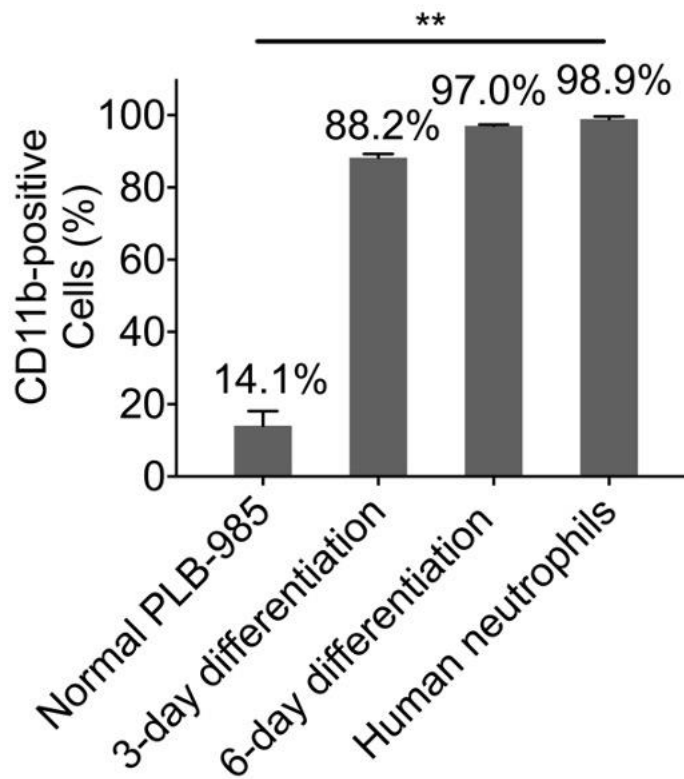


Figure 3-11. Expression level of human neutrophil-surface antigen CD11b on differentiated PLB-985 cells. The mean percentage of CD11b expression was analyzed. Error bars represent SD of 3-4 independent repeats (n = 3-4). (Partial data were adapted from Shi et al., 2021)

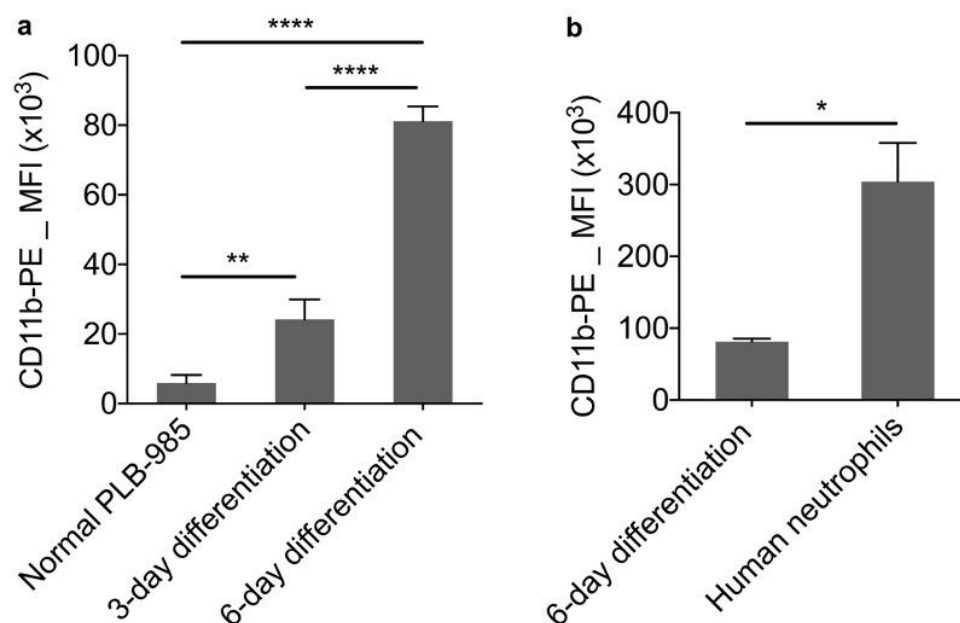


Figure 3-12. Expression level of human neutrophil-surface antigen CD11b on differentiated PLB-985 cells. Mean fluorescence intensity of cells expressed CD11b were quantified by flow cytometry. Error bars represent SD of 3-4 independent repeats (n = 3-4). * P < 0.05, ** P < 0.01, **** P < 0.0001.

3.4.5 Generation and Visualization of NETs

Immunofluorescence was carried out to visualize NETs, which were generated from human neutrophils or differentiated PLB-985 cells by stimulating with 20 nM or 100 nM PMA for 2 hours or overnight. A marker of NETs, Histone H3 (citruiline R2 + R8 + R17), was used to confirm NETosis. As shown in Figure 3-13, both human neutrophils and differentiated PLB cells successfully released their DNA and Histone H3 to form NETs. Both PMA concentrations of 20 nM and 100 nM worked well in stimulating NETosis, as did the stimulation time range of 2 hours to overnight. Autofluorescence and antibody staining controls are shown in Figure 3-14.

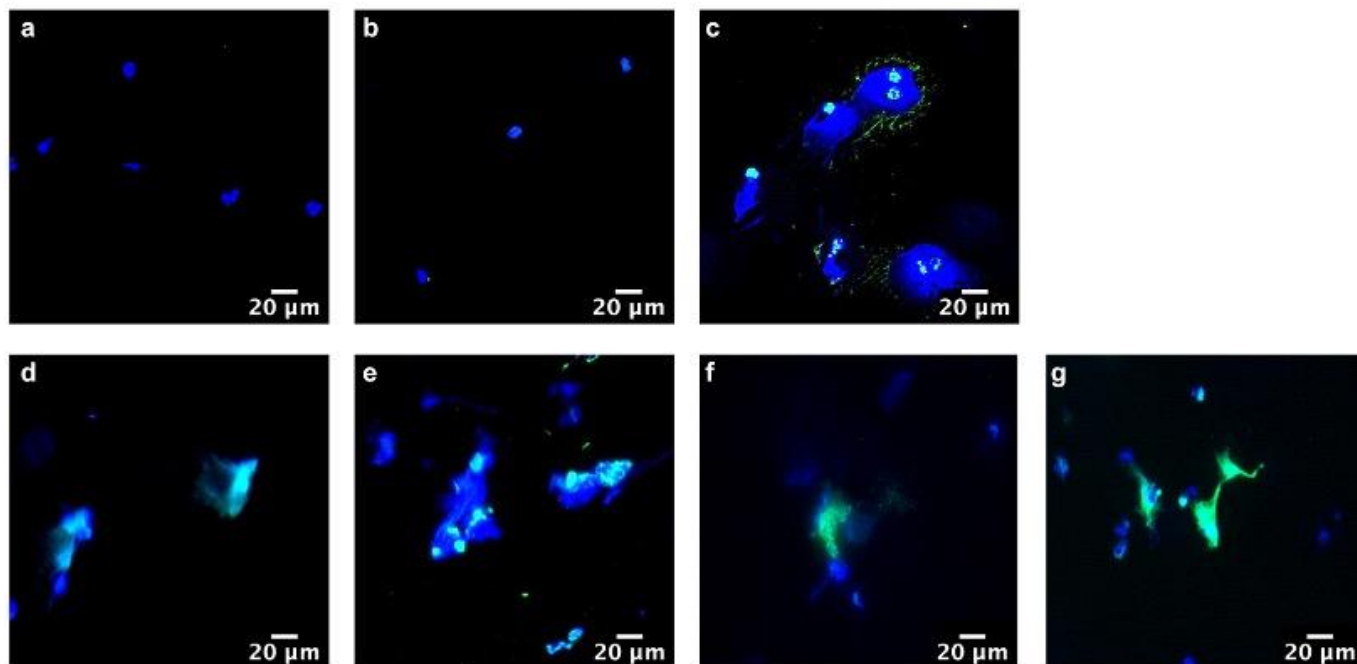


Figure 3-13. Immunofluorescence images of NETs. (a) Human neutrophils. (b) Differentiated PLB-985 cells. (c) NETs generated from differentiated PLB-985 cells by stimulating with 20 nM PMA for 2 hours. (d) NETs generated from human neutrophils by stimulating with 20 nM PMA for 2 hours. (e) NETs generated from human neutrophils by stimulating with 100 nM PMA for 2 hours. (f) NETs generated from human neutrophils by stimulating with 20 nM PMA for overnight. (g) NETs generated from human neutrophils by stimulating with 100 nM PMA for overnight. Blue: DAPI-stained DNA. Green (cyan in overlay with blue): Alexa Fluor 488 labelled Histone H3 (citrulline R2 + R8 + R17). Scale bars showing 20 μm . ($n \geq 3$) (Please see attached movie of human NETs formation.) (Partial data were adapted from Shi et al., 2021)

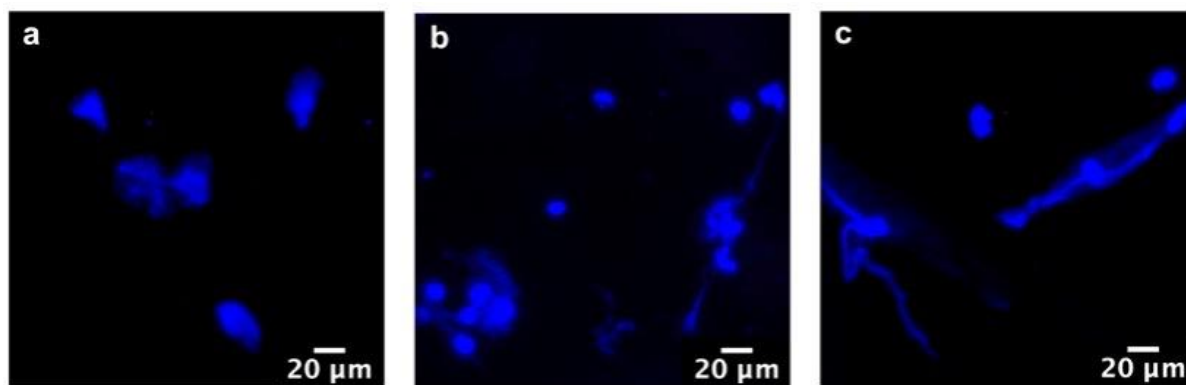


Figure 3-14. Immunofluorescence staining controls. Images showing NETs generated from human neutrophils. **(a)** DAPI only. **(b)** without primary antibody. **(c)** without secondary antibody, Blue: DAPI-stained DNA. Primary antibody: anti-Histone H3 (citrulline R2 + R8 + R17). Secondary antibody: Goat anti-Rabbit IgG H&L (Alexa Fluor® 488). Scale bars showing 20 μm . ($n \geq 3$) (Shi et al., 2021)

3.5 Discussion

In this chapter, a neutrophil-like cell model was established by differentiating PLB-985 cells. According to result from Wright's staining results, differentiated PLB-985 cells changed into irregular shapes comparable with normal PLB-985 cells, consistent with flow cytometry FSC/SSC data. Unlike the isolated human neutrophils, the nuclei of both normal and differentiated PLB-985 cells were difficult to identify. Therefore, it is unclear whether this neutrophil-like cell model has a similar multilobed nucleus as compared with primary neutrophils using Wright's stain. Pivot-Pajot et al. (2010) used transmission electron microscopy (TEM) to visualize normal PLB-985 cells, differentiated PLB-985 cells and human neutrophils. They observed that normal PLB-985 cells had round nuclei and lacked granules in their cytoplasm. After differentiation, their nuclei changed into a lobed morphology, and granules were observed in their cytoplasm, similar to human neutrophil (Pivot-Pajot et al., 2010). According to the data presented in this chapter, differentiated PLB-985 cells changed into a neutrophil-like morphology, but were not exactly the same as primary neutrophils.

To further compare the neutrophil-like cell model with human neutrophils, the expression levels of neutrophil cell-surface markers CD16 (FcγRIII), CD66b and CD11b on this cell model were evaluated. My findings indicate that differentiated PLB-985 cells demonstrated significantly less CD16 (FcγRIII) and CD66b, a marker for specific, secondary and tertiary granules (Mollinedo et al.,

2003; Pivot-Pajot et al., 2010), when compared with primary neutrophils. Future studies should try extending experiments beyond 6-day differentiation to check whether the expression of CD16 and CD66b could be increased. CD11b is a marker for secondary, tertiary granules and secretory vesicles, and is related to adhesion, migration and degranulation of neutrophils (Anderson et al., 2000; Borregaard et al., 2007; Schleiffenbaum et al., 2018). The expression of CD11b increased with differentiation time, and on the last day of differentiation the percentage of cells expressing CD11b was comparable to that of primary neutrophils. But differentiated PLB-985 cells had lower CD11b MFI value than isolated neutrophils, suggesting that these cells may have fewer CD11b receptors on their membrane surfaces than primary human neutrophils. As CD11b and CD66b have also been used as activation markers on granulocytes (Torsteinsdóttir et al., 1999; Carrigan et al., 2005), a high expression level of both suggests that primary neutrophils may be activated during isolation. The capability of NETosis was also investigated in isolated neutrophils and the neutrophil-like cell model. Data presented in this thesis show that both human neutrophils and differentiated PLB-985 cells successfully formed NETs after stimulation with 20-100 nM PMA. Notably, PLB-985 cell line is also capable of monocytic maturation in the presence of other stimuli (Tucker et al., 1987), and human monocytes have also been confirmed to form extracellular traps (Granger et al., 2017). Therefore, neutrophil-like cells and NETs generated from this cell line may contain some monocytic features.

This chapter also shows that human neutrophils, which were isolated by the standard density gradient centrifugation method, had a sufficiently high purity (94.7%). However, the effects of other components in isolated neutrophils (e.g., eosinophils, basophils, lymphocytes, and platelets) need to be considered in future experiments. In addition, the presence of platelets was quantified, with results suggesting that the CD41 antibody and its isotype control worked well in platelet samples but not in isolated neutrophil samples (platelet data are only preliminary), as the platelet percentage of 16.14% platelets seemed higher than that observed in Wright's stain images. Nevertheless, with alternative platelet marker CD42b, 2.69% platelets were identified in isolated neutrophils samples, which was more compatible with the Wright's stain results. These findings suggest that CD42b may be more effective and accurate than CD41 when quantifying small amounts of platelets in this cell mixture.

In conclusion, differentiated PLB-985 cells are a suitable neutrophil-like model to be used when studying neutrophils and NETs, particularly to avoid the use of human blood during optimization steps. But the lack of some neutrophil-surface antigens indicates that this neutrophil-like cell model did not acquire all the properties of primary neutrophils and its functions and characteristics may be somewhat between those of primary neutrophils and monocytes. Therefore, it will be essential to confirm key data with PLB-985 cells using also primary neutrophils.

Chapter 4 Effects of Neutrophils and NETs on Coagulation

4.1 Introduction

As reviewed in chapter 1, neutrophils and NETs have recently been found in both arterial and venous thrombi. However, the role of neutrophils and NETs in clotting seem to be complex since some conflicting results were found in previous studies. For example, expression of TF has been observed in human and mice neutrophils in some studies, while data from other studies question a role for TF expression in human granulocytes (Østerud et al., 2000; Ritis et al., 2007; Darbousset et al., 2012; Alkarithi et al., 2021). An increased thrombotic risk has been found in patients with chronic diseases in which NETs form, and a possible role of NETs in thrombosis has been shown in baboon and mouse models (Martinod and Wagner, 2014). However, as described in chapter 1, a recent study suggested that intact NETs cannot trigger clotting, while NET components (DNA or histones) purified from human neutrophils could promote clotting. They hypothesized their findings may be explained by the interactions of histone-histone and histone-DNA (Denis F Noubouossie et al., 2019), but there is insufficient evidence yet to confirm this. The mechanisms behind the effects of neutrophils and NETs on coagulation remain to be further studied. This chapter aims at investigating the effects of neutrophils and NETs on coagulation *in vitro*, and whether they influence clot properties, such as structure and stability.

4.2 Objectives

This chapter aims to determine the role of neutrophils and NETs in blood coagulation *in vitro*, to explore whether neutrophils and NETs have different effects on coagulation, then to investigate how they affect the resistance of clots to thrombolysis.

4.3 Methods

4.3.1 Role of Neutrophils and NETs in Clot Formation and Dissolution

Normal pooled plasma (NPP), human neutrophils and neutrophil supernatant were obtained as described in section 2.1. PLB-985 cells were differentiated into neutrophil-like cells as described in section 2.2. NETs were generated and collected from either human neutrophils or differentiated PLB-985 cells as described in section 2.4.2. Turbidity measurements were carried out in purified fibrinogen and NPP clotting systems to investigate the effects of human neutrophils, differentiated PLB-985 cells and their NETs in clot formation and dissolution (section 2.9). The effects of human serum albumin (HSA) and phorbol 12-myristate 13-acetate (PMA), which were used in NETs generation and thus may have remained in NETs samples, were also explored by turbidity measurements.

4.3.2 Data Analysis

GraphPad Prism 7 or Microsoft Excel were used to represent the data graphically. All statistical analyses were performed using GraphPad Prism 7. A

normal distribution of the data was checked by D'Agostino-Pearson omnibus (K2), Shapiro-Wilk (W) test, Anderson-Darling (A2*) or Kolmogorov-Smirnov (distance) tests. The equality of variances was checked by Brown-Forsythe test or F test. Two-tailed unpaired t-test, two-tailed unpaired t test with Welch's correction, one-way ANOVA followed by Tukey's multiple comparisons test, Brown-Forsythe and Welch ANOVA tests followed by Dunnett's T3 multiple comparisons test were used for parametric data. Mann Whitney test and Kruskal-Wallis test followed by Dunn's multiple comparisons test were used for non-parametric data. P-values < 0.05 were considered to indicate statistical significance.

4.4 Results

4.4.1 Effects of Neutrophils and NETs on Clot Formation with Purified Fibrinogen

First, the role of neutrophils and NETs in clotting were detected by turbidity measurements using a purified fibrinogen system. A neutrophil-like cell model (differentiated PLB-985 cells, see chapter 3 for details) and their NETs (PLB-985 NETs) were used to practice and optimise experiments in this chapter prior using human neutrophils and NETs. In a purified fibrinogen system, the addition of either differentiated PLB-985 cells or PLB-985 NETs had no significant effect on clot formation (Figure 4-1 a). The lag time of clotting triggered by differentiated PLB-985 cells alone or PLB-985 NETs alone were significantly longer than thrombin control ($P < 0.05$) (Figure 4-1 c). In addition, clots

triggered by differentiated PLB-985 cells alone or PLB-985 NETs alone showed significantly lower maximum absorbance ($P < 0.001$, $P < 0.01$, respectively) and slower turbidity V_{max} ($P < 0.01$) than the thrombin control (Figure 4-1 d & e).

Human neutrophils and human NETs were used to confirm the results using the neutrophil-like cell model. In agreement with the PLB-985 data, human neutrophils and human NETs had no significant effect on clot formation in a purified fibrinogen system (Figure 4-1 b). The lag time of clotting triggered by human neutrophils alone was about 6-fold longer than that of the thrombin control (Figure 4-1 c). The lag time of clotting triggered by human NETs alone was about 5-fold longer than that of the thrombin control (Figure 4-1 c). Clotting triggered by human neutrophils alone or human NETs alone showed significantly lower maximum absorbance ($P < 0.01$, $P < 0.0001$, respectively), when compared to thrombin control (Figure 4-1 d). They also showed significantly lower turbidity V_{max} ($P < 0.01$) than that of the thrombin control (Figure 4-1 e). In addition, clotting triggered by human neutrophils alone showed significantly higher maximum absorbance ($P < 0.05$) than human NETs alone (Figure 4-1 d).

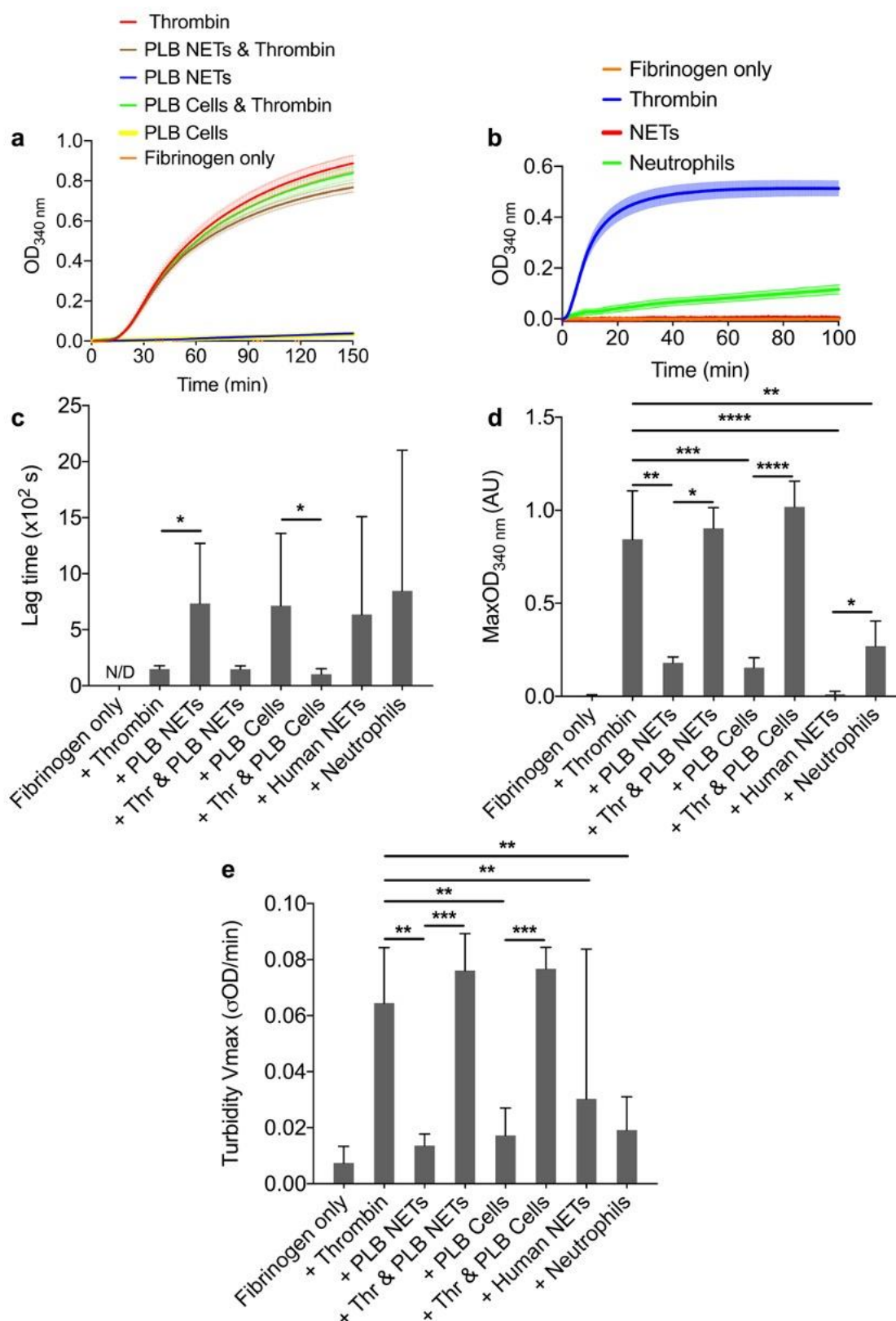


Figure 4-1. Comparison of clot formation in a purified fibrinogen system in the presence of PLB NETs and cells versus human NETs and neutrophils. Differentiated PLB-985 cells or human neutrophils (200,000 cells/100 μ l) or their NETs (generated from 200,000 cells/100 μ l) were added to purified fibrinogen. (a) and (b) Turbidity curves showing the kinetics of clot formation. (c) Lag time, (d) MaxOD and (e) turbidity Vmax were quantified. Other concentrations: thrombin (0.1 U/ml), fibrinogen (2 mg/ml), CaCl₂ (1.5 mM). Error bars represent \pm SD of three independent repeats in triplicates. N/D stands for not detectable. * $P < 0.05$, ** $P < 0.01$, *** $P < 0.001$, **** $P < 0.0001$. (Partial data were adapted from Shi et al., 2021)

4.4.2 Effects of Neutrophils and NETs on Clot Formation in Plasma

The role of neutrophils and NETs in clotting were detected by turbidity measurements in normal pooled plasma (NPP). Differentiated PLB-985 cells and PLB-985 NETs were again used before human neutrophils and human NETs. Unlike in purified fibrinogen systems, both differentiated PLB-985 cells and PLB-985 NETs triggered clotting in plasma, in the absence of any other coagulant triggers (Figure 4-2 a). The addition of PLB-985 NETs significantly shortened the lag time of clotting ($P < 0.01$) and increased the turbidity V_{max} ($P < 0.001$), when compared to thrombin control (Figure 4-2 c & e). But, the addition of neither differentiated PLB-985 cells nor PLB-985 NETs apparently affected the maximum absorbance (Figure 4-2 d).

Human neutrophils and human NETs were also used in NPP turbidity measurements. Both human neutrophils and human NETs triggered clotting in plasma, independent of any other coagulant triggers (Figure 4-2 b). As shown in Figure 4-2 c, the lag time of clotting triggered by human NETs alone was 5-fold longer than that of the thrombin control ($P < 0.05$). The lag time of human NETs was also significantly longer than human neutrophils ($P < 0.0001$). Clotting triggered by human neutrophils alone showed significantly higher maximum absorbance than clotting triggered by human NETs alone ($P < 0.05$) (Figure 4-2 d). Clotting triggered by human NETs alone had significantly lower maximum absorbance than thrombin control ($P < 0.01$) (Figure 4-2 d), and the addition of

thrombin significantly ($P < 0.05$) increased the maximum absorbance of NET-induced clotting but did not affect that of neutrophil-induced clotting (Figure 4-2 d). Only human neutrophils, but not human NETs, statistically slowed the turbidity V_{max} compared to thrombin control (Figure 4-2 e).

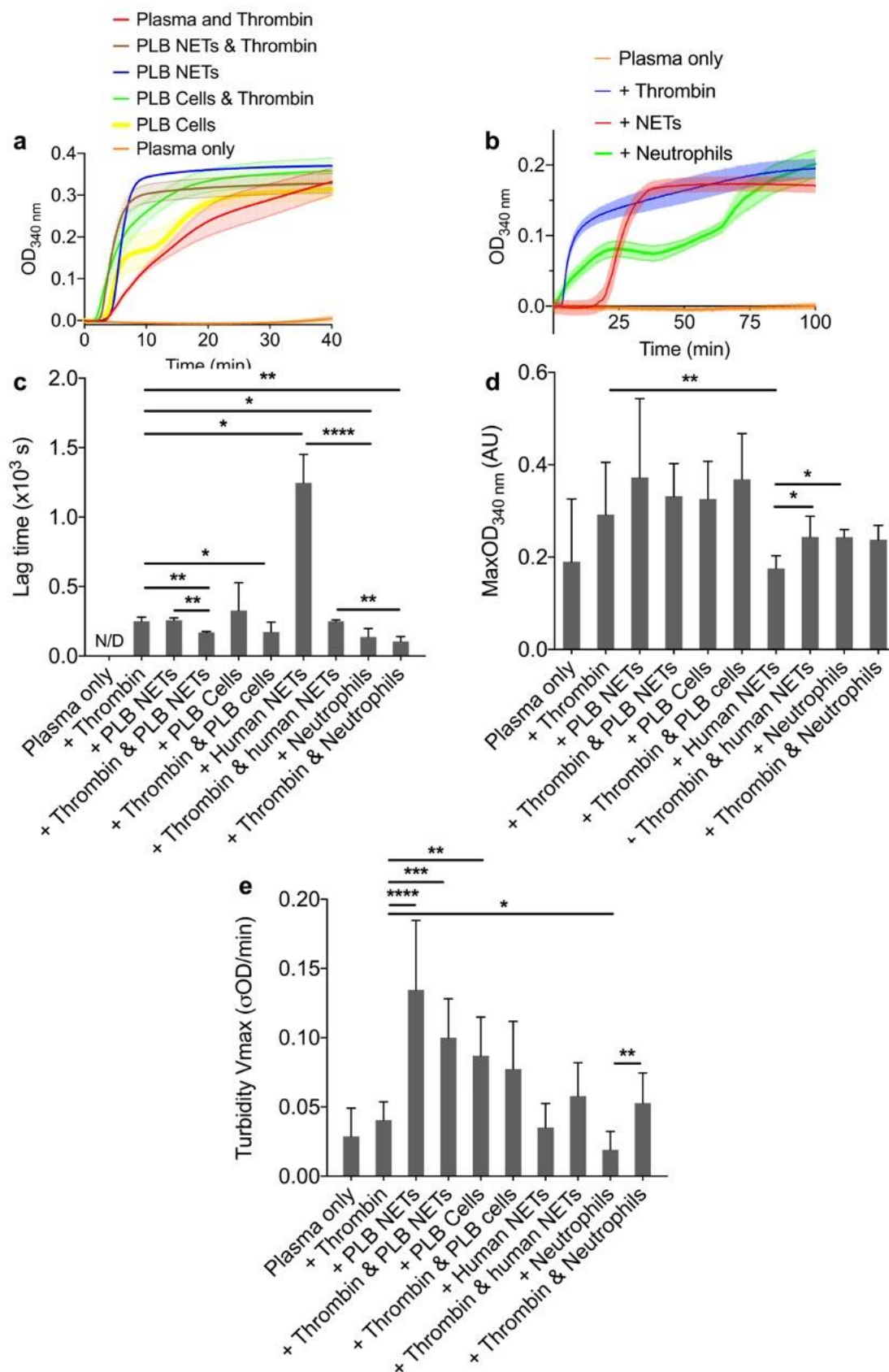


Figure 4-2. Comparison of clot formation in plasma in the presence of PLB NETs and cells versus human NETs and neutrophils. Differentiated PLB-985 cells or human neutrophils (200,000 cells/100 μ l) or their NETs (generated from 200,000 cells/100 μ l) were added to plasma. (a) and (b) Turbidity curves showing the kinetics of clot formation. (c) Lag time, (d) MaxOD and (e) turbidity Vmax were quantified. Other concentrations: thrombin (0.1 U/ml), plasma (diluted 1:6), CaCl₂ (3.33 mM). Error bars represent \pm SD of three independent repeats in triplicates. N/D stands for not detectable. * $P < 0.05$, ** $P < 0.01$, *** $P < 0.001$, **** $P < 0.0001$. (Partial data were adapted from Shi et al., 2021)

The effects of PMA, which was used to stimulate NETs formation, on clot formation were investigated in purified fibrinogen and plasma. PMA only significantly delayed ($P < 0.01$) the lag time of thrombin-induced clotting in plasma (Figure 4-3 b), and had no other effect on clot formation in either purified fibrinogen or plasma (Figure 4-3). Clots formed in plasma had a notably longer lag time and lower MaxOD than clots formed using purified fibrinogen (Figure 4-3 b & c), which may be due to the naturally occurring inhibitors of coagulation present in the plasma and plasma was used in a 1:6 dilution. The effects of 2% HSA, which was supplemented in NETs stimulation media, on clot formation were investigated in purified fibrinogen. As shown in figure 4-4, HSA only significantly increased ($P < 0.05$) the MaxOD of thrombin-induced clotting, and had no other effect on clot formation in purified fibrinogen.

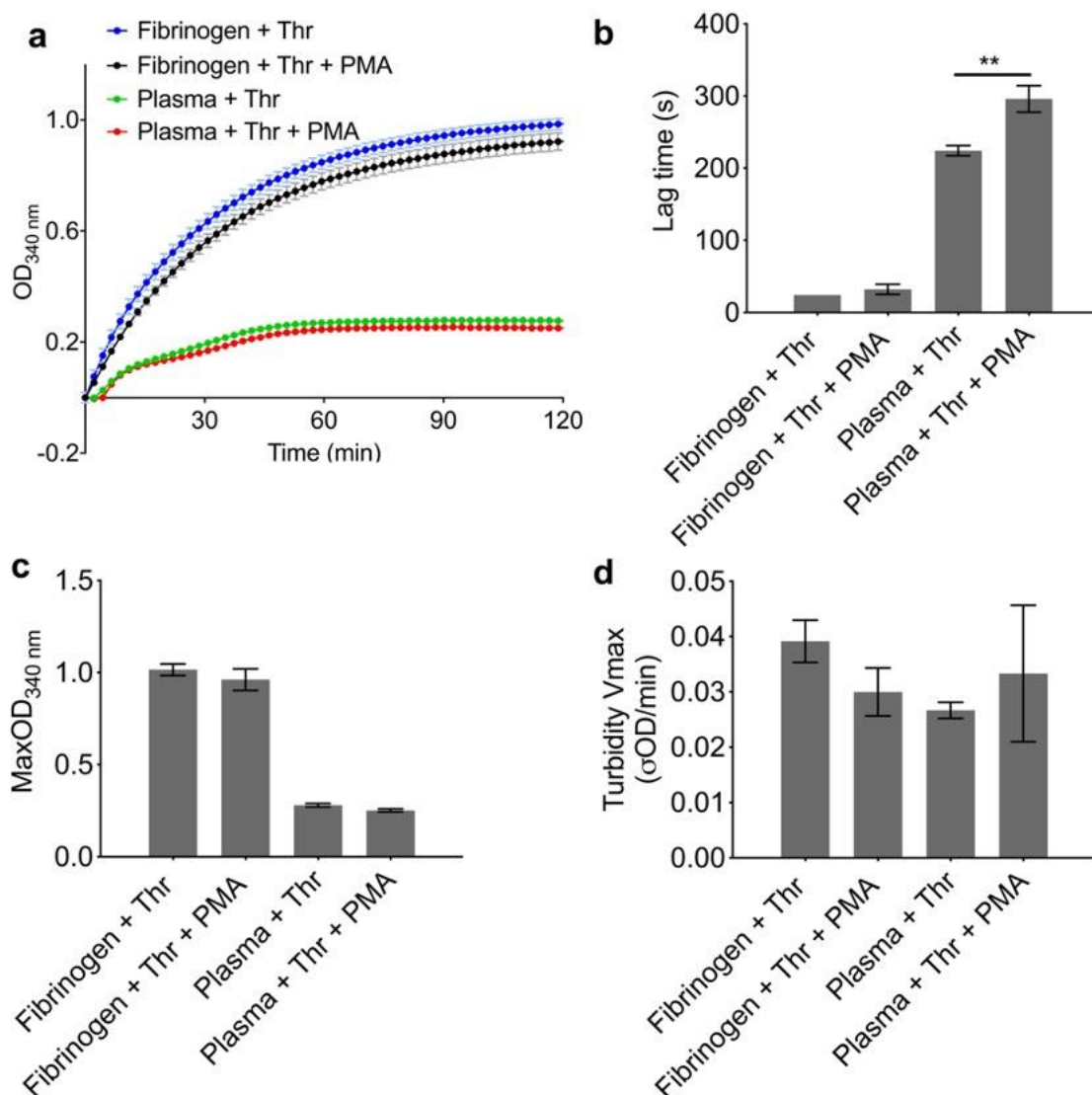


Figure 4-3. Effects of PMA on clot formation in purified fibrinogen and plasma. (a) Turbidity curve showing the kinetics of clot formation. (b) Lag time, (c) MaxOD and (d) turbidity Vmax were quantified. Other concentrations: fibrinogen (2 mg/ml), plasma (diluted 1:6), PMA (20 nM), thrombin (0.1 U/ml), CaCl₂ (1.5 mM in purified fibrinogen or 3.33 mM in plasma). Error bars represent \pm SD of three repeats (n = 3). ** P < 0.01. (Partial data were adapted from Shi et al., 2021)

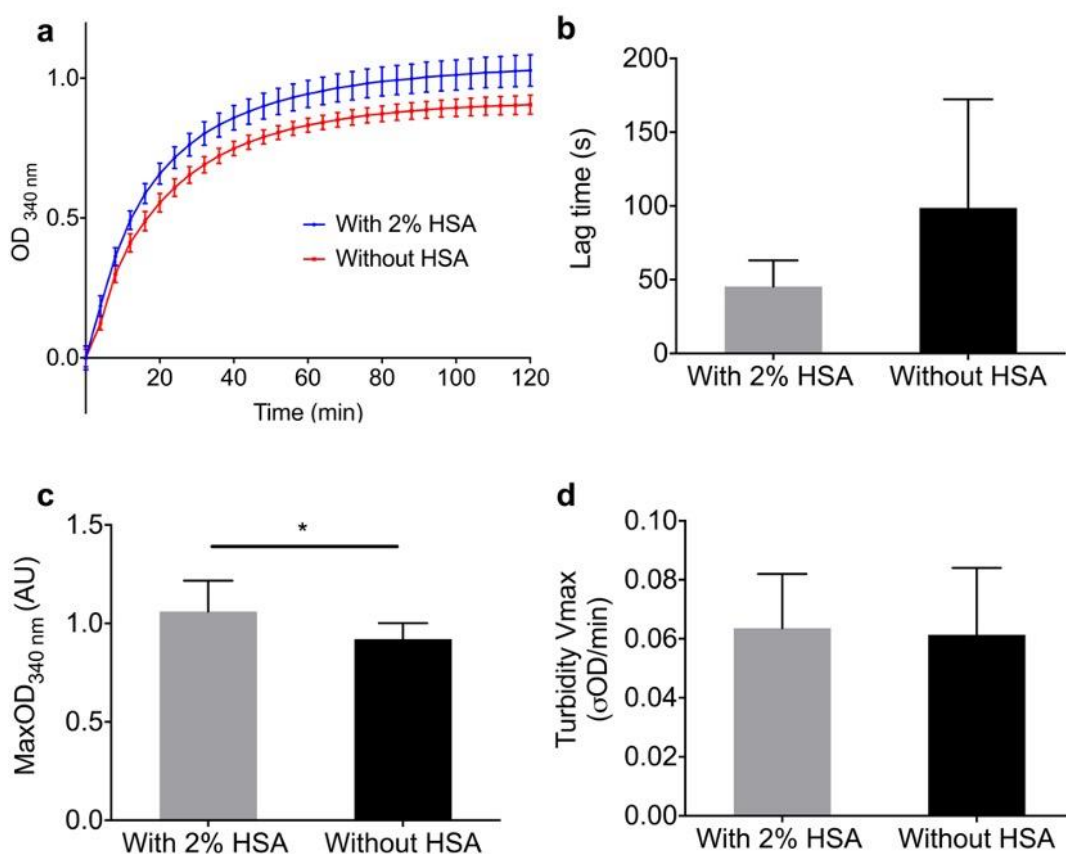


Figure 4-4. Effects of human serum albumin (HSA) on clot formation with purified fibrinogen. (a) Turbidity curve showing the kinetics of clot formation. (b) Lag time, (c) MaxOD and (d) turbidity Vmax were quantified. Other concentrations: 2 mg/ml fibrinogen, 0.1 U/ml thrombin, 1.5 mM CaCl₂. Error bars represent SD of three independent repeats in triplicates. * P < 0.05.

To determine whether the procoagulant effects of human neutrophils required presence of the cells themselves or were caused by any proteins they may release, the supernatant of human neutrophils was tested in NPP turbidity measurements. Figure 4-5 shows that the neutrophil supernatant also triggered clotting without the addition of any other coagulation triggers. Clotting triggered by the supernatant had a significantly longer lag time than neutrophils ($P < 0.001$) (Figure 4-5 b), but they showed a similar value of the final maximum

absorbance and turbidity Vmax (Figure 4-5 c & d). Neutrophil isolation media (Lympholyte-poly) did not notably affect clot formation in plasma (Figure 4-5 a).

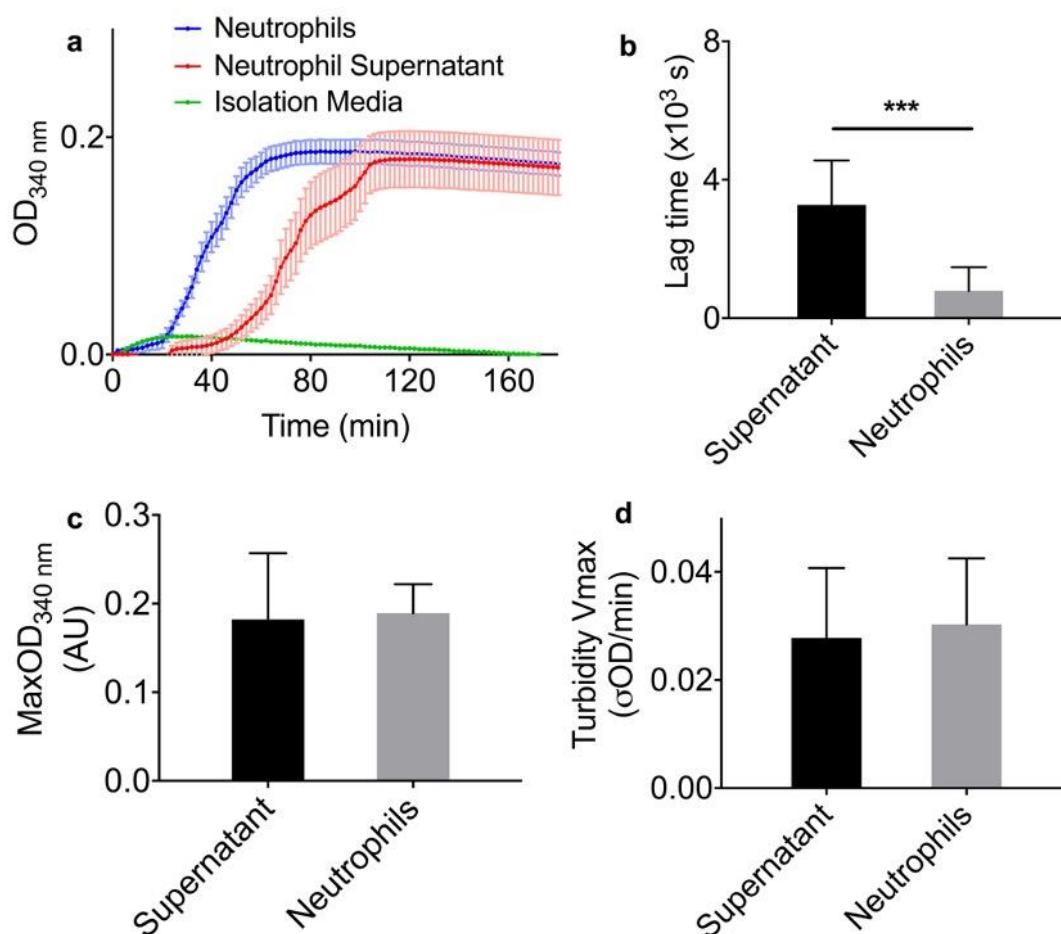


Figure 4-5. Effects of human neutrophil supernatant on clot formation in plasma. (a) Clot polymerization curves, which obtained by turbidity, showing the effects of neutrophil isolation media, human neutrophils (200,000 cells/100 μ l) and their supernatant on clot formation when added to plasma. (b) Lag time, (c) MaxOD and (d) turbidity Vmax were quantified. Other concentrations: plasma (diluted 1:6), CaCl₂ (3.33 mM). Error bars represent SD of three independent repeats in triplicates. *** P < 0.001. (Partial data were adapted from Shi et al., 2021)

Next, whether red blood cell (RBC) lysis buffer, which is used during neutrophil isolation, could activate neutrophils was investigated. As compared with neutrophils isolated normally, adding additional RBC lysis buffer did not apparently affect neutrophil-induced clotting in plasma (Figure 4-6).

Interestingly, when neutrophils were isolated without using RBC lysis buffer, the remaining RBCs significantly shortened the lag time ($P < 0.05$) and increased the turbidity Vmax ($P < 0.01$) of neutrophil-induced clotting (Figure 4-6 b & d).

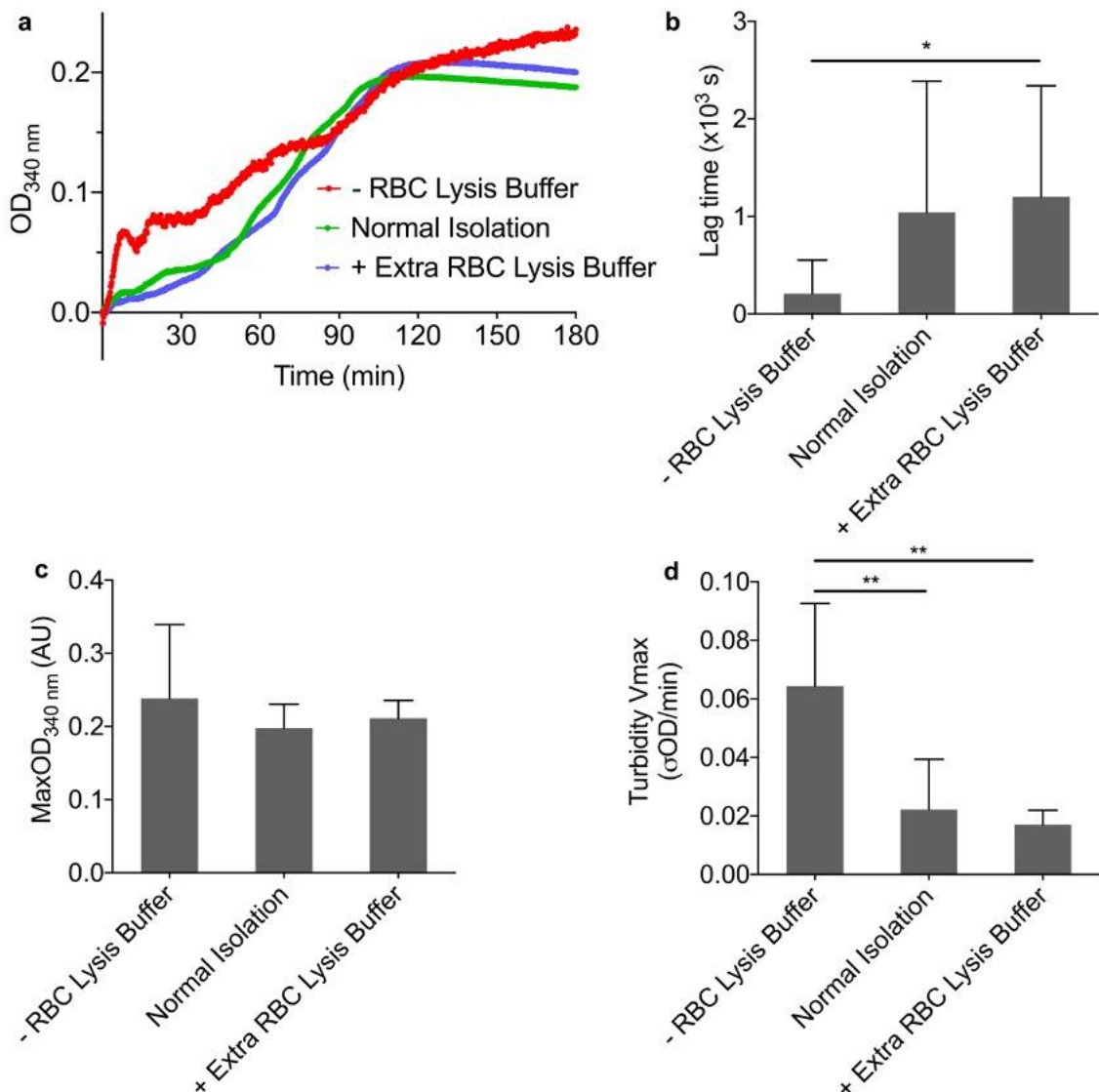


Figure 4-6. Effects of RBC lysis buffer on the procoagulant effects of human neutrophils in plasma. “-RBC lysis buffer”: neutrophils were isolated without adding RBC lysis buffer. “Normal isolation”: neutrophils were isolated with adding RBC lysis buffer. “+Extra RBC lysis buffer”: neutrophils were isolated in the normal method, but extra RBC lysis buffer (final dilution 1:3) was added when turbidity measurements were carried out. Final concentrations: plasma (diluted 1:6), CaCl₂ (3.33 mM), neutrophils (200,000 cells/100 μl). (b) Lag time, (c) MaxOD and (d) turbidity Vmax were quantified. Error bars represent SD of 2-3 independent repeats in triplicates. * $P < 0.05$, ** $P < 0.01$.

4.4.3 Effects of Neutrophils and NETs on Clot Dissolution in Plasma

The role of human neutrophils or human NETs in plasma clot dissolution was also investigated by turbidity measurements. As shown in Figure 4-7 a, neutrophil-induced and NET-induced plasma clots had significantly lower average rate of lysis ($P < 0.0001$) than thrombin control. Neutrophil-induced clots showed statistically lower average rate of lysis ($P < 0.01$) than NET-induced clots. However, only neutrophils decreased the average rate of lysis ($P < 0.05$) if thrombin was added simultaneously. Consistent with the reduced lysis rates, both neutrophil- and NET-induced clots took significantly longer time to reach 50% lysis ($P < 0.001$, $P < 0.0001$, respectively) than thrombin control (Figure 4-7 b). Notably, in the absence of thrombin, neutrophils and NETs played a greater role in increasing the resistance of clots to thrombolysis.

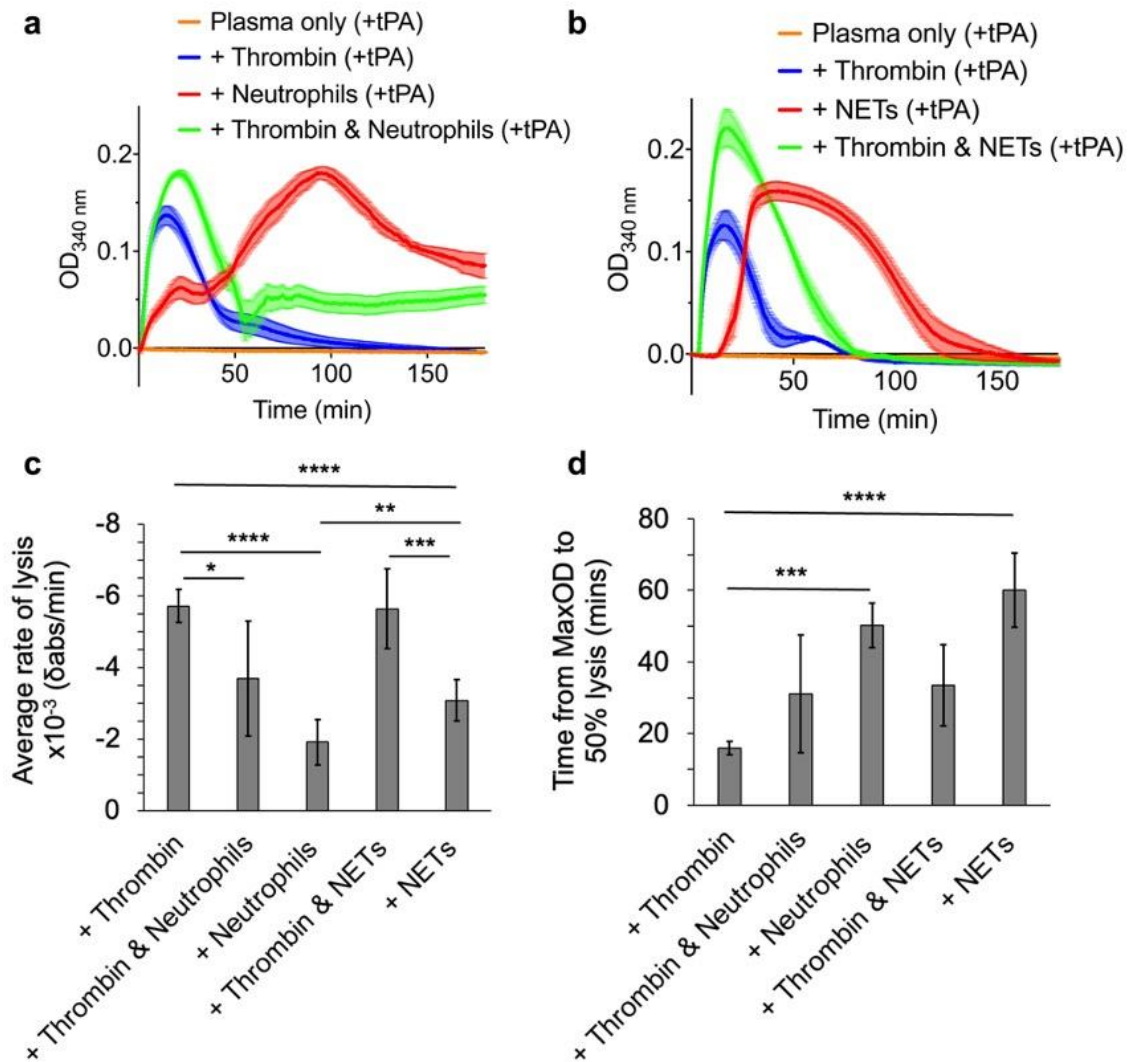


Figure 4-7. Effect of human neutrophils or human NETs on clot dissolution in plasma. Neutrophils (200,000 cells/100 μ l) or NETs (generated from 200,000 cells/100 μ l) were added in plasma to trigger clotting, thrombin (0.1 U/ml) was used as a control. **(c)** Average rate of lysis and **(d)** time from MaxOD to 50% lysis were quantified. Other concentrations: plasma (diluted 1:6), CaCl₂ (3.33 mM), tPA (0.03 mg/ μ l). Error bars represent \pm SD of three independent repeats in triplicates. * $P < 0.05$, ** $P < 0.01$, *** $P < 0.001$, **** $P < 0.0001$. (Partial data were adapted from Shi et al., 2021)

4.5 Discussion

In this chapter, the role of neutrophils and NETs in clot formation and dissolution were investigated. In a purified fibrinogen system, when compared to clotting triggered by thrombin, the significantly longer lag time, lower maximum absorbance and slower turbidity V_{max} suggest that neither neutrophils nor NETs triggered noteworthy fibrin polymerization. They could not induce clot formation in the absence of thrombin. However, neutrophils and NETs induced significant clotting without the addition of any other coagulation trigger in plasma. These findings suggest that some components in plasma may interact with neutrophils and NETs, resulting in the formation of blood clots. PMA and HSA that may remain in NETs samples have some minor effects on thrombin-induced clotting but did not explain the findings of clot formation with neutrophils and NETs in plasma presented in this chapter. Neutrophils and NETs also delayed dissolution of plasma clots, indicating that they could increase the resistance of clots to thrombolysis.

To further explore the potential mechanisms behind the procoagulant effects of neutrophils, and whether the cells themselves or factors secreted by the cells may be responsible, the role of neutrophil supernatant in clot formation was investigated. Turbidity results show that neutrophil supernatant had a similar effect on clot formation as neutrophils themselves, except for a somewhat longer time for protofibril formation (lag time). This finding suggests that isolated neutrophils may have been partially activated, and then induced clotting via

some mediators they released. RBC lysis buffer had no apparent contribution to the activation of neutrophils. Notably, NET-induced clotting also had a significantly longer lag time than neutrophil-induced clotting. This may be due to some mediators on the surface of neutrophils, but possibly lost in NETs and neutrophil supernatant, shortening the time for protofibril formation. Human neutrophil-induced clotting had a higher maximum absorbance than human NET-induced clotting in both the purified fibrinogen and plasma systems, suggesting there may be additional interactions between neutrophils and fibrinogen.

Differentiated PLB-985 cells were used as a neutrophil-like cell model in this chapter. In general, results obtained with differentiated PLB-985 cells and PLB-985 NETs were similar when compared to those with human neutrophils and human NETs. For example, cells and NETs from both PLB-985 and neutrophil origin showed no effect on clot formation in purified fibrinogen, but could induce clotting independently of thrombin in plasma. However, unlike the differences between human neutrophils and human NETs, there was no significant difference between clotting triggered by differentiated PLB-985 cells and by PLB-985 NETs. The other aspect that is different from human NETs, was that PLB-985 NETs significantly shortened the time of protofibril formation (lag time) and significantly increased the rate of clot formation (turbidity V_{max}) in plasma, compared with thrombin control. Thus, the PLB-985 cell model could be a suitable substitute for human neutrophils (NETs) in some coagulation-related

studies, but important differences remain compared to primary neutrophils that need to be considered.

In conclusion, neutrophils and NETs interact with components of plasma to promote clotting and enhance the resistance of clots to thrombolysis. Although NETs are generated from neutrophils, their procoagulant effects and the underlying mechanisms was different. Future experiments are required to investigate which coagulation factors interact with neutrophils or NETs, and which neutrophil factors, proteins or enzymes may be involved in the procoagulant effects of neutrophils. It is likely that quiescent, circulating and not-activated neutrophils may not trigger clotting, or that there are some mechanisms in circulation that prevent neutrophil-induced clotting (or neutrophil protein-induced clotting). To explore this, the first challenge may be to keep neutrophils fully quiescent during isolation and subsequent *in vitro* experiments. Generally, to limit neutrophil activation, buffers used to isolate neutrophils are free of Ca^{2+} and Mg^{2+} , but that may not be sufficient as the whole blood from which the cells originate do contain such ions. Thus, further optimization of the methods for the isolation of neutrophils may still be explored in future studies.

Chapter 5 Role of Neutrophils and NETs in Overall Structure of Clots

5.1 Introduction

Neutrophils and NETs were shown to promote clotting and delay thrombolysis, likely in a different manner (as described in Chapter 4). Therefore, their individual effects on clot structure are also worthy of consideration. Clot structure, which is directly related to the stability and fibrinolysis resistance of clots, is generally determined by some properties, such as fibrin fibre thickness, fibre density and porosity. The fibrin fibre thickness and fibre density can be directly examined using specialized microscopy techniques, such as laser scanning confocal microscopy and scanning electron microscopy (SEM). The porosity can be indirectly studied by clot permeability, which uses a pressure-driven system to quantify fluid flow through clots and uses flow characteristics to calculate porosity or average pore-size (Mihalko and Brown, 2020).

A previous study examined the effects of NETs on clot stability using human granulocyte DNA and commercial histones. The authors of this study found that the DNA-histone complexes increased the median diameter of fibre from 84 to 123 nm, which improved the stability and rigidity of clots (Longstaff et al., 2013). Another study has shown that intact human NETs are able to act as fibrin-independent scaffolds for platelet and RBC binding and aggregation in thrombi. Platelets and RBCs were still held together by the NET-scaffold when fibrin was removed using tissue plasminogen activator (tPA) (Fuchs et al., 2010). However, how intact NETs affect fibrin fibre thickness and the molecular of structural interaction between NETs and fibrin fibres are not yet fully

understood. The role of neutrophils on clot structure and whether it differs from that of NETs also remains to be further explored.

5.2 Objectives

This chapter aims to explore and compare the role of PLB-985 cell model, human neutrophils, and their respective NETs on the overall structure of clots using microscopy and imaging methods. Additionally, the permeability of human neutrophil- and human NET-induced clots is assessed to quantitatively investigate overall pore-size and network structure.

5.3 Methods

5.3.1 Visualization of inner Structure of Clots

Normal pooled plasma (NPP) and human neutrophils were obtained as described in section 2.1. PLB-985 cells were differentiated into neutrophil-like cells as described in section 2.2. NETs were generated and collected from either human neutrophils or differentiated PLB-985 cells as described in section 2.4. Plasma clot formation was triggered by thrombin only (control), differentiated PLB-985 cells, PLB-985 NETs, human neutrophils or human NETs. The structure of clots was analysed by laser scanning confocal microscopy (section 2.8) and scanning electron microscopy (SEM) (section 2.13).

To explore whether atomic force microscopy (AFM) is a feasible method to observe the interaction between fibrin fibres and cells or between fibrin fibres and NETs at the molecular level, differentiated PLB-985 cells and PLB-985 NETs were used in the optimization of this method (section 2.12).

5.3.2 Permeability of Clots

Permeability is carried out to analyse the degree to which liquid is able to pass through clots. Plasma clot formation was triggered by thrombin only (control), human neutrophils or human NETs. The permeation system was set up and the permeability coefficient (K_s , Darcy constant) was calculated as described in section 2.15. A high permeability coefficient reflects a porous clot structure.

5.3.3 Data Analysis

AFM images were analysed using the NanoScope Analysis x86 v190r1 software. Contrast and brightness of optical, fluorescence and SEM images were adjusted by Fiji-Image J. Fibrin fibre diameter (80 fibres from 3-5 clots), NET fibre diameter and other components shown in SEM images were analysed by Fiji-Image J. Fibrin fibres in confocal images (3-4 clots, 20 positions of each clot) were counted by Fiji-Image J macros designed by Dr Fraser Macrae and Dr Cedric Duval, Ariëns group, Leeds Institute of Cardiovascular and Metabolic Medicine, University of Leeds. Statistical analyses of permeation data were performed using GraphPad Prism 7. Distribution of the data was checked for normality by D'Agostino-Pearson omnibus (K_2), Shapiro-Wilk (W)

test Anderson-Darling (A2*) or Kolmogorov-Smirnov (distance) tests. The equality of variances was checked by Brown-Forsythe test or F test. Kruskal-Wallis test followed by Dunn's multiple comparisons test was used for non-parametric data. P-values < 0.05 were considered to indicate statistical significance.

5.4 Results

5.4.1 Effects of Neutrophil-like Cells and Human Neutrophils on Clot

Structure

As described in chapter 3, differentiated PLB-985 cells were used as a neutrophil-like cell model in this study. Confocal images show similar structures for differentiated PLB-985 cell-induced and thrombin-induced clots (Figure 5-1 a & b). However, unlike differentiated PLB-985 cells, human neutrophil-induced clots showed a weaker network structure composed of thinner fibrin fibres interspersed between the cells (Figure 5-1 c). Neutrophils did not apparently alter the structure of clots when added in combination with thrombin, as compared with thrombin only control (Figure 5-1 d).

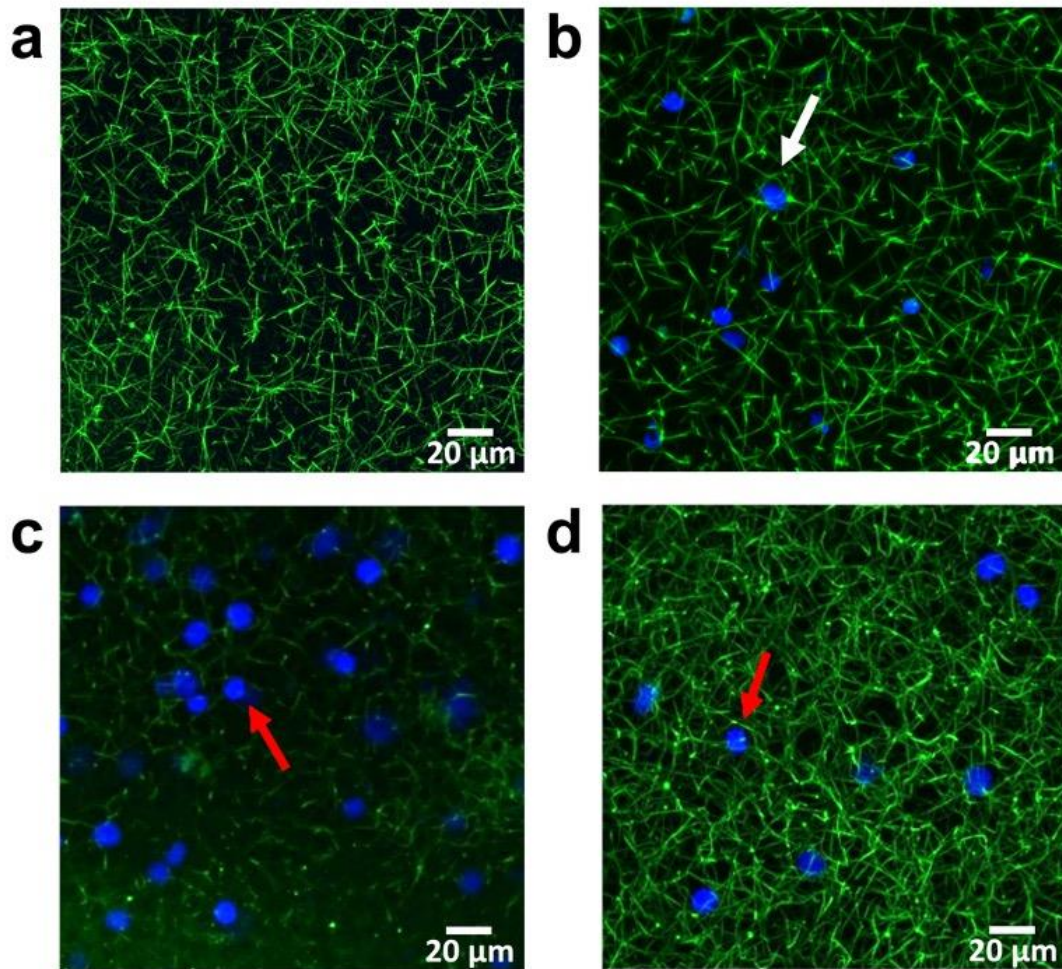


Figure 5-1. Confocal Z-stacks images of differentiated PLB-985 cell-induced and human neutrophil-induced plasma clots. (a) Clot triggered by thrombin. (b) Clot triggered by differentiated PLB-985 cells. (c) Clot triggered by human neutrophils. (d) Clot triggered by thrombin and human neutrophils. Final concentrations: plasma (1:6), CaCl_2 (3.33 mM), thrombin (0.1U/ml), differentiated PLB-985 cells (200,000 cells/100 μl), human neutrophils (200,000 cells/100 μl). Blue: DAPI-stained DNA. Green: Alexa Fluor 488 labeled fibrinogen. White arrow indicates differentiated PLB-985 cells. Red arrows indicate human neutrophils. Scale bars shows 20 μm . ($n \geq 3$) (Partial data were adapted from Shi et al., 2021)

The effects of different cell types on the three-dimensional structure of clots were further investigated using SEM, which allows for higher resolution images at higher magnification. SEM images showed that the membrane surface of PLB-985 cell formed many flaps after differentiation, which were similar to those

seen on the surface of human neutrophil (Figure 5-2). The difference in diameter between normal PLB-985 cells (8.22 μm), differentiated PLB-985 cells (8.17 μm) and human neutrophils (8.52 μm) were minor. Filamentous structures were observed on the membrane surface of the normal PLB-985 cells, differentiated PLB-985 cells and human neutrophils (Figure 5-2 a, c, d). The average filament diameter of normal PLB-985 cells (117.2 nm), differentiated PLB-985 cells (114.3 nm) and human neutrophils (94.4 nm) were not statistically different. Cells seemed to connect with each other via some of these filaments (Figure 5-2 b). As shown in Figure 5-3, the fibrin fibres wrapped around the cells and formed a network structure in differentiated PLB-985 cell-induced clots. The overall structure of differentiated PLB-985 cell-induced clots was visibly looser than that of thrombin-induced clots. Interestingly, the overall clot structure of neutrophil-induced clots was remarkably different from the other conditions. Neutrophils were surrounded by lots of small fibres, and these clots failed to form a substantial fibre network. Comparing the confocal and SEM images of neutrophil induced clots (Figure 5-1 c and 5-3) there seems to be clearer presence of fibrin fibres in the confocal images than in the SEM images. The reason(s) for this are not entirely clear. However, some fibrin fibres can also be seen in the SEM images, as well as the confocal images, thus it is likely that some degree of fibrin fibre network has been formed. Please see Appendix 3 for more SEM images.

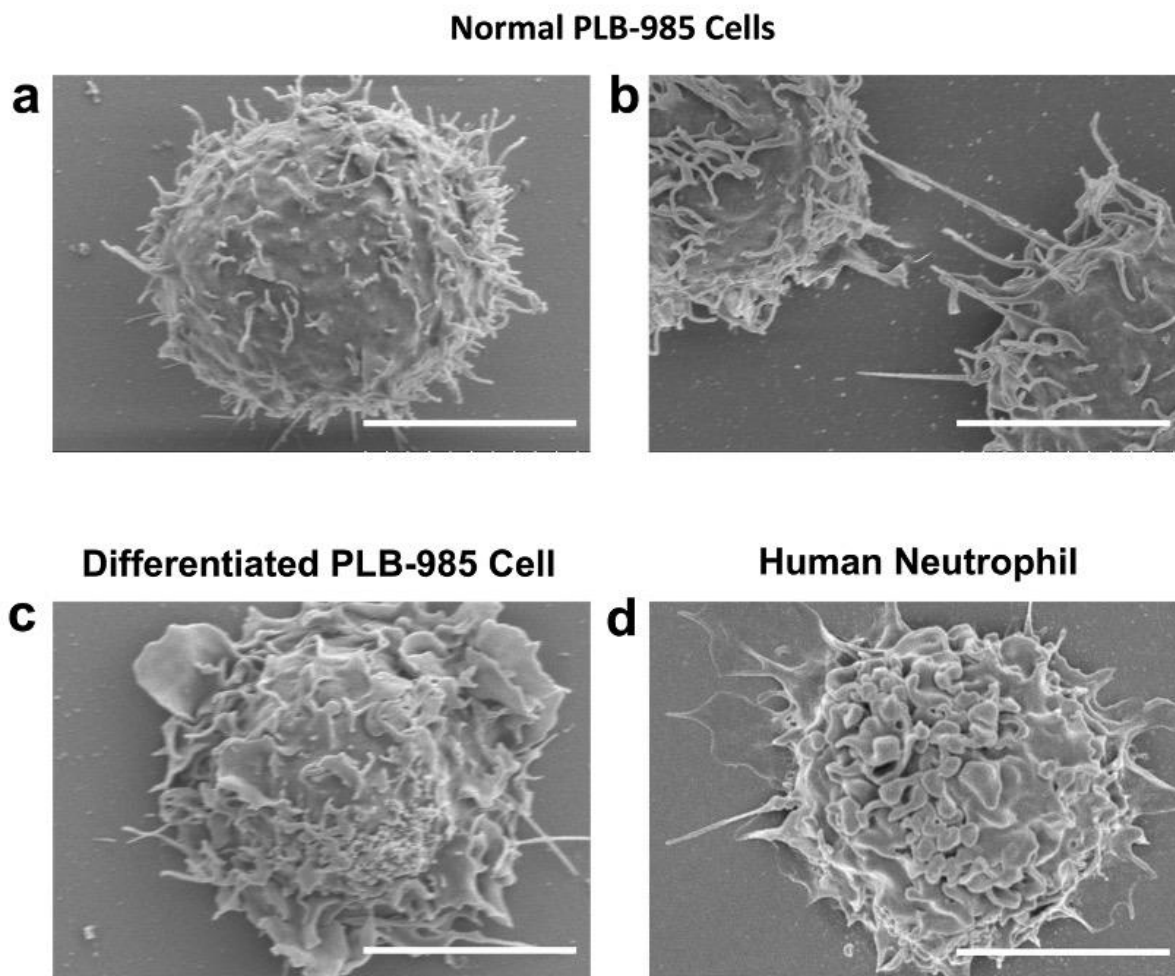
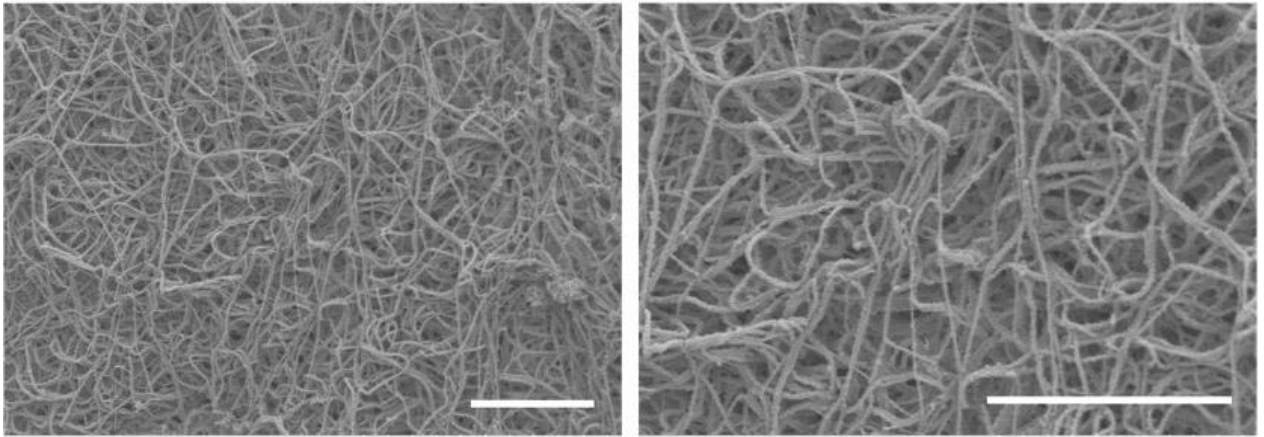
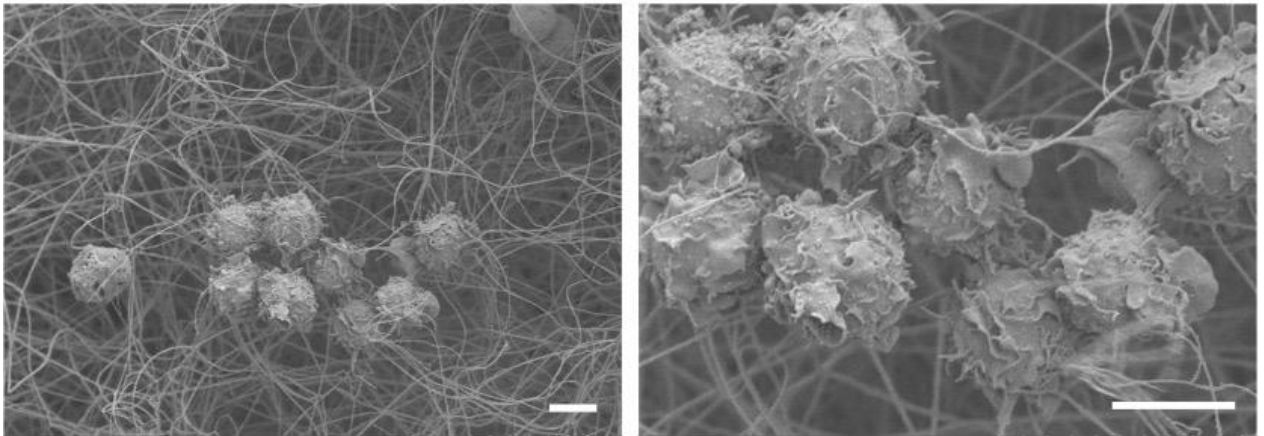


Figure 5-2. SEM images of normal PLB-985 cells (**a**, **b**), differentiated PLB-985 cell (**c**) and human neutrophil (**d**). Scale bars are 5 μm . ($n \geq 3$)

Thrombin-induced Clots



Differentiated PLB-985 Cell-induced Clots



Human Neutrophil-induced Clots

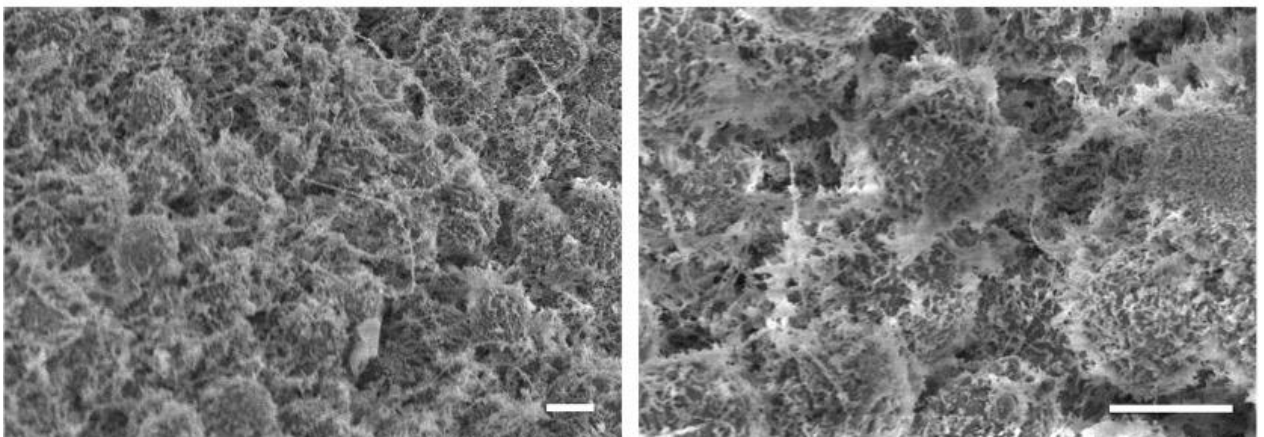


Figure 5-3. SEM images of differentiated PLB-985 cell-induced and human neutrophil-induced plasma clots. Thrombin-induced clots were used as a control. Final concentrations: Plasma (diluted 1:3), 10 mM CaCl₂, 1 U/ml thrombin. Scale bars are 5 μ m. (n \geq 3)

5.4.2 Effects of PLB-985 NETs and Human NETs on Clot Structure

The role of PLB-985 NETs and human NETs in clot structure were also investigated using laser scanning confocal and scanning electron microscopy. Confocal images show that the fibrin fibres of both PLB-985 NET-induced and human NET-induced clots formed a normal network structure (Figure 5-4 a & b). Figure 5-4 (c) and (d) show two positions of a same clot triggered by human NETs only, where fibrin fibres were denser when surrounding a big cluster of NETs, and looser with big holes in the area without NETs. When adding human NETs and thrombin together, the fibrin fibres still accumulated around NETs, as compared with thrombin only control (Figure 5-4 e & f).

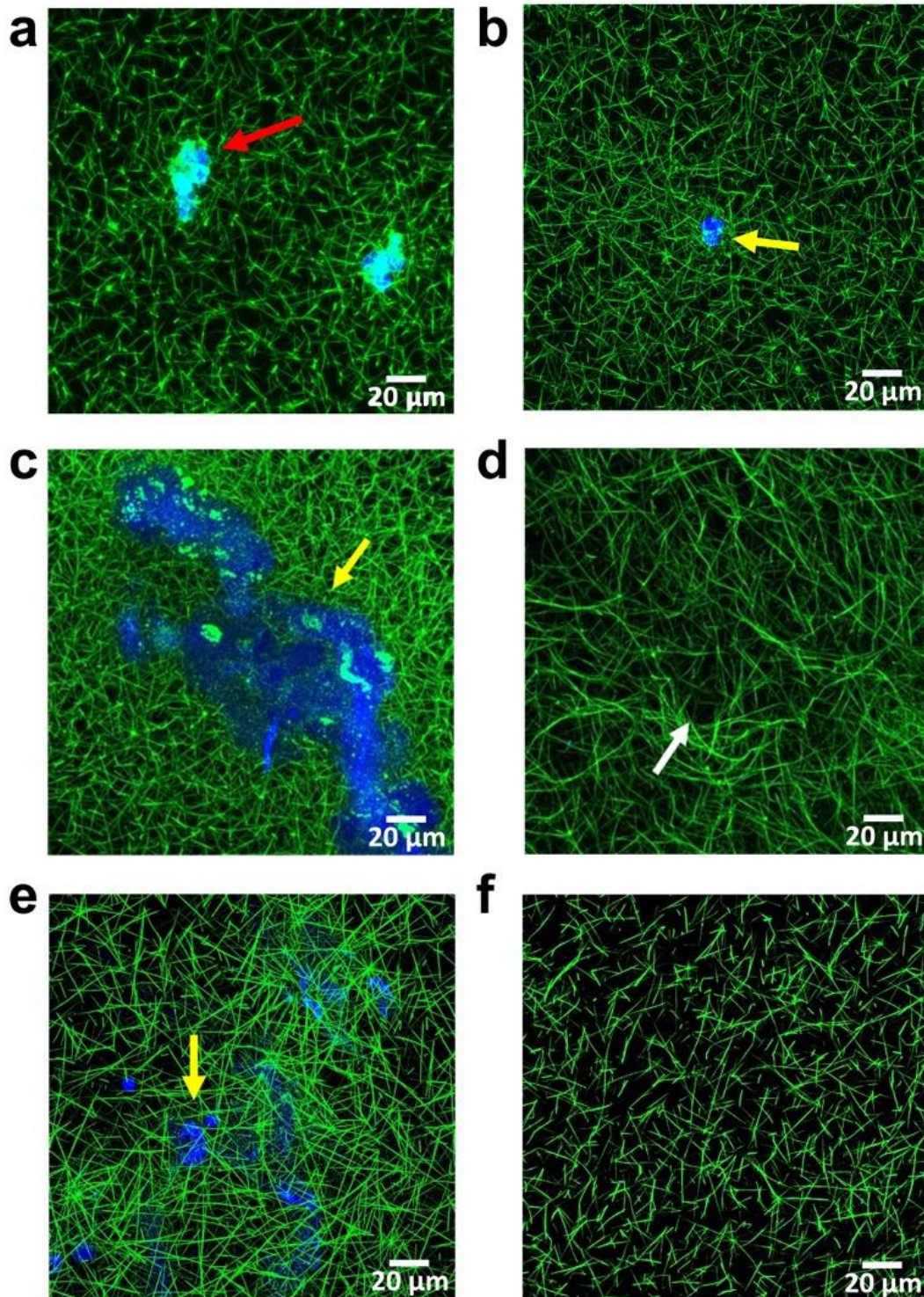


Figure 5-4. Confocal Z-stacks images of PLB-985 NET-induced and human NET-induced plasma clots. (a) Clot triggered by PLB-985 NETs only. (b), (c) and (d) Clot triggered by human NETs only, images c & d showing two positions of a same clot. (e) Clot triggered by thrombin and human NETs. (f) Clot triggered by thrombin only. Final concentrations: plasma was diluted 1:6 (except e & f was 1:3), CaCl_2 (3.33 mM), thrombin (0.1U/ml), PLB-985 NETs (generated from 200,000 cells/100 μl), human NETs (generated from 200,000 cells/100 μl). Blue: DAPI-stained DNA. Green: Alexa Fluor 488 labeled fibrinogen. Red arrow indicates PLB-985 NETs, yellow arrows indicate human NETs, white arrow indicates large pores. ($n \geq 3$) (Please see Appendix 2 for images of broken PLB-985 NET-induced clots) (Partial data were adapted from Shi et al., 2021)

The three-dimensional structure of NETs and NET-induced clots was observed under SEM. As Figure 5-5 shows, the overall structure of PLB-985 NETs and human NETs under SEM microscopy were similar, and the fibres of NETs were made up of many minute DNA fibres. The single NET fibre diameter of PLB NETs was around 22.3 - 39.5 nm, and that of human NETs around 9.70 - 29.1 nm. Notably, some spherical particles were found in PLB-985 NETs but not in human NETs. The diameter range of these particles ranged from 182.2 to 1051.6 nm. Both PLB-985 NET-induced clot and human NET-induced clot formed a normal network structure, and there were no apparent visual differences between them (Figure 5-6 and Figure 5-7). It is difficult to accurately distinguish NET fibres and fibrin fibres, due to their similar structure observed under SEM. But, in the images with higher magnification (Figure 5-6 and 5-7), it is obvious that some long smooth fibres with uniform thickness are entangled by other fine fibres, which may likely represent fibrin and NET fibres, respectively. In some images, NETs structure, and thin and thick fibres intertwined with NETs can clearly be observed. Particularly, in Figure 5-6 bottom image, the PLB-985 NET fibres, fibrin fibres and some spherical particles seemed to be mixed within a denser mesh. Please see Appendix 3 for more SEM images.

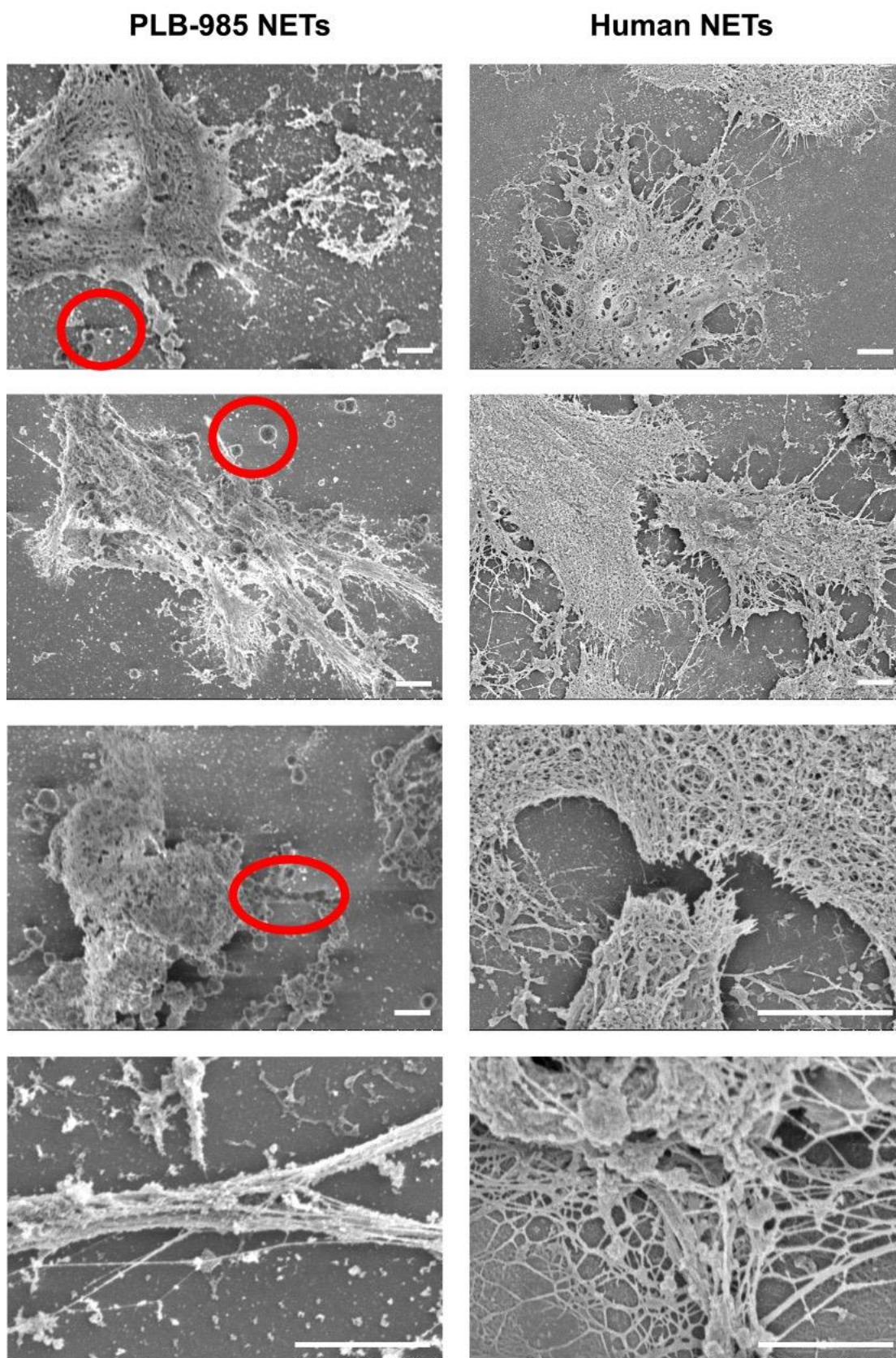


Figure 5-5. SEM images of PLB-985 NETs and human NETs. Scale bars are 2 μm . Red circle: spherical particles, either individually or in a series. ($n \geq 3$)

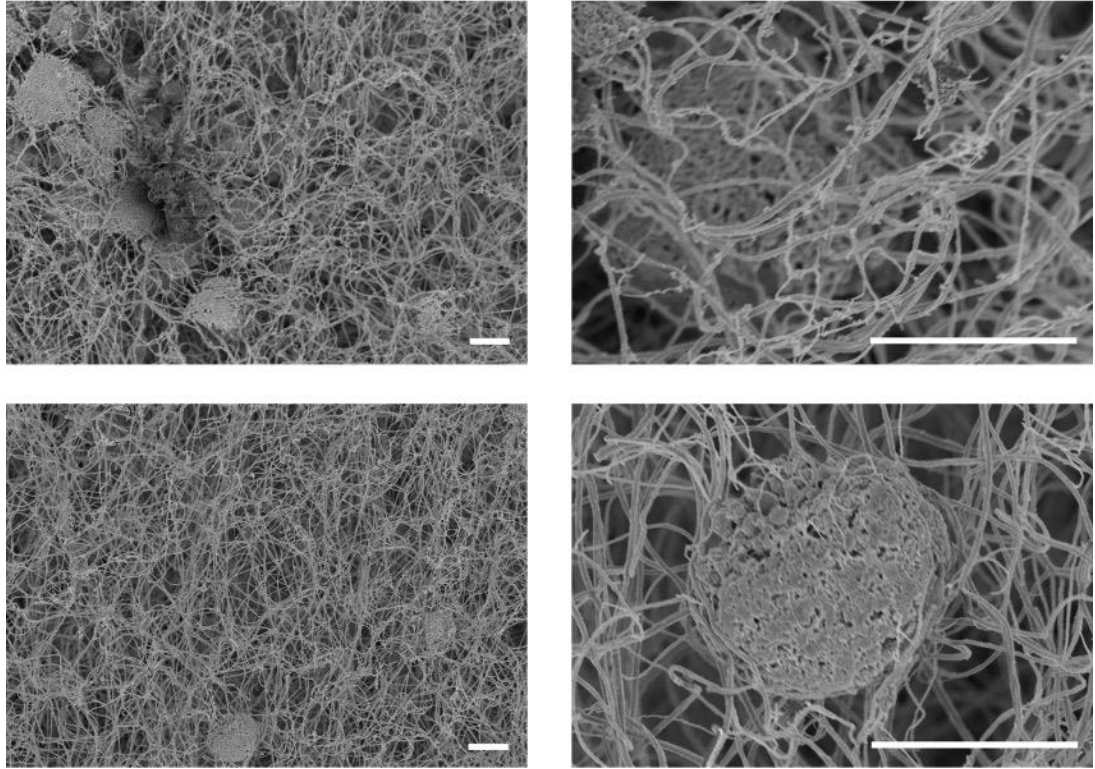
PLB-985 NET-induced Clots

Figure 5-6. SEM images of PLB-985 NET-induced plasma clots. Final concentrations: Plasma (diluted 1:3), 10 mM CaCl₂, 1 U/ml thrombin. Scale bars are 5 μ m. (n \geq 3)

Human NET-induced Clots

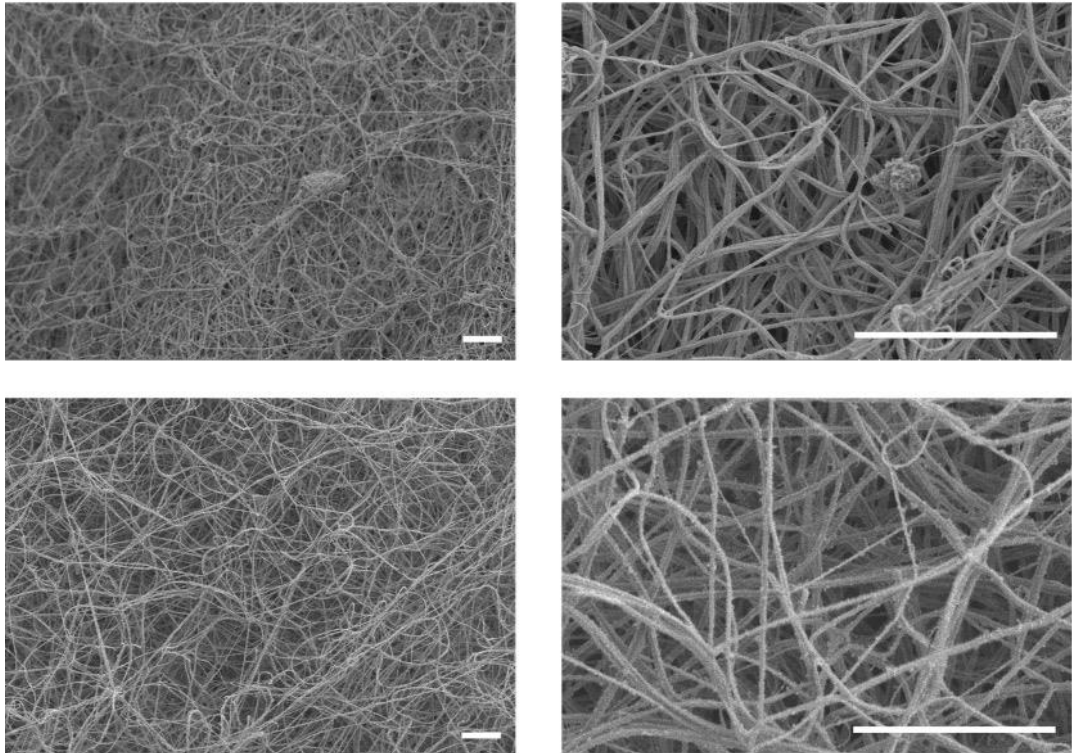


Figure 5-7. SEM images of human NET-induced plasma clots. Final concentrations: Plasma (diluted 1:3), 10 mM CaCl₂, 1 U/ml thrombin. Scale bars are 5 μ m. (n \geq 3)

Fibrin fibre diameter and density of clots were quantified. According to Figure 5-8, differentiated PLB-985 cells significantly increased the fibrin fibre thickness ($P < 0.0001$), while the fibre thickness of human neutrophil-induced clots was not analyzable. Both human NETs and PLB-985 NETs significantly increased the fibrin fibre thickness ($P < 0.0001$). The fibrin fibre thickness of PLB-985 NET-induced clots was statistically thicker ($P < 0.01$) than that of differentiated PLB-985 cell-induced clots. As shown in Figure 5-9, except human NETs, clots triggered by human neutrophils, differentiated PLB-985 cells or PLB-985 NETs

all formed significantly less fibrin fibres, compared with thrombin control ($P < 0.0001$). The presence of cells and some large NETs clusters may affect the final counting, also the fibrin fibres of neutrophil-induced clots may be too thin for software to count accurately.

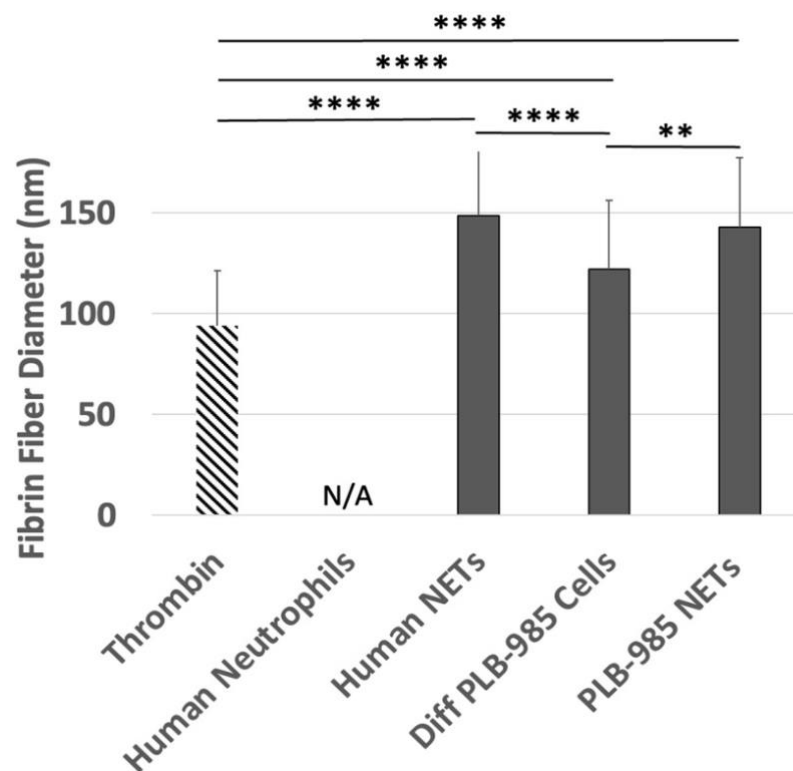


Figure 5-8. Effects of human neutrophils, human NETs, differentiated PLB-985 cells and PLB-985 NETs on the fibrin fibre thickness in plasma. Final concentrations: plasma (diluted 1:6), cells (200,000 cells/100 μ l), NETs (generated from 200,000 cells/100 μ l), thrombin (0.1 U/ml) and CaCl_2 (3.33 mM). Error bars represent SD ($n = 80$). N/A stands for not analyzable. ** $P < 0.01$, **** $P < 0.0001$.

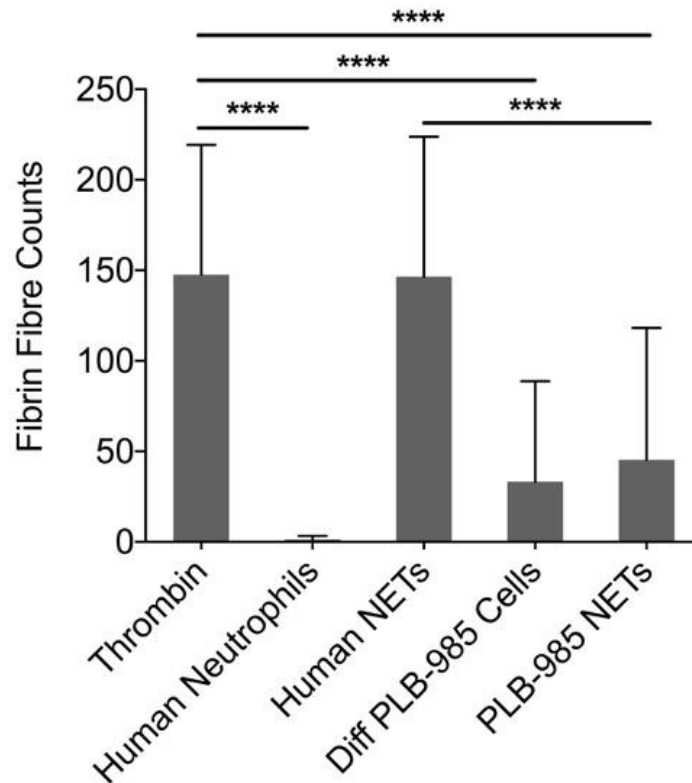


Figure 5-9. Effects of human neutrophils, human NETs, differentiated PLB-985 cells and PLB-985 NETs on the density (fibrin fibre counts) of plasma clots. Final concentrations: plasma (diluted 1:6), cells (200,000 cells/100 μ l), NETs (generated from 200,000 cells/100 μ l), thrombin (0.1 U/ml) and CaCl_2 (3.33 mM). Error bars represent SD (n = 60-80). **** P < 0.0001.

5.4.3 AFM Scanning of Neutrophil-like Cell Model

In this section, a method was optimised for imaging differentiated PLB-985 cells and PLB-985 NETs by AFM. First, differentiated PLB-985 cells and PLB-985 NETs were scanned in air. As shown in Figure 5-10, the membrane surface of dried differentiated PLB-985 cells were rugged. A single air-dried cell had a horizontal diameter of around 13.53 μm and a height of 378.66-829.03 nm (Figure 5-10 c). Figure 5-11 shows that the main body of dried PLB-985 NETs had a height of around 1.49 μm (Figure 5-11 c), and the remaining part released

from main body (i.e. NETs) had a height from 5.51 nm to 397.82 nm (Figure 5-11 d). The NET fibre enlarged in Figure 5-11 (a) had a height of 59.42 nm and was around 0.53 μm in horizontal thickness (Figure 5-11 e). The analyses of single fibres of air-dried PLB-985 NETs are shown in Figure 5-12. The size of two fibres circled in Figure 5-12 (c) was 0.12 μm in horizontal thickness with 16.27 nm in height and 0.20 μm in horizontal thickness with 36.33 nm height, from left to right respectively. Differentiated PLB-985 cells and PLB-985 NETs were also scanned in liquid. In liquid, differentiated PLB-985 cells retained a smooth membrane surface (Figure 5-13). A single cell had a horizontal diameter of around 13.53 μm and height of 3.95 μm . No image could be obtained during scanning of PLB-985 NETs in liquid, because the probe remained stuck to the sample surface and the scanning was interrupted before completion. Please see Appendix 4 for more AFM images.

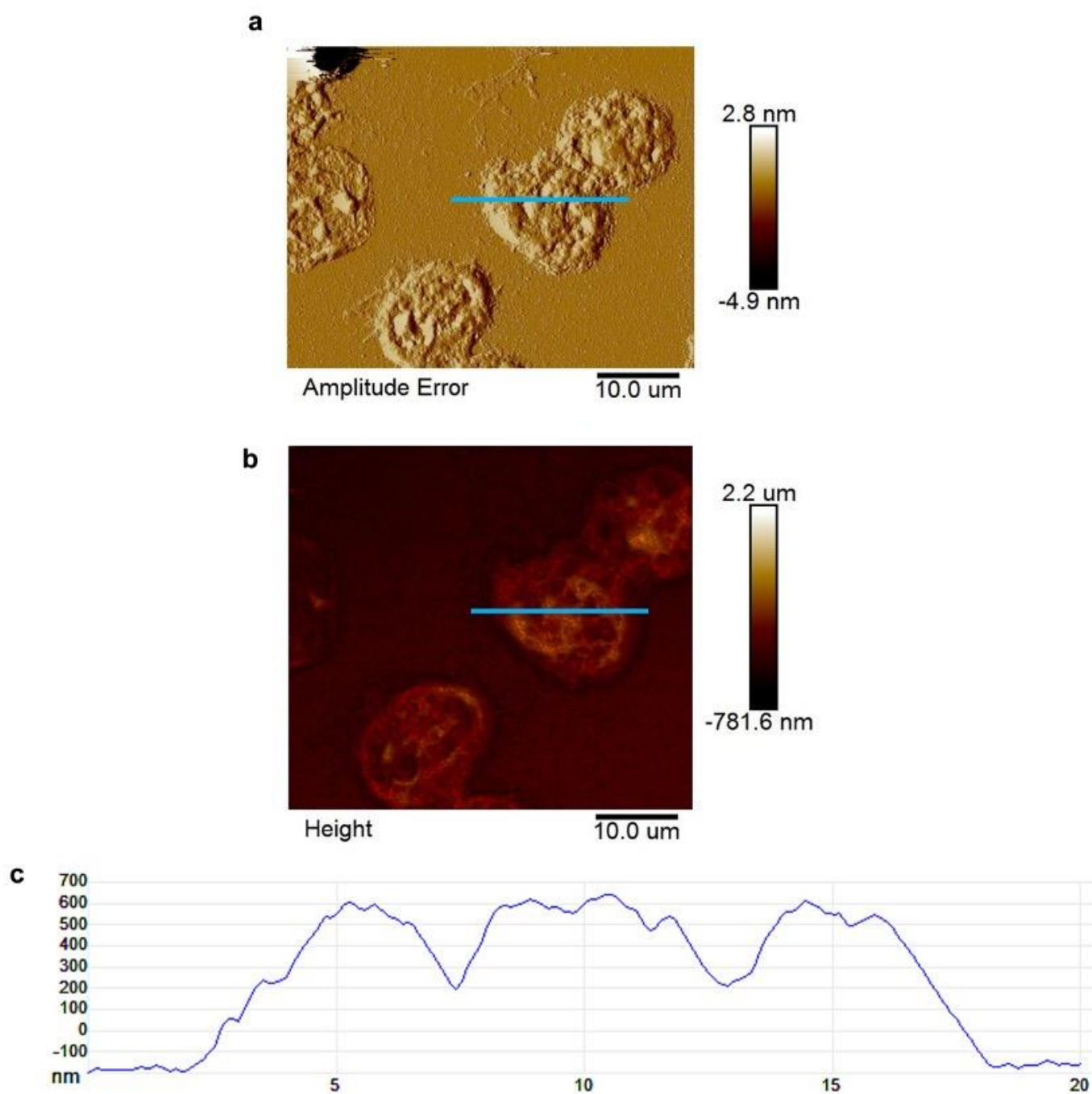


Figure 5-10. AFM analyses of air-dried differentiated PLB-985 cells. **(a)** Amplitude error channel reflects a three-dimensional image of cells. **(b)** Height channel reflects the size range of cells. **(c)** Height profile taken along the blue line in panel **(a)** and **(b)**.

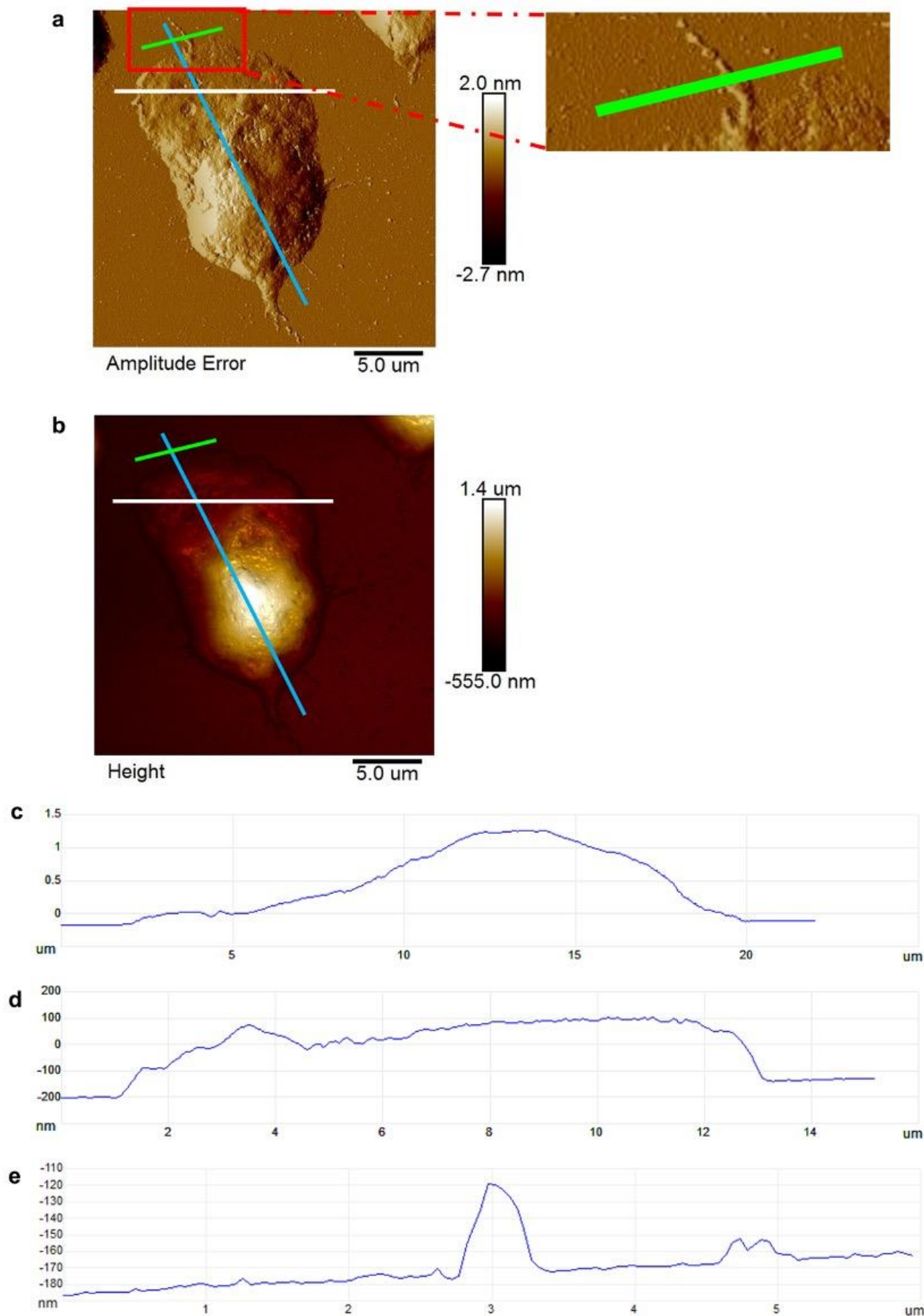


Figure 5-11. AFM analyses of air-dried PLB-985 NETs. (a) Amplitude error channel reflects a three-dimensional image of NETs. (b) Height channel reflects the size range of NETs. (c) Height profile taken along the blue line in panel (a) and (b). (d) Height profile taken along the white line in panel (a) and (b). (e) Height profile taken along the green line in panel (a) and (b).

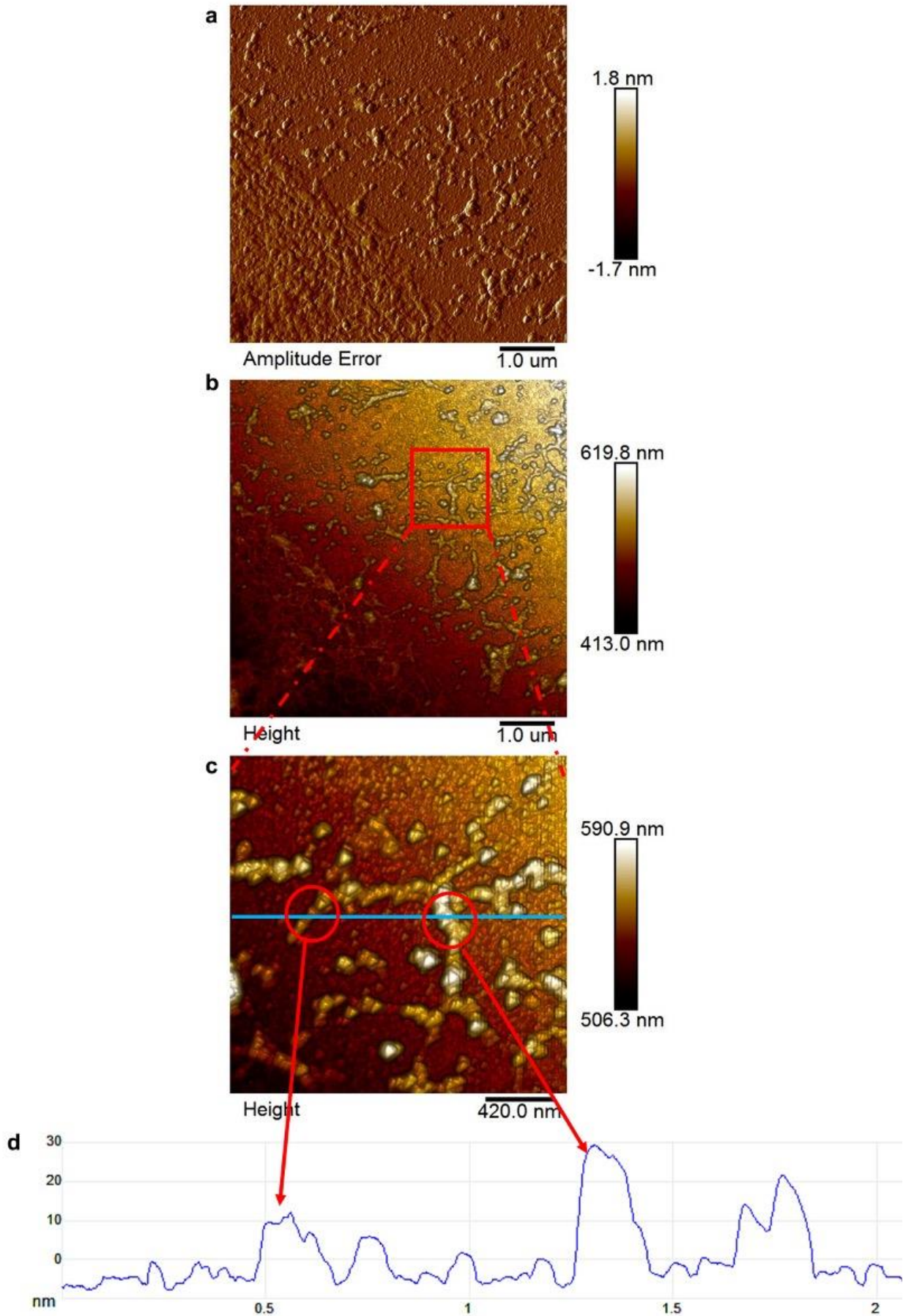


Figure 5-12. AFM analyses of the single fibres of air-dried PLB-985 NETs. **(a)** Amplitude error channel reflects a three-dimensional image of NETs. **(b and c)** Height channel reflects the size range of NETs. **(d)** Height profile taken along the blue line in panel **(c)**.

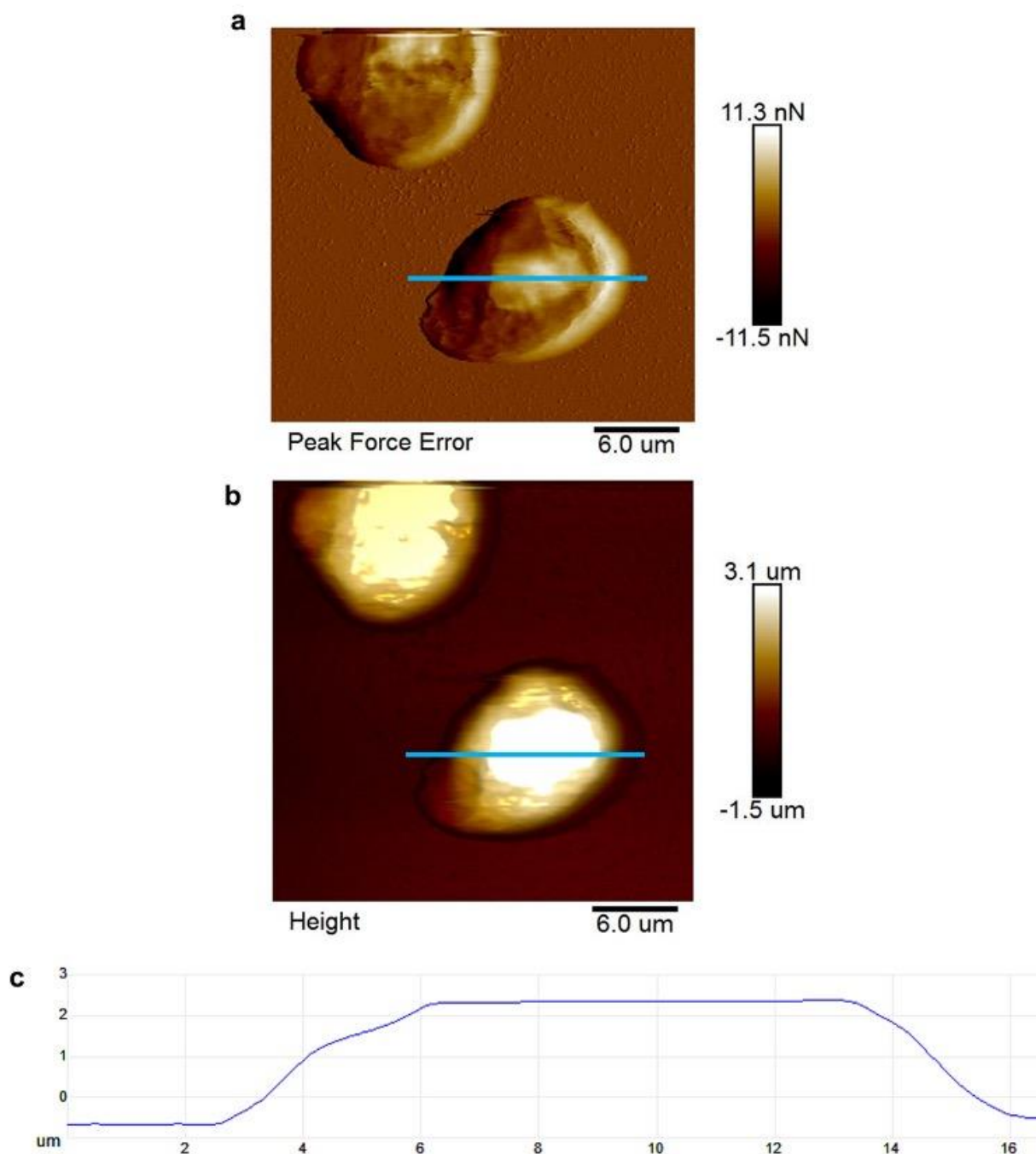


Figure 5-13. AFM analyses of differentiated PLB-985 cells in PBS buffer. (a) Peak force error channel reflects a three-dimensional image of cells. (b) Height channel reflects the size range of cells. (c) Height profile taken along the blue line in panels (a) and (b).

5.4.4 Effects of Human Neutrophils and NETs on Clot Permeability

The porosity of human neutrophil-induced clots and human NET-induced clots was analysed using permeability assays (Figure 5-14). Thrombin-induced clots were used as controls. Human neutrophil-induced clots showed a significantly higher permeability coefficient than thrombin only control ($P < 0.01$). Moreover, neutrophil-induced clots were easily ruptured during permeation experiments as they were likely mechanically weak and could not withstand the flowing liquid. There was no significant difference between human NET-induced clots and the thrombin only control. In the presence of thrombin, the addition of human neutrophils and NETs did not statistically alter the permeability coefficient of clots.

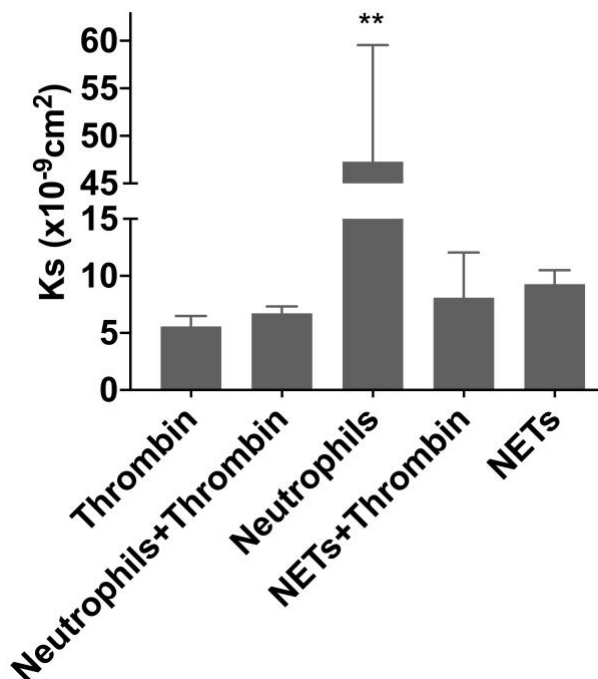


Figure 5-14. Effects of human neutrophils and human NETs on the permeability of plasma clots. The permeability coefficient (Darcy constant [Ks]) of clots was quantified. Final concentrations: plasma (diluted 1:6), human neutrophils (200,000 cells/100 μ l), NETs (generated from 200,000 cells/100 μ l), thrombin (0.1 U/ml) and CaCl₂ (3.33 mM). Error bars represent SEM of three independent repeats in triplicates. ** $P < 0.01$. (Data were adapted from Shi et al., 2021)

5.5 Discussion

This chapter investigated the role of neutrophils and NETs in clot structure and permeability, and compared the differences between PLB-985 and human samples. Results showed that differentiated PLB-985 cell formed a membrane surface with many flaps, which was similar to human neutrophils. Additionally, NETs generated from differentiated PLB-985 cells and human neutrophils generally appear similar in confocal and SEM. AFM and SEM data showed that the thickness of NET fibres was variable but about 8-18 times larger than a single DNA helix (2 nm), indicating that each NET fibre is made up of multiple strands of DNA. Interestingly, lots of filamentous structures were observed on the membrane surface of PLB-985 cells and human neutrophils. It is possible that these filamentous structures are nanotubes. A previous study has observed similar nanotubes (diameter: 50-200 nm) on cultured rat pheochromocytoma PC12 cells. It has been proposed that nanotubes could be a common phenomenon that occurs in long-distance communication between cells, and that it allows cells to transfer organelles between each other (Rustom et al., 2004). Although there is no direct evidence in the literature showing that neutrophils or PLB-985 cells contain nanotubes, they have been observed in monocytes, macrophages, endothelial cells and tumor cells (Jash et al., 2018).

Data also showed that differentiated PLB-985 cell-induced clots formed thicker fibrin fibres as compared to thrombin control, although the overall structure was looser. In contrast, human neutrophil did not trigger plasma to form strong fibres

by themselves. The overall structure of human neutrophil-induced clots appears to be weak and less stable, as a lot of small broken fibres were observed on the surface of neutrophils, which may explain why neutrophil-induced clots showed high permeability. The different effects on clot structure comparing differentiated PLB-985 cells with human neutrophils may be explained by the ability of cancer cell lines to generate and release TF-containing microvesicles (Ettelaie et al., 2016). As a cancer cell line, PLB-985 cells may also be able to release TF-containing microvesicles, or at least express TF on their cell membrane, likely contributing to the formation of thrombin in the plasma and thus the generation of “normal” fibrin fibres (compared with thrombin control) in differentiated PLB-985 cell-induced clots. The spherical particles observed in SEM images of PLB-985 NETs may represent some of such microvesicles. The general size of microvesicles is 100–1000 nm, which is consistent with the size of the particles observed in this chapter.

The overall structure of human NETs-induced clots and PLB-985 NET-induced clots were generally similar. Both increased the thickness of fibrin fibres as compared with thrombin control, which may strengthen the structure of clots. When comparing PLB-985 NETs and differentiated PLB-985 cells, the effects of increasing fibrin fibre thickness was enhanced by the formation of NETs. Interestingly, some apparently NET-like structures (denser mesh) were observed in PLB-985 NET-induced clots, but no such structures were found in human NET-induced clots. Moreover, many spherical particles, which were only

observed in PLB-985 NETs, appeared within these NET-like structures. These spherical particles may be able to enhance NETs stability during clot formation, but this needs to be confirmed in future studies. A previous study has shown that pure DNA and histones decreased clot permeability (Varjú et al., 2015). On the contrary, no effects of NETs on clot permeability were found in this chapter. Confocal results suggested that fibrin fibres were denser around NET clusters. However, the fibrin network was porous in other areas lacking NET clusters. This may be one reason why NETs did not alter the overall permeability of clots, as such opposing effects on pore-size could cancel each other out.

There are clear advantages and limitations for both confocal microscopy and SEM. SEM is able to show more minute details at the molecular level with high resolution and high magnification, but it can only provide black-and-white images, making it difficult to distinguish between similar structures such as NET fibres and fibrin fibres. Confocal microscopy can easily distinguish the NET fibres and fibrin fibres by fluorescence labeling, but the resolution is substantially lower than that of SEM, so the confocal images lose many finer details. To find a better method to observe the interactions between neutrophils and fibrin fibres or between NET fibres and fibrin fibres, AFM was chosen for further study, because it not only has a high resolution but also allow samples to be labelled with fluorescent dyes. Parallel AFM/confocal imaging using a state-of-the-art system has recently become available at the University of Leeds for combined AFM and fluorescence imaging, an approach that should be explored

in future studies. AFM can also reliably measure a variety of properties of samples under physiologically relevant conditions, such as fibre diameter, clot stiffness and resistance to deformation (Mihalko and Brown, 2020). AFM is a powerful technique, but it is more difficult to operate than confocal microscopy and SEM. Due to the nature of some samples, which had a sticky sample surface (e.g., NETs in liquid), the probe was easily stuck and the scanning interrupted. Additionally, most types of AFM equipment were originally designed to scan small molecules, e.g., in the in-liquid AFM images of plb-985 cells (Figure 5-13), the top of the cell is too flat and seems to be cut off, suggesting the AFM scanner may have reached its upper limit. AFM experiments have not yet been performed in human neutrophils and human NETs samples due to time limitations and temporary laboratory closure in response to the COVID-19 pandemic, but may be performed in future studies.

In conclusion, NETs and neutrophils affect clot structure in a distinctive manner. NETs increased density of clots in the areas immediately surrounding them, also increased fibrin fibre thickness, but did not significantly decrease the permeability of clots. Neutrophil-induced clots on the other hand failed to form analyzable fibrin fibres, and neutrophil-induced clots were weak with a high permeability. Unlike primary neutrophils, differentiated PLB-985 cells also increased fibrin fibre thickness, but thinner than that of PLB-985 NET-induced clots. AFM could be a better method to investigate the interaction between neutrophils (NETs) and fibrin fibres, but further method optimization is required

to scan neutrophil-induced or NET-induced clots via AFM, and in parallel studies using combined AFM/fluorescence imaging. Future studies are required to investigate whether differentiated PLB cells can release TF-containing microvesicles and whether the spherical particles observed in SEM images of PLB-985 NETs correspond to these microvesicles.

Chapter 6 Potential Mechanisms of Neutrophil- and NET-Induced Clotting

6.1 Introduction

NETs are hypothesized to promote clotting via the intrinsic pathway, as they could present a negatively charged surface which is suggested to activate factor XII (FXII) (Griep et al., 1985). An *in vivo* study has previously observed reduced NET-induced clot formation in FXII- and FXI-deficient mice (von Brühl et al., 2012), but this requires confirmation with human samples. NETs are generated by neutrophils, but the coagulation pathway that neutrophils exploit to promote clotting is not yet fully understood either.

Therefore, this chapter investigates whether FXII, FXI and FVII are involved in the procoagulant effects of human neutrophils and NETs *in vitro*. Neutrophils are known to release a number of pro- and anti-coagulant mediators (such as matrix metalloproteinases (MMP), cathepsin G, elastase and proteinase 3), which are stored in the cytoplasmic granules (Swystun and Liaw, 2016).

However, it is not clear which mediator(s) play a role in the neutrophil-induced clot formation described in Chapter 4. This chapter also explores which neutrophil proteins may be involved in the procoagulant effects of human neutrophils. As described in chapter 5, human neutrophil-induced clots did not form a notable network structure, but produced many tiny fibrin fibres. It is well known that thrombin cleaves fibrinopeptide A (FpA) from fibrinogen to form protofibrils, and then cleaves fibrinopeptide B (FpB) to allow the protofibrils to aggregate laterally into fibres (Undas and Ariëns, 2011). Since human neutrophil-induced clots only formed small fibrin fibres as described in chapter

5, these clots were hypothesized to release less FpA and FpB. Therefore, the release of FpA and FpB in neutrophil-induced clotting was also analysed in this chapter.

6.2 Objectives

This chapter aims to investigate the coagulation pathway mechanisms responsible for neutrophil- and NET-induced clotting, and explore which mediators released by neutrophils may contribute to neutrophil-induced clotting.

6.3 Methods

6.3.1 Inhibition of FXII and TF in Plasma

Normal pooled plasma (NPP), human neutrophils and neutrophil supernatant were obtained as described in section 2.1. NETs were generated and collected from human neutrophils as described in section 2.4.2. A TF antibody, Murine MAb Against Human Tissue Factor (Invitech), was used as an inhibitor of the TF pathway. Corn trypsin inhibitor (CTI) was used to inhibit FXII in plasma. A specific FXIIa chromogenic activity assay was carried out to detect the efficacy of CTI as described in section 2.10. TF antibody (diluted 1:50) and CTI (1.6 μM) were added in human neutrophil and NETs turbidity experiments to investigate whether TF and FXII were involved in the procoagulant effects of neutrophils and NETs (All other conditions were the same described in Chapter 4). In addition to experiments with inhibitors, FXII-, FXI- and FVII-deficient plasmas

were also used as a replacement of normal pooled plasma (NPP) in human neutrophil and NETs turbidity experiments.

6.3.2 Detection of Procoagulant Mediators Released from Neutrophils

To investigate which mediators released from neutrophils may contribute to the procoagulant effects of neutrophils; their supernatant was collected as described in section 2.1, and then sent to R. George for protein identification using mass spectrometry (section 2.11).

To explore the role of RBC lysis buffer in the activation of neutrophils, neutrophils were isolated with or without adding RBC lysis buffer, with other isolation steps remaining essentially the same as described in section 2.1.1. Turbidity measurements for neutrophils (normal isolation), neutrophils isolated without RBC lysis buffer, and neutrophils (normal isolation) with extra RBC lysis buffer (final dilution 1:3) were carried out in plasma as described in section 2.9.2.

6.3.4 Quantitative Detection of FpA and FpB Release in Neutrophil-induced Clots by ELISA

Clot supernatant was collected as described in section 2.14. Enzyme-linked immunosorbent assays (ELISA) for FpA and FpB were carried out as described in section 2.16.

6.3.5 Data Analysis

GraphPad Prism 7 or Microsoft Excel were used to represent the data graphically. All statistical analyses were performed using GraphPad Prism 7. A normal distribution of the data was checked by D'Agostino-Pearson omnibus (K2), Shapiro-Wilk (W), Anderson-Darling (A2*) or Kolmogorov-Smirnov (distance) tests ($P > 0.05$). The equality of variances was checked by Brown-Forsythe or F test ($P > 0.05$). Two-tailed unpaired t-test, one-way ANOVA followed by Tukey's multiple comparisons, Brown-Forsythe and Welch ANOVA tests followed by Dunnett's T3 multiple comparisons test were used for parametric data. Mann Whitney test and Kruskal-Wallis followed by Dunn's multiple comparisons tests were used for non-parametric data. P-values < 0.05 were considered to indicate statistical significance.

6.4 Results

6.4.1 Coagulation Pathway Mechanisms Involved in Neutrophil- and NETs-induced Clotting

First, TF antibody (final dilution 1:50) and 1.6 μM CTI were used to block TF and FXII respectively in plasma turbidity experiments. The efficacy of CTI was detected by a FXIIa specific chromogenic activity assay in a purified system. Figure 6-1 (a) shows that 0.2 μM CTI fully blocked 30 nM FXIIa in the purified system. The concentration of FXIIa in neutrophil-induced plasma clotting (Figure 6-1 (a) black line) was less than 30 nM. However, 1.6 μM CTI did not apparently block FXIIa in the plasma system (Figure 6-1 b). The same was

observed with TF antibody, which also did not notably block TF in a plasma-based system (Figure 6-1 c).

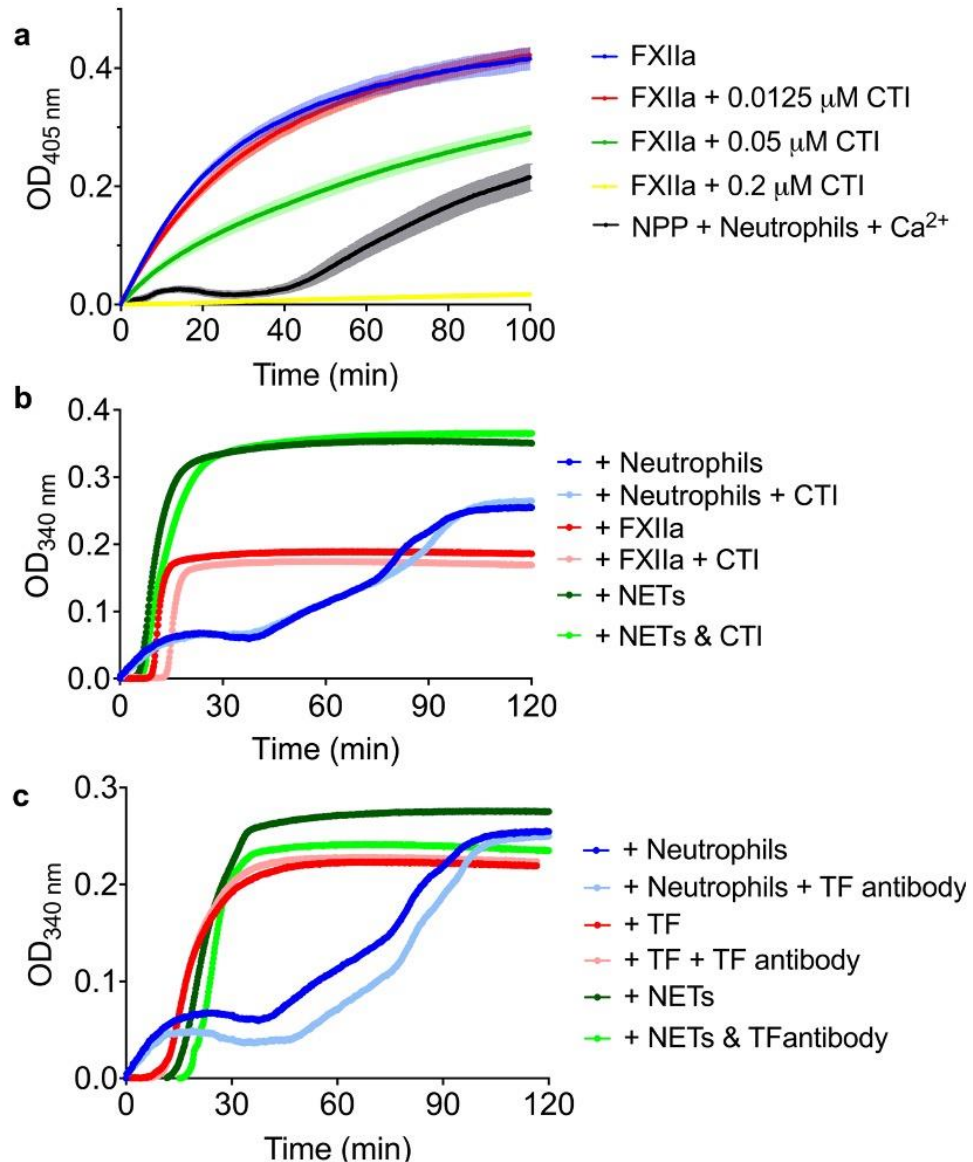


Figure 6-1. Role of TF inhibitor (TF antibody) and FXII Inhibitor (CTI) in the procoagulant effects of human neutrophils and NETs in plasma. **(a)** Chromogenic activity assay was carried out in a purified HBS buffer system with FXIIa (30 nM) with CTI (0.0125 μM , 0.05 μM or 0.2 μM) added to block FXII. Plasma (diluted 1:5), human neutrophils (200,000 cells/100 μl) and CaCl₂ (5 mM) were added instead of 30 nM FXIIa as a control to show an approximate concentration of FXIIa that may be present in the turbidity of plasma system. **(b) & (c)** Turbidity measurements were carried out in plasma. Final concentrations in turbidity: plasma (diluted 1:6), CaCl₂ (3.33 mM), human neutrophils (200,000 cells/100 μl), NETs (generated from 200,000 cells/100 μl), FXIIa (30 nM), TF (diluted 1:250), TF antibody (diluted 1:50), CTI (1.6 μM). (n = 3-9) (Partial data were adapted from Shi et al., 2021)

As inhibition could not be achieved with CTI or TF antibody in plasma, FXII-, FXI- and FVII-deficient plasmas were next used in turbidity instead of inhibitors, to seek to understand the respective roles of these coagulation factors in NETs- and neutrophil-induced clotting. FXII-, FXI- and FVII-deficient plasmas did not inhibit the procoagulant effects of human NETs (Figure 6-2 a), the FXI-deficient plasma even resulted in a significantly higher MaxOD ($P < 0.01$) than NPP control (Figure 6-2 d). In contrast, FXI-deficient plasma significantly inhibited the procoagulant effects of human neutrophils with statistically significant lower MaxOD ($P < 0.0001$) than NPP control (Figure 6-2 c & d). FXI-deficient plasma fully inhibited the procoagulant effects of neutrophil supernatant in turbidity experiments (Figure 6-2 b, d, e, f). FXII- and FVII-deficient plasmas reduced the procoagulant effects of both human neutrophils and neutrophil supernatant to some extent, but clots still formed at later timepoints. FXII-deficient plasma significantly delayed the time to MaxOD of clots triggered by neutrophils ($P < 0.001$) and neutrophil supernatant ($P < 0.01$) (Figure 6-2 f).

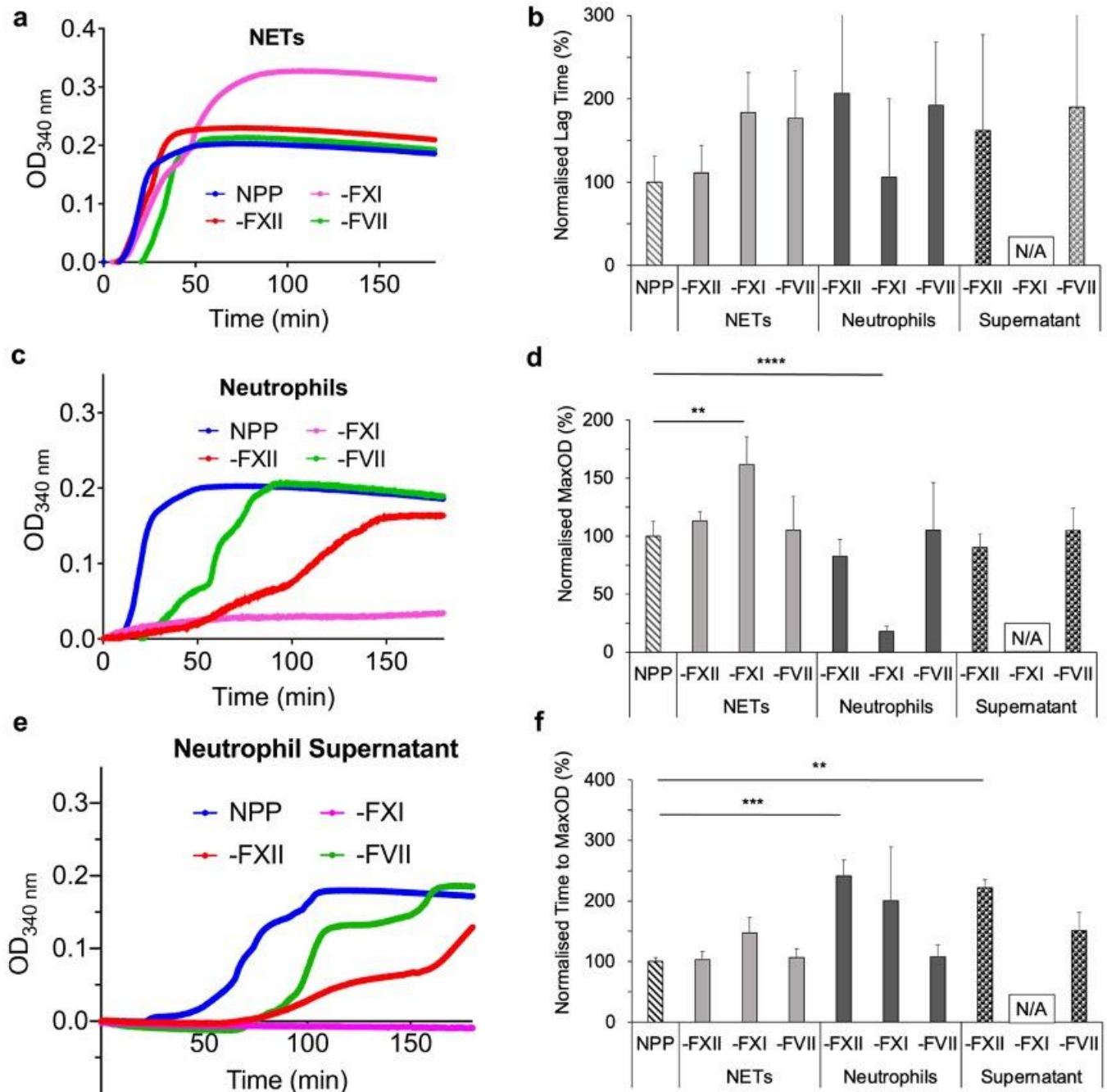


Figure 6-2. Effects of FXII-, FXI- and FVII-deficient plasmas on the procoagulant effects of human neutrophils, NETs and neutrophil supernatant. NPP was used as the positive control. **(b)** Normalized percentage of lag time, **(d)** normalized percentage of MaxOD and **(f)** normalized percentage of time to MaxOD were quantified. Final concentrations: plasmas (diluted 1:6) and CaCl_2 (3.33 mM), neutrophils (200,000 cells/100 μl), NETs (generated from 200,000 cells/100 μl). Error bars represent SD. NPP data represents 8-9 repeats, deficient plasma data represents 3-6 repeats. N/A stands for not analyzable. * $P < 0.05$, ** $P < 0.01$, *** $P < 0.001$, **** $P < 0.0001$. (Partial data were adapted from Shi et al., 2021)

Self-coagulation of plasma was also investigated using turbidity. As shown in Figure 6-3, only FXI-deficient plasma did not clot (without addition of coagulation triggers) before centrifugation and filtration. All other plasmas showed accelerated self-coagulation prior to centrifugation and filtration. For this reason, throughout this study, all plasmas were subsequently first centrifuged at 10,000 RCF for 10 min and then filtered through a 0.2 μm filter prior to use. Nevertheless, self-coagulation was still occasionally observed in NPP after ~55 mins after centrifugation and filtration (Figure 6-3 b).

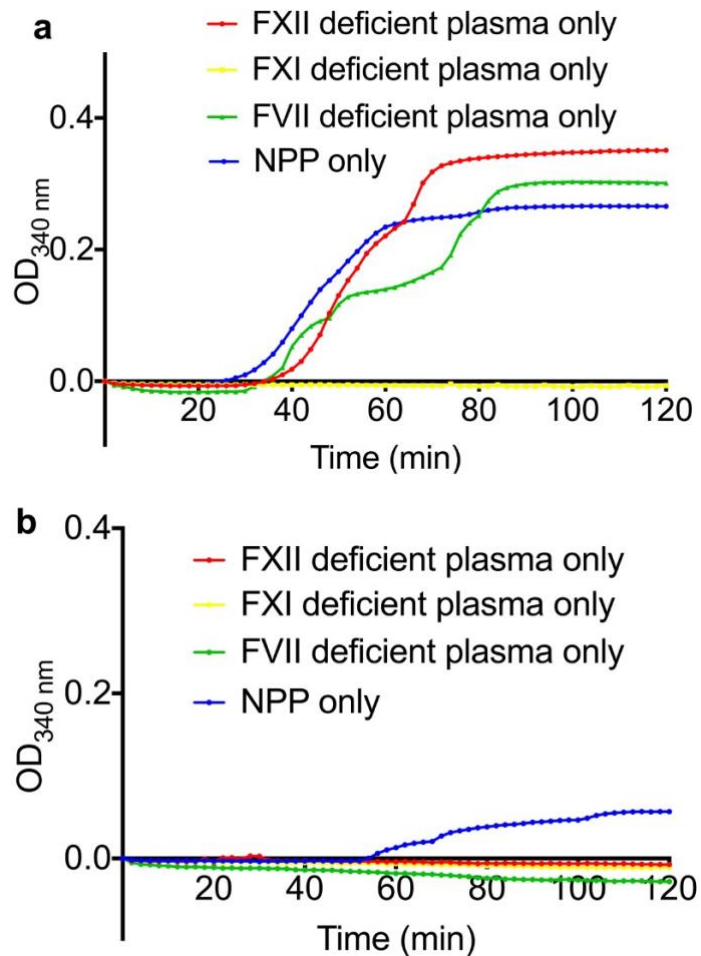


Figure 6-3. Self-coagulation of plasmas before and after centrifugation and filtration. **(a)** Plasmas without centrifugation and filtration. **(b)** Plasmas which were spun at 10,000 RCF for 10 min and filtered through a 0.2 µm filter. Final concentrations: plasmas (diluted 1:6) and CaCl₂ (3.33 mM). (n = 4-9)

6.4.2 Release of FpA and FpB during Neutrophil-induced Clotting

The release of FpA and FpB during neutrophil-induced clotting was quantified by ELISA. Figure 6-3 shows that neutrophil-induced clotting released significantly lower amounts of FpA than thrombin control ($P < 0.05$). The concentration of FpB released from neutrophil-induced clotting was also somewhat lower than thrombin control, but this did not reach statistical significance. Neutrophil-induced clotting released similar amounts of FpA (0.46

ng/ml) and FpB (0.43 ng/ml). In addition, FpA released from plasma only control was similar to that from neutrophil-induced clotting, but significantly lower ($P < 0.05$) than that of the thrombin control. FpB released from plasma only control was significantly lower ($P < 0.05$) than both neutrophil-induced clotting and thrombin control. Plasma only control released less FpB (0.22 ng/ml) than FpA (0.46 ng/ml), by about half.

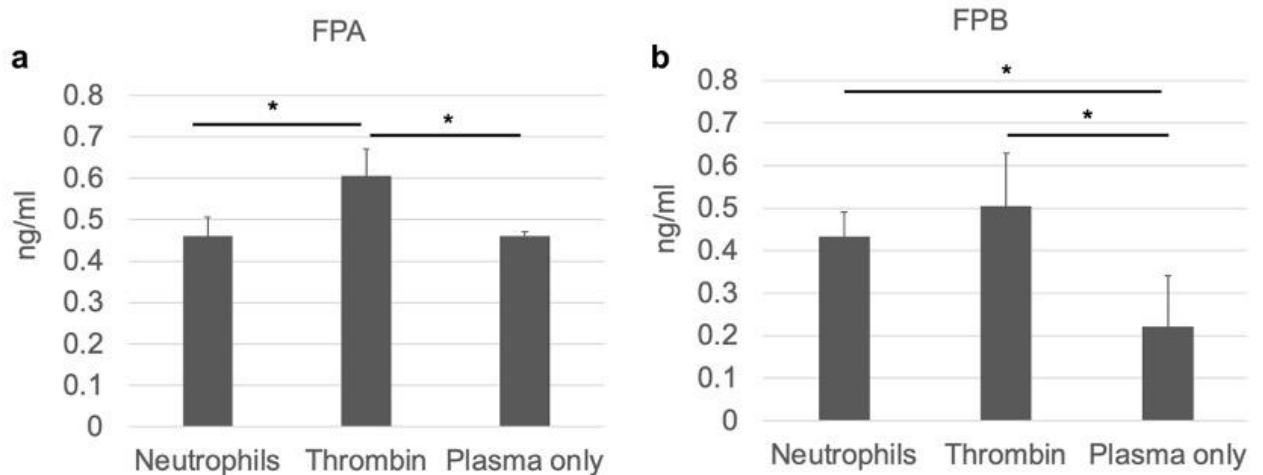


Figure 6-4. Release of FPA and FPB in neutrophil-induced clots. (a) Fibrinopeptide A concentration in the supernatant of clots (b) Fibrinopeptide B concentration in the supernatant of clots. “Neutrophils”: clots triggered by neutrophils only. “Thrombin”: clots triggered by thrombin only. “Plasma only”: plasma without adding any coagulation trigger. Final concentrations: Plasma (diluted 1:3), 10 mM CaCl₂, 1 U/ml thrombin, neutrophils (200,000 cells/100 μl), NETs (generated from 200,000 cells/100 μl). Error bars represent SD of 3-5 independent repeats in duplicate. * $P < 0.05$.

6.4.3 Mediators that may Contribute to Neutrophil-induced Clotting

The procoagulant effects of human neutrophils could be based on the effects of mediators released from neutrophils as discussed in chapter 4. Possible mediators in neutrophil supernatant were analysed by mass spectrometry (Table 6-1). Several possible mediators were observed in the supernatant,

including protein S100-A8, cDNA, glyceraldehyde-3-phosphate dehydrogenase, annexin, phosphoglycerate kinase 1, myeloperoxidase (MPO), neutrophil defensin 1, amongst others.

Table 6-1. Mass spectrometry data showing the composition of human neutrophil supernatant (Adapted from Shi et al., 2021). Please see Appendix 5 for the entire original table.

Accession *	Protein Description	-10lgP **
H6VRF8	Keratin 1, GN=KRT1 PE=3 SV=1	176.5
P13645	Keratin type I cytoskeletal 10, GN=KRT10 PE=1 SV=6	155.61
P35908	Keratin type II cytoskeletal 2 epidermal, GN=KRT2 PE=1 SV=2	150.21
P35527	Keratin type I cytoskeletal 9, GN=KRT9 PE=1 SV=3	147.8
P05109	Protein S100-A8, GN=S100A8 PE=1 SV=1	122.94
B7ZAL5	cDNA FLJ79229 highly similar to Lactotransferrin, PE=2 SV=1	120.31
B4DUI5	Triosephosphate isomerase, PE=2 SV=1	109.63
B2R4M6	Protein S100, PE=2 SV=1	103.9
B4DVQ0	cDNA FLJ58286 highly similar to Actin cytoplasmic 2, PE=2 SV=1	103.84
A0A0M4FNU3	Fructose-bisphosphate aldolase (Fragment), GN=ALDOA PE=3 SV=1	91.97
P04406	Glyceraldehyde-3-phosphate dehydrogenase, GN=GAPDH PE=1 SV=3	89.44
P13647	Keratin type II cytoskeletal 5, GN=KRT5 PE=1 SV=3	87.82
B4DJI1	cDNA FLJ52549 highly similar to L-lactate dehydrogenase A chain, PE=2 SV=1	77.88
A0A4D5RAJ5	Annexin, PE=3 SV=1	72.46
P00558	Phosphoglycerate kinase 1, GN=PGK1 PE=1 SV=3	72.41
P05164	Myeloperoxidase, GN=MPO PE=1 SV=1	69.62
B4DEK3	cDNA FLJ56959 highly similar to Vascular endothelial growth factor receptor 2, PE=2 SV=1	69.24
B2R4C5	Lysozyme, GN=LYZ PE=2 SV=1	67.95
A0A0K0K1H9	Epididymis secretory protein Li 48 (Fragment), GN=HEL-S-48 PE=2 SV=1	67.16
K7EPF6	6-phosphogluconate dehydrogenase decarboxylating (Fragment), GN=PGD PE=1 SV=1	63.71
P59665	Neutrophil defensin 1, GN=DEFA1 PE=1 SV=1	61.61
B4E3A8	cDNA FLJ53963 highly similar to Leukocyte elastase inhibitor, PE=2 SV=1	60.26
B7Z4U6	cDNA FLJ55803 highly similar to Gelsolin, PE=2 SV=1	59.14
B4DE36	Glucose-6-phosphate isomerase, PE=2 SV=1	57.29
A0A384NPR0	Epididymis secretory sperm binding protein, PE=2 SV=1	53.55
D6RA82	Annexin, GN=ANXA3 PE=1 SV=1	44.84
A0A0K0K1K8	Enolase 1 (Alpha) isoform CRA_a, GN=ENO1 PE=3 SV=1	44.18
Q59ES1	Leukotriene A4 hydrolase variant (Fragment), PE=2 SV=1	44.14

GN: gene name, PE: protein existence, SV: sequence version.

* Accession: The accession number of the protein as seen in the FASTA database.

** -10lgP: The protein confidence score. The protein matches in the reports are ordered by this score. Proteins with a high -10lgP score show many peptides that have good quality sequences.

6.5 Discussion

This chapter investigated whether TF, FXII, FXI or FVII are involved in the procoagulant effects of neutrophils and NETs. The TF and FXII inhibitors (TF antibody and CTI) were first used to block TF and FXII in turbidity experiments, but results showed that they did not work efficiently in plasma. Some components in plasma may affect the reaction of these two inhibitors, since the FXII inhibitor was separately shown to inhibit FXII efficiently in a purified system. Therefore, FXII-, FXI- and FVII-deficient plasmas were then used in turbidity experiments. None of FXII-, FXI- and FVII-deficient plasmas inhibited the procoagulant effects of NETs, suggesting that NETs likely triggered clotting through other components than FVII, FXII and FXI in plasma. However, FXI-deficient plasma significantly reduced the procoagulant effects of neutrophils and fully blocked the procoagulant effects of neutrophil supernatant. FXII- and FVII-deficient plasmas also delayed neutrophil-induced and neutrophil supernatant-induced clotting, but to a lesser extent. Therefore, neutrophils (or neutrophil released mediators) likely trigger clotting mainly via FXI, while FXII and FVII are involved to a lesser extent. Notably, some components in plasma seem to trigger self-coagulation, possibly via FXI, as FXI-deficient plasma was the only plasma that did not self-coagulate. Some of these components may be smaller than 0.2 μm , as the self-coagulation was sometimes still observed in NPP after extensive high-speed centrifugation and filtration (through a 0.2 μm filter).

ELISA results showed that less FpA and FpB were released from neutrophil-induced clots, compared with thrombin control. Interestingly, neutrophils prompted release of FpB as compared with plasma only control. A previous study has indicated that the release levels of FpA and FpB may not be specific markers of thrombin activity, as t-PA, urokinase and plasmin can directly release FpA and/or FpB from fibrinogen independently of thrombin (Glas-Greenwalt, 1995). Moreover, another study has shown that leukocyte enzymes could release fragments containing FpA from fibrinogen (Weitz et al., 1986). However, there is no direct evidence showing that neutrophil enzymes could cleave fibrinogen and release FpB. As discussed in chapter 5, neutrophil-induced clots lacked the more substantial fibrin scaffold formation as observed in control clots. The increased release level of FpB in neutrophil-induced clotting may thus be due to the effects of neutrophil enzymes, but independent of thrombin activity.

The expression of FpA and FpB in plasma only controls was much higher than expected, which may be due to non-specific binding of the antibodies to other proteins (e.g., native fibrinogen). Alternatively, it is possible that the plasma indeed contains FpA and FpB if protofibrils had already formed before the plasma was used in experiments. The plasma may also be affected by other factors, for example, a previous study found an increased FpA level in patients with malignancy without clinical signs of venous thromboembolism or

disseminated intravascular coagulation (DIC) (Peuscher et al., 1980). Further studies are required to investigate the origin of the FpA and FpB in the plasma.

This chapter also explored which mediators released by neutrophils may contribute to neutrophil-induced clotting. Mass spectrometry data showed that the neutrophil supernatant contains a number of proteins, enzymes and cDNA. Among them, neutrophil defensin has previously been shown to accelerate clotting and increase clot stability in mice (Abu-Fanne et al., 2019). However, proteins well-known to be involved in coagulation, such as elastase and cathepsin G, were not found in the supernatant. It is, nevertheless, possible that these proteins could be further released by neutrophils during the clotting process. The cDNA in neutrophil supernatant appears to have a distinct function from the DNA in NETs, because their kinetics of clot formation were significantly different. MPO and annexin were also observed in neutrophil supernatant. They are involved in several anticoagulant effects, e.g., MPO has been shown to inhibit phospholipid-dependent coagulation (Beckmann et al., 2017), annexin A4 is known to inhibit the activation of factor XII, and annexin A2 contributes to increased fibrinolysis (Chapin and Hajjar, 2015; Nakayama et al., 2020).

However, no significant anticoagulant effects of these proteins were observed in this study, as clots still formed in neutrophils supernatant that contained them.

In conclusion, FXII, FXI and FVII were not involved in the procoagulant effects of NETs, suggesting other components in plasma are responsible for the

observations described in previous chapters. Neutrophils, or mediators they release, triggered clotting mainly through the intrinsic pathway and partially through the extrinsic pathway. However, the interactions between neutrophil released mediators and coagulation factors (particularly FXI) needs to be further investigate in future studies. To further confirm results from congenital FXII-, FXI- and FVII-deficient plasmas, normal clotting controls triggered by TF and depleted deficient plasmas should be used in future studies. The effects of neutrophil enzymes on fibrinopeptides release are also worthy of further exploration. The specificity of two ELISA kits could be further characterized using purified fibrinogen samples, samples in which fibrin is formed but in the presence of a fibrin polymerization inhibitor (GPRP acetate) and fibrinogen-deficient plasma to determine the specificity of the FpA and FpB ELISA systems. Additionally, FpA and FpB levels in the plasma could be analysed using other detection methods (e.g., high performance liquid chromatography).

Chapter 7 General Discussion

7.1 General discussion

The aims of this thesis were to investigate the role of neutrophils and NETs in blood coagulation, clot stability, clot structure and clot porosity, to decipher how neutrophils and NETs interact with the fibrin network and identify novel mechanisms that contribute to thrombosis and thromboinflammation. The formation of NETs is currently considered as a key part of the procoagulant effects of neutrophils (von Brühl et al., 2012; Kapoor et al., 2018; Denis F. Noubouossie et al., 2019). Hitherto, no published study has described the procoagulant effects of neutrophils and NETs separately. Findings of this thesis suggested that neutrophils themselves are able to influence coagulation in a distinct manner when compared with NETs. This thesis mostly investigated the action of neutrophils and NETs as separate elements, in order to better compare the differences between these two procoagulant cellular mechanisms.

7.1.1 NETs and Mediators Released by Neutrophils Induced Coagulation in Plasma

As summarized in Table 7-1, neutrophils and NETs have no significant procoagulant effects in purified fibrinogen, but both could induce clotting in plasma without adding any other coagulant trigger. Thus, some components in plasma may interact with neutrophils and NETs, resulting in clot formation. These findings seem inconsistent with the opinion of Denis F Noubouossie et al., that intact NETs cannot promote coagulation (described in section 1.8) (Denis F Noubouossie et al., 2019), but are in agreement with other previous

studies (Fuchs et al., 2010; von Brühl et al., 2012) showing that intact NETs contributed to clotting. The procoagulant effects observed in neutrophils may be contributed by mediators released by neutrophils, since neutrophil supernatant also promoted clotting in plasma (Table 7-1). Moreover, small amounts of contaminating cells (up to 5.3% of the total preparation), including platelets, eosinophils, basophils and lymphocytes, were observed in isolated neutrophil samples. Although they were not apparently observed in the eventual clots, their role in the procoagulant effects of neutrophils needs to be investigated in future experiments.

According to the mass spectrometry results, some mediators were found that have previously been reported to demonstrate procoagulant effects in the neutrophil supernatant, such as neutrophil defensin, which promotes fibrin polymerization and contributes to a denser clot formation (Abu-Fanne et al., 2019). Neutrophils likely released additional procoagulant mediators during the clotting process, since the generation of protofibrils in plasma occurred faster with neutrophils compared to their supernatant alone. Interestingly, some proteins, which have anticoagulant effects, were also found in the neutrophil supernatant, e.g. annexin which contributes to fibrinolysis and inhibits FXII. (Chapin and Hajjar, 2015; Nakayama et al., 2020). But it seems that procoagulant mediators were more dominant under the experimental conditions of this study. As neutrophils release both procoagulant and anticoagulant

mediators, the mechanisms behind neutrophil-induced clotting may be complex and requires further investigation.

	Human Neutrophils	Human NETs	Neutrophil Supernatant	Diff PLB-985 Cells	PLB-985 NETs
Promote Clotting in Purified Fibrinogen	No (Minute MaxOD)	No	—	No	No
Promote Clotting in NPP	Yes	Yes	Yes	Yes	Yes
Promote Clotting in -FXII Plasma	Delayed	Yes	Delayed	—	—
Promote Clotting in -FXI Plasma	No (Minute MaxOD)	Yes	No	—	—
Promote Clotting in -FVII Plasma	Delayed	Yes	Delayed	—	—
Clot Lysis Rate	Delayed	Delayed	—	—	—
Clot Permeability	High	Normal	—	—	—
Fibrin Fibre Morphology	Tiny and Abnormal	Normal	—	Normal	Normal
Fibrin Fibre Thickness	Thinner	Thicker	—	Thicker	Thicker
Fibrin Fibre Counts (Clot Density)	Less (May be too thin for software to count)	Normal (Denser surrounding NETs)	—	Less	Less (Denser surrounding NETs)

Table 7-1. A summary of effects of human neutrophils, human NETs, differentiated PLB-985 cells and PLB-985 NETs on coagulation. Data were compared with clots induced by 0.1 U/ml thrombin. “—” represents there is no data to display.

7.1.2 Neutrophil and NETs Altered Clot Structure in a Different Manner

The overall structure of clots induced by neutrophils or NETs was significantly different (Table 7-1), although both neutrophils and NETs generated from neutrophils could promote clotting. SEM images showed that neutrophil-induced clots only formed short and thin fibres on the surface of the neutrophils, and the

overall structure appeared to be fragile and unstable, which was consistent with the high permeability of these clots. This kind of structure may be explained by the opposite effects of procoagulant and anticoagulant mediators released by neutrophils. In contrast, NET-induced clots showed substantial fibrin fibre network structures, and even formed thicker fibrin fibres when compared with thrombin control. However, NETs did not statistically increase the permeability of clots. Confocal results suggested that NETs increased the density of fibrin fibres in the close vicinity of them, but that the fibrin network was more porous in other areas, which may explain why the overall permeability of clots was not apparently influenced. Interestingly, both neutrophils and NETs prolonged clot lysis time compared to thrombin control clots. For neutrophil clots, the delayed clot lysis rate may be due to the compact and thinner fibers having reduced contact surfaces for tPA. For human NETs clots, it may be due to the thicker fibrin fibres. Thicker fibrin fibres normally associate with lower density of clot, like clots induced by differentiated PLB-985 cells and PLB-985 NETs. But the overall density of human NETs clots did not apparently alter in this study. Human NETs may show more efficient procoagulant effects than human neutrophils, differentiated PLB-985 cells and PLB-985 NETs. Additionally, when thrombin was added together with neutrophils (NETs), the role of neutrophils and NETs in increasing the resistance of clots to thrombolysis appeared reduced when compared with thrombin control. The formation of thicker fibrin fibres may explain the increased resistance of NET-induced clots to thrombolysis. It could be that some components in neutrophils and NETs may

interact with tPA, and that this interaction may be disturbed by thrombin, but this possible explanation is speculative, and requires further investigation.

To explore why neutrophil-induced clots failed to generate normal fibrin fibres, the release of FpA and FpB were detected by ELISA. Neutrophils only significantly increased the release of FpB. The release of FpA and FpB was significantly less than that of thrombin control clots, which is consistent with the abnormal structure of neutrophil-induced clots observed under SEM. It has been shown that FpA and FpB could be released from fibrinogen by other enzymes (e.g., tPA) independently of thrombin (Glas-Greenwalt, 1995).

Leukocyte enzymes have also been shown to release FpA from fibrinogen (Weitz et al., 1986). Combined with the tiny fibrin fibres observed in neutrophil-induced clots, the increased release of FpB in neutrophil-induced clots may be unrelated to thrombin activity, but may be related to the direct effects of an enzyme released by the neutrophil. Moreover, in view of the observation of no substantial thrombin generation by the neutrophils, these SEM results also shows some agreement with previous studies that questioned the expression of TF in neutrophils (Østerud et al., 2000; Østerud, 2004; Sovershaev et al., 2008).

7.1.3 Neutrophil and NETs Initiated Different Coagulation Pathways

This thesis also explored the coagulation pathways through which neutrophils and NETs induce clotting (Table 7-1). FXII-, FXI- and FVII-deficient plasmas were used in turbidity experiments since the inhibitors of TF and FXII did not

work efficiently in plasma. The procoagulant effects of both neutrophils and their supernatant were inhibited most significantly in FXI-deficient plasma.

Furthermore, clotting induced by neutrophils or their supernatant was somewhat delayed in FXII- and FVII-deficient plasmas. Therefore, it is likely that both the intrinsic and extrinsic pathways are involved in the procoagulant effects of neutrophils or their mediators, with FXI mainly responsible for the effect, while FXII and FVII were partially involved. A limitation of this study is that the control of normal pooled plasma itself contained relatively higher levels FpA and FpB than expected. Self-coagulation was observed in all plasmas, except in FXI-deficient plasma. The addition of high-speed centrifugation and filtration steps could significantly reduce this phenomenon. Thus, some components in plasma seem to trigger self-coagulation via FXI, and it could be that some components may promote the release of fibrinopeptides (mainly FpA) from fibrinogen. However, the specificity of the ELISA kits for FpA and FpB needs to be tested in control experiments to investigate for any non-specific interactions of the antibodies included in the kits.

In contrast to the findings in neutrophils, the absence of FXII, FXI and FVII did not inhibit the procoagulant effects of NETs in plasma, suggesting that NETs may interact with other components than FVII, FXII and FXI in plasma to promote clotting. As described in chapter 1, some previous studies have indicated different opinions from this study. They suggested that NETs promote clotting via intrinsic or extrinsic pathways, as NETs have been reported to

contain negatively charged DNA and to be decorated with TF (von Brühl et al., 2012; Martinod and Wagner, 2014). For the involvement of TF in NET-induced clotting, as discussed above, this study suggested that neutrophil samples did not contain or release TF, so the NETs used in this study may not be decorated with TF either. Moreover, NETs still clotted FVII-deficient plasma. Thus, this study suggested that the pro-coagulant effects of NETs do not appear to be TF-based. As for the involvement of FXII, one possible explanation is that although NETs are negatively charged, the granular proteins attached on NETs are positively charged (Fuchs et al., 2007), thereby the intact NETs may be electrically neutral and cannot initiate clotting via FXII. Another possible explanation may be that von Brühl et al. carried their study in mouse models, while this thesis is based on the use of human plasmas *in vitro*, so the conflicting findings may be due to different experimental conditions and species differences. Moreover, both neutrophils and NETs were presented in the mice model used by von Brühl et al., thus the reduced thrombus formation they observed in FXII deficiency may be due to the blocking of procoagulant effects of the neutrophils but not NETs. However, the exact reasons for some of these apparent discrepancies still need to be explored in future studies.

7.1.4 Comparison of Neutrophil and Neutrophil-like Cells

In this thesis, a neutrophil-like cell model was also established with the PLB-985 cell line. 97% PLB-985 cells expressed CD11b on the last day of differentiation. However, they demonstrated lower CD11b MFI value than human neutrophils.

The expression of two other neutrophil surface markers (CD16 [FcγRIII] and CD66b) in differentiated PLB-985 cells was less than human neutrophils.

Therefore, differentiated PLB-985 cells may have fewer CD11b receptors on their membrane surface than human neutrophils, and they may not display all the properties of neutrophils. But in general, they appeared to have differentiated into neutrophil-like cells. SEM and Wright's staining showed consistent results that differentiated PLB-985 cells changed into irregular shapes compared to normal PLB-985 cells, and formed a neutrophil-like membrane surface which has many 'flap-like' structures. Similar to primary neutrophils, differentiated PLB-985 cells were able to generate NETs. Data presented in this thesis also suggested that the fibres of both the human neutrophil NETs and PLB-985 NETs were made up of multiple strands of DNA.

Similar to human neutrophils and human NETs, differentiated PLB-985 cells and PLB-985 NETs also had no effect on clotting in purified fibrinogen, but induced clotting independently of thrombin in plasma (Table 7-1). PLB-985 NETs also increased the thickness of fibrin fibres as compared to thrombin control. However, unlike the small and thin fibrin fibres observed in human neutrophil-induced clots, differentiated PLB-985 cell-induced clots formed thicker fibrin fibres than thrombin control and demonstrated substantial fibrin fibre network structures (Table 7-1). Since many spherical particles which are likely to be microvesicles were observed in SEM image, differentiated PLB-985 cells may be able to release microvesicles that contains coagulant factors,

resulting in the formation of normal fibrin fibres. Furthermore, because PLB-985 are an immortalized and thus neoplastic cell line, they likely express TF, which will activate coagulation through the extrinsic pathway. Basically, the neutrophil-like cell model established with PLB-985 cells could be a suitable substitute for human neutrophils and NETs in coagulation-related studies, and could be used to reduce the need for human blood during optimization steps. But due to the significant other differences compared with human neutrophils, key results need to be confirmed with primary neutrophils.

7.2 Conclusion

In summary, neutrophils and NETs promoted clotting and affected clot structure in a different manner. NETs increased fibrin fibre thickness, and induced a denser fibre network in the area immediately surrounding them, which may increase the stability of clots. However, neutrophils could not trigger the formation of normal fibrin fibres, and the overall structure of neutrophil-induced clot was weak with a high permeability. NETs may interact with components other than FXII, FXI and FVII in plasma to trigger clotting. In contrast, neutrophils (or mediators they release) likely trigger clotting mainly through the intrinsic pathway. Differentiated PLB-985 cells are a suitable neutrophil-like cell model, and could be used in coagulation-related studies, but some differences between them and primary neutrophils need to be considered.

This study has provided new insights into the role of neutrophils and NETs in coagulation, and suggested a possibility that NETs may promote clotting by a special pathway in addition to the known intrinsic and extrinsic pathways, the future elucidation of which may lead to the development of new strategies for the treatment of thromboinflammation.

7.3 Future Studies

- Research should continue to elucidate which coagulant factors interact with NETs to promote clotting.
- The mediators that are released by neutrophils and which may be involved in the procoagulant effects of neutrophils should be further studied and defined. The interactions between such mediators and coagulation factors (especially FXI, FXII and FVII) should be further investigated. Since neutrophils do not unduly trigger clotting everywhere in vessels, future studies should address whether there is some kind of “balance” between procoagulant and anticoagulant mediators released from neutrophils in circulation, in physiology and in disease.
- The mechanism by which neutrophils delay clot lysis also needs to be further investigated in future studies, because it cannot be fully explained by the characteristics of the neutrophil clots that have been found so far (e.g., porous and abnormal structure).

- The origin of the FpA and FpB in the plasma and neutrophil-induced clots is also unclear, whether they were released due to the effects of neutrophils or residual platelets needs to be further investigated.
- Further studies could investigate whether the spherical particles observed in SEM images of PLB-985 NETs are microvesicles or other components. Whether these spherical particles can contribute to maintain the structure of NETs during clot formation (as discussed in chapter 5) should also be explored in future studies.

References

- Abcam 2015. Counting cells using a hemocytometer. *Protocols*. **000**.
- Abu-Fanne, R., Stepanova, V., Litvinov, R.I., Abdeen, S., Bdeir, K., Higazi, M., Maraga, E., Nagaswami, C., Mukhitov, A.R., Weisel, J.W., Cines, D.B. and Higazi, A.A.R. 2019. Neutrophil α -defensins promote thrombosis in vivo by altering fibrin formation, structure, and stability. *Blood*. **133**(5).
- Adan, A., Alizada, G., Kiraz, Y., Baran, Y. and Nalbant, A. 2017. Flow cytometry: basic principles and applications. *Critical Reviews in Biotechnology*. **37**(2), pp.163–176.
- Alkarithi, G., Duval, C., Shi, Y., Macrae, F.L. and Ariëns, R.A.S. 2021. Thrombus Structural Composition in Cardiovascular Disease. *Arteriosclerosis, Thrombosis, and Vascular Biology*. **0**(0), ATVBAHA.120.315754.
- Anderson, S.I., Hotchin, N.A. and Nash, G.B. 2000. Role of the cytoskeleton in rapid activation of CD11b/CD18 function and its subsequent downregulation in neutrophils. *Journal of cell science*.
- Ariëns, R.A.S. 2013. Fibrin(ogen) and thrombotic disease. *Journal of Thrombosis and Haemostasis*. **11**(SUPPL.1).
- Ariëns, R.A.S., Lai, T.S., Weisel, J.W., Greenberg, C.S. and Grant, P.J. 2002. Role of factor XIII in fibrin clot formation and effects of genetic polymorphisms. *Blood*. **100**(3).
- Ariens, R.A.S., Philippou, H., Nagaswami, C., Weisel, J.W., Lane, D.A. and Grant, P.J. 2000. The factor XIII V34L polymorphism accelerates thrombin activation of factor XIII affects cross-linked fibrin structure. *Blood*. **96**(3).
- Ashkenazi, A. and Marks, R.S. 2009. Luminol-dependent chemiluminescence of human phagocyte cell lines: Comparison between DMSO differentiated PLB 985 and HL 60 cells. *Luminescence*. **24**(3), pp.171–177.
- Aydin, S. 2015. A short history, principles, and types of ELISA, and our laboratory experience with peptide/protein analyses using ELISA. *Peptides*. **72**.

- Baker, S.R., Zabczyk, M., Macrae, F.L., Duval, C., Undas, A. and Ariëns, R.A.S. 2019. Recurrent venous thromboembolism patients form clots with lower elastic modulus than those formed by patients with non-recurrent disease. *Journal of Thrombosis and Haemostasis*.
- Beckmann, L., Dicke, C., Spath, B., Lehr, C., Sievers, B., Klinker, A., Baldus, S., Rudolph, V. and Langer, F. 2017. Myeloperoxidase Is a Negative Regulator of Phospholipid-Dependent Coagulation. *Thrombosis and Haemostasis*. **117**(12).
- Bombeli, T. and Spahn, D.R. 2004. Updates in perioperative coagulation: Physiology and management of thromboembolism and haemorrhage. *British Journal of Anaesthesia*. **93**(2).
- Borregaard, N., Sørensen, O.E. and Theilgaard-Mönch, K. 2007. Neutrophil granules: a library of innate immunity proteins. *Trends in Immunology*.
- Bridge, K.I., Philippou, H. and Ariëns, R.A.S. 2014. Clot properties and cardiovascular disease. *Thrombosis and Haemostasis*. **112**(5).
- Brill, A., Fuchs, T.A., Savchenko, A.S., Thomas, G.M., Martinod, K., De Meyer, S.F., Bhandari, A.A. and Wagner, D.D. 2012. Neutrophil extracellular traps promote deep vein thrombosis in mice. *Journal of Thrombosis and Haemostasis*. **10** (1), pp.136–144.
- von Brühl, M.-L., Stark, K., Steinhart, A., Chandraratne, S., Konrad, I., Lorenz, M., Khandoga, A., Tirniceriu, A., Coletti, R., Köllnberger, M., Byrne, R.A., Laitinen, I., Walch, A., Brill, A., Pfeiler, S., Manukyan, D., Braun, S., Lange, P., Riegger, J., Ware, J., Eckart, A., Haidari, S., Rudelius, M., Schulz, C., Ehtler, K., Brinkmann, V., Schwaiger, M., Preissner, K.T., Wagner, D.D., Mackman, N., Engelmann, B. and Massberg, S. 2012. Monocytes, neutrophils, and platelets cooperate to initiate and propagate venous thrombosis in mice in vivo. *The Journal of Experimental Medicine*. **209**(4), pp.819–835.
- Butenas, S. 2012. Tissue Factor Structure and Function. *Scientifica*. **2012**.

- Carrigan, S.O., Wepler, A.L., Issekutz, A.C. and Stadnyk, A.W. 2005. Neutrophil differentiated HL-60 cells model Mac-1 (CD11b/CD18)-independent neutrophil transepithelial migration. *Immunology*. **115**(1).
- Carvalho, F.A., Connell, S., Miltenberger-Miltenyi, G., Pereira, S.V., Tavares, A., Ariëns, R.A.S. and Santos, N.C. 2010. Atomic force microscopy-based molecular recognition of a fibrinogen receptor on human erythrocytes. *ACS Nano*. **4**(8).
- Chan, Y.K., Tsai, M.H., Huang, D.C., Zheng, Z.H. and Hung, K.D. 2010. Leukocyte nucleus segmentation and nucleus lobe counting. *BMC Bioinformatics*. **11**(1), p.558.
- Chandler, W.L. 2013. Fibrinolytic Testing. *Transfusion Medicine and Hemostasis: Clinical and Laboratory Aspects: Second Edition.*, pp.871–874.
- Chapin, J.C. and Hajjar, K.A. 2015. Fibrinolysis and the control of blood coagulation. *Blood Reviews*. **29**(1), pp.17–24.
- Chernysh, I.N., Nagaswami, C., Kosolapova, S., Peshkova, A.D., Cuker, A., Cines, D.B., Cambor, C.L., Litvinov, R.I. and Weisel, J.W. 2020. The distinctive structure and composition of arterial and venous thrombi and pulmonary emboli. *Scientific Reports*. **10**(1).
- Clark, S.R., Ma, A.C., Tavener, S.A., McDonald, B., Goodarzi, Z., Kelly, M.M., Patel, K.D., Chakrabarti, S., McAvoy, E., Sinclair, G.D., Keys, E.M., Allen-Vercoe, E., DeVinney, R., Doig, C.J., Green, F.H.Y. and Kubes, P. 2007. Platelet TLR4 activates neutrophil extracellular traps to ensnare bacteria in septic blood. *Nat. Med.* **13**(4), pp.463–469.
- Colman, R.W. 2006. Are hemostasis and thrombosis two sides of the same coin? *The Journal of Experimental Medicine*. **203**(3), pp.493–495.
- Dahlbäck, B. and Villoutreix, B.O. 2005. The anticoagulant protein C pathway. *FEBS Letters*. **579**(15).
- Darbousset, R., Thomas, G.M., Mezouar, S., Frère, C., Bonier, R., Mackman, N., Renné, T., Dignat-George, F., Dubois, C. and Panicot-Dubois, L. 2012.

Tissue factor-positive neutrophils bind to injured endothelial wall and initiate thrombus formation. *Blood*.

Darby, B.C., Chien, P., Rossman, M.D. and Schreiber, A.D. 2018.

Monocyte/Macrophage FcγRIII, Unlike FcγRIII on Neutrophils, Is Not a Phosphatidylinositol-Linked Protein. . **75**(12), pp.2396–2400.

Duerschmied, D., Suidan, G.L., Demers, M., Herr, N., Carbo, C., Brill, A., Cifuni, S.M., Mauler, M., Cicko, S., Bader, M., Idzko, M., Bode, C. and Wagner, D.D. 2013. Platelet serotonin promotes the recruitment of neutrophils to sites of acute inflammation in mice. *Blood*. **121**(6).

Duval, C., Ali, M., Chaudhry, W.W., Ridger, V.C., Ariëns, R.A.S. and Philippou, H. 2016. Factor XIII A-Subunit V34L Variant Affects Thrombus Cross-Linking in a Murine Model of Thrombosis. *Arteriosclerosis, Thrombosis, and Vascular Biology*. **36**(2), pp.308–316.

Duval, C., Allan, P., Connell, S.D.A., Ridger, V.C., Philippou, H. and Ariëns, R.A.S. 2014. Roles of fibrin α- and γ-chain specific cross-linking by FXIIIa in fibrin structure and function. *Thrombosis and Haemostasis*. **111**(5).

Eddy, J.L., Schroeder, J.A., Zimble, D.L., Bellows, L.E. and Lathem, W.W. 2015. Impact of the pla protease substrate α2-antiplasmin on the progression of primary pneumonic plague. *Infection and Immunity*. **83**(12).

Ettelaie, C., Collier, M.E.W., Featherby, S., Benelhaj, N.E., Greenman, J. and Maraveyas, A. 2016. Analysis of the potential of cancer cell lines to release tissue factor-containing microvesicles: Correlation with tissue factor and PAR2 expression. *Thrombosis Journal*. **14**(1).

Fay, P.J. 2004. Activation of factor VIII and mechanisms of cofactor action. *Blood Reviews*. **18**(1).

Flemmig, M. and Melzig, M.F. 2012. Serine-proteases as plasminogen activators in terms of fibrinolysis. *Journal of Pharmacy and Pharmacology*. **64**(8).

Fuchs, T.A., Abed, U., Goosmann, C., Hurwitz, R., Schulze, I., Wahn, V., Weinrauch, Y., Brinkmann, V. and Zychlinsky, A. 2007. Novel cell death

- program leads to neutrophil extracellular traps. *Journal of Cell Biology*. **176**(2), pp.231–241.
- Fuchs, T.A., Brill, A., Duerschmied, D., Schatzberg, D., Monestier, M., Myers, D.D., Wroblewski, S.K., Wakefield, T.W., Hartwig, J.H. and Wagner, D.D. 2010. Extracellular DNA traps promote thrombosis. *Proceedings of the National Academy of Sciences*.
- Furie, B. and Furie, B.C. 2008. Mechanisms of Thrombus Formation. *New England Journal of Medicine*.
- G, C. and S, F. 2017. The Two Faces of Thrombosis: Coagulation Cascade and Platelet Aggregation. Are Platelets the Main Therapeutic Target? *Journal of Thrombosis and Circulation: Open Access*. **03**(01), pp.1–6.
- Glas-Greenwalt, P. 1995. *Fibrinolysis in Disease - The Malignant Process, Interventions in Thrombogenic Mechanisms, and Novel Treatment Modalities* [Online]. [Accessed 13 November 2021]. Available from: [https://books.google.co.uk/books?id=tOvMR7QJ3gC&pg=PA143&dq=enzymes+other+than+thrombin+can+release+FPA+and+FPB&hl=zh-CN&sa=X&ved=2ahUKEwietrOvvZX0AhVnQEEAHXW0ByIQ6AF6BAgFEAl#v=onepage&q=enzymes other than thrombin can release FPA and FPB&f=false](https://books.google.co.uk/books?id=tOvMR7QJ3gC&pg=PA143&dq=enzymes+other+than+thrombin+can+release+FPA+and+FPB&hl=zh-CN&sa=X&ved=2ahUKEwietrOvvZX0AhVnQEEAHXW0ByIQ6AF6BAgFEAl#v=onepage&q=enzymes%20other%20than%20thrombin%20can%20release%20FPA%20and%20FPB&f=false).
- Goldhaber, S.Z. 2010. Risk Factors for Venous Thromboembolism. *Journal of the American College of Cardiology*. **56**(1).
- Granger, V., Faille, D., Marani, V., Noël, B., Gallais, Y., Szely, N., Flament, H., Pallardy, M., Chollet-Martin, S. and Chaisemartin, L. 2017. Human blood monocytes are able to form extracellular traps. *Journal of Leukocyte Biology*.
- Griep, M.A., Fujikawa, K. and Nelsestuen, G.L. 1985. Binding and Activation Properties of Human Factor XII, Prekallikrein, and Derived Peptides with Acidic Lipid Vesicles. *Biochemistry*.

- Harper, M.T. and Poole, A.W. 2013. Chloride channels are necessary for full platelet phosphatidylserine exposure and procoagulant activity. *Cell Death and Disease*. **4**(12).
- Heemskerk, J.W.M., Mattheij, N.J.A. and Cosemans, J.M.E.M. 2013. Platelet-based coagulation: Different populations, different functions. *Journal of Thrombosis and Haemostasis*. **11**(1).
- Hethershaw, E.L., Cilia La Corte, A.L., Duval, C., Ali, M., Grant, P.J., Ariëns, R.A.S. and Philippou, H. 2014. The effect of blood coagulation factor XIII on fibrin clot structure and fibrinolysis. *Journal of Thrombosis and Haemostasis*. **12**(2).
- Higure, A., Okamoto, K., Hirata, K., Todoroki, H., Nagafuchi, Y., Takeda, S., Katoh, H., Itoh, H., Ohsato, K. and Nakamura, S. 1996. Macrophages and neutrophils infiltrating into the liver are responsible for tissue factor expression in a rabbit model of acute obstructive cholangitis. *Thrombosis and Haemostasis*. **75**(5).
- Ito, T., Thachil, J., Asakura, H., Levy, J.H. and Iba, T. 2019. Thrombomodulin in disseminated intravascular coagulation and other critical conditions - A multi-faceted anticoagulant protein with therapeutic potential. *Critical Care*. **23**(1).
- Jackson, S.P., Darbousset, R. and Schoenwaelder, S.M. 2019. Thromboinflammation: Challenges of therapeutically targeting coagulation and other host defense mechanisms. *Blood*. **133**(9).
- Jash, E., Prasad, P., Kumar, N., Sharma, T., Goldman, A. and Sehrawat, S. 2018. Perspective on nanochannels as cellular mediators in different disease conditions. *Cell Communication and Signaling*. **16**(1).
- Jochum, M., Lander, S., Heimbürger, N. and Fritz, H. 1981. Effect of human granulocytic elastase on isolated human antithrombin iii. *Hoppe-Seyler's Zeitschrift für Physiologische Chemie*.
- Kaemmar, S.B. 2011. Introduction to Bruker's ScanAsyst and PeakForce Tapping AFM Technology. *Application note*. **133**(Rev. A0), p.12.

- Kapoor, S., Opneja, A. and Nayak, L. 2018. The role of neutrophils in thrombosis. *Thromb. Res.* **170**, pp.87–96.
- Kashi, M., Jacquin, A., Dakhil, B., Zaimi, R., Mahé, E., Tella, E. and Bagan, P. 2020. Severe arterial thrombosis associated with Covid-19 infection. *Thrombosis Research.* **192**.
- Kato, H. 2002. Regulation of functions of vascular wall cells by tissue factor pathway inhibitor: Basic and clinical aspects. *Arteriosclerosis, Thrombosis, and Vascular Biology.* **22**(4).
- Kato, H. 1996. Tissue factor pathway inhibitor; Its structure, function and clinical significance *In: Polish Journal of Pharmacology.*
- Kattula, S., Byrnes, J.R. and Wolberg, A.S. 2017. Fibrinogen and Fibrin in Hemostasis and Thrombosis. *Arteriosclerosis, Thrombosis, and Vascular Biology.* **37**(3), pp.e13–e21.
- Kerbikov, O., Orekhov, P., Borskaya, E. and Nosenko, N. 2021. High incidence of venous thrombosis in patients with moderate-to-severe COVID-19. *International Journal of Hematology.* **113**(3).
- Kleinschnitz, C., Stoll, G., Bendszus, M., Schuh, K., Pauer, H.U., Burfeind, P., Renné, C., Gailani, D., Nieswandt, B. and Renné, T. 2006. Targeting coagulation factor XII provides protection from pathological thrombosis in cerebral ischemia without interfering with hemostasis. *Journal of Experimental Medicine.* **203**(3).
- Von Köckritz-Blickwede, M. and Nizet, V. 2009. Innate immunity turned inside-out: Antimicrobial defense by phagocyte extracellular traps. *Journal of Molecular Medicine.* **87**(8), pp.775–783.
- Koshiar, R.L., Somajo, S., Norström, E. and Dahlbäck, B. 2014. Erythrocyte-derived microparticles supporting activated protein C-mediated regulation of blood coagulation. *PLoS ONE.* **9**(8).
- Lam, W. and Moosavi, L. 2019. *Physiology, Factor V.*
- LaPelusa, A. and Dave, H.D. 2021. Physiology, Hemostasis *In: StatPearls.*
- De Lau, L.M.L., Cheung, E.Y.L., Kluft, C., Leebeek, F.W.G., Meijer, P., Laterveer, R., Dippel, D.W.J. and De Maat, M.P.M. 2008. Strongly

- increased levels of fibrinogen elastase degradation products in patients with ischemic stroke. *British Journal of Haematology*. **143**(5).
- Levi, M. and Van Der Poll, T. 2005. Two-way interactions between inflammation and coagulation. *Trends in Cardiovascular Medicine*. **15**(7).
- Libby, P. and Aikawa, M. 2002. Stabilization of atherosclerotic plaques: New mechanisms and clinical targets. *Nature Medicine*. **8**(11).
- Licari, L.G. and Kovacic, J.P. 2009. Thrombin physiology and pathophysiology. *Journal of Veterinary Emergency and Critical Care*. **19**(1).
- Lippi, G. and Favaloro, E.J. 2018. Venous and Arterial Thromboses: Two Sides of the Same Coin? *Seminars in Thrombosis and Hemostasis*. **44**(3).
- Longstaff, C. and Kolev, K. 2015. Basic mechanisms and regulation of fibrinolysis. *Journal of Thrombosis and Haemostasis*. **13**(S1), pp.S98–S105.
- Longstaff, C., Varjú, I., Sótonyi, P., Szabó, L., Krumrey, M., Hoell, A., Bóta, A., Varga, Z., Komorowicz, E. and Kolev, K. 2013. Mechanical stability and fibrinolytic resistance of clots containing fibrin, DNA, and histones. *J. Biol. Chem.* **288**(10), pp.6946–6956.
- Lorand, L. 2001. Factor XIII: Structure, activation, and interactions with fibrinogen and fibrin *In: Annals of the New York Academy of Sciences*.
- Macrae, F.L., Duval, C., Papareddy, P., Baker, S.R., Yuldasheva, N., Kearney, K.J., McPherson, H.R., Asquith, N., Konings, J., Casini, A., Degen, J.L., Connell, S.D., Philippou, H., Wolberg, A.S., Herwald, H. and Ariëns, R.A.S. 2018. A fibrin biofilm covers blood clots and protects from microbial invasion. *Journal of Clinical Investigation*. **128**(8), pp.3356–3368.
- Malkhassian, D. and Sharma, S. 2019. *Physiology, Factor XIII*.
- Margetic, S. 2012. Inflammation and hemostasis. *Biochemia Medica*.
- Marin-Esteban, V., Turbica, I., Dufour, G., Semiramoth, N., Gleizes, A., Gorges, R., Beau, I., Servin, A.L., Moal, V.L. Le, Sandré, C. and Chollet-Martin, S. 2012. Afa/Dr diffusely adhering Escherichia coli strain C1845 induces neutrophil extracellular traps that kill bacteria and damage human enterocyte-like cells. *Infection and Immunity*.

-
- Martinod, K. and Deppermann, C. 2021. Immunothrombosis and thromboinflammation in host defense and disease. *Platelets*. **32**(3).
- Martinod, K. and Wagner, D.D. 2014. Thrombosis: Tangled up in NETs. *Blood*. **123**(18), pp.2768–2776.
- Mast, A.E. 2016. Tissue Factor Pathway Inhibitor: Multiple Anticoagulant Activities for a Single Protein. *Arteriosclerosis, Thrombosis, and Vascular Biology*. **36**(1).
- Maugeri, N. and Manfredi, A.A. 2015. Tissue Factor Expressed by Neutrophils: Another Piece in the Vascular Inflammation Puzzle *In: Seminars in Thrombosis and Hemostasis*.
- Mayadas, T.N., Cullere, X. and Lowell, C.A. 2014. The Multifaceted Functions of Neutrophils. *Annual Review of Pathology: Mechanisms of Disease*. **9**(1), pp.181–218.
- Mazurkiewicz-Pisarek, A., Płucienniczak, G., Ciach, T. and Plucienniczak, A. 2016. The factor VIII protein and its function. *Acta Biochimica Polonica*. **63**(1).
- McAdoo, S.P. and Dhaun, N. 2021. Resolving thromboinflammation. *Blood*. **137**(11).
- Meltzer, M.E., Doggen, C.J.M., De Groot, P.G., Rosendaal, F.R. and Lisman, T. 2009. The impact of the fibrinolytic system on the risk of venous and arterial thrombosis. *Seminars in Thrombosis and Hemostasis*. **35**(5).
- Mihalko, E. and Brown, A.C. 2020. Clot Structure and Implications for Bleeding and Thrombosis. *Seminars in Thrombosis and Hemostasis*. **46**(1).
- Mohammed, B.M., Matafonov, A., Ivanov, I., Sun, M. fu, Cheng, Q., Dickeson, S.K., Li, C., Sun, D., Verhamme, I.M., Emsley, J. and Gailani, D. 2018. An update on factor XI structure and function. *Thrombosis Research*. **161**.
- Mollinedo, F., Martin-Martin, B., Calafat, J., Nabokina, S.M. and Lazo, P.A. 2003. Role of Vesicle-Associated Membrane Protein-2, Through Q-Soluble N-Ethylmaleimide-Sensitive Factor Attachment Protein Receptor/R-Soluble N-Ethylmaleimide-Sensitive Factor Attachment Protein Receptor

-
- Interaction, in the Exocytosis of Specific and Tertiary . *The Journal of Immunology*. **170**(2), pp.1034–1042.
- Monroe, D.M., Hoffman, M. and Roberts, H.R. 2002. Platelets and thrombin generation. *Arteriosclerosis, Thrombosis, and Vascular Biology*. **22**(9).
- Monroe, D.M., Hoffman, M. and Roberts, H.R. 1996. Transmission of a procoagulant signal from tissue factor-bearing cells to platelets. *Blood Coagulation and Fibrinolysis*. **7**(4).
- Monroe, D.M., Roberts, H.R. and Hoffman, M. 1994. Platelet procoagulant complex assembly in a tissue factor-initiated system. *British Journal of Haematology*. **88**(2).
- Moroi, M. and Jung, S.M. 2004. Platelet glycoprotein VI: Its structure and function. *Thrombosis Research*. **114**(4).
- Mosesson, M.W. 2005. Fibrinogen and fibrin structure and functions.pdf. , pp.1894–1904.
- Murayama, C., Kimura, Y. and Setou, M. 2009. Imaging mass spectrometry: Principle and application. *Biophysical Reviews*. **1**(3).
- Mussbacher, M., Kral-Pointner, J.B., Salzman, M., Schrottmaier, W.C. and Assinger, A. 2019. Mechanisms of Hemostasis: Contributions of Platelets, Coagulation Factors, and the Vessel Wall
- Muszbek, L., Bereczky, Z., Bagoly, Z., Komáromi, I. and Katona, É. 2011. Factor XIII: A coagulation factor with multiple plasmatic and cellular functions. *Physiological Reviews*. **91**(3).
- Næss, I.A., Christiansen, S.C., Romundstad, P., Cannegieter, S.C., Rosendaal, F.R. and Hammerstrøm, J. 2007. Incidence and mortality of venous thrombosis: A population-based study. *Journal of Thrombosis and Haemostasis*. **5**(4).
- Nakamura, S., Imamura, T. and Okamoto, K. 2004. Tissue factor in neutrophils: Yes. *Journal of Thrombosis and Haemostasis*.
- Nakayama, M., Miyagawa, H., Kuranami, Y., Tsunooka-Ota, M., Yamaguchi, Y. and Kojima-Aikawa, K. 2020. Annexin A4 inhibits sulfatide-induced

activation of coagulation factor XII. *Journal of Thrombosis and Haemostasis*.

Nesheim, M. 2003. Thrombin and fibrinolysis. *Chest*. **124**(3 SUPPL.), pp.33S-39S.

Nieswandt, B. and Watson, S.P. 2003. Platelet-collagen interaction: Is GPVI the central receptor? *Blood*. **102**(2).

Noubouossie, Denis F., Reeves, B.N., Strahl, B.D. and Key, N.S. 2019. Neutrophils: Back in the thrombosis spotlight. *Blood*.

Noubouossie, Denis F, Whelihan, M.F., Yu, Y., Sparkenbaugh, E., Pawlinski, R., Monroe, D.M. and Key, N.S. 2019. In vitro activation of coagulation by human neutrophil DNA and histone proteins but not neutrophil extracellular traps. . **129**(8), pp.1021–1030.

Oh, H., Siano, B. and Diamond, S. 2008. Neutrophil Isolation Protocol. *Journal of Visualized Experiments*.

Østerud, B., Rao, L.V.M. and Olsen, J.O. 2000. Induction of tissue factor expression in whole blood: Lack of evidence for the presence of tissue factor expression in granulocytes. *Thrombosis and Haemostasis*.

Østerud, B. 2004. Tissue factor in neutrophils: No. *Journal of Thrombosis and Haemostasis*. **2**(2), pp.218–220.

Owens, A.P. and Mackman, N. 2010. Tissue factor and thrombosis: The clot starts here. *Thrombosis and Haemostasis*. **104**(3).

Palta, S., Saroa, R. and Palta, A. 2014. Overview of the coagulation system. *Indian Journal of Anaesthesia*.

Pedruzzi, E., Fay, M., Elbim, C., Gaudry, M. and Gougerot-Pocidallo, M.A. 2002. Differentiation of PLB-985 myeloid cells into mature neutrophils, shown by degranulation of terminally differentiated compartments in response to N-formyl peptide and priming of superoxide anion production by granulocyte-macrophage colony-stimulating factor. *British Journal of Haematology*. **117**(3).

Periayah, M.H., Halim, A.S. and Saad, A.Z.M. 2017. Mechanism action of platelets and crucial blood coagulation pathways in Hemostasis.

International Journal of Hematology-Oncology and Stem Cell Research.
11(4).

- Petersen, L.C., Bojrn, S.E. and Nordfang, O. 1992. Effect of leukocyte proteinases on tissue factor pathway inhibitor. *Thrombosis and Haemostasis.*
- Peuscher, F.W., Cleton, F.J., Armstrong, L., Stoepman-van Dalen, E.A., van Mourik, J.A. and van Aken, W.G. 1980. Significance of plasma fibrinopeptide A (fpA) in patients with malignancy. *Journal of Laboratory and Clinical Medicine.* **96(1).**
- Peyvandi, F., Garagiola, I. and Baronciani, L. 2011. Role of von Willebrand factor in the haemostasis. *Blood Transfusion.* **9(SUPPL. 2).**
- Pieters, J., Lindhout, T. and Hemker, H. 1989. In situ-generated thrombin is the only enzyme that effectively activates factor VIII and factor V in thromboplastin-activated plasma. *Blood.* **74(3).**
- Pieters, M., Undas, A., Marchi, R., De Maat, M.P.M., Weisel, J.W. and Ariëns, R.A.S. 2012. An international study on the standardization of fibrin clot permeability measurement: Methodological considerations and implications for healthy control values. *Journal of Thrombosis and Haemostasis.* **10(10)**, pp.2179–2181.
- Pilsczek, F.H., Salina, D., Poon, K.K.H., Fahey, C., Yipp, B.G., Sibley, C.D., Robbins, S.M., Green, F.H.Y., Surette, M.G., Sugai, M., Bowden, M.G., Hussain, M., Zhang, K. and Kubes, P. 2010. A Novel Mechanism of Rapid Nuclear Neutrophil Extracellular Trap Formation in Response to *Staphylococcus aureus*. *The Journal of Immunology.* **185(12).**
- Pitchford, S., Pan, D. and Welch, H.C.E. 2017. Platelets in neutrophil recruitment to sites of inflammation. *Current Opinion in Hematology.* **24(1).**
- Pivot-Pajot, C., Chouinard, F.C., Amine El Azreq, M., Harbour, D. and Bourgoin, S.G. 2010. Characterisation of degranulation and phagocytic capacity of a human neutrophilic cellular model, PLB-985 cells. *Immunobiology.* **215(1)**, pp.38–52.

- Van der Poll, T., De Jonge, E. and Levi, M. 2001. Regulatory role of cytokines in disseminated intravascular coagulation. *Seminars in Thrombosis and Hemostasis*. **27**(6).
- Previtali, E., Bucciarelli, P., Passamonti, S.M. and Martinelli, I. 2011. Risk factors for venous and arterial thrombosis. *Blood Transfus.* **9**(2), pp.120–38.
- Prinyakupt, J. and Pluempitiwiriwajew, C. 2015. Segmentation of white blood cells and comparison of cell morphology by linear and naïve Bayes classifiers. *BioMedical Engineering Online*. **14**(1), pp.1–19.
- Ramesh, N., Salama, M., Dangott, B. and Tasdizen, T. 2012. Isolation and two-step classification of normal white blood cells in peripheral blood smears. *Journal of Pathology Informatics*. **3**(1).
- Raskob, G.E., Angchaisuksiri, P., Blanco, A.N., Büller, H., Gallus, A., Hunt, B.J., Hylek, E.M., Kakkar, T.L., Konstantinides, S. V., McCumber, M., Ozaki, Y., Wendelboe, A. and Weitz, J.I. 2014. Thrombosis: A Major Contributor to Global Disease Burden. *Seminars in Thrombosis and Hemostasis*. **40**(7), pp.724–735.
- Renné, T., Pozgajová, M., Grüner, S., Schuh, K., Pauer, H.U., Burfeind, P., Gailani, D. and Nieswandt, B. 2005. Defective thrombus formation in mice lacking coagulation factor XII. *Journal of Experimental Medicine*. **202**(2).
- Rezaie, A.R. and Giri, H. 2020. Anticoagulant and signaling functions of antithrombin. *Journal of Thrombosis and Haemostasis*. **18**(12).
- Ritis, K., Doumas, M., Mastellos, D., Micheli, A., Giaglis, S., Magotti, P., Rafail, S., Kartalis, G., Sideras, P. and Lambris, J.D. 2007. A novel C5aR-tissue factor crosstalk in neutrophils links innate immunity to coagulation pathways. *Molecular Immunology*.
- Rodgers, G.M. 2009. Role of antithrombin concentrate in treatment of hereditary antithrombin deficiency: An update. *Thrombosis and Haemostasis*. **101**(5).
- Rosales, C. 2018. Neutrophil: A cell with many roles in inflammation or several cell types? *Front. Physiol.*

- Rossaint, J., Margraf, A. and Zarbock, A. 2018. Role of platelets in leukocyte recruitment and resolution of inflammation. *Frontiers in Immunology*. **9**(NOV).
- Ruggeri, Z.M. 2007. The role of von Willebrand factor in thrombus formation. *Thrombosis Research*. **120**(SUPPL. 1).
- Ruggeri, Z.M. and Mendolicchio, G.L. 2007. Adhesion mechanisms in platelet function. *Circulation Research*. **100**(12).
- Rustom, A., Saffrich, R., Markovic, I., Walther, P. and Gerdes, H.H. 2004. Nanotubular Highways for Intercellular Organelle Transport. *Science*. **303**(5660), pp.1007–1010.
- Sang, Y., Roest, M., de Laat, B., de Groot, P.G. and Huskens, D. 2021. Interplay between platelets and coagulation. *Blood Reviews*. **46**.
- Scandura, J.M. and Walsh, P.N. 1996. Factor X bound to the surface of activated human platelets is preferentially activated by platelet-bound factor IXa. *Biochemistry*. **35**(27).
- Schillers, H., Medalsy, I., Hu, S., Slade, A.L. and Shaw, J.E. 2016. PeakForce Tapping resolves individual microvilli on living cells. *Journal of Molecular Recognition*. **29**(2).
- Schleiffenbaum, B., Moser, R., Patarroyo, M. and Fehr, J. 2018. The cell surface glycoprotein Mac-1 (CD11b / CD18) mediates neutrophil adhesion and modulates degranulation independently of its quantitative cell surface expression . Information about subscribing to The Journal of Immunology is online at : INDEPENDENT. . **1**.
- Schwartz, M.L., Pizzo, S. V., Hill, R.L. and McKee, P.A. 1973. Human Factor XIII from plasma and platelets. Molecular weights, subunit structures, proteolytic activation, and cross-linking of fibrinogen and fibrin. *Journal of Biological Chemistry*. **248**(4).
- Shi, Y., Gauer, J.S., Baker, S.R., Philippou, H., Connell, S.D. and Ariëns, R.A.S. 2021. Neutrophils can promote clotting via FXI and impact clot structure via neutrophil extracellular traps in a distinctive manner in vitro. *Scientific Reports*. **11**(1).

- Sillen, M. and Declerck, P.J. 2021. Thrombin activatable fibrinolysis inhibitor (Tafi): An updated narrative review. *International Journal of Molecular Sciences*. **22**(7).
- Simon, D.I., Chen, Z., Xu, H., Li, C.Q., Dong, J.F., McIntire, L. V., Ballantyne, C.M., Zhang, L., Furman, M.I., Berndt, M.C. and López, J.A. 2000. Platelet glycoprotein Iba is a counterreceptor for the leukocyte integrin Mac-1 (CD11b/CD18). *Journal of Experimental Medicine*. **192**(2).
- Sollberger, G., Tilley, D.O. and Zychlinsky, A. 2018. Neutrophil Extracellular Traps: The Biology of Chromatin Externalization. *Developmental Cell*. **44**(5).
- Sovershaev, M.A., Lind, K.F., Devold, H., Jørgensen, T., Hansen, J.B., Østerud, B. and Egorina, E.M. 2008. No evidence for the presence of tissue factor in high-purity preparations of immunologically isolated eosinophils. *Journal of Thrombosis and Haemostasis*.
- Sumaya, W., Wallentin, L., James, S.K., Siegbahn, A., Gabrysch, K., Himmelmann, A., Ajjan, R.A. and Storey, R.F. 2020. Impaired Fibrinolysis Predicts Adverse Outcome in Acute Coronary Syndrome Patients with Diabetes: A PLATO Sub-Study. *Thrombosis and Haemostasis*. **120**(3).
- Swystun, L.L. and Liaw, P.C. 2016. The role of leukocytes in thrombosis. *Blood*. **128**(6), pp.753–762.
- Tanaka, T., Narazaki, M. and Kishimoto, T. 2014. Il-6 in inflammation, Immunity, And disease. *Cold Spring Harbor Perspectives in Biology*. **6**(10).
- Tanguay, J.F., Geoffroy, P., Sirois, M.G., Libersan, D., Kumar, A., Schaub, R.G. and Merhi, Y. 2004. Prevention of in-stent restenosis via reduction of thrombo-inflammatory reactions with recombinant P-selectin glycoprotein ligand-I. *Thrombosis and Haemostasis*. **91**(6).
- Todoroki, H., Nakamura, S., Higure, A., Okamoto, K., Takeda, S., Nagata, N., Itoh, H. and Ohsato, K. 2000. Neutrophils express tissue factor in a monkey model of sepsis. *Surgery*.
- Torsteinsdóttir, I., Arvidson, N.G., Hällgren, R. and Håkansson, L. 1999. Enhanced expression of integrins and CD66b on peripheral blood

- neutrophils and eosinophils in patients with rheumatoid arthritis, and the effect of glucocorticoids. *Scandinavian Journal of Immunology*.
- Tracy, P.B., Rohrbach, M.S. and Mann, K.G. 1983. Functional prothrombinase complex assembly on isolated monocytes and lymphocytes. *Journal of Biological Chemistry*. **258**(12).
- Tucker, K.A., Lilly, M.B., Heck, L. and Rado, T.A. 1987. Characterization of a new human diploid myeloid leukemia cell line (PLB-985) with granulocytic and monocytic differentiating capacity. *Blood*. **70**(2).
- Undas, A. and Ariëns, R.A.S. 2011. Fibrin clot structure and function: A role in the pathophysiology of arterial and venous thromboembolic diseases. *Arteriosclerosis, Thrombosis, and Vascular Biology*. **31**(12), pp.88–99.
- Varjú, I., Longstaff, C., Szabó, L., Farkas, Á.Z., Varga-Szabó, V.J., Tanka-Salamon, A., Machovich, R. and Kolev, K. 2015. DNA, histones and neutrophil extracellular traps exert anti-fibrinolytic effects in a plasma environment. *Thrombosis and Haemostasis*.
- Venkateswarlu, D., Perera, L., Darden, T. and Pedersen, L.G. 2002. Structure and dynamics of zymogen human blood coagulation factor X. *Biophysical Journal*. **82**(3).
- Viskup, R.W., Tracy, P.B. and Mann, K.G. 1987. The isolation of human platelet factor V. *Blood*. **69**(4).
- Voetsch, B. and Loscalzo, J. 2004. Genetic Determinants of Arterial Thrombosis. *Arteriosclerosis, Thrombosis, and Vascular Biology*. **24**(2).
- Walsh, P.N. 2004. Platelet coagulation-protein interactions. *Seminars in Thrombosis and Hemostasis*. **30**(4).
- Watanabe-Kusunoki, K., Nakazawa, D., Ishizu, A. and Atsumi, T. 2020. Thrombomodulin as a Physiological Modulator of Intravascular Injury. *Frontiers in Immunology*. **11**.
- Weisel, J.W. and Litvinov, R.I. 2017. Fibrin formation, structure and properties. *Sub-Cellular Biochemistry*.
- Weitz, J.I., Landman, S.L., Crowley, K.A., Birken, S. and Morgan, F.J. 1986. Development of an assay for in vivo human neutrophil elastase activity.

- Increased elastase activity in patients with α 1-proteinase inhibitor deficiency. *Journal of Clinical Investigation*. **78**(1).
- Whelihan, M.F., Zachary, V., Orfeo, T. and Mann, K.G. 2012. Prothrombin activation in blood coagulation: The erythrocyte contribution to thrombin generation. *Blood*. **120**(18).
- Whyte, C.S. and Mutch, N.J. 2021. uPA-mediated plasminogen activation is enhanced by polyphosphate. *Haematologica*. **106**(2).
- Wolberg, A.S. 2007. Thrombin generation and fibrin clot structure. *Blood Reviews*. **21**(3), pp.131–142.
- Xu, R.G., Gauer, J.S., Baker, S.R., Slater, A., Martin, E.M., McPherson, H.R., Duval, C., Manfield, I.W., Bonna, A.M., Watson, S.P. and Ariëns, R.A.S. 2021. GPVI (Glycoprotein VI) interaction with fibrinogen is mediated by avidity and the fibrinogen α c-Region. *Arteriosclerosis, Thrombosis, and Vascular Biology*.
- Yipp, B.G. and Kubes, P. 2013. NETosis: How vital is it? *Blood*. **122**(16).
- Zacchi, L.F., Roche-Recinos, D., Pegg, C.L., Phung, T.K., Napoli, M., Aitken, C., Sandford, V., Mahler, S.M., Lee, Y.Y., Schulz, B.L. and Howard, C.B. 2021. Coagulation factor IX analysis in bioreactor cell culture supernatant predicts quality of the purified product. *Communications Biology*. **4**(1).
- Zawrotniak, M. and Rapala-Kozik, M. 2013. Neutrophil extracellular traps (NETs) - Formation and implications. *Acta Biochimica Polonica*. **60**(3), pp.277–284.
- Zhou, P., Li, T., Jin, J., Liu, Y., Li, B., Sun, Q., Tian, J., Zhao, H., Liu, Z., Ma, S., Zhang, S., Novakovic, V.A., Shi, J. and Hu, S. 2020. Interactions between neutrophil extracellular traps and activated platelets enhance procoagulant activity in acute stroke patients with ICA occlusion. *EBioMedicine*. **53**.
- Zöller, B., Svensson, P.J., Dahlbäck, B., Lind-Hallden, C., Hallden, C. and Elf, J. 2020. Genetic risk factors for venous thromboembolism. *Expert Review of Hematology*. **13**(9).

Zucoloto, A.Z. and Jenne, C.N. 2019. Platelet-Neutrophil Interplay: Insights Into Neutrophil Extracellular Trap (NET)-Driven Coagulation in Infection. *Frontiers in Cardiovascular Medicine*. **6**.

Appendices

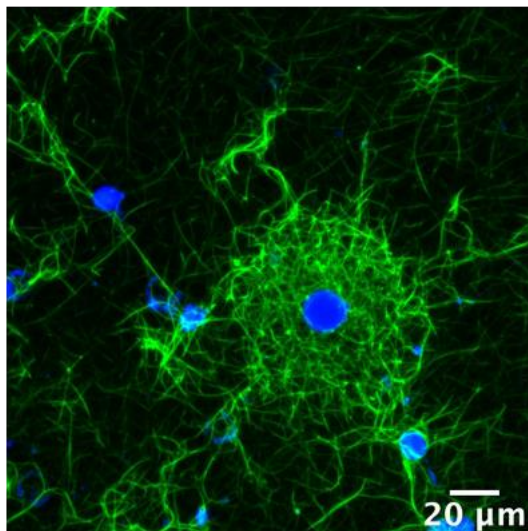
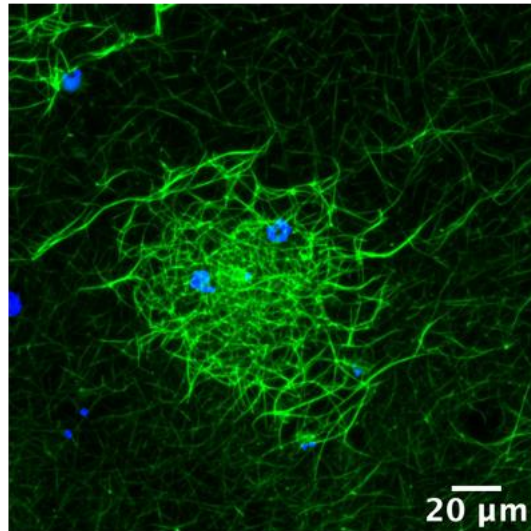
Appendix 1.

Publications	<p><u>Shi Y</u>, Baker SR, Gauer JS, Philippou H, Connell SD, Ariëns RAS. Neutrophils can promote clotting via FXI and impact clot structure via neutrophil extracellular traps in a distinctive manner <i>in vitro</i>. <i>Sci Rep</i> 11, 1718 (2021). https://doi.org/10.1038/s41598-021-81268-7</p>
	<p>Alkarithi, G., Duval, C., <u>Shi, Y.</u>, Macrae, F.L. and Ariëns, R.A.S. 2021. Thrombus Structural Composition in Cardiovascular Disease. <i>Arteriosclerosis, Thrombosis, and Vascular Biology</i>. 0(0), ATVBAHA.120.315754.</p>
Presentations at Conferences	<p>2019 'Making a Difference' - Faculty of Medicine and Health Postgraduate Research Conference</p> <ul style="list-style-type: none"> • Presentation: Poster • Title: Role of Neutrophils in Fibrin Structure and Function • Author(s): <u>Y. Shi</u>, H. Philippou, S.D. Connell, R.A.S. Ariëns
	<p>2019 European Congress on Thrombosis and Haemostasis (ECTH) Congress</p> <ul style="list-style-type: none"> • Presentation: Poster • Title: Neutrophil Extracellular Traps Accelerate Clotting and Produce a Denser Clot Structure in Plasma • Author(s): <u>Y. Shi</u>, S.R. Baker, H. Philippou, S.D. Connell, R.A.S. Ariëns
	<p>2020 International Society on Thrombosis and Haemostasis (ISTH) Virtual Congress</p> <ul style="list-style-type: none"> • Presentation: Poster

	<ul style="list-style-type: none"> • Title: Neutrophils and Neutrophil Extracellular Traps (NETs) can promote clotting and impact clot structure in a distinctive manner • Author(s): <u>Y. Shi</u>, S.R. Baker, J.S. Gauer, H. Philippou, S.D. Connell, R.A.S. Ariëns <p>2021 British Society for Haemostasis & Thrombosis (BSHT) Virtual Scientific Meeting:</p> <ul style="list-style-type: none"> • Presentation: Oral (Scientists in Training) • Title: Neutrophils can Promote Clotting via FXI and Impact Clot Structure via Neutrophil Extracellular Traps in a Distinctive Manner <i>in vitro</i> • Author(s): <u>Y. Shi</u>, J.S. Gauer, S.R. Baker, H. Philippou, S.D. Connell, R.A.S. Ariëns <p>2021 International Society on Thrombosis and Haemostasis (ISTH) Virtual Congress:</p> <ul style="list-style-type: none"> • Presentation: Poster • Title: Neutrophils can Promote Clotting by Secreting Proteins that Activate FXI while NETs Promote Clotting Independently of FXI <i>In Vitro</i> • Author(s): Y. Shi, J.S. Gauer, S.R. Baker, H. Philippou, S.D. Connell, R.A.S. Ariëns <p>2022 British Society for Haemostasis & Thrombosis (BSHT) Annual Scientific Meeting</p> <ul style="list-style-type: none"> • Presentation: Oral (Scientists in Training) • Title: Neutrophils and NETs Produce Clots with Different Types of Fibrin Fibres <p>Author(s): <u>Y. Shi</u>, H. McPherson, T. Feller, J.S. Gauer, H. Philippou, S.D. Connell, R.A.S. Ariëns</p>
Award	Shortlisted and Winner of the 1 st prize at the 2021 BSHT Annual Meeting Scientist in Training Session

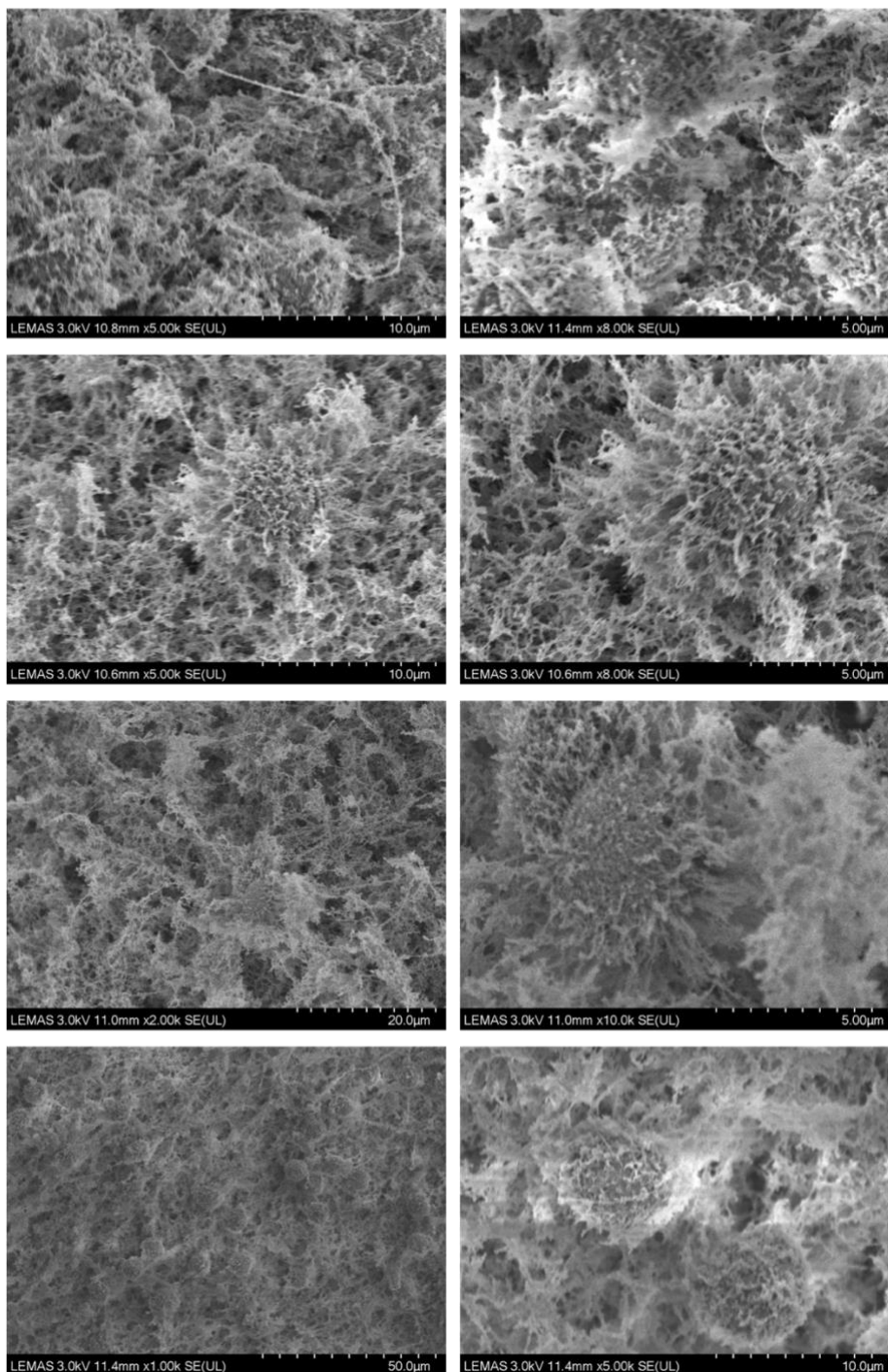
Appendix 2. Confocal images of broken PLB-985 cell-induced clots.

Confocal Z-stacks images of PLB-985 NET-induced plasma clots. Final concentrations: plasma was diluted 1:6, CaCl_2 (3.33 mM), PLB-985 NETs (generated from 200,000 cells/100 μl). Blue: DAPI-stained DNA. Green: Alexa Fluor 488 labeled fibrinogen. Please see attached movie of a three-dimensional clot.

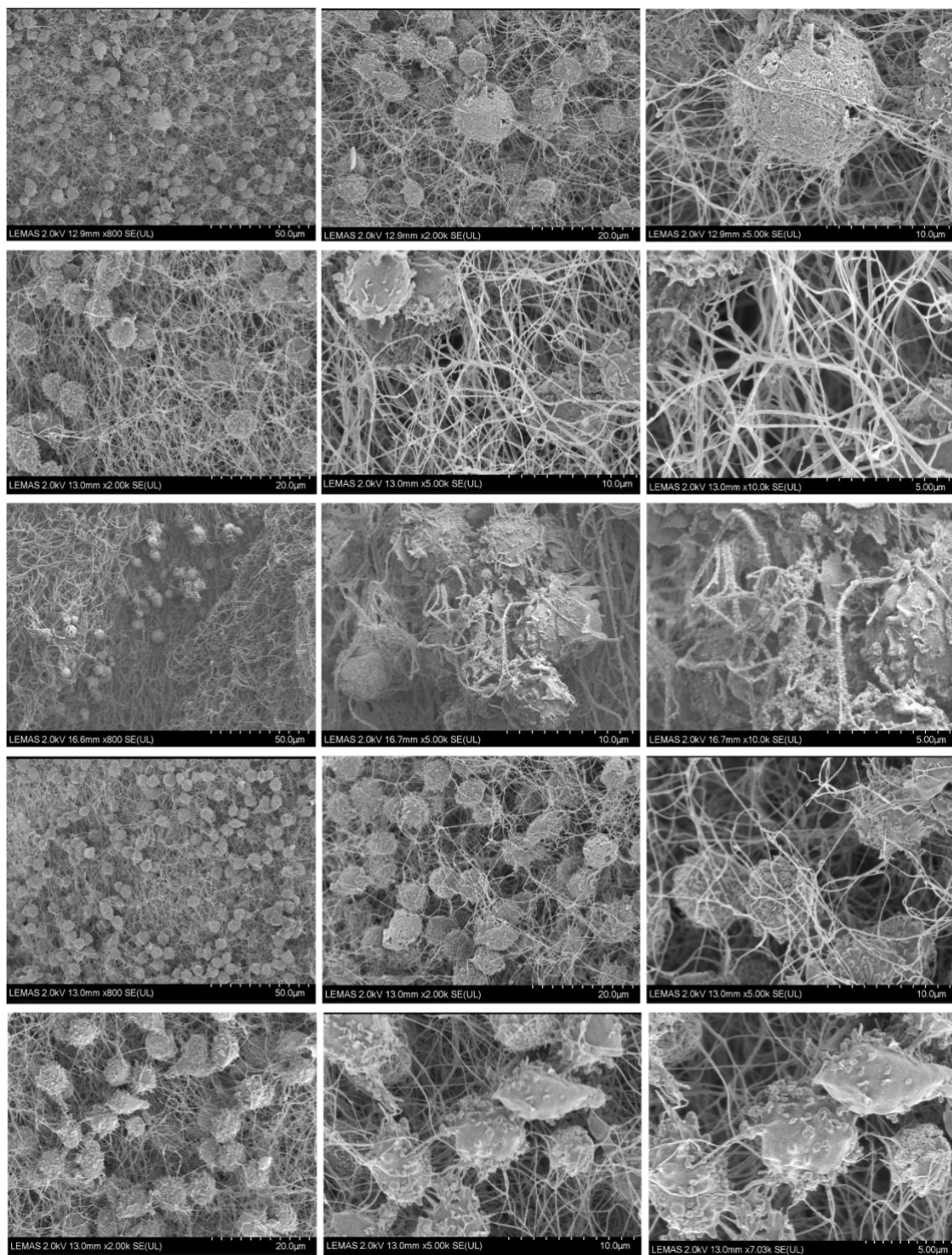
Diff PLB-985 Cell-Induced Clots (Broken)

Appendix 3. Additional SEM images of clots induced by differentiated PLB-985 cells, human neutrophils, PLB-985 NETs and human NETs. Thrombin-induced clots were used as a control. Final concentrations: Plasma (diluted 1:3), 10 mM CaCl₂, 1 U/ml thrombin. Some images were used in the fibrin fibre thickness analysis.

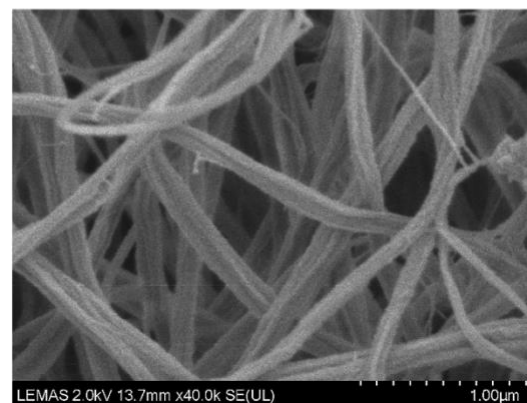
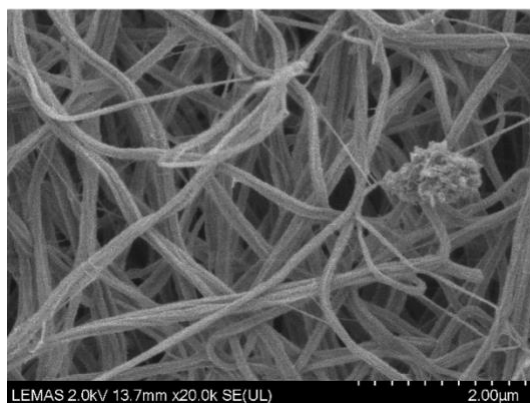
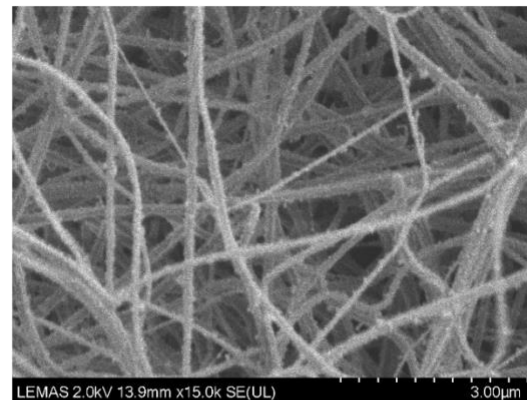
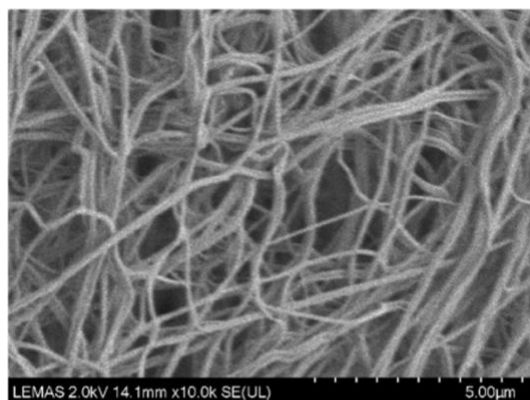
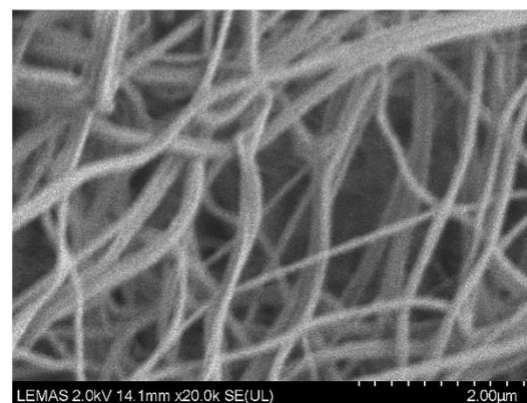
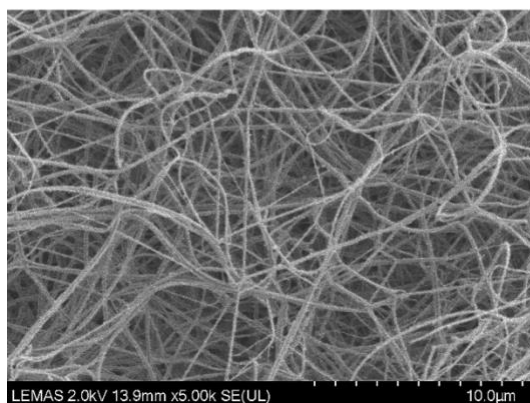
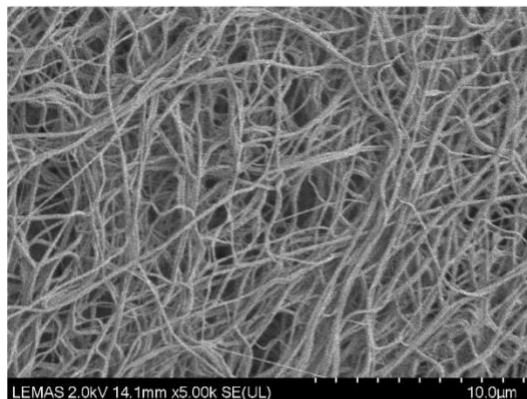
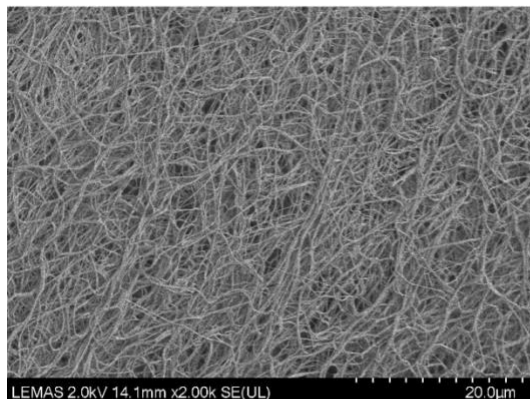
Human Neutrophil-induced Clots



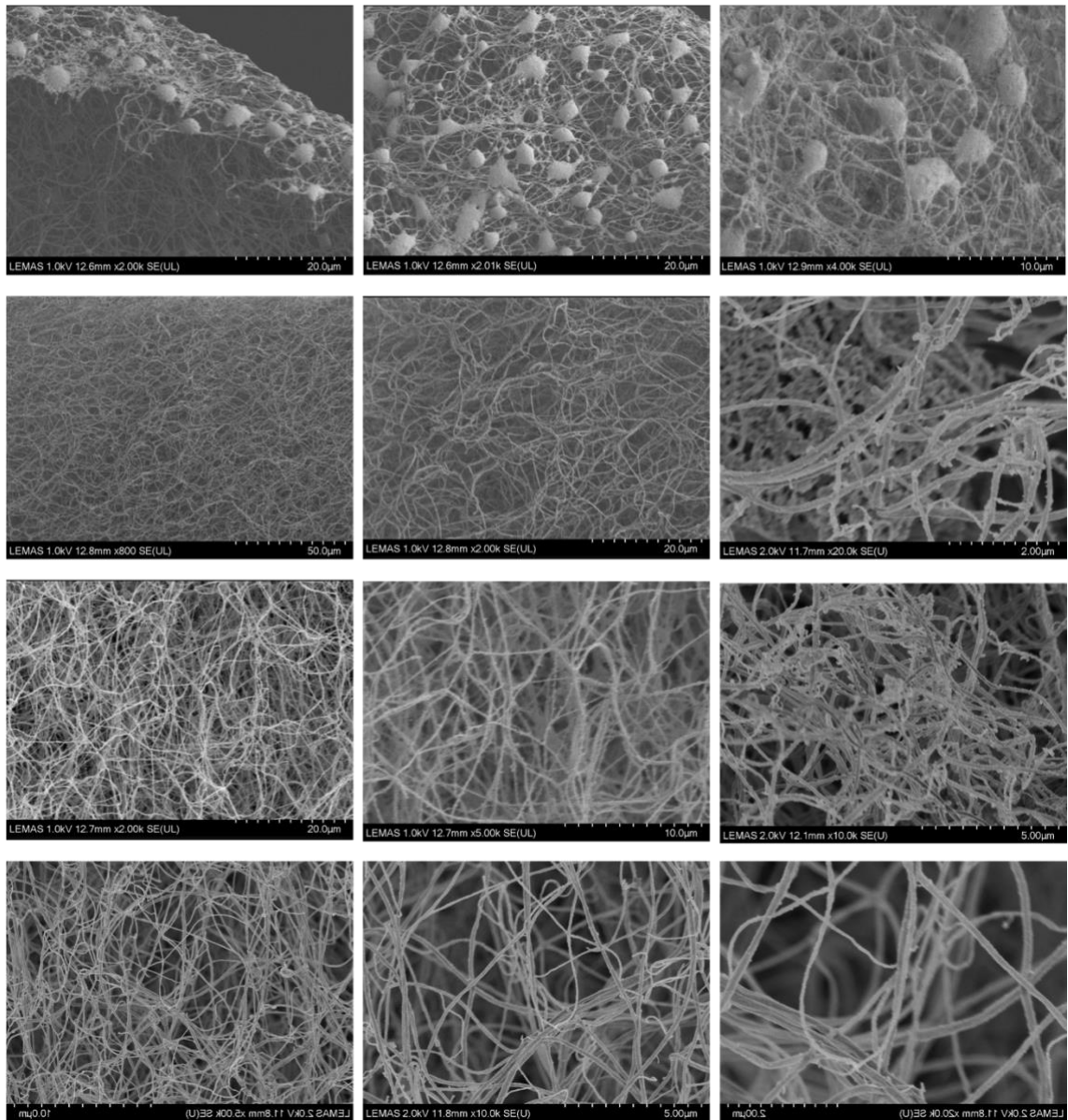
Diff PLB-985 Cell-induced Clots



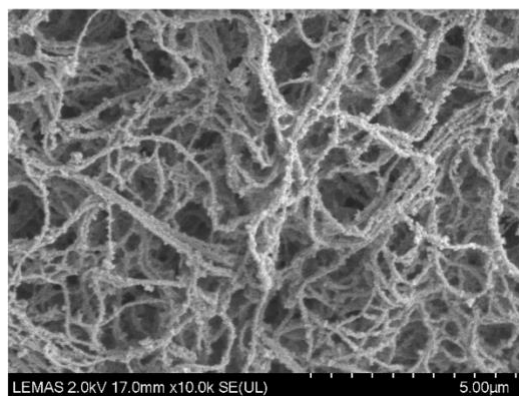
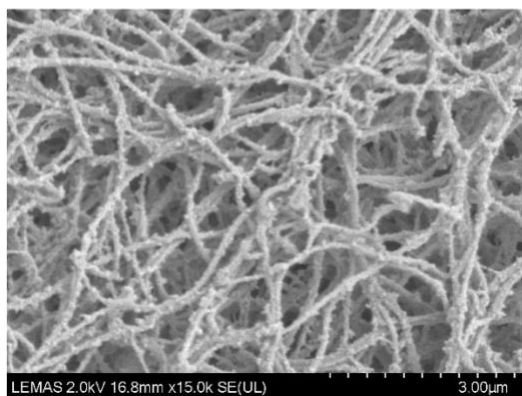
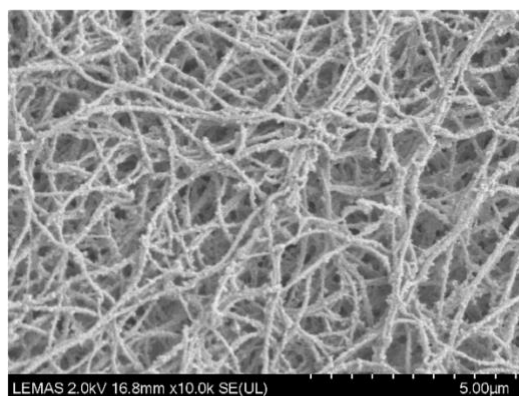
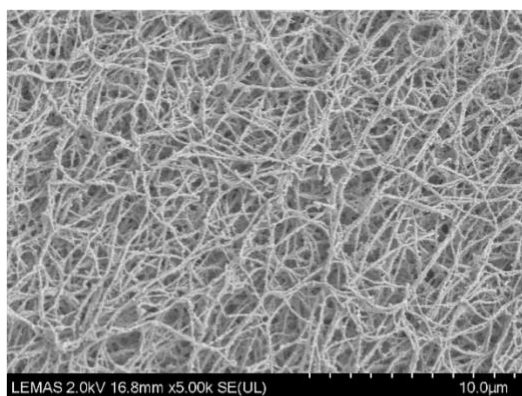
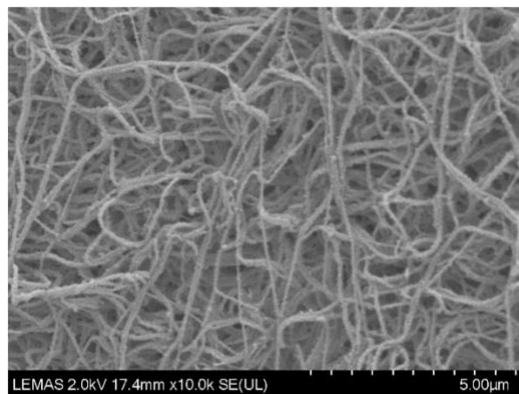
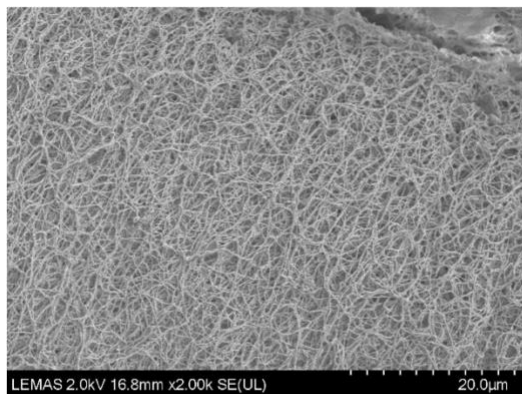
Human NET-induced Clots



PLB-985 NET-induced Clots



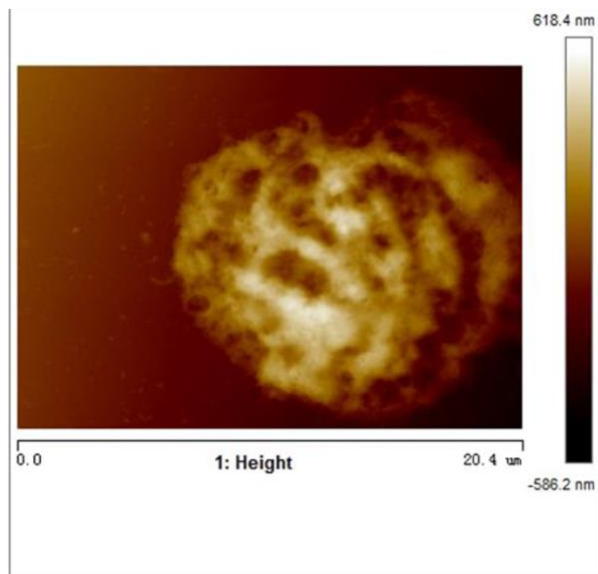
Thrombin-induced Clots



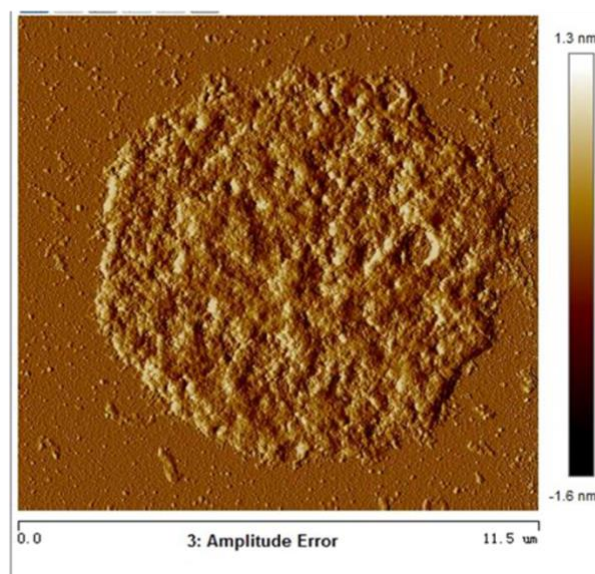
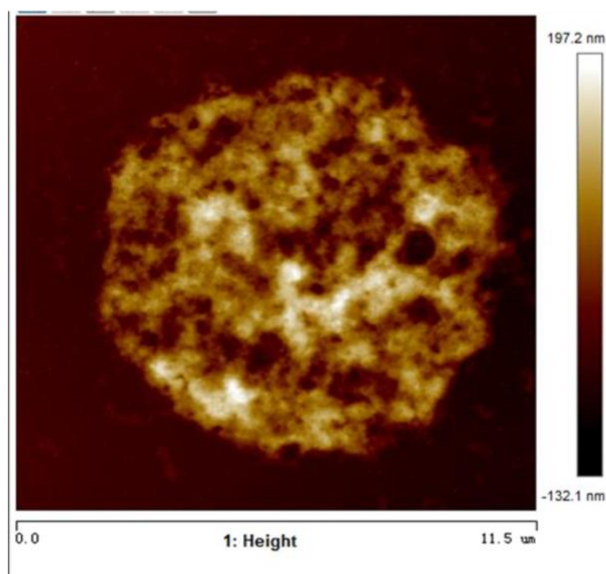
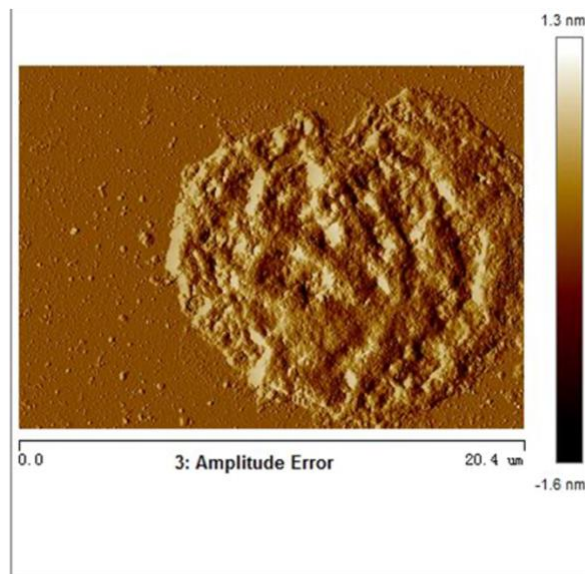
Appendix 4. Additional AFM images.

Appendix 4.1 Air-dried PLB-985 Cells. Height channel reflects the size range of cells. Amplitude error channel reflects a three-dimensional image of cells.

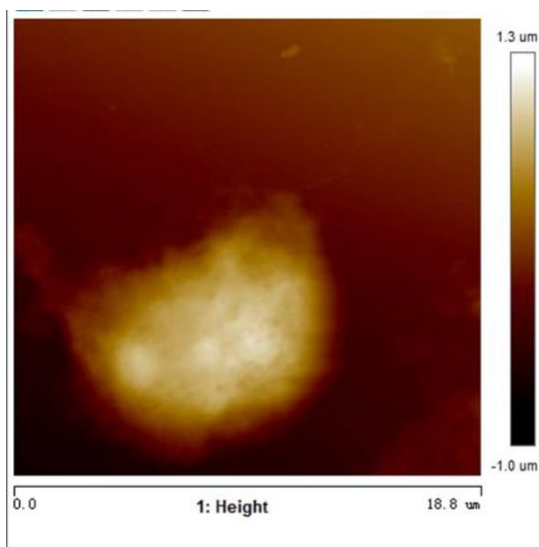
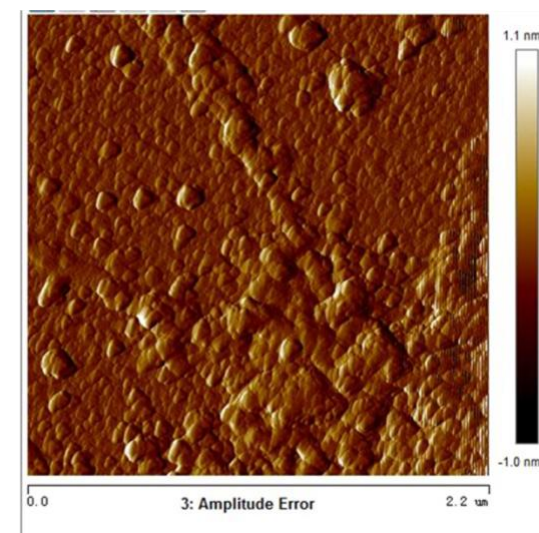
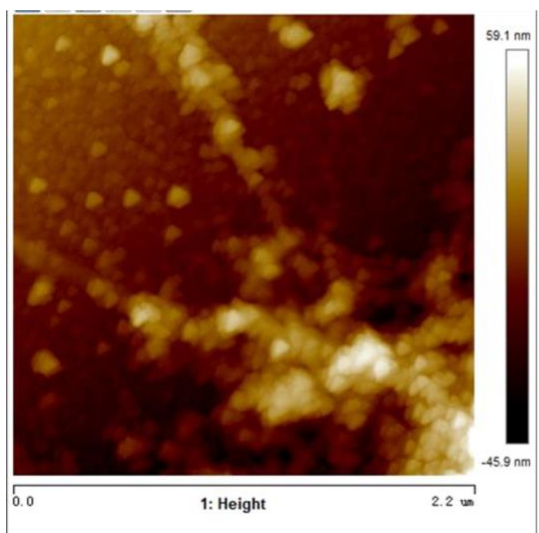
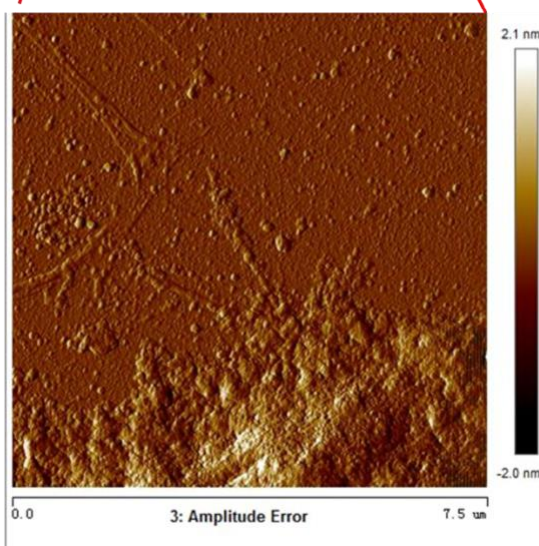
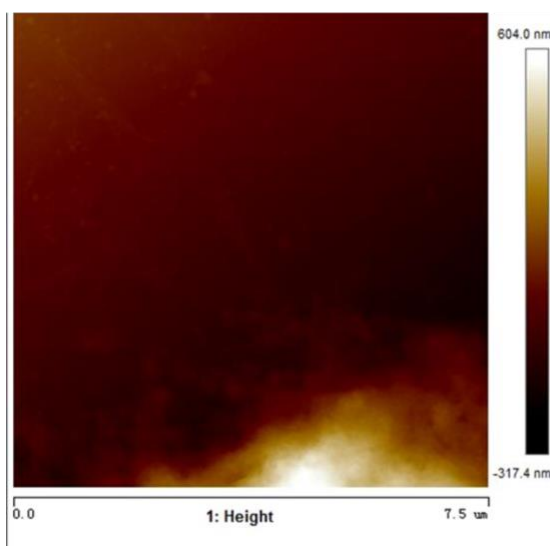
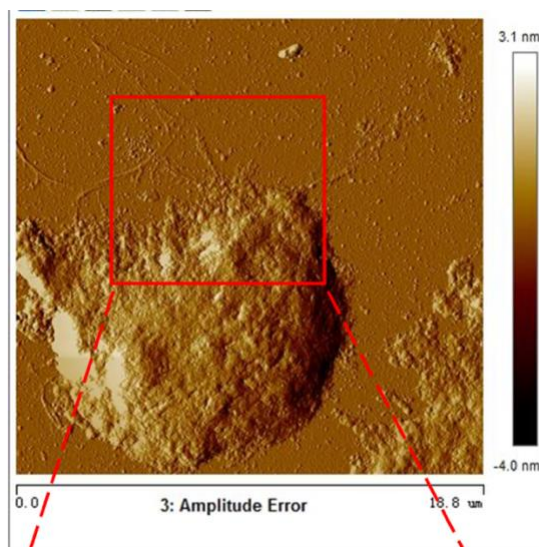
Height



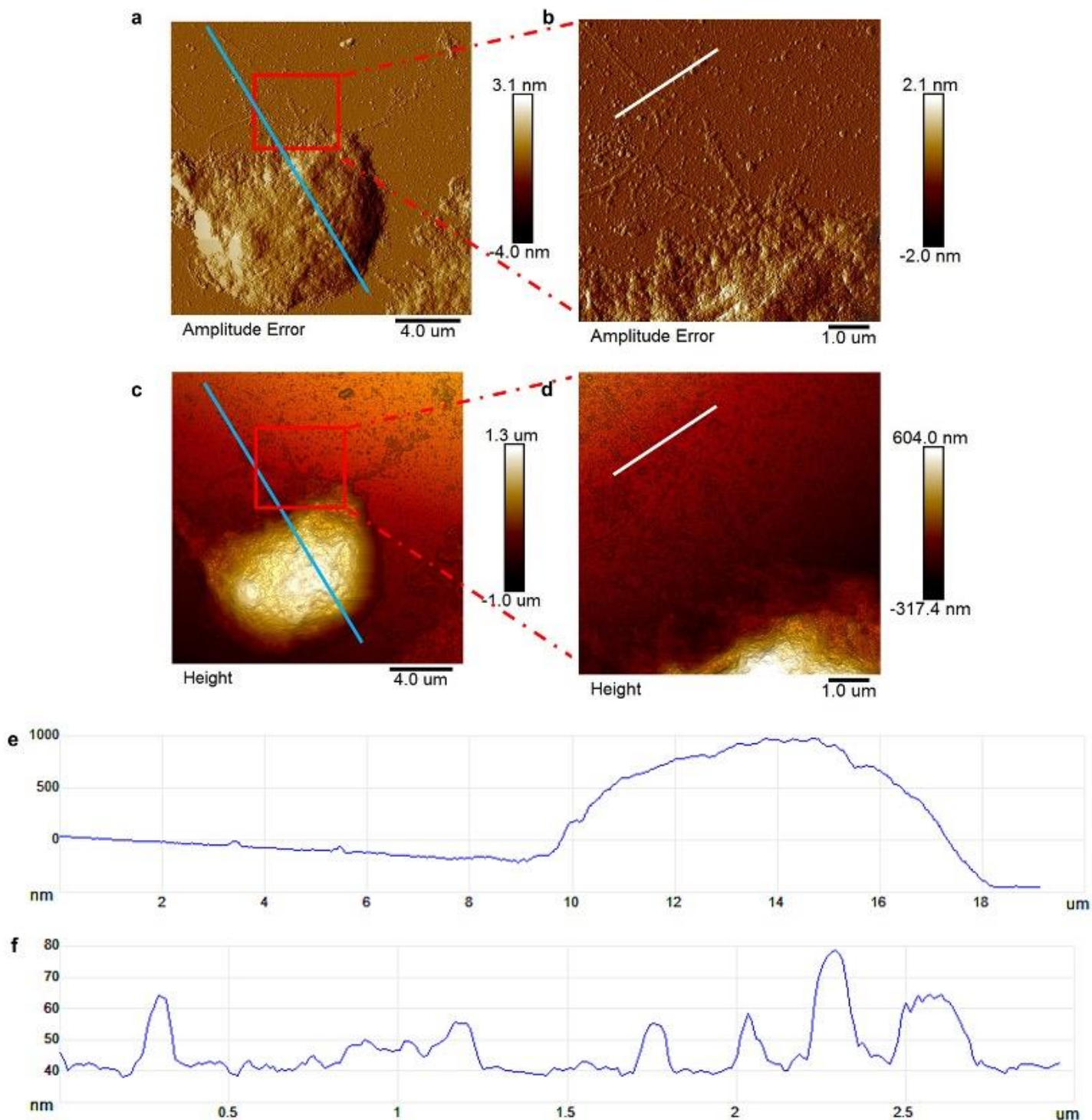
Amplitude Error



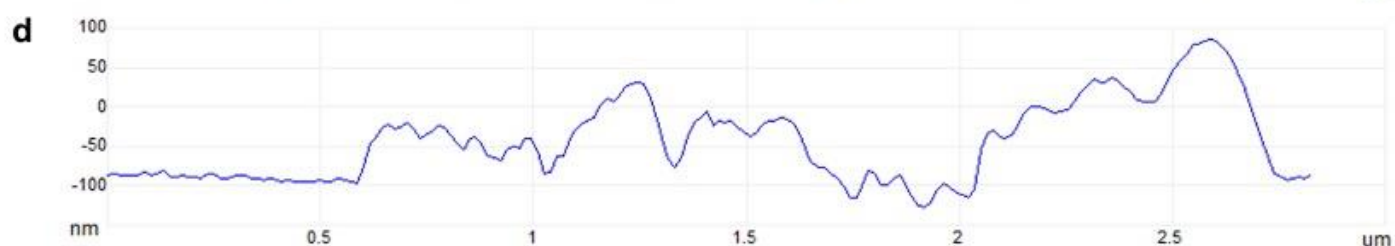
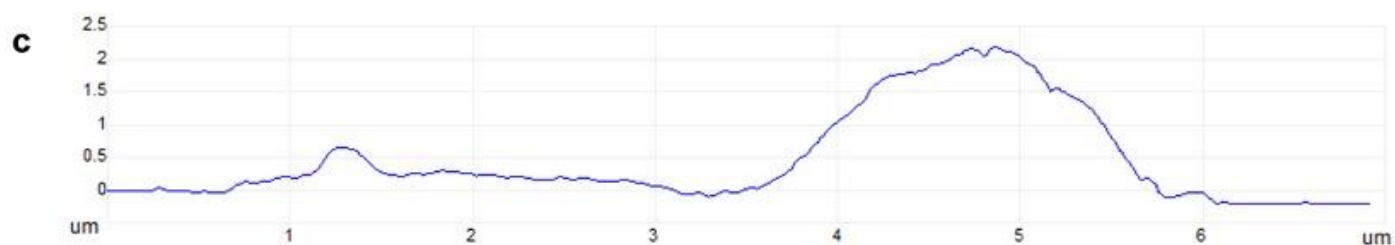
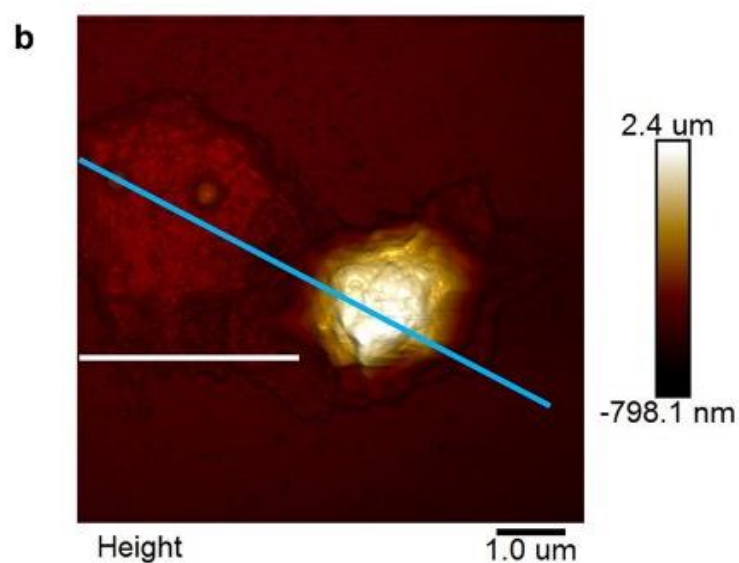
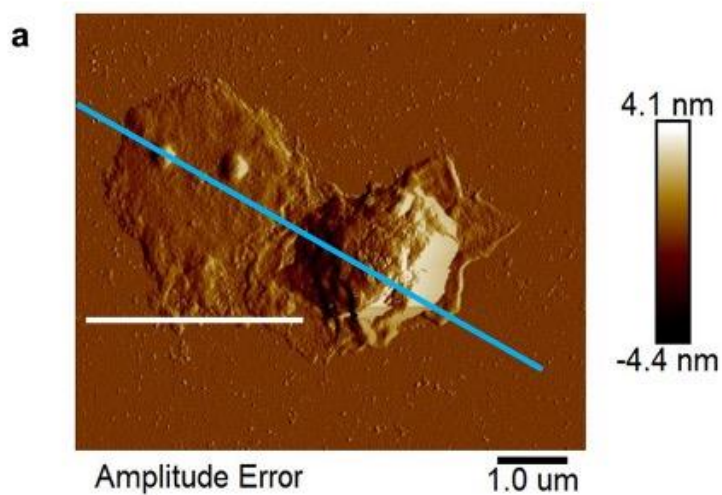
Appendix 4.2 Air-dried PLB-985 NETs. Height channel reflects the size range of NETs. Amplitude error channel reflects a three-dimensional image of NETs.

Height**Amplitude Error**

Appendix 4.3. AFM analyses of air-dried PLB-985 NETs. **(a)** Amplitude error channel reflects a three-dimensional image of NETs. **(b)** Height channel reflects the size range of NETs. **(c)** Height profile taken along the blue line in panel **a** and **c**. **(f)** Height profile taken along the white line in panel **b** and **d**.



Appendix 4.4. AFM analyses of air-dried PLB-985 NETs. **(a)** Amplitude error channel reflects a three-dimensional image of NETs. **(b)** Height channel reflects the size range of NETs. **(c)** Height profile taken along the blue line in panel **a** and **b**. **(d)** Height profile taken along the white line in panel **a** and **b**.



Appendix 5. Mass spectrometry data showing the composition of human neutrophil supernatant.

Part 1/2										
Protein Group	Protein ID	Accession	-10lgP	Coverage (%)	Coverage (%) Sample 1	Area Sample 1	#Peptides	#Unique	#Spec Sample 1	PTM
1	1	H6VRF8	176.5	25	25	1.39E+06	18	14	22	Oxidation (M)
3	8	P13645	155.61	20	20	2.96E+05	12	9	13	Oxidation (M)
5	10	P35908	150.21	16	16	1.05E+05	9	6	9	
2	9	P35527	147.8	21	21	9.12E+05	13	12	15	Oxidation (M)
6	24	P05109	122.94	61	61	8.52E+05	8	8	9	Carbamidomethylation
4	11	B7ZAL5	120.31	13	13	2.40E+05	10	10	10	Carbamidomethylation
14	33	B4DUI5	109.63	23	23	4.97E+04	4	4	4	Carbamidomethylation
8	49	B2R4M6	103.9	56	56	3.58E+05	5	5	6	
9	37	B4DVQ0	103.84	13	13	1.16E+05	5	5	6	Oxidation (M)
13	51	A0A0M4FNU3	91.97	11	11	5.70E+04	4	4	4	Carbamidomethylation
7	27	P04406	89.44	14	14	2.79E+05	5	5	6	Deamidation (NQ); Oxidation (M)
11	32	P13647	87.82	7	7	3.17E+04	4	3	4	
16	75	B4DJI1	77.88	10	10	2.53E+04	3	3	3	Carbamidomethylation
20	90	A0A4D5RAJ5	72.46	10	10	1.78E+04	3	3	3	
10	47	P00558	72.41	9	9	6.22E+04	5	5	5	
18	108	P05164	69.62	4	4	3.53E+04	3	3	3	Carbamidomethylation; Oxidation (M)
23	119	B4DEK3	69.24	15	15	1.52E+04	2	2	2	
22	122	B2R4C5	67.95	11	11	9.46E+04	2	2	2	
15	82	A0A0K0K1H9	67.16	9	9	5.75E+04	4	4	4	
19	109	K7EPF6	63.71	11	11	2.91E+04	3	3	3	
29	184	P59665	61.61	19	19	3.27E+04	2	2	2	Carbamidomethylation
30	191	B4E3A8	60.26	6	6	4.36E+04	2	2	2	
17	95	B7Z4U6	59.14	4	4	4.98E+04	3	3	3	
21	113	B4DE36	57.29	3	3	2.48E+04	2	2	2	
27	154	A0A384NPR0	53.55	9	9	2.77E+04	2	2	2	
31	218	D6RA82	44.84	6	6	2.30E+04	2	2	2	
24	135	A0A0K0K1K8	44.18	3	3	2.49E+04	2	2	2	
32	220	Q59ES1	44.14	10	10	1.75E+04	2	2	2	Carbamidomethylation

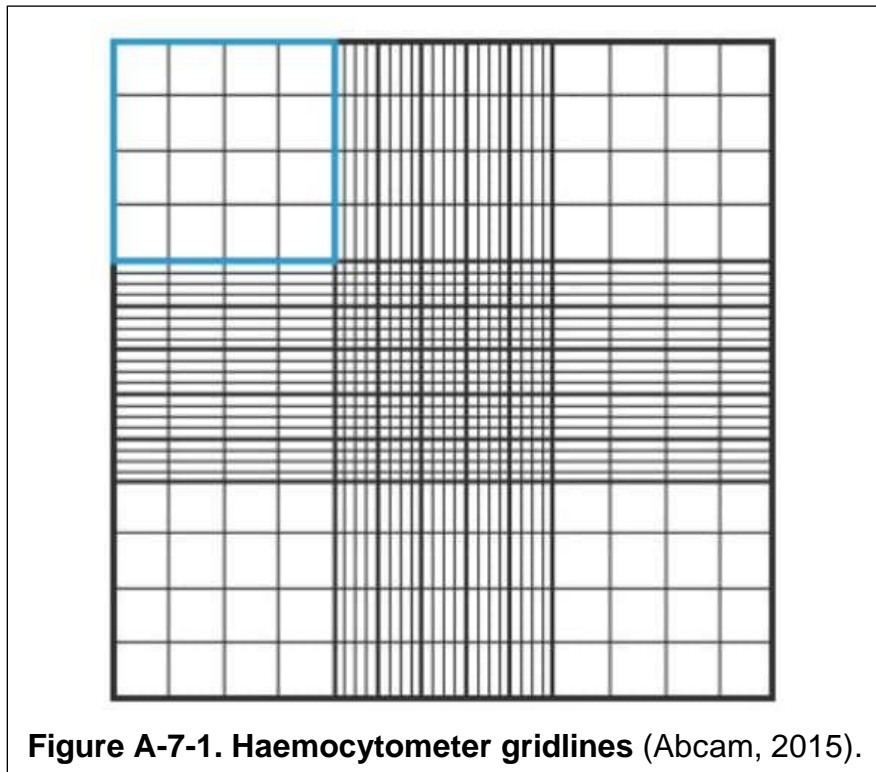
Part 2/2			
Protein Group	Protein ID	Avg. Mass	Description
1	1	66053	Keratin 1 OS=Homo sapiens OX=9606 GN=KRT1 PE=3 SV=1
3	8	58827	Keratin type I cytoskeletal 10 OS=Homo sapiens OX=9606 GN=KRT10 PE=1 SV=6
5	10	65433	Keratin type II cytoskeletal 2 epidermal OS=Homo sapiens OX=9606 GN=KRT2 PE=1 SV=2
2	9	62064	Keratin type I cytoskeletal 9 OS=Homo sapiens OX=9606 GN=KRT9 PE=1 SV=3
6	24	10835	Protein S100-A8 OS=Homo sapiens OX=9606 GN=S100A8 PE=1 SV=1
4	11	73170	cDNA FLJ79229 highly similar to Lactotransferrin OS=Homo sapiens OX=9606 PE=2 SV=1
14	33	22871	Triosephosphate isomerase OS=Homo sapiens OX=9606 PE=2 SV=1
8	49	13210	Protein S100 OS=Homo sapiens OX=9606 PE=2 SV=1
9	37	37349	cDNA FLJ58286 highly similar to Actin cytoplasmic 2 OS=Homo sapiens OX=9606 PE=2 SV=1
13	51	31579	Fructose-bisphosphate aldolase (Fragment) OS=Homo sapiens OX=9606 GN=ALDOA PE=3 SV=1
7	27	36053	Glyceraldehyde-3-phosphate dehydrogenase OS=Homo sapiens OX=9606 GN=GAPDH PE=1 SV=3
11	32	62378	Keratin type II cytoskeletal 5 OS=Homo sapiens OX=9606 GN=KRT5 PE=1 SV=3
16	75	33593	cDNA FLJ52549 highly similar to L-lactate dehydrogenase A chain OS=Homo sapiens OX=9606 PE=2 SV=1
20	90	31647	Annexin OS=Homo sapiens OX=9606 PE=3 SV=1
10	47	44615	Phosphoglycerate kinase 1 OS=Homo sapiens OX=9606 GN=PGK1 PE=1 SV=3
18	108	83869	Myeloperoxidase OS=Homo sapiens OX=9606 GN=MPO PE=1 SV=1
23	119	18542	cDNA FLJ56959 highly similar to Vascular endothelial growth factor receptor 2 OS=Homo sapiens OX=9606 PE=2 SV=1
22	122	16537	Lysozyme OS=Homo sapiens OX=9606 GN=LYZ PE=2 SV=1
15	82	42896	Epididymis secretory protein Li 48 (Fragment) OS=Homo sapiens OX=9606 GN=HEL-S-48 PE=2 SV=1
19	109	27884	6-phosphogluconate dehydrogenase decarboxylating (Fragment) OS=Homo sapiens OX=9606 GN=PGD PE=1 SV=1
29	184	10201	Neutrophil defensin 1 OS=Homo sapiens OX=9606 GN=DEFA1 PE=1 SV=1
30	191	38685	cDNA FLJ53963 highly similar to Leukocyte elastase inhibitor OS=Homo sapiens OX=9606 PE=2 SV=1
17	95	75752	cDNA FLJ55803 highly similar to Gelsolin OS=Homo sapiens OX=9606 PE=2 SV=1
21	113	60186	Glucose-6-phosphate isomerase OS=Homo sapiens OX=9606 PE=2 SV=1
27	154	19301	Epididymis secretory sperm binding protein OS=Homo sapiens OX=9606 PE=2 SV=1
31	218	32119	Annexin OS=Homo sapiens OX=9606 GN=ANXA3 PE=1 SV=1
24	135	47169	Enolase 1 (Alpha) isoform CRA_a OS=Homo sapiens OX=9606 GN=ENO1 PE=3 SV=1
32	220	24242	Leukotriene A4 hydrolase variant (Fragment) OS=Homo sapiens OX=9606 PE=2 SV=1

Appendix 6. Buffer preparation

0.5 M Ethylenediaminetetraacetic acid (EDTA), pH 8.0	18.61 g of disodium EDTA•2H ₂ O was added to 80 ml of double-distilled water (ddH ₂ O). Solution was stirred on a magnetic stirrer. PH was adjusted to 8.0 by adding sodium hydroxide (NaOH) to allow the disodium salt of EDTA dissolve into solution. Once the salt was fully dissolved, the solution was topped up to 100 ml using ddH ₂ O (if necessary). Finally, solution was filtered with a 0.2 µm filter and sterilised by autoclaving.
HEPES-buffered saline (HBS, 10 mM HEPES, 150 mM NaCl)	2.38 g of HEPES (4-(2-hydroxyethyl)-1-piperazineethanesulfonic acid) and 8.766 g sodium chloride were added to 800 ml of ddH ₂ O. Solution was stirred on a magnetic stirrer until salt was completely dissolved. PH was adjusted to 7.4. the solution was topped up to 1000 ml. Finally, solution was filtered with a 0.2 µm filter and sterilised by autoclaving.
Saline (154 mM sodium chloride)	4.5 g sodium chloride was dissolved in 500 ml ddH ₂ O. Solution could also be made by diluting the 5 M stock in ddH ₂ O (15.4 ml in 500 ml).
2% Glutaraldehyde	Solution was made by diluting the 25% stock in Saline (4 ml in 50 ml).
Sodium cacodylate buffer	10.7 g sodium cacodylate was added in 1000 ml of ddH ₂ O, pH was adjusted to 7.4.

Appendix 7. Cell counting protocol (Abcam, 2015).

1. Glass haemocytometer was cleaned with 74% alcohol before use. The coverslip was moistened with ddH₂O and affixed to the haemocytometer.
2. Flasks were gently swirled to ensure the cells are evenly distributed. 10 µl cell suspension was added in 90 µl Trypan Blue, mixed gently.
3. 10 µl of Trypan Blue-treated cell suspension was gently filled into both chambers of the haemocytometer.
4. The grid lines of the haemocytometer were focused under a microscope with a 10x objective lens.
5. Live cells (cells do not stained by Trypan Blue) using a hand tally counter in one set of 16 squares (Figure A-7-1). Cells were only counted when they were located within a square or on the right-hand or bottom boundary line. All four sets of 16 corners were counted.



6. The number of cells/ml in the original cell suspension was calculated as following: 1) take the average cell count from each of the sets of 16 corner squares; 2) multiply by 10,000; 3) multiply by 10 to correct for the 1:10 dilution from the Trypan Blue addition.

For example, if the cell counts for each of the 16 squares were 22, 19, 21, 18, the average cell count would be:

$$(22 + 19 + 21 + 18) \div 4 = 20$$

$$20 \times 10,000 = 200,000$$

$$200,000 \times 10 = 2,000,000 \text{ cells/ml in original cell suspension.}$$

Appendix 8. Patient Information Sheet

Leeds Institute of Cardiovascular and Metabolic Medicine

Division of Cardiovascular & Diabetes Research
LIGHT Laboratories
Clarendon Way
University of Leeds
Leeds, LS2 9JT

T +44 (0) 113 343 7743
E e.hethershaw@leeds.ac.uk



UNIVERSITY OF LEEDS

Role of different components on fibrin clot structure and function

Volunteer Information Sheet

You are being invited to take part in a research study. Before you decide it is important for you to understand why the research is being done and what it will involve. Please take the time to read the following information carefully and discuss it if you wish. Please ask us if there is anything that is not clear or if you would like more information. Take time to decide whether or not you wish to take part.

Purpose of the study

People at risk of cardiovascular problems, e.g. heart attack, can have differences in their components (proteins) of the blood clotting system. These differences can be beneficial, detrimental, or not have any effect. We hope to understand the contribution of these differences to cardiovascular problems, and thus aid future drug development against these diseases.

Why have I been chosen?

You have been chosen because you are between 18 and 70 years old and are generally healthy.

Do I have to take part?

It is up to you whether or not to take part. If you do decide to participate, you will be given this information sheet to keep, asked to sign a consent form, may be asked to give telephone or email address (so we can contact you again asking if you would be willing to provide subsequent blood donations), and may be asked to complete a questionnaire detailing basic information. Completing any part of this questionnaire is voluntary. You do not have to provide any information if you do not want to. Your answers will be treated in confidence and will not be identifiable. We will hold your information securely in accordance with the Data Protection Act (1998). Your name and contact details (if you choose to provide these) will be kept solely on the consent form. Your volunteer ID code will be the only link between your name and contact details, and any stored samples and questionnaires. If you do decide to take part, you are still free to withdraw at any time and without giving a reason. If you do decide to participate, your blood sample will either:

- be tested within 6 hours of being taken and any remaining discarded after 6 hours
- separated into different components (e.g. plasma, cells, proteins) and either tested on the same day or stored for future use

If you do decide to participate, it is accepted that your sample is a gift and may be retained for use in future ethically approved research.

What will happen to me if I take part?

The study will take approximately 15 minutes of your time on one or more occasions when you will be asked to come to the LIGHT laboratories in the University of Leeds where you will see one of our research nurses or Dr Hethershaw. Up to 54 mls of blood (which is the equivalent of about 4 tablespoons) will be taken from a vein on the inside of your arm. Additionally, you may be asked to complete a questionnaire detailing basic information.

What will happen to any samples I give?

The blood sample provided will be labelled with your volunteer ID code only so that you can not be identified. The whole blood will then either:

- be used as is and tested on the same day
- separated into different components (e.g. plasma, cells, proteins) and either tested on the same day or stored for future use

Standard blood clotting assays will be used to test the effects of the different components of blood clotting system with your sample. Any stored samples will also be labelled with your volunteer ID code as the only identifier and so you can not be identified.

What are the possible disadvantages and risks of taking part?

Giving a blood sample may be uncomfortable and there is a slight risk of bruising from the needle piercing the vein to take the blood.

What is there is a problem?

If you have a concern about any aspect of this study, you should contact one of the researchers who will do their best to answer your questions. Our contact numbers are at the end of this information sheet. If you are harmed by taking part in this study, there are no special compensation arrangements. If you are harmed due to someone's negligence, then you may have grounds for a legal action but you may have to pay for this.

Will my taking part in this study be kept confidential?

All information which is collected about you during the course of this research will be kept strictly confidential.

Contact Details

If you require any further information please contact us on the telephone numbers below. Thank-you for reading this information sheet and for considering participating in the research.

Dr Emma Hethershaw
0113 343 7743
e.hethershaw@leeds.ac.uk

Julie Bailey – Research Nurse
0113 343 7702

Appendix 9. Patient Consent Form

Leeds Institute of Cardiovascular and Metabolic Medicine

Division of Cardiovascular & Diabetes Research
LIGHT Laboratories
Clarendon Way
University of Leeds
Leeds, LS2 9JT

T +44 (0) 113 343 7768
F +44 (0) 113 343 6603
E h.philippou@leeds.ac.uk



UNIVERSITY OF LEEDS

Consent Form Role of different components on fibrin clot structure and function Blood Donation

Volunteer ID code:

Date sample taken:

Date test(s) performed:

Date sample discarded:

Please initial box

1. I confirm that I have read and understood the volunteer information sheet for the above study and have had the opportunity to ask questions.
2. I understand that my participation is voluntary and that I am free to withdraw at any time, without giving any reason, without any legal rights being affected.
3. I agree that my sample is a gift and may be retained for use in future ethically approved research.
4. I understand that any samples and questionnaires will be labelled with my volunteer code only so that I can not be identified from them.

Name of volunteer

Date

Signature

Contact details (optional)

Name of person taking consent

Date

Signature

Professor Mark Kearney
Institute Director

Version 3
17/11/2016

Appendix 10. Publication which has arisen from the work presented in this thesis (author accepted version).

Neutrophils can Promote Clotting via FXI and Impact Clot Structure via Neutrophil Extracellular Traps in a Distinctive Manner *in vitro*

Y. Shi¹, J.S. Gauer¹, S.R. Baker^{1,2}, H. Philippou¹, S.D. Connell³, R.A.S. Ariëns^{1*}

¹Discovery and Translational Science Department, Institute of Cardiovascular and Metabolic Medicine, University of Leeds, Leeds, LS2 9LU, United Kingdom.

²Department of Physics, Wake Forest University, Winston Salem, NC, United States.

³The Astbury Centre for Structural Molecular Biology, Molecular & Nanoscale Physics, University of Leeds, Leeds, LS2 9JT, United Kingdom.

*Address correspondence to Robert A.S. Ariëns, LIGHT Laboratories, University of Leeds, Clarendon Way, Leeds, LS2 9JT, United Kingdom. Phone: +44 (0) 113 34 3437734; Email: r.a.s.ariens@leeds.ac.uk.

Abstract

Neutrophils and neutrophil extracellular traps (NETs) have been shown to be involved in coagulation. However, the interactions between neutrophils or NETs and fibrin(ogen) in clots, and the mechanisms behind these interactions are not yet fully understood. In this *in vitro* study, the role of neutrophils or NETs on clot structure, formation and dissolution was studied with a combination of confocal microscopy, turbidity and permeation experiments. Factor (F)XII, FXI and FVII-deficient plasmas were used to investigate which factors may be involved in the procoagulant effects. We found both neutrophils and NETs promote clotting in plasma without the addition of other coagulation triggers, but not in purified fibrinogen, indicating that other factors mediate the interaction. The procoagulant effects of neutrophils and NETs were also observed in FXII- and FVII-deficient plasma. In FXI-deficient plasma, only the procoagulant effects of NETs were observed, but not of neutrophils. NETs increased the density of clots, particularly in the vicinity of the NETs, while neutrophils-induced clots were less stable and more porous. In conclusion, NETs accelerate clotting and contribute to the formation of a denser, more lysis resistant clot architecture. Neutrophils, or their released mediators, may induce clotting in a different manner to NETs, mediated by FXI.

Introduction

Neutrophils, which are produced in the bone marrow, are the most abundant class of leukocyte^{1,2}. Neutrophils are known to participate in the innate inflammatory system as the earliest line of defense against microbial infection^{3,4}. Recently, there has been increasing evidence that blood coagulation is associated with neutrophils⁵⁻⁷, including evidence that neutrophils contribute to thrombosis by interacting with both the injured endothelium and fibrin(ogen)⁸⁻¹⁰. Neutrophils can also influence thrombosis through the release of a number of active proteases and other agents such as matrix metalloproteinases (MMP), serine proteases (e.g., cathepsin G and elastase) and platelet-activating factor (PAF)^{5,11}. For instance, cathepsin G and elastase are known to activate platelets¹²⁻¹⁴, factor V, VIII and X¹⁵⁻¹⁷. Moreover, MMP, cathepsin G and elastase cleave and inactivate tissue factor pathway inhibitor (TFPI)^{18,19} and elastase degrades antithrombin III²⁰.

A key function via which neutrophils contribute to innate immune responses and also to thrombosis is the generation of neutrophil extracellular traps (NETs), which are released by activated neutrophils, and contain DNA and granular proteins (histone 3)^{21,22}. There are various stimuli that can induce the generation of NETs (NETosis), such as bacteria, activated platelets and Phorbol 12-myristate 13-acetate (PMA)^{23,24}. NETosis is a special type of cell death process that differs from apoptosis and necrosis, which enables neutrophils to retain their antibacterial function after the end of their lives²⁵. It is widely known that NETs have properties of trapping and killing bacteria and pathogens^{26,27}. More recently, NETs have also been shown to be involved in the regulation of procoagulant factors (e.g. Factor XII and platelet and von Willebrand factor (vWF))^{22,28}. Thereby, NETs are able to provide a scaffold for the aggregation and adhesion of platelets and red blood cells, which may result in increased stability of clots^{31,32}. This scaffold can be dismantled by the anticoagulant heparin and DNAses^{32,34}. Histones are able to recruit fibrinogen and vWF, which can trigger platelet aggregation³⁰⁻³², and can also induce platelet aggregation directly^{32,35}. Histones also interact with fibrinogen and contribute to the heparin-induced platelet aggregation, a process enhanced by their regulation of $\alpha\text{IIb}\beta\text{3}$ activation, the integrin receptor on platelets³⁵.

Although previous studies have shown that neutrophils and NETs are involved in both arterial and venous thrombosis³⁶⁻⁴⁰, questions remain whether neutrophils contribute to coagulation independently or via NETs, whether both neutrophils and NETs promote clotting via the intrinsic pathway and how procoagulant factors interact with neutrophils or NETs. This *in vitro* study aims to investigate the role of neutrophils and NETs in blood coagulation, fibrin formation, clot structure/density and clot stability, to decipher how neutrophils or NETs interact with the fibrin network. The role of neutrophils or NETs on clot formation and clot dissolution was analysed by turbidity and lysis assays, clot structure was determined by confocal microscopy, and clot stability and pore

size were investigated using permeation studies. We found that both partially activated neutrophils and NETs promote clotting in plasma independently of additional triggers. We also found that the procoagulant effects of NETs are independent of FXI, FXII or FVII. However, the procoagulant effects of neutrophils are mediated via FXI, to a lesser extent by FXII, but not by FVII.

Results

Neutrophil-Surface Antigens on Neutrophils and PLB-985 Cells

To determine the purity of isolated human neutrophils, flow cytometry was carried out to analyse the expression of human neutrophil surface markers CD66b and CD16 on isolated human neutrophils. After isolation, 99.7% of cells expressed CD66b, 93.9% of cells expressed CD16, and 93.6% of cells expressed both (Fig. 1a). To identify whether PLB-985 cells differentiated into a functional neutrophil-like phenotype, the expression of CD16 and CD66b on differentiated PLB-985 cells was investigated via flow cytometry on day 6 of treatment, with untreated PLB-985 cells as the negative control. The expression of CD16 on differentiated cells (1.3%, $p = 0.0389$) was significantly higher than that on untreated cells (0.2%) (Fig. 1b). However, both CD16 and CD66b (3.3%) had a very low expression level on differentiated PLB-985 cells (Fig. 1b and 1c). In order to find a positive marker for the differentiation of PLB-985 cells, the expression of another human neutrophil surface marker CD11b on differentiated cells was investigated by flow cytometry. Surface markers were detected on day 3 and day 6 of differentiation, isolated human neutrophils were used as positive control and untreated PLB-985 cells were used as negative control. As shown in Figure 1d, differentiated PLB-985 cells had significantly increased expression level of CD11b ($P < 0.0001$) after treatment, as compared with untreated cells (13.1%). Namely, 89.2% of cells expressed CD11b on day 3 of differentiation and 97.0% of cells expressed CD11b on day 6 of differentiation. As days of treatment increased so did the expression level of CD11b on differentiated PLB-985 cells. The expression levels of CD11b on differentiated PLB-985 cells on day 6 of differentiation was similar to isolated blood neutrophils (96.6%).

Visualization of NETs

Immunofluorescence was carried out to visualize NETs which were generated from isolated human neutrophils and differentiated PLB-985 cells. To better observe NETs, we stained samples for DNA using the blue dye 4',6-diamidino-2-phenylindole (DAPI) and labeled them green with Alexa Fluor 488 labelled Histone H3 (citrulline R2 + R8 + R17), a marker for NETosis. Human neutrophils not stimulated with Phorbol 12-myristate 13-acetate (PMA) were used as negative control (Fig. 1e). Both human neutrophils and differentiated PLB-985 cells released their DNA and citrullinated histone H3 to form NETs upon stimulation with PMA (Fig. 1f and 1g) (The videos of NETosis can be found as Supplementary videos online). We found that NETosis happened when human neutrophils were treated with either 20 nM or 100 nM PMA for

either two hours or overnight (Supplementary Fig. S1 online). Controls for immunofluorescence are shown in Supplementary Fig. S2 online.

Role of Neutrophils and NETs in Clot Formation

Turbidity measurements were carried out to investigate the role of neutrophils or NETs in clot formation. In a purified fibrinogen system (Fig. 2a), both neutrophils and NETs did not trigger noteworthy fibrin polymerisation, when compared to the positive control (clotting triggered by thrombin), as evidenced by the low maximum absorbance. However, in plasma, clot formation was observed in samples containing neutrophils or NETs, independent of thrombin (Fig. 2b). The lag time of clotting triggered by human NETs in plasma was at least 4-fold ($P < 0.0001$) greater than thrombin only controls (Supplementary Fig. S3 online).

In order to determine if proteins secreted by neutrophils could promote clotting, the supernatant of human neutrophils was collected, added to normal pooled plasma (NPP) and clot formation was investigated by turbidity. Figure 3 shows that the supernatant of neutrophils also promoted clotting, with a slightly longer lag phase and a similar final maximum absorbance as clotting initiated by neutrophils themselves. We next analysed the neutrophil supernatant by mass spectrometry, which indicated that the neutrophils supernatant contained protein S100-A8, cDNA, glyceraldehyde-3-phosphate dehydrogenase, annexin, phosphoglycerate kinase 1, myeloperoxidase (MPO), neutrophil defensin 1 and other proteins (Supplementary Table S1 online).

Role of Neutrophils or NETs in Clot Dissolution

Lysis analysis was next carried out to investigate the role of human neutrophils or NETs in clot dissolution. Clots in the presence of human neutrophils had significantly ($P < 0.001$) lower average rate of lysis than thrombin only controls (Fig. 4a) and took significantly ($P < 0.05$) longer to reach 50% lysis when compared with controls (Fig. 4b). These effects were observed both with and without the addition of thrombin alongside neutrophils. NETs-induced clots had significantly ($P < 0.0001$) lower average rate of lysis than thrombin only controls, but when thrombin was added with NETs, clots had a similar average rate of lysis compared to controls (Fig. 4a). Clots in the presence of NETs took significantly ($P < 0.01$) longer time than controls to reach 50% lysis (Fig. 4b). We observed more pronounced effects of NETs on lysis in the absence of thrombin ($P < 0.0001$).

Factors Involved in the Procoagulant Effects of Neutrophils and NETs

To investigate through which pathway neutrophils/NETs promote clotting, tissue factor (TF) and FXII Inhibitors (TF antibody and Corn trypsin inhibitor (CTI)) were used to block TF and FXII in turbidity. Nevertheless, we saw no effect of these inhibitors in plasma-based experiments (Supplementary Fig. S4 online). Next, FXII-, FXI- and FVII-deficient plasmas were used in turbidity to investigate the procoagulant effects of human neutrophils and NETs.

Procoagulant effects of neutrophils were still observed in FXII- and FVII-deficient plasmas (Fig. 5a), while procoagulant effects of NETs were still observed in all of these deficient plasmas (Fig. 5b). The time to MaxOD of neutrophil-induced clotting was significantly lengthened in FXII- ($P < 0.0001$) and FXI-deficient ($P < 0.001$) plasmas (Fig. 5d). In FXI-deficient plasma, NETs induced clotting with a significantly ($P < 0.001$) higher MaxOD than NPP controls, but samples containing neutrophils only had significantly ($P < 0.0001$) lower MaxOD than NPP controls (Fig. 5c).

Role of Neutrophils and NETs in Clot Structure and Permeability

Confocal microscopy was used to investigate the effect of human neutrophils and NETs on the overall fibrin fibre network structure of clots. Neutrophils did not visually alter the clot density in the presence of thrombin (Fig. 6b). Unlike the turbidity data, the procoagulant effects of neutrophils were not obvious in the absence of thrombin (Fig. 6c). On the other hand, NETs visually triggered clotting (Fig. 6d and 6f). Compared to thrombin only controls (Fig. 6a), NETs increased the density of clots, particularly in the areas immediately surrounding the NETs (Fig. 6e and 6f). In areas where no NETs were formed, we observed large pores (Fig. 6e and 6g). Permeation experiments were carried out to investigate the permeability of clots. Neutrophil-induced clots were weak and easily ruptured during experiments, showing a significantly ($P < 0.001$) higher permeation coefficient than other conditions (Fig. 6h). When thrombin was added to neutrophils, the clot permeability matched that of control clots. NETs did not significantly affect the permeation coefficient of clots (Fig. 6h). NETs-induced clot permeability and stability were independent of thrombin.

Discussion

The role of neutrophils and NETs in coagulation *in vivo* has been investigated in several previous studies. Pühr-Westerheide and colleagues found that neutrophils contribute to platelet aggregation, thereby promoting clotting in the microvasculature⁴¹. However, Rumbaut and colleagues suggested that microvascular clotting could be neutrophil-independent in the presence of lipopolysaccharide (LPS)⁴². In addition, NETs have been shown to play a crucial role in coagulation in lower-shear vessels, but some studies show that they may be dispensable in those with high-shear^{32,33,41}. The procoagulant effects of neutrophils and NETs *in vivo* are complex and varied. In this *in vitro* study, we investigated the mechanisms of how neutrophils and NETs interact with fibrin(ogen) in blood clotting using both differentiated PLB-985 cells and isolated human neutrophils. According to our flow cytometry results, 93.6% of isolated cells from human neutrophils expressed both CD16 and CD66b markers. CD66b, a specific marker for secondary and tertiary granules^{43,44}, is mainly expressed on neutrophils and eosinophils⁴⁵. CD16 is also expressed on neutrophils, natural killer cells and macrophages, but not on eosinophils⁴⁶.

Therefore, our data indicate that highly pure neutrophils were harvested after isolation from human blood.

The expression of neutrophil cell-surface markers (CD16, CD66b and CD11b) on differentiated PLB-985 cells was also evaluated using flow cytometry. CD11b is a marker for secondary, tertiary granules and secretory vesicles⁴⁷, it also plays an important role in adhesion, migration and degranulation of neutrophils^{48,49}. Although the expression of CD16 on PLB-985 cells significantly increased upon stimulation with 1.25% Dimethyl sulfoxide (DMSO), expression was still much weaker than that of human neutrophils. Additionally, both normal and differentiated PLB-985 cells had low CD66b expression. However, the expression of CD11b on PLB-985 cells dramatically increased upon differentiation by DMSO to a similar level to that of human neutrophils. Citrullinated histone H3 (H3Cit) plays an important role in the decondensation of chromatin, as the release of decondensed chromatin is an essential process of NETosis, H3Cit has recently been considered as a biomarker of NETs formation⁵⁰. Our immunofluorescence results using a green dye marker for histone H3 show that both human neutrophils and differentiated PLB-985 cells successfully formed NETs which are positive for H3Cit. These findings suggest that even though DMSO-differentiated PLB-985 cells did not possess the same granules as human neutrophils, the “NETosis” capabilities of these differentiated cells are similar to that of human neutrophils. Our data altogether show that PLB-985 cells are different from neutrophils and their extracellular traps may therefore not be fully identical to NETs. Nevertheless, experiments using this cell line were conducted prior to using human neutrophils in order to set up methods as well as prevent unnecessary blood draw. However, since this cell line cannot fully differentiate into primary neutrophils, it could not be a substitute for mature neutrophils, and human neutrophils were always needed to confirm experimental results.

Our turbidity results show that differentiated PLB cells, human neutrophils and their NETs had no significant influence on clot formation in a purified fibrinogen system in the absence of thrombin. However, in plasma they distinctly promoted clotting independently of thrombin. Previous studies showed that neutrophils contribute to clot formation via NETs^{6,27,33}. To investigate the potential mechanism of neutrophil-induced clotting, we analysed neutrophil supernatant by mass spectrometry and used it in turbidity experiments. Several mediators were observed in the neutrophil supernatant, including MPO, a marker of neutrophil activation⁵¹. Although cDNA was also observed in the supernatant, no histones (e.g., H3Cit) were detected. Therefore, these findings suggest that neutrophils were potentially activated to release proteins/enzymes and DNA, but did not form NETs during isolation. We also found that neutrophil-induced clotting had a significantly shorter lag time than both supernatant-induced and NETs-induced clotting, but with fluctuating turbidity curves for both neutrophil-induced and supernatant-induced clots, particularly before reaching MaxOD. This may indicate that, after isolation, neutrophils were still undergoing further

activation during the pre-coagulation period. The procoagulant effects we observed in neutrophil experiments may be due to mediators released from activated neutrophils. Confocal images show that NETs increased the local clot density, while neutrophils-induced clots were less stable. Altogether, our results show that neutrophils and NETs have different effects on clot formation, despite the NETs being generated from neutrophils.

A 1985 study by Griep *et.al.*, indicated that negatively charged surfaces (e.g. DNA) can activate FXII⁵². A more recent study has shown that NETs promote coagulation via the intrinsic pathway, where the authors observed reduced thrombus formation in mice injected with the FXII inhibitor PCK (not depicted) or in FXII- and FXI-deficient mice³³. In contrast, our results suggest that the procoagulant effects of NETs are not mediated through FVII, FXII or FXI but likely involve other components present in the plasma. We observed that FXII- and FXI-deficient plasmas reduced the procoagulant effects of partially activated neutrophils via lengthening the time to the maximum absorbance. Our results with deficient plasmas also highly suggest that partially activated neutrophils or mediators they release could induce clotting via FXI. However, there are currently no studies showing that the proteins we detected by mass spectrometry have direct interactions with FXI. Interestingly, anticoagulant protein annexin, which has been shown to inhibit the activation of factor XII⁵³, was observed in the neutrophils' supernatant. However, it has no apparent inhibitory effect on coagulation in plasmas containing FXII.

Previous studies have shown that NETs increase the fiber thickness and strengthen the clot structure, resulting in decreased permeability and delayed clot lysis^{34,54,55}. In this study, we confirmed that both partially activated neutrophils and NETs delayed clot lysis to varying degrees. However, our permeation data show that there were no significant differences in permeability between NET-induced clots and thrombin-induced clots, suggesting their average pore sizes are similar. This may be due to the fact that NETs only increased the density of fibrin fibers in areas directly surrounding them, whereas away from NETs, large pores were visible, indicating that the overall permeability of clots was not altered. Moreover, this finding indicates that the procoagulant effects of NETs could be concentration dependent, since we observed a denser clot structure in areas with more NETs.

To conclude, our data show that partially activated neutrophils and NETs independently promote clotting in plasma via novel mechanisms *in vitro*, and that FXI and to a lesser degree FXII play a role in the procoagulant effects of neutrophils but not NETs. We also find that partially activated neutrophils and NETs delay clot lysis and that clot density is visually increased in the immediate areas surrounding NETs. We propose that the procoagulant effects of neutrophils could be induced by neutrophil-secreted proteins. These findings provide unique mechanistic insights into the cross-talk between neutrophils, NETs and blood coagulation, with important implications for diseases of

thrombosis such as stroke, deep vein thrombosis and heart attacks. Targeting mechanisms involved in this cross-talk provide tempting new prospects for future therapeutics.

Methods

Human Neutrophils Isolation

Whole blood samples were obtained from the antecubital vein of healthy volunteers with minimal stasis, discarding the first 2.5 ml, and collected on 0.5 M Ethylenediaminetetraacetic acid (EDTA) or using EDTA Vacutainers. Normally, 5 to 10 ml of blood were needed for carrying out one subsequent experiment. Human neutrophils were isolated as previously described⁵⁶. All reagents that could be filtered were filtered with a 0.2 µm filter prior to use. First, 5 ml of whole blood was carefully layered on the top of 5 ml Lympholyte-poly (Cedarlane). Samples were centrifuged at 500 RCF, 23°C for 35 minutes without brakes. Blood was separated into six clear bands, and the layer of neutrophils and all of the isolation media below this layer were carefully transferred into a new Falcon tubes. Cells were then washed once with Hanks' Balanced Salt solution (HBSS) (without Ca²⁺/Mg²⁺) and centrifuged at 350 RCF for 10 minutes. After centrifugation, the supernatant was removed, then 2 ml of Red Blood Cell (RBC) Lysis Buffer (Roche) was added to the tube to lyse the residual RBC, and the cell pellet was gently resuspended. Cells were then washed once with 10 ml HBSS (without Ca²⁺/Mg²⁺) and centrifuged at 250 RCF for 5 mins. Finally, the supernatant was discarded and the pellet was resuspended in 4 ml of HBSS (with Ca²⁺/Mg²⁺) or HEPES-buffered saline (HBS) ((If required for subsequent experiments, these buffers could be supplemented with 2% w/v human serum albumin (HSA) or 2% v/v fetal bovine serum (FBS)). All Blood donors provided informed written consent according to the declaration of Helsinki, and this study was approved by the University of Leeds Medicine and Health Faculty Research Ethics Committee, reference number HSLTLM12045.

PLB-985 Cell Culture and Differentiation

The PLB-985 cell line (ACC-139), established from human acute myeloid leukemia and previously reported as a suitable neutrophil-like cell model⁴⁴, was purchased from DSMZ. PLB-985 cells were cultured and differentiated as previously described⁴⁴. In short, cells were cultured in RPMI 1640 medium (R8758, Sigma-Aldrich) supplemented with 10% heat-inactivated FBS at 37°C in a 5% CO₂ with air humidified incubator. Medium was renewed every 2 days. For differentiation, cells were treated in RPMI 1640 medium supplemented with 1.25% Dimethyl Sulfoxide (DMSO, Sigma-Aldrich) and heat-inactivated FBS at 37°C in 5% CO₂ for 5 days. This treatment medium was renewed on day 3. The treated cells were used in experiments on day 6.

NETs Generation

For immunofluorescence, round cover-slips that were pre-coated with poly-L-lysine (0.01% solution, Sigma-Aldrich) were placed in wells of a 24-well cell culture plate, then isolated neutrophils or PLB-985 cells were seeded (~200,000 cells) in 500 μ l RPMI 1640 medium (supplemented with 2% FBS) per well and incubated at 37°C in a 5% CO₂. After 1 hour, the supernatant was gently removed, after which 100 nM PMA (Sigma-Aldrich), which diluted in RPMI 1640 or HBS, were added in each well. Cells were incubated at 37°C in a 5% CO₂ incubator overnight (minimally 2 hr). All reagents that could be filtered were filtered with a 0.2 μ m filter prior to use.

For turbidity assays, cells were treated with 20 nM PMA in a T25 flask, incubated at 37°C in 5% CO₂ for 4 hr prior to experiments. After treatment, samples were centrifuged at 500 RCF for 5 mins to precipitate residual cells or debris, then the supernatant was centrifuged at 17,000 RCF for 15 mins at 4°C to harvest NETs. NETs were washed once with HBS by centrifugation at 17,000 RCF for 15 mins at 4°C, then the supernatant was discarded, and NETs were resuspended in HBS. Before resuspended NETs were used in experiments, double-stranded DNA (dsDNA) was quantified using LabTech-Nanodrop ND100 spectrophotometer at a wavelength of 260 nm to confirm that the NET concentration was consistent in every experiment. All reagents that could be filtered were filtered with a 0.2 μ m filter prior to use.

Turbidity Measurements

Turbidity measurements were used to analyse the kinetics of clot formation and fibrinolysis as previously described^{57,58}. Final concentrations were as follows: *Fibrinogen System*: 2 mg/ml Human Fibrinogen (von Willebrand factor and plasminogen depleted, Enzyme Research Laboratories), 1.5 mM CaCl₂ and 200,000 cells or NETs (pre-generated from 200,000 cells) were diluted in HBS and premixed in a 96-well plate. 0.1 U/ml thrombin (Merck) was added to initiate clotting. The absorbency was read at 340nm, every 12 seconds for 4 hours at 37°C by Multiskan FC Microplate Photometer (Thermo Fisher Scientific) or a PowerWave HT Microplate Spectrophotometer (BioTek). For lysis, tPA (0.03mg/ μ l) was added while other conditions remained unchanged. All experiments were performed in triplicate. *Plasma System*: Plasma (diluted 1:6), 3.33 mM Ca²⁺ and 200,000 cells or NETs (pre-generated from 200,000 cells) were diluted in HBS and premixed in a 96-well plate. 0.1 U/ml thrombin was added to initiate clotting. The absorbency was read at 340 nm, every 12 seconds for 4 hours at 37°C by Multiskan FC Microplate Photometer. For lysis, tPA (0.03 mg/ μ l) was added and all other conditions remained unchanged. FXII-, FXI- and FVII-deficient plasmas were purchased from George King Bio-Medical, Inc., USA. All experiments were performed in triplicate. All reagents that could be filtered were filtered with a 0.2 μ m filter prior to use.

Immunofluorescence & Fluorescence Microscopy

Immunofluorescence was carried out to visualize NETs, which were generated on round coverslips as described above. Anti-Histone H3 (citrulline R2 + R8 +

R17) antibody (ab5103) and Goat anti-Rabbit IgG H&L (Alexa Fluor 488) (ab150077) were obtained from Abcam. All reagents that could be filtered were filtered with a 0.2 μm filter prior to use. Samples on 24-well plates were fixed with paraformaldehyde (PFA, 4% in PBS, Sigma-Aldrich) for 30 mins inside a fume hood at room temperature, followed by washing 3x with 1 ml PBS per well. Then, samples were incubated in 0.5% Triton X-100 (diluted in PBS) for 1 min at room temperature. After washing 3x with PBS, samples were incubated in blocking buffer (1% w/v bovine serum albumin (BSA), 22.52 mg/ml glycine in PBST (PBS with 0.1% v/v Tween 20)) for 30 mins at room temperature to block non-specific binding of the antibodies. Following one washing step with 1% BSA in PBST, samples were incubated in 500 μl primary antibody (anti-Histone H3, 1:250 diluted in 1% BSA) per well overnight at 4°C. The following day, coverslips were washed 3x with PBS, then incubated with secondary antibody (Goat Anti-Rabbit IgG H&L (Alexa Fluor 488), 1:500 diluted in 1% BSA) for 1 hour at room temperature in the dark. Coverslips were then washed 3x with PBS, followed by incubating with 300 nM 4',6-Diamidino-2-Phenylindole, Dihydrochloride (DAPI, Sigma-Aldrich) for 1-5 min in the dark. After washing twice with distilled water, coverslips were mounted upside down onto glass slides with antifade mounting medium (Vector Laboratories). Slides were allowed to dry for at least 1 hour at room temperature in the dark. Slides were imaged via 20x (0.8 NA) or 40x (1.0 NA) lenses with Diode 405 nm laser and Argon 488nm laser filter by using an Airyscan Upright Confocal Microscope (Zeiss LSM880) or Fluorescence Microscope (Zeiss AX10 - Zen software).

Fluorescent Labeling was carried out to visualize clots. FITC labeled fibrinogen (25 $\mu\text{g}/\text{ml}$) was added into plasma. All reagents that could be filtered were filtered with a 0.2 μm filter prior to use. The reaction mixture was prepared by diluting plasmas (diluted 1:6 or 1:3), CaCl_2 (3.33 mM) and 200,000 cells (with 100 nM PMA) or NETs (pre-generated from 200,000 cells) in HBS. Thrombin (0.1U/ml) was added to initiate clotting. Then 30 μl of the mixture was immediately transferred into a well of an uncoated 8-well Ibidi slide (Ibidi GmbH). The slide was placed into a dark humidity chamber for 2 hr at room temperature. Slides were imaged via 40x oil immersion objective lens (1.4 NA) with Diode 405 nm laser and Argon 488nm laser filter by using an Airyscan Inverted Confocal Microscope (Zeiss LSM880). Optical Z-stacks (9.4-10 μm , 21-23 slices) were combined to form 3D images via Fiji-ImageJ.

Clot Permeation

Permeability of clots was analysed as previously described. All reagents that could be filtered were filtered with a 0.2 μm filter prior to use. Clot samples were prepared using similar methods as described for confocal microscopy above, with the following alterations: plasma was diluted 1:3 and the 6-channel Ibidi slide was used. Clotting slides were placed horizontally in the moist chamber for 2 hours then a syringe was connected to each channel. Syringes were filled with permeation buffer to a set height (4 cm) and clots were washed in this manner for 90-120 mins. Flow-through of buffer was subsequently measured by

collecting and weighing the buffer flow-through every 5 mins for 20-40 mins. Volume of buffer flow-through, correlated to weight assuming 1 g = 1 mL, over time was plotted and fitted by linear regression ($R^2 \approx 0.99$). The permeation coefficient (Ks, Darcy constant), corresponding to pore size, was calculated as previously described⁵⁹.

Statistical Analysis

All statistical analyses were performed using GraphPad Prism 7. A normal distribution of the data used in two-tailed unpaired t-test was checked by Shapiro-Wilk (W) test ($P > 0.05$). Differences in the expression levels of CD16 ($W = 0.9306$) and CD66b ($W = 0.9355$) on differentiated PLB-985 cells were determined by two-tailed unpaired t-test. Differences in the lag time ($W = 0.9445$), maximum optical density (MaxOD) ($W = 0.9713$) and turbidity Vmax ($W = 0.9130$) of human neutrophil supernatant were determined by two-tailed unpaired t test. Other turbidity and lysis data were determined by one-way ANOVA analysis with Tukey's multiple comparisons test ($\text{Alpha} = 0.05$). Differences in Ks were determined by one-way ANOVA with Tukey's multiple comparisons test ($\text{Alpha} = 0.05$). Contrast of confocal and fluorescence images were adjusted by Fiji-Image J. P-values < 0.05 were considered to indicate statistical significance. All methods and analyses were performed in accordance with the relevant guidelines and regulations.

Data Availability Statement

The datasets generated during and/or analysed during the current study are available from the corresponding author on reasonable request.

References

1. Mayadas, T. N., Cullere, X. & Lowell, C. A. The Multifaceted Functions of Neutrophils. *Annu. Rev. Pathol. Mech. Dis.* **9**, 181–218 (2014).
2. Edwards, S. W. *Biochemistry and Physiology of the Neutrophil*. *Biochemistry and Physiology of the Neutrophil* (1994). doi:10.1017/cbo9780511608421
3. Rosales, C. Neutrophil: A cell with many roles in inflammation or several cell types? *Front. Physiol.* (2018). doi:10.3389/fphys.2018.00113
4. Selders, G. S., Fetz, A. E., Radic, M. Z. & Bowlin, G. L. An overview of the role of neutrophils in innate immunity, inflammation and host-biomaterial integration. *Regen. Biomater.* (2017). doi:10.1093/rb/rbw041
5. Swystun, L. L. & Liaw, P. C. The role of leukocytes in thrombosis. *Blood* **128**, 753–762 (2016).
6. Kapoor, S., Opneja, A. & Nayak, L. The role of neutrophils in thrombosis. *Thromb. Res.* **170**, 87–96 (2018).

7. Noubouossie, D. F., Reeves, B. N., Strahl, B. D. & Key, N. S. Neutrophils: Back in the thrombosis spotlight. *Blood* **133**, (2019).
8. Darbousset, R. *et al.* Tissue factor-positive neutrophils bind to injured endothelial wall and initiate thrombus formation. *Blood* (2012). doi:10.1182/blood-2012-06-437772
9. Flick, M. J. *et al.* Leukocyte engagement of fibrin(ogen) via the integrin receptor α M β 2/Mac-1 is critical for host inflammatory response *in vivo*. *J. Clin. Invest.* (2004). doi:10.1172/JCI20741
10. Kuijper, P. H. *et al.* Neutrophil adhesion to fibrinogen and fibrin under flow conditions is diminished by activation and L-selectin shedding. *Blood* **89**, 2131–8 (1997).
11. Korkmaz, B., Horwitz, M. S., Jenne, D. E. & Gauthier, F. Neutrophil Elastase, Proteinase 3, and Cathepsin G as Therapeutic Targets in Human Diseases. *Pharmacol. Rev.* (2010). doi:10.1124/pr.110.002733
12. Goel, M. S. & Diamond, S. L. Neutrophil cathepsin G promotes prothrombinase and fibrin formation under flow conditions by activating fibrinogen-adherent platelets. *J. Biol. Chem.* (2003). doi:10.1074/jbc.M211956200
13. LaRosa, C. A. *et al.* Human neutrophil cathepsin G is a potent platelet activator. *J. Vasc. Surg.* (1994). doi:10.1016/S0741-5214(94)70106-7
14. Renesto, P. & Chignard, M. Enhancement of cathepsin G-induced platelet activation by leukocyte elastase: Consequence for the neutrophil-mediated platelet activation. *Blood* (1993). doi:10.1182/blood.v82.1.139.bloodjournal821139
15. Allen, D. H. & Tracy, P. B. Human coagulation factor V is activated to the functional cofactor by elastase and cathepsin G expressed at the monocyte surface. *J. Biol. Chem.* (1995). doi:10.1074/jbc.270.3.1408
16. Gale, A. J. & Rozenshteyn, D. Cathepsin G, a leukocyte protease, activates coagulation factor VIII. *Thromb. Haemost.* (2008). doi:10.1160/TH07-08-0495
17. Plescia, J. & Altieri, D. C. Activation of Mac-1 (CD11b/CD18)-bound factor X by released cathepsin G defines an alternative pathway of leucocyte initiation of coagulation. *Biochem. J.* (1996). doi:10.1042/bj3190873
18. Petersen, L. C., Bojrn, S. E. & Nordfang, O. Effect of leukocyte proteinases on tissue factor pathway inhibitor. *Thromb. Haemost.* (1992). doi:10.1055/s-0038-1648489
19. Belaaouaj, A. A., Li, A., Wun, T. C., Welgus, H. G. & Shapiro, S. D. Matrix metalloproteinases cleave tissue factor pathway inhibitor: Effects on coagulation. *J. Biol. Chem.* (2000). doi:10.1074/jbc.M004218200
20. Jochum, M., Lander, S., Heimburger, N. & Fritz, H. Effect of human granulocytic elastase on isolated human antithrombin iii. *Hoppe. Seylers. Z. Physiol. Chem.* (1981). doi:10.1515/bchm2.1981.362.1.103
21. Von Köckritz-Blickwede, M. & Nizet, V. Innate immunity turned inside-out: Antimicrobial defense by phagocyte extracellular traps. *J. Mol. Med.* **87**, 775–783 (2009).

22. Zawrotniak, M. & Rapala-Kozik, M. Neutrophil extracellular traps (NETs) - Formation and implications. *Acta Biochim. Pol.* **60**, 277–284 (2013).
23. Clark, S. R. *et al.* Platelet TLR4 activates neutrophil extracellular traps to ensnare bacteria in septic blood. *Nat. Med.* **13**, 463–469 (2007).
24. Petretto, A. *et al.* Neutrophil extracellular traps (NET) induced by different stimuli: A comparative proteomic analysis. *PLoS One* (2019). doi:10.1371/journal.pone.0218946
25. Fuchs, T. A. *et al.* Novel cell death program leads to neutrophil extracellular traps. *J. Cell Biol.* **176**, 231–241 (2007).
26. Pfeiler, S., Stark, K., Massberg, S. & Engelmann, B. Propagation of thrombosis by neutrophils and extracellular nucleosome networks. *Haematologica* **102**, 206–213 (2017).
27. Nagareddy, P. & Smyth, S. S. Inflammation and thrombosis in cardiovascular disease. *Curr. Opin. Hematol.* **20**, 457–463 (2013).
28. Martinod, K., Wagner, D. D., Martinod, K. & Wagner, D. D. Thrombosis : tangled up in NETs Review Article Thrombosis : tangled up in NETs. *Blood* **123**, 2768–2776 (2014).
29. Ward, C. M., Tetaz, T. J., Andrews, R. K. & Berndt, M. C. Binding of the von Willebrand factor A1 domain to histone. *Thromb. Res.* (1997). doi:10.1016/S0049-3848(97)00096-0
30. Massberg, S. *et al.* Reciprocal coupling of coagulation and innate immunity via neutrophil serine proteases. *Nat. Med.* (2010). doi:10.1038/nm.2184
31. Ammollo, C. T., Semeraro, F., Xu, J., Esmon, N. L. & Esmon, C. T. Extracellular histones increase plasma thrombin generation by impairing thrombomodulin-dependent protein C activation. *J. Thromb. Haemost.* (2011). doi:10.1111/j.1538-7836.2011.04422.x
32. Fuchs, T. A. *et al.* Extracellular DNA traps promote thrombosis. *Proc. Natl. Acad. Sci.* (2010). doi:10.1073/pnas.1005743107
33. von Brühl, M.-L. *et al.* Monocytes, neutrophils, and platelets cooperate to initiate and propagate venous thrombosis in mice *in vivo*. *J. Exp. Med.* **209**, 819–835 (2012).
34. Longstaff, C. *et al.* Neutralisation of the anti-coagulant effects of heparin by histones in blood plasma and purified systems. *Thromb. Haemost.* **115**, 591–599 (2016).
35. Fuchs, T. A., Bhandari, A. A. & Wagner, D. D. Histones induce rapid and profound thrombocytopenia in mice. *Blood* (2011). doi:10.1182/blood-2011-01-332676
36. Brill, A. *et al.* Neutrophil extracellular traps promote deep vein thrombosis in mice. *J. Thromb. Haemost.* **10** (1), 136–144 (2012).
37. Laridan, E., Martinod, K. & De Meyer, S. F. Neutrophil Extracellular Traps in Arterial and Venous Thrombosis. *Semin. Thromb. Hemost.* **45**, 86–93 (2019).
38. Hisada, Y. *et al.* Neutrophils and neutrophil extracellular traps enhance venous thrombosis in mice bearing human pancreatic tumors. *Haematologica* (2020). doi:10.3324/haematol.2019.217083

39. Vilalta, N. *et al.* The Relationship between Leukocyte Counts and Venous Thromboembolism: Results from RETROVE Study. *Biol. Med.* **09**, (2017).
40. Hagberg, I. A., Roald, H. E. & Lyberg, T. Adhesion of leukocytes to growing arterial thrombi. *Thromb. Haemost.* (1998). doi:10.1055/s-0037-1615370
41. Pühr-Westerheide, D. *et al.* Neutrophils promote venular thrombosis by shaping the rheological environment for platelet aggregation. *Sci. Rep.* (2019). doi:10.1038/s41598-019-52041-8
42. Rumbaut, R. E. *et al.* Endotoxin enhances microvascular thrombosis in mouse cremaster venules via a TLR4-dependent, neutrophil-independent mechanism. *Am. J. Physiol. - Hear. Circ. Physiol.* (2006). doi:10.1152/ajpheart.00305.2005
43. Mollinedo, F., Martin-Martin, B., Calafat, J., Nabokina, S. M. & Lazo, P. A. Role of Vesicle-Associated Membrane Protein-2, Through Q-Soluble N-Ethylmaleimide-Sensitive Factor Attachment Protein Receptor/R-Soluble N-Ethylmaleimide-Sensitive Factor Attachment Protein Receptor Interaction, in the Exocytosis of Specific and Tertiary . *J. Immunol.* **170**, 1034–1042 (2003).
44. Pivot-Pajot, C., Chouinard, F. C., Amine El Azreq, M., Harbour, D. & Bourgoin, S. G. Characterisation of degranulation and phagocytic capacity of a human neutrophilic cellular model, PLB-985 cells. *Immunobiology* **215**, 38–52 (2010).
45. Torsteinsdóttir, I., Arvidson, N. G., Hällgren, R. & Håkansson, L. Enhanced expression of integrins and CD66b on peripheral blood neutrophils and eosinophils in patients with rheumatoid arthritis, and the effect of glucocorticoids. *Scand. J. Immunol.* (1999). doi:10.1046/j.1365-3083.1999.00602.x
46. Darby, C., Chien, P., Rossman, M. D. & Schreiber, A. D. Monocyte/macrophage FcγRIII, unlike FcγRIII on neutrophils, is not a phosphatidylinositol-linked protein. *Blood* (1990). doi:10.1182/blood.v75.12.2396.2396
47. Borregaard, N., Sørensen, O. E. & Theilgaard-Mönch, K. Neutrophil granules: a library of innate immunity proteins. *Trends Immunol.* (2007). doi:10.1016/j.it.2007.06.002
48. Schleiffenbaum, B., Moser, R., Patarroyo, M. & Fehr, J. The cell surface glycoprotein Mac-1 (CD11b/CD18) mediates neutrophil adhesion and modulates degranulation independently of its quantitative cell surface expression. *J. Immunol.* (1989).
49. Anderson, S. I., Hotchin, N. A. & Nash, G. B. Role of the cytoskeleton in rapid activation of CD11b/CD18 function and its subsequent downregulation in neutrophils. *J. Cell Sci.* (2000).
50. Thålin, C. *et al.* Citrullinated histone H3 as a novel prognostic blood marker in patients with advanced cancer. *PLoS One* (2018). doi:10.1371/journal.pone.0191231

51. Boettcher, M. *et al.* Markers of neutrophil activation and extracellular traps formation are predictive of appendicitis in mice and humans: a pilot study. *Sci. Rep.* (2020). doi:10.1038/s41598-020-74370-9
52. Griep, M. A., Fujikawa, K. & Nelsestuen, G. L. Binding and Activation Properties of Human Factor XII, Prekallikrein, and Derived Peptides with Acidic Lipid Vesicles. *Biochemistry* (1985). doi:10.1021/bi00336a047
53. Nakayama, M. *et al.* Annexin A4 inhibits sulfatide-induced activation of coagulation factor XII. *J. Thromb. Haemost.* (2020). doi:10.1111/jth.14789
54. Varjú, I. *et al.* DNA, histones and neutrophil extracellular traps exert anti-fibrinolytic effects in a plasma environment. *Thromb. Haemost.* (2015). doi:10.1160/TH14-08-0669
55. Longstaff, C. *et al.* Mechanical stability and fibrinolytic resistance of clots containing fibrin, DNA, and histones. *J. Biol. Chem.* **288**, 6946–6956 (2013).
56. Oh, H., Siano, B. & Diamond, S. Neutrophil Isolation Protocol. *J. Vis. Exp.* (2008). doi:10.3791/745
57. Baker, S. R. *et al.* Recurrent venous thromboembolism patients form clots with lower elastic modulus than those formed by patients with non-recurrent disease. *J. Thromb. Haemost.* (2019). doi:10.1111/jth.14402
58. Duval, C. *et al.* Factor XIII A-Subunit V34L Variant Affects Thrombus Cross-Linking in a Murine Model of Thrombosis. *Arterioscler. Thromb. Vasc. Biol.* **36**, 308–316 (2016).
59. Pieters, M. *et al.* An international study on the standardization of fibrin clot permeability measurement: Methodological considerations and implications for healthy control values. *J. Thromb. Haemost.* **10**, 2179–2181 (2012).

Acknowledgements

This work was supported by a British Heart Foundation (BHF) Programme Grant (RG/18/11/34036) and Wellcome Investigator Award (204951/B/16/Z) to RASA. We thank R. George (Biomolecular Mass Spectrometry Facility, University of Leeds) for protein identification by mass spectrometry. We also thank H. McPherson, S. Heal and L. Hardy for assistance with turbidity and lysis measurements.

Author Contributions

R.A.S. Ariëns, S.D. Connell and H. Philippou conceived the study, Y. Shi conducted the experiments, J.S. Gauer and S.R. Baker assisted with the experiments and the analysis of the data. Y. Shi and R.A.S. Ariëns wrote the manuscript. All authors reviewed the manuscript.

Competing Interests

The author(s) declare no competing interests.

Figure Legends

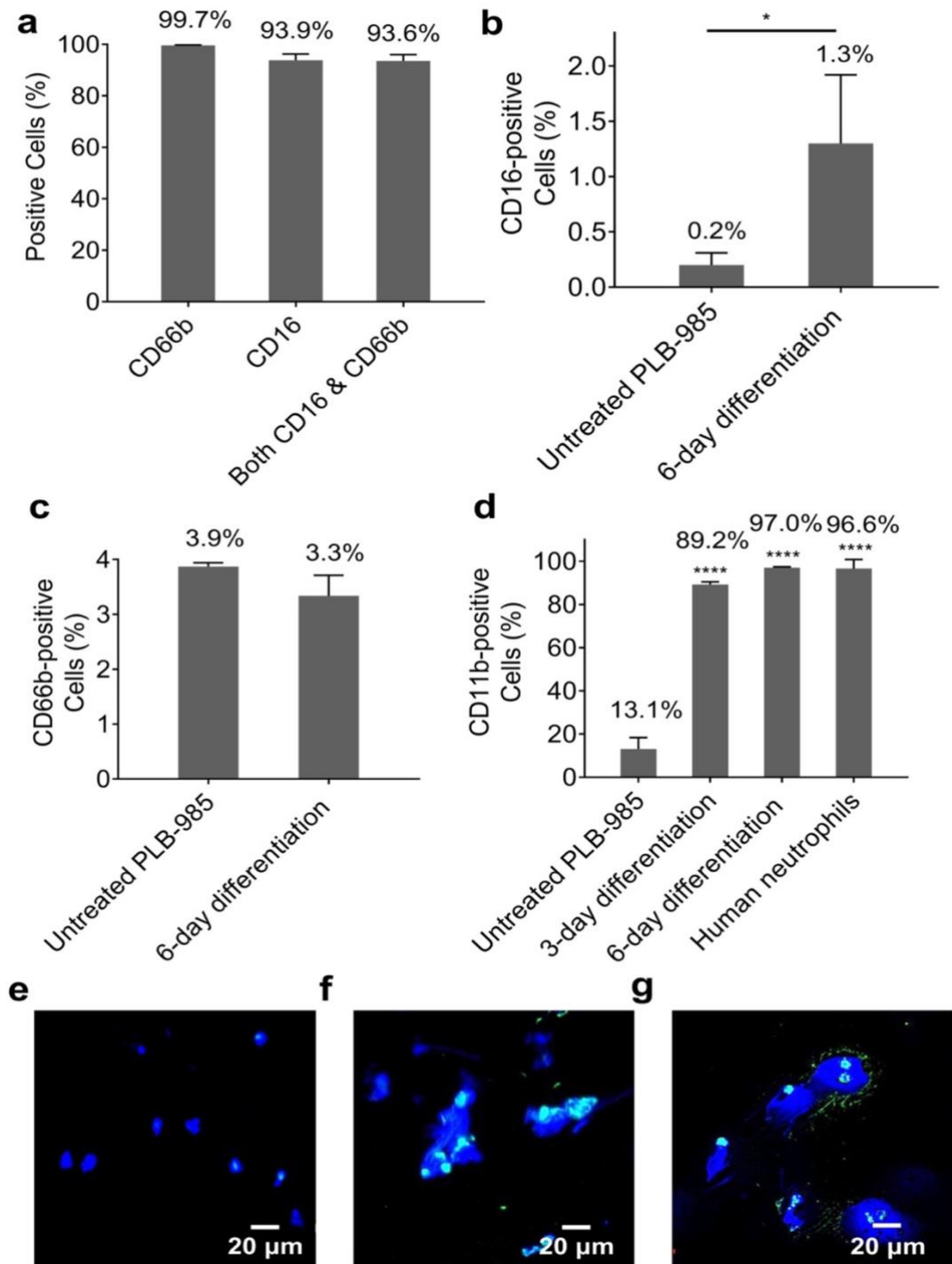


Figure 1. Expression of neutrophil-surface antigens on isolated human neutrophils and differentiated PLB-985 cells and the capacity of NETosis of these cells. The expression of antigens on cells was detected in living cells via

flow cytometry. (a) Expression levels of CD16 and CD66b on human neutrophils were used as the positive control. Expression levels of (b) CD16 and (c) CD66b on differentiated PLB-985 cells were detected on the day 6 of treatment with 1.25% DMSO, untreated cells were used as the negative control. (d) Expression level of CD11b on differentiated PLB-985 cells was detected on the day 3 and day 6 of treatment with 1.25% DMSO, untreated PLB-985 cells were used as a negative control, and human neutrophils were used as a positive control. Error bars represent SD of three technical replicates. * $P < 0.05$, **** $P < 0.0001$. (e) Unstimulated human neutrophils using fluorescence microscopy. (f) NETs generated from isolated human neutrophils stimulated with PMA. (g) NETs generated from differentiated PLB-985 cells stimulated with PMA. Blue: DAPI-stained DNA. Green (cyan in overlay with blue): Alexa Fluor 488 labelled Histone H3 (citrulline R2 + R8 + R17).

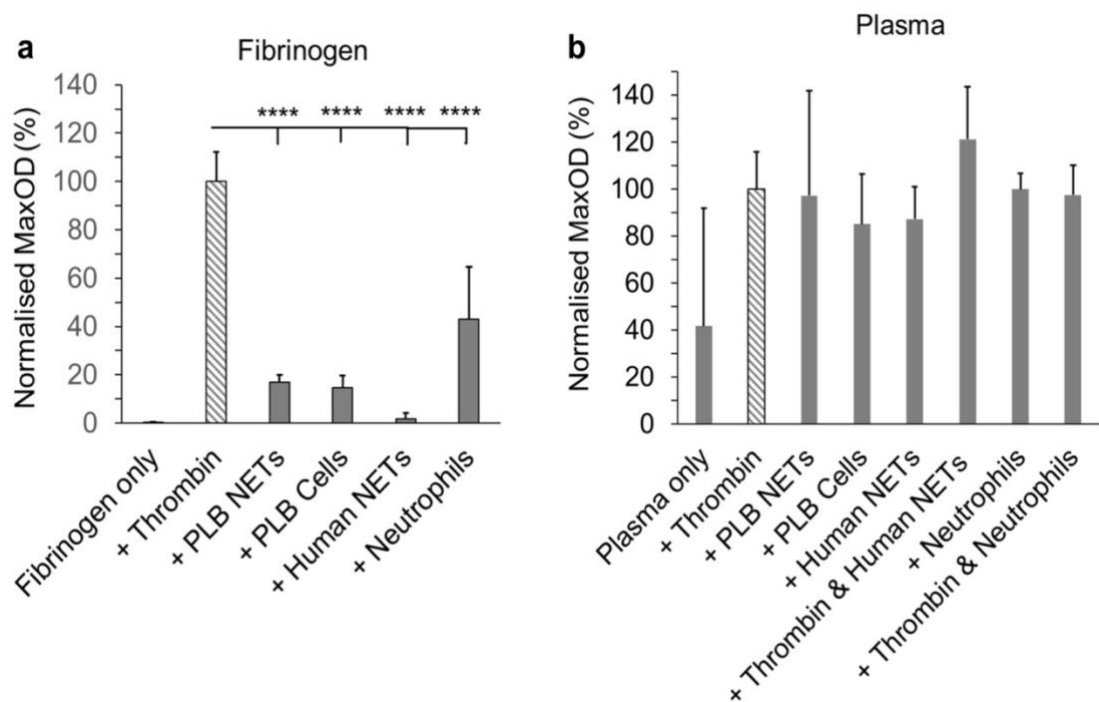


Figure 2. Effects of neutrophils and NETs on coagulation. Turbidity measurements were carried out in (a) a purified fibrinogen system or in (b) NPP. Differentiated PLB-985 cells or human neutrophils (200,000 cells/100 μ l) or NETs (generated from 200,000 cells/100 μ l) were added to purified fibrinogen or plasma. Normalized percentage of MaxOD (compared to thrombin only controls) was quantified. Other concentrations: thrombin (0.1 U/ml), fibrinogen (2 mg/ml), plasma (diluted 1:6) and CaCl_2 (1.5 mM in purified fibrinogen or 3.33 mM in plasma). Error bars represent SD of three technical replicates in triplicates. **** $P < 0.0001$.

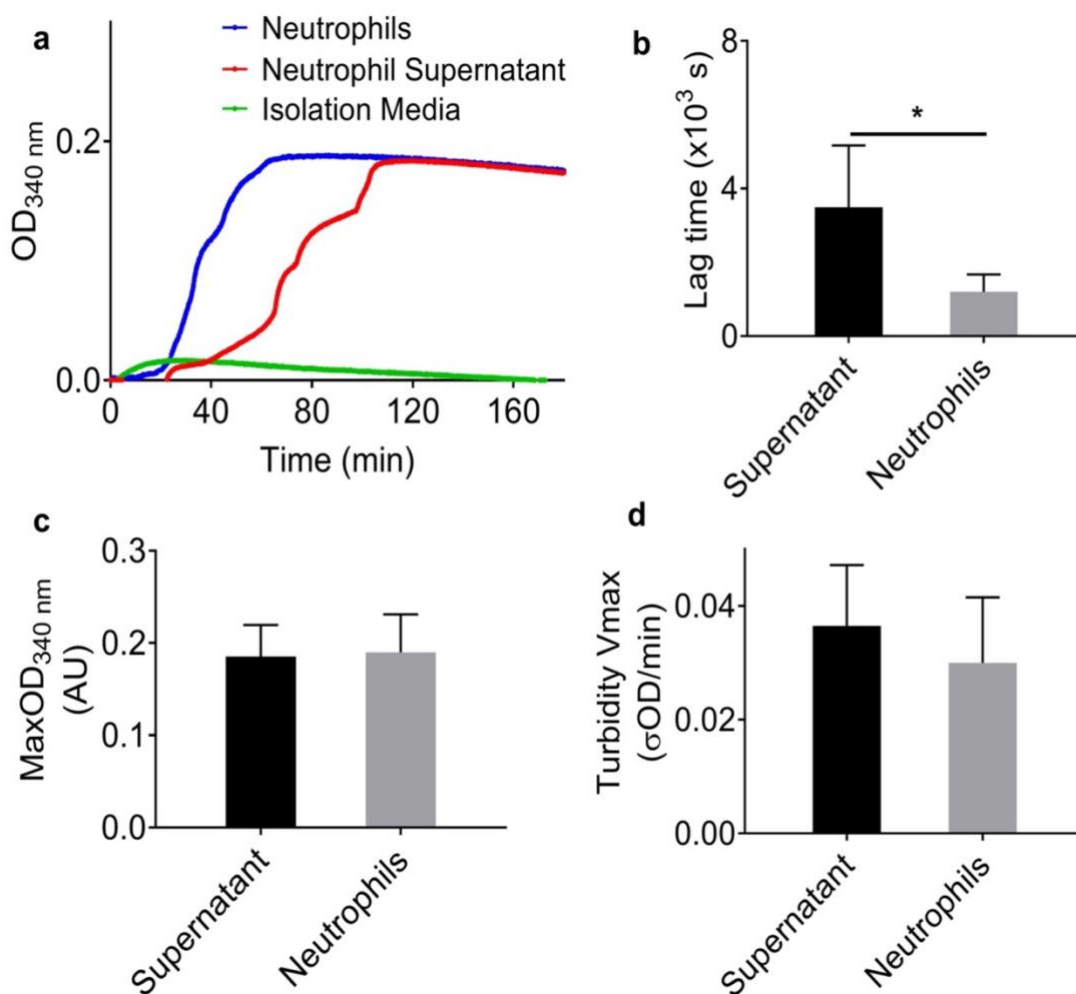


Figure 3. Effects of human neutrophil supernatant on clot formation. (a) Clot polymerization curves, obtained by turbidity, showing the effects of human neutrophils (200,000 cells/100 μ l) and their supernatant on clot formation when added to NPP. (b) Lag time, (c) MaxOD and (d) maximum rate of clot formation (turbidity Vmax) were quantified. Other concentrations: plasma (diluted 1:6) and CaCl₂ (3.33 mM). Error bars represent SD of 5-6 replicates. * P < 0.05.

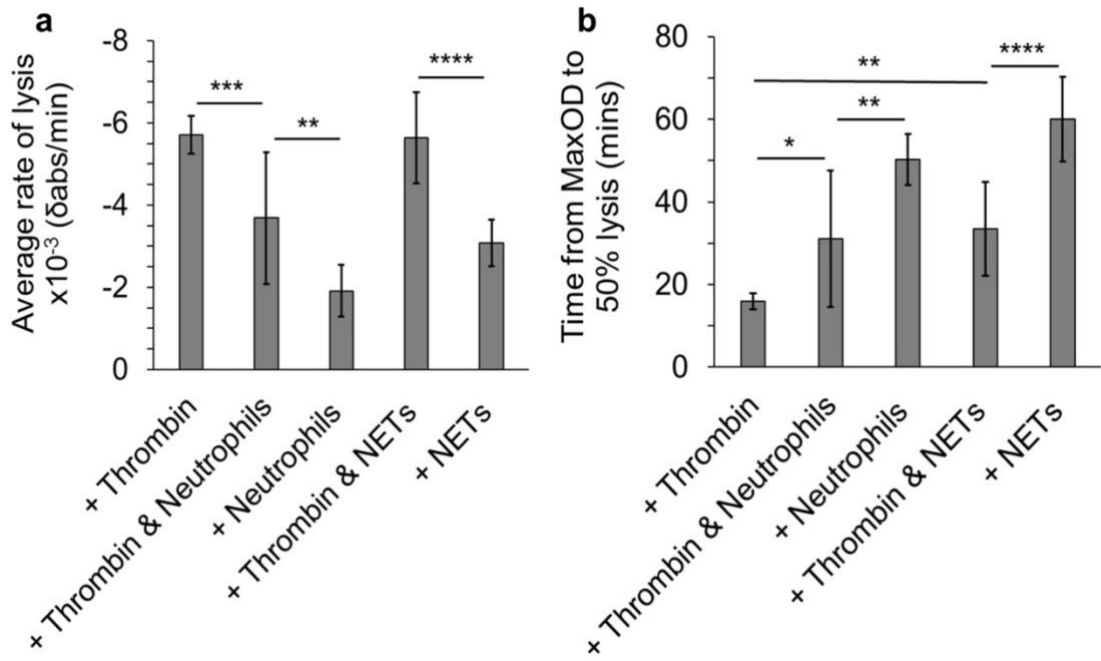


Figure 4. Lysis analysis of the effect of human neutrophils or human NETs on clot dissolution. Neutrophils (200,000 cells/100 μ l) or NETs (generated from 200,000 cells/100 μ l) were added to plasma. (a) Average rate of lysis and (b) time from MaxOD to 50% lysis were quantified. Other concentrations: plasma (diluted 1:6), CaCl₂ (3.33 mM) and thrombin (0.1 U/ml), Error bars represent \pm SD of three technical replicates in triplicates. * P < 0.05, ** P < 0.01, *** P < 0.001, **** P < 0.0001.

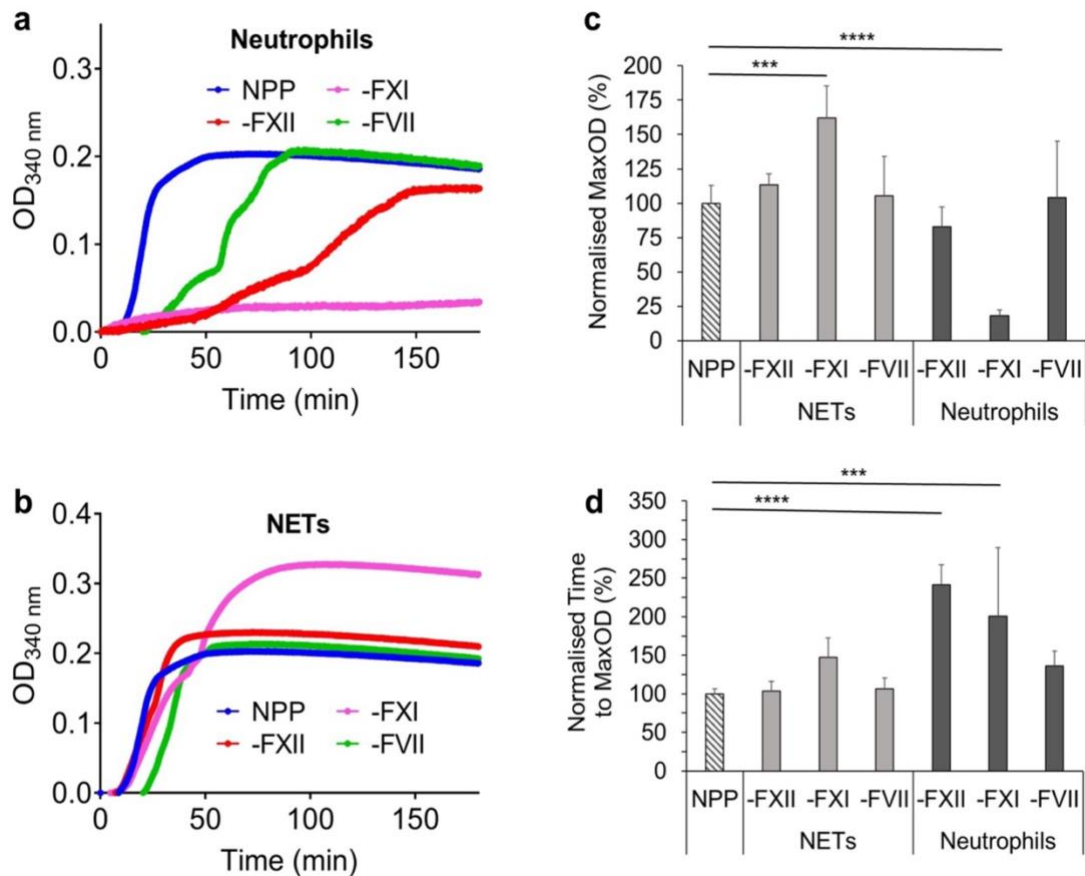


Figure 5. Turbidity analysis of the effect of human neutrophils and human NETs on FXII, FXI and FVII deficient plasmas. (a) Human neutrophils (200,000 cells/100 μ l) or (b) human NETs (generated from 200,000 cells/100 μ l) were added into FXII, FXI or FVII deficient plasmas, NPP was used as the positive control. (c) Normalized percentage of MaxOD and (d) normalized percentage of time to MaxOD were quantified. Other concentrations: plasmas (diluted 1:6) and CaCl_2 (3.33 mM). Error bars represent SD. NPP data represents 8 replicates, deficient plasma data represents 4-6 replicates. *** $P < 0.001$, **** $P < 0.0001$.

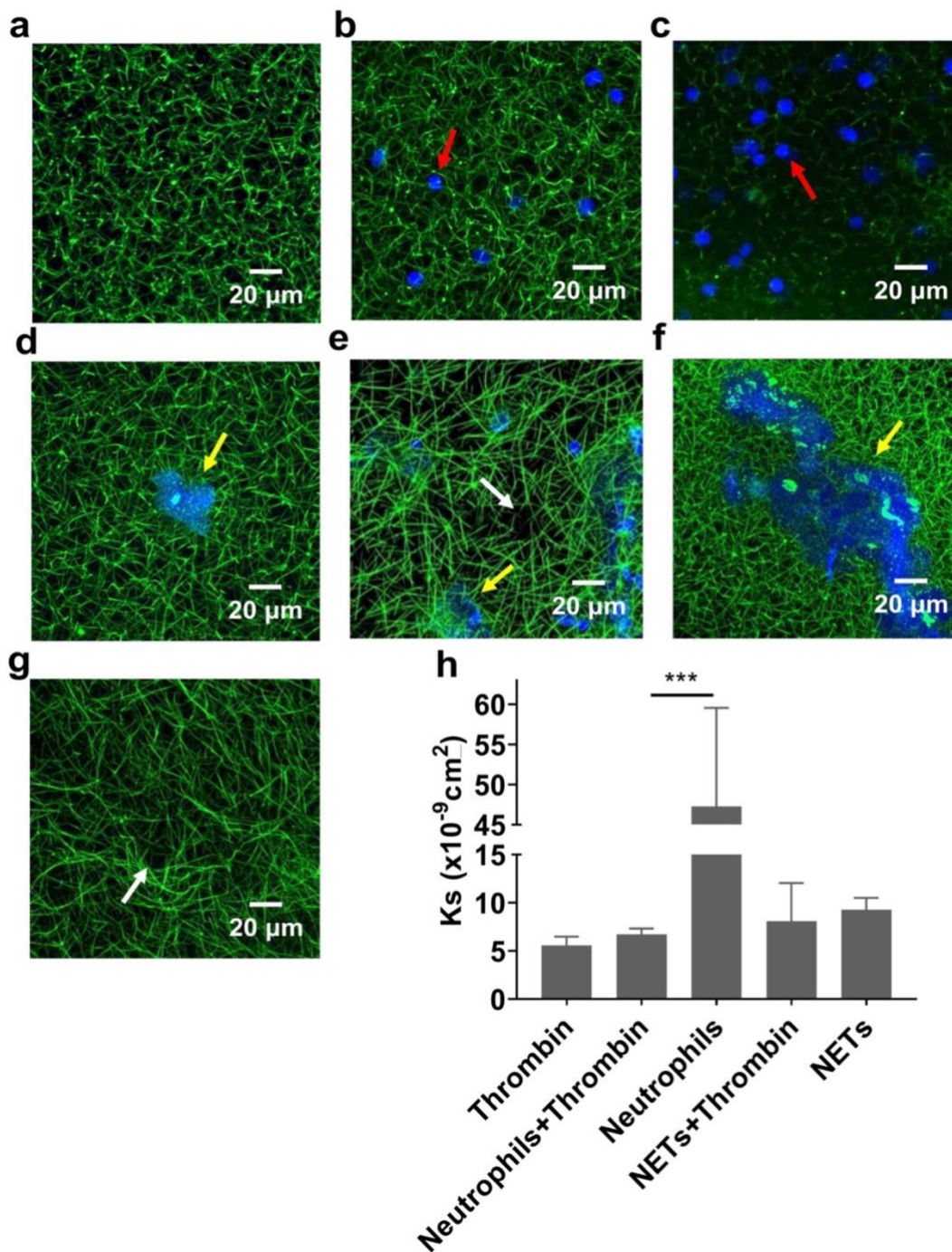


Figure 6. Clot density and the permeability of clots with human neutrophils or human NETs. (a) The overall structure of NPP clots triggered with only thrombin, (b) thrombin and neutrophils (200,000 cells/100 μ l), (c) neutrophils only, (d and e) thrombin and NETs (generated from 200,000 cells/100 μ l) and (f

and **g**) NETs only were visualized by an confocal microscopy with a 40× oil immersion objective lens (1.4 NA). **f** and **g** are images of two positions from the same slide. Blue: DAPI-stained DNA. Green: Alexa Fluor 488 labeled fibrinogen. Red arrows indicate neutrophils, yellow arrows indicate NETs and white arrows indicate large pores. (**h**) The permeation coefficient (Darcy constant [Ks]) of clots were quantified. Other concentrations: plasma was diluted 1:6 for confocal (except in figure **e** was 1:3) and 1:3 for permeation, CaCl₂ (3.33 mM), thrombin (0.1U/ml). Error bars represent SEM of three technical replicates in triplicates. *** P < 0.001.

Appendix 11. Conference Abstracts
Abstract 1_FMH PGR 2019
**‘Making a Difference’ - Faculty of Medicine and Health Postgraduate
Research Conference**

Title (max of 10 words)	Role of Neutrophils in Fibrin Structure and Function
Aim/Research Question(s)	How do Cells, Fibrin and Neutrophil Extracellular Traps (NETs) Integrate in Thrombi and Blood Clots?
Background	<p>Blood clots are known to contain platelets, fibrin and red blood cells. Recent studies have shown that neutrophils, which traditionally play an important role in inflammatory responses, are also involved in the formation of clots via Neutrophil extracellular traps (NETs). NETs are formed via neutrophils extruding their DNA and granular proteins in response to microbial and inflammatory stimuli. Recent studies indicate a major role for NETs in thrombosis. However the exact interactions of neutrophils or NETs with fibrin(ogen) and the mechanisms behind this interaction are not yet fully understood.</p>
Methods	<p>Turbidity measurements were used to measure the kinetics of clots formation. Confocal microscopy and permeation analysis were used to investigate the effects of NETs on overall clot network structure. Magnetic tweezers are currently being used to investigate clot stiffness and viscous properties.</p>
Results/Findings	<p>NETs had no significant influence on clot formation with purified fibrinogen. However, NETs increased the speed of clot formation in pooled normal plasma both with and without thrombin. Blocking tissue factor reduced the effect of NETs on promoting clot formation to some</p>

	level, but blocking Factor XII did not significantly influence this effect. We also found that clots with NETs were denser than those without NETs.
Conclusions or recommendations	NETs may interact with other components inside pooled normal plasma, and result in promoting clot formation and the formation of a denser clot architecture. Tissue factor may be involved in this interaction, but factor XII may have less effect. My next aim is to investigate the effects of these structural changes on clot mechanical properties.

Abstract 2_ECTH 2019**Neutrophil Extracellular Traps Accelerate Clotting and Produce a Denser Clot Structure in Plasma**

Yu Shi*¹, Stephen Baker¹, Helen Philippou¹, Simon Connell², Robert A. S. Ariens¹

¹Institute of Cardiovascular and Metabolic Medicine, ²Molecular & Nanoscale Physics, Leeds, United Kingdom

Please indicate your presentation preference: Oral Presentation

Please indicate your type of research: Basic Laboratory Research

Please indicate if you are under 35 years of age at the time of ECTH 2019: Yes

Background: The neutrophil is a type of leukocyte that is involved in innate inflammatory processes. Neutrophils are capable of extruding their DNA and granular proteins as traps for microbes, called Neutrophil Extracellular Traps or NETs. Neutrophils and NETs have been implicated in both arterial and venous thrombosis. NETs have been suggested to provide a “scaffold” for thrombosis and to increase the resistance of clots to fibrinolysis and thrombolysis. However, the exact interactions between neutrophils or NETs and fibrin(ogen), and the mechanisms behind this interaction are not yet fully understood.

Aims: This study aims to investigate the role of NETs in blood coagulation, fibrin formation, clot stability and clot mechanical properties, in order to decipher how NETs interact with the fibrin network, and to ultimately elucidate novel mechanisms that contribute to thrombosis.

Methods: Turbidity measurements were used to measure the kinetics of clots formation. Confocal microscopy and permeation analysis were used to investigate the effects of NETs on overall clot network structure. Magnetic tweezers are being used to investigate effects on clot stiffness and viscous properties.

Results: Neutrophils themselves did not significantly promote clot formation. NETs had no significant influence on clot formation with purified fibrinogen. However, NETs increased the speed of clot formation in pooled normal plasma both with and without thrombin. Blocking tissue factor and factor XII did not significantly influence this effect. Our confocal results suggested that clots with NETs were denser than those without NETs.

Summary/Conclusion: NETs may interact with other components of the plasma, resulting in accelerated clotting and the formation of a denser clot architecture. These effects are not mediated through tissue factor or factor XII but could involve other components present in the plasma.

Abstract 3_ISTH 2020

Theme: Blood Cells and Vessel Wall

Neutrophils and Neutrophil Extracellular Traps**Title: (NETs) can promote clotting and impact clot structure in a distinctive manner**

Author(s): Y. Shi¹, S.R. Baker², J.S. Gauer¹, H. Philippou¹, S.D. Connell³, R.A.S. Ariens¹

¹University of Leeds, Leeds Institute of Cardiovascular and Metabolic Medicine, Discovery and Translational Science Department, Leeds, United Kingdom, ²Wake Institute(s): Forest University, Department of Physics, Winston Salem, NC, United States, ³University of Leeds, The Astbury Centre for Structural Molecular Biology, Molecular & Nanoscale Physics, Leeds, United Kingdom

Disclosure: I have no potential conflict of interest.

Text: Background: Neutrophils release mediators (e.g. matrix metalloproteinases and serine proteases) which can influence thrombus formation. Neutrophil Extracellular Traps (NETs), which are extruded from neutrophils, have been shown to provide a “scaffold” for thrombosis and to increase the resistance of clots to fibrinolysis and thrombolysis. However, the interactions between neutrophils or NETs and fibrin(ogen) in clots, as well as the mechanisms behind these interactions are not yet fully understood.

Aims: To investigate the role of neutrophils/NETs in blood coagulation, fibrin formation, clot stability and clot mechanical properties, in order to decipher how neutrophils/NETs interact with the fibrin network.

Methods: Human neutrophils were isolated from whole blood by the standard density gradient centrifugation method. Neutrophils were stimulated by Phorbol 12-myristate 13-acetate to generate NETs. Turbidity measurements were used to measure the kinetics of clot formation. Confocal microscopy was used to investigate the effects of neutrophils/NETs on overall clot network structure. Permeation experiments were carried out to investigate clot porosity.

Results: Neutrophils and NETs promoted clot formation in pooled normal plasma without the addition of other triggers of coagulation. Both also delayed clot lysis. The procoagulant effect of neutrophils and NETs were also observed in FXII- and FVII-deficient plasma. However, the procoagulant effect of neutrophils was not observed, while NETs still induced clotting, in FXI-deficient plasma.

NETs increased the density of clots, particularly in the areas immediately surrounding the NETs, but neutrophils did not. Neutrophil-induced clots were weak and showed large pores. NETs did not significantly affect the average pore size of clots.

Conclusions: NETs accelerate clotting and contribute to the formation of a denser clot architecture. These effects are not mediated through FVII, FXII or FXI but likely involve other components present in the plasma. Neutrophils, or mediators they release, induce clotting via FXI.

Abstract 4_BSHT 2021

Title: Neutrophils can Promote Clotting via FXI and Impact Clot Structure via Neutrophil Extracellular Traps in a Distinctive Manner *in vitro*

Author(s): Y. Shi¹, J.S. Gauer¹ S.R. Baker^{1,2}, H. Philippou¹, S.D. Connell³, R.A.S. Ariens¹ (R.A.S.Ariens@leeds.ac.uk)

Affiliation (s): ¹University of Leeds, Leeds Institute of Cardiovascular and Metabolic Medicine, Discovery and Translational Science Department, Leeds, United Kingdom, ²Wake Forest University, Department of Physics, Winston Salem, NC, United States, ³University of Leeds, The Astbury Centre for Structural Molecular Biology, Molecular & Nanoscale Physics, Leeds, United Kingdom

Background: Neutrophils release mediators (e.g. matrix metalloproteinases and serine proteases) which can influence thrombus formation. Neutrophil Extracellular Traps (NETs), which are extruded from neutrophils, have been shown to provide a “scaffold” for thrombosis and to increase the resistance of clots to fibrinolysis and thrombolysis. However, the interactions between neutrophils or NETs and fibrin(ogen) in clots, as well as the mechanisms behind these interactions are not yet fully understood.

Aims: To investigate the role of neutrophils/NETs in blood coagulation, fibrin formation, clot stability and clot porosity, in order to decipher how neutrophils/NETs interact with the fibrin network.

Methods: Human neutrophils were isolated from whole blood by the standard density gradient centrifugation method. Neutrophils were stimulated by Phorbol 12-myristate 13-acetate to generate NETs. Turbidity measurements were used to measure the kinetics of clot formation. Confocal microscopy was used to investigate the effects of neutrophils/NETs on overall clot network structure. Permeation experiments were carried out to investigate clot porosity.

Results: Neutrophils and NETs promote clotting in plasma without the addition of other coagulation triggers, but not in purified fibrinogen, indicating that other factors mediate the interaction. Both neutrophils and NETs also delayed clot lysis in plasma. The procoagulant effects of neutrophils and NETs were also observed in FXII- and FVII-deficient plasma. In FXI-deficient plasma, only the procoagulant effects of NETs were observed, but not of neutrophils. NETs increased the density of clots, particularly in the vicinity of the NETs, while neutrophils-induced clots were less stable and more porous.

Conclusions: NETs accelerate clotting and contribute to the formation of a denser clot architecture that is more resistant to lysis. Neutrophils, or their released mediators, may induce clotting in a different manner to NETs, mediated by FXI.

Abstract 5_ISTH 2021**Title:**

Neutrophils can Promote Clotting by Secreting Proteins that Activate FXI while NETs Promote Clotting Independently of FXI *In Vitro*

Authors:

Y. Shi ¹, J.S. Gauer ¹, S.R. Baker ^{1,2}, H. Philippou ¹, S.D. Connell ³, R.A.S. Ariens ¹

¹University of Leeds, Leeds Institute of Cardiovascular and Metabolic Medicine, Discovery and Translational Science Department, Leeds, United Kingdom, ²Wake Forest University, Department of Physics, Winston Salem, NC, United States, ³University of Leeds, The Astbury Centre for Structural Molecular Biology, Molecular & Nanoscale Physics, Leeds, United Kingdom

Theme:

Regulation of Coagulation

Background:

Neutrophils release mediators (e.g. matrix metalloproteinases and serine proteases) which can influence thrombus formation. Neutrophil Extracellular Traps (NETs), which are extruded from neutrophils, have been shown to provide a “scaffold” for thrombosis and to increase the resistance of clots to fibrinolysis and thrombolysis. However, the interactions between neutrophils or NETs and fibrin(ogen) in clots, as well as the mechanisms behind these interactions are not yet fully understood.

Aims:

To investigate the role of neutrophils/NETs in blood coagulation, fibrin formation, clot stability and clot porosity, in order to decipher how neutrophils/NETs interact with the fibrin network.

Methods:

Human neutrophils were isolated from whole blood by the standard density gradient centrifugation method. Neutrophils were stimulated by Phorbol 12-myristate 13-acetate to generate NETs. Turbidity measurements were used to measure the kinetics of clot formation. Confocal microscopy was used to investigate the effects of neutrophils/NETs on overall clot network structure. Permeation experiments were carried out to investigate clot porosity.

Results:

Neutrophils and NETs promote clotting in plasma without the addition of other coagulation triggers, but not in purified fibrinogen, indicating that other factors mediate the interaction. Both neutrophils and NETs also delayed clot lysis in plasma. The procoagulant effects of neutrophils and NETs were also observed in FXII- and FVII-deficient plasma. In FXI-deficient plasma, only the procoagulant effects of NETs were observed, but not of neutrophils. NETs increased the density of clots, particularly in the vicinity of the NETs, while neutrophils-induced clots were less stable and more porous.

Conclusions:

NETs accelerate clotting and contribute to the formation of a denser clot architecture that is more resistant to lysis. Neutrophils, or their released mediators, may induce clotting in a different manner to NETs, mediated by FXI.

Title: Neutrophils and NETs Produce Clots with Different Types of Fibrin Fibers**Authors:**

Y. Shi ¹, H. McPherson ¹, T. Feller ^{1,2}, J.S. Gauer ¹, H. Philippou ¹, S.D. Connell ², R.A.S. Ariëns ¹

¹University of Leeds, Leeds Institute of Cardiovascular and Metabolic Medicine, Discovery and Translational Science Department, Leeds, United Kingdom, ²University of Leeds, The Astbury Centre for Structural Molecular Biology, Molecular & Nanoscale Physics, Leeds, United Kingdom

Background:

Previously we showed neutrophil extracellular traps (NETs) promoted clotting independently of FXII, FXI and FVII, and contributed to the formation of a denser clot architecture that is more resistant to lysis. We also found neutrophils induced blood clotting in a different manner than NETs, specifically mediated by FXI. Hitherto, effects of neutrophils and NETs on fibrin fiber structure and fibrinopeptide release are unknown.

Aims:

To compare effects of differentiated PLB-985 cells (a neutrophil-like cell model), human neutrophils and their NETs on the structure of fibrin fibers, and investigate the effects of neutrophils on fibrinopeptide release.

Methods:

Human neutrophils were isolated from whole blood by standard density gradient centrifugation method. PLB-985 cells were differentiated in 1.25% (v/v) DMSO. Neutrophils and differentiated PLB-985 cells were stimulated by PMA to generate NETs. Scanning electron microscopy (SEM) was used to image the fiber structure of clots. Atomic force microscopy (AFM) was used to detect the diameter of PLB-985 NET fibers. ELISAs were carried out to analyze fibrinopeptide A and B in neutrophil-induced clots.

Results:

Differentiated PLB-985 cells, PLB-985 NETs and human NETs induced the formation of a network structure of clots (Fig 1), and significantly increased the diameter of fibrin fibers. Human neutrophils increased the release of fibrinopeptide B in plasma, but the structure of human neutrophil-induced clots was lacking an overall “scaffold” structure (Fig 1). AFM data showed that the thickness of NET fibers was variable but thicker than a single DNA helix (2 nm), suggesting that NET fibers are made up of multiple strands of DNA.

Conclusions:

Differentiated PLB-985 cells, PLB-985 NETs and human NETs increased fibrin fiber thickness, which may enhance the clot stability. Human neutrophils on the other hand failed to produce normal fibrin fibers.

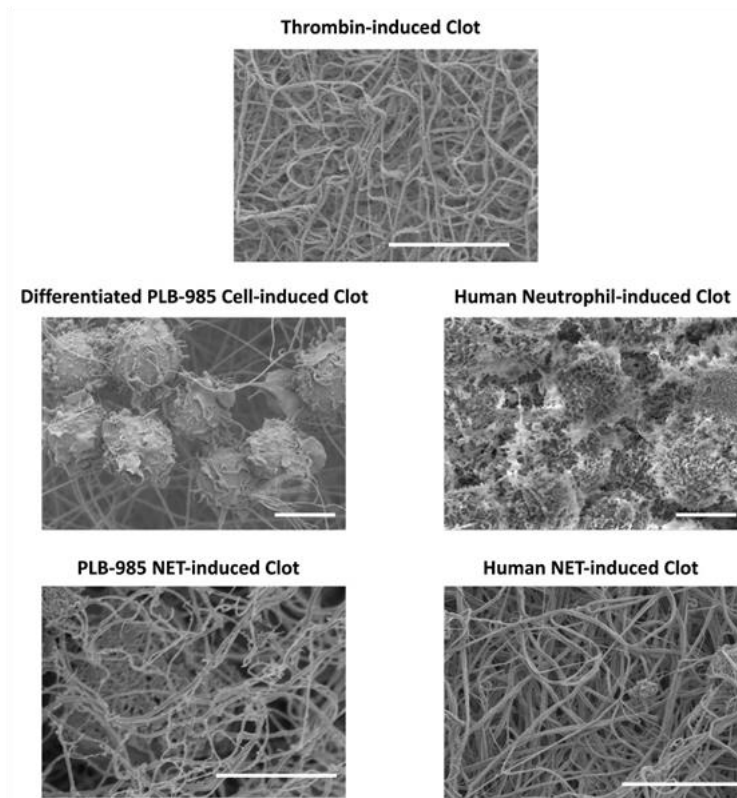


Figure 1. SEM images of plasma clots. Clots were induced by differentiated PLB-985 cells, PLB-985 NETs, human neutrophils and human NETs, respectively. 1 U/ml Thrombin-induced clot was used as a control. Final concentrations: Plasma (diluted 1:3), 10 mM CaCl₂. Scale bars are 5 μm.